



Titre: Sol and gel behavior of chitosan-glycerophosphate systems
Title:

Auteur: Jaepyoung Cho
Author:

Date: 2005

Type: Mémoire ou thèse / Dissertation or Thesis

Référence: Cho, J. (2005). Sol and gel behavior of chitosan-glycerophosphate systems [Ph.D. thesis, École Polytechnique de Montréal]. PolyPublie.
Citation: <https://publications.polymtl.ca/7551/>

 **Document en libre accès dans PolyPublie**
Open Access document in PolyPublie

URL de PolyPublie: <https://publications.polymtl.ca/7551/>
PolyPublie URL:

Directeurs de recherche:
Advisors:

Programme: Unspecified
Program:

UNIVERSITÉ DE MONTRÉAL

**SOL AND GEL BEHAVIOR OF CHITOSAN-
GLYCEROPHOSPHATE SYSTEMS**

JAEPYOUNG CHO

**DÉPARTEMENT DE GÉNIE CHIMIQUE
ÉCOLE POLYTECHNIQUE DE MONTRÉAL**

**THÈSE PRÉSENTÉE EN VUE DE L'OBTENTION
DU DIPLÔME DE PHILOSOPHIAE DOCTOR
(GÉNIE CHIMIQUE)**

Juin 2005

© Jaepyoung Cho, 2005.



Library and
Archives Canada

Bibliothèque et
Archives Canada

Published Heritage
Branch

Direction du
Patrimoine de l'édition

395 Wellington Street
Ottawa ON K1A 0N4
Canada

395, rue Wellington
Ottawa ON K1A 0N4
Canada

Your file Votre référence

ISBN: 978-0-494-16986-5

Our file Notre référence

ISBN: 978-0-494-16986-5

NOTICE:

The author has granted a non-exclusive license allowing Library and Archives Canada to reproduce, publish, archive, preserve, conserve, communicate to the public by telecommunication or on the Internet, loan, distribute and sell theses worldwide, for commercial or non-commercial purposes, in microform, paper, electronic and/or any other formats.

The author retains copyright ownership and moral rights in this thesis. Neither the thesis nor substantial extracts from it may be printed or otherwise reproduced without the author's permission.

AVIS:

L'auteur a accordé une licence non exclusive permettant à la Bibliothèque et Archives Canada de reproduire, publier, archiver, sauvegarder, conserver, transmettre au public par télécommunication ou par l'Internet, prêter, distribuer et vendre des thèses partout dans le monde, à des fins commerciales ou autres, sur support microforme, papier, électronique et/ou autres formats.

L'auteur conserve la propriété du droit d'auteur et des droits moraux qui protègent cette thèse. Ni la thèse ni des extraits substantiels de celle-ci ne doivent être imprimés ou autrement reproduits sans son autorisation.

In compliance with the Canadian Privacy Act some supporting forms may have been removed from this thesis.

Conformément à la loi canadienne sur la protection de la vie privée, quelques formulaires secondaires ont été enlevés de cette thèse.

While these forms may be included in the document page count, their removal does not represent any loss of content from the thesis.

Bien que ces formulaires aient inclus dans la pagination, il n'y aura aucun contenu manquant.


Canada

UNIVERSITÉ DE MONTRÉAL

ÉCOLE POLYTECHNIQUE DE MONTRÉAL

Cette thèse intitulée :

**SOL AND GEL BEHAVIOR OF CHITOSAN-
GLYCEROPHOSPHATE SYSTEMS**

présentée par: **CHO Jaepyoung**

en vue de l'obtention du diplôme de : **Philosophiae Doctor**

a été dûment acceptée par le jury d'examen constitué de:

M. DE CRESCENZO Gregory, Ph. D., président

Mme HEUZEY Marie-Claude, Ph. D., membre et directrice de recherche

M. BÉGIN André, Ph. D., membre et codirecteur de recherche

M. CARREAU Pierre J., Ph. D., membre et codirecteur de recherche

Mme HOEMANN Caroline, Ph. D., membre

M. BUI VAN Tam, Ph. D., membre

Acknowledgments

I am deeply indebted to my research director, Professor Marie-Claude Heuzey, and codirectors, Professor Pierre J. Carreau and Dr. André Bégin, for their patience and encouragement. I also would like to thank them for providing abundant time to discuss my research results. The useful discussions enabled me to finish my Ph. D. work. In addition, I gratefully acknowledge the financial support of Conseil de Recherches en Pêche et en Agroalimentaire du Québec (CORPAQ).

I would like to thank all of my colleagues, Ali Ahmari, Julien Ferec, Stephane Guillaud, Melina Hamdine, Dr. Saeid Savarmand, Shant Shahbikian, Baptiste Mary, Christophe Mobuchon, in my research group, Centre de recherche en Plasturgie et Composites (CREPEC), for their good friendship, interesting discussions and comments.

I would like to share my joy with my Christian family in University Bible Fellowship. I really thank them for their prayer support and encouragement. Especially, I am indebted to Mr. John Giesbrecht for providing me weekly one-to-one bible study, encouragement, advice and good friendship.

Finally, I would like to thank my mother for her unlimited love, support and prayer. I acknowledge the patience and encouragement of my sisters (Eunjin, Haejin, Hwajin and Heejung) and my brother-in laws (Mr. Seongjun Lee, Mr. Kunsoo Kim, Dr. Junghwan Ryu and Mr. Dukwoo Park). Additionally, I would like to share my joy with my four nephews (Jungbin, Juhyun, Hohyun and Injae) and three nieces (Subin, Hyunju and Sunhwa).

Résumé

Le chitosane, un biopolymère extrait des carapaces de crustacés, présente un grand intérêt pour ses propriétés de non toxicité, de biodégradabilité et biocompatibilité. Il peut être utilisé comme agent antifongique, anti-tumeur, anti-allergène et activateur immunitaire. De nos jours, ses applications sont innombrables dans les domaines nutraceutique, cosmétique, pharmaceutique et biomédical. Une étude récente (Chinité et al., 2001) a porté sur la possibilité de produire un gel homogène thermoréversible de chitosane en présence de β -glycerophosphate et de l'utiliser comme recteur in-situ de matériaux thérapeutiques. Les mécanismes de gélification ainsi que la nature des gels ont été explorés. Une analyse plus élargie pourrait cependant s'étendre à des gels physiques de chitosane. Dans la présente étude, le comportement sol-gel des systèmes chitosan-glycerophosphate a été abordé d'un point de vue rhéologique et physico-chimique. Les effets de la force ionique, des additifs, de la concentration des polymères et de la température ont été étudiés systématiquement.

Il a été montré que les concentrations de croisement (C^*) et d'enchevêtrement (C_e) varient de façon exponentielle avec la force ionique (I) avec les exposants $2/9$ et $1/15$ respectivement. Dans le domaine dilué ($C_C < C^*$), la viscosité intrinsèque décroît avec l'augmentation de la force ionique et la chaîne macromoléculaire devient plus flexible et plus compacte à cause de la diminution de la répulsion électrostatique. À la longueur de persistance calculée à partir de la viscosité intrinsèque diminue également et

a été estimée à 24nm pour un solvant θ . Des précipités blanchâtres se sont formés quand la force ionique était de 0.7M.

Dans le domaine concentré ($C_C > C_e$), la diminution de la force ionique due à l'effet écran généré par le sel ajouté, a engendré une chute des propriétés rhéologiques dynamiques et non linéaires. Cependant ces dernières augmentent lorsque la concentration du chitosane devient plus importante du fait du nombre important d'enchevêtrements et d'interactions polymère-polymère. A concentration de polymère élevée, le mode de relaxation est plus complexe. Les temps de relaxation (τ_H) et les plateaux de viscosité (η_0) suivent également une relation exponentielle du type : $\tau_H \sim C_C^{3.1}$ et $\eta_0 \sim C_C^{4.1}$. La viscosité est aussi largement dépendante de la concentration de l'urée, du glycerophosphate (GP) et du chitosane. L'énergie d'activation (E_{af}) diminue lorsque la concentration de GP diminue, tandis qu'elle augmente lorsque la concentration du chitosane augmente. À basse température, l'ajout de l'urée a pour effet de réduire les propriétés viscoélastiques et les temps de relaxation des solutions chitosane-GP. Cela est dû à la diminution des interactions polymère-polymère.

Le processus de gélification se déroulant au chauffage a montré trois phases : 1) une première phase au comportement liquide ($G' < G''$) est observée; 2) une phase d'accélération ($G' > G''$) et 3) une phase lente ($G' > G''$). La gélification physique est généralement assurée par des interactions ioniques, hydrogènes et hydrophobes. Ces interactions sont très sensibles à la variation de la température. La protonation du chitosane ($-\text{NH}_3^+$) décroît lorsque la température augmente, tandis que l'ionisation du solvant GP ou $(-\text{OP})(\text{O}^-)_2$ croît, générant une force ionique plus importante. Le ratio

chitosane/anion décroît également, indiquant aussi une diminution des interactions ioniques telles que le pontage ionique. D'un autre côté, l'augmentation de la force ionique, principalement due à la forte ionisation du GP à haute température, favorise les interactions hydrophobes entre les chaînes de polymères. L'augmentation de la température modifie également la distribution des liaisons hydrogènes, favorisant plutôt les interactions polymère-polymère que les interactions polymère-solvant. Ainsi la gélification induite par le chauffage pourrait être gouvernée par les interactions hydrophobes. Cette hypothèse a été appuyée par les résultats de gélification en présence d'urée.

La température de gélification (T_{gel}) définie comme étant le point de croisement des modules G' et G'' , décroît lorsque les concentrations de chitosane et de glycérophosphate augmentent. Le processus de gélification est accéléré quand la force ionique dans les solutions de chitosane croît. Par contre, elle est retardée lorsque de l'urée est ajoutée.

L'énergie d'activation de gélification (E_{ga}) dans chaque système a été calculée à partir d'un modèle de cinétique non isotherme. Lorsque la concentration de chitosane est augmentée de 0.10 à 0.20M, E_{ag} diminue de 3000 à 500kJ/mol dans deuxième zone. La concentration de GP affecte de façon insignifiante. E_{ga} ne montre ainsi aucune influence sur la cinétique de gélification. Dans la dernière zone la valeur la plus basse de E_{ag} , laisse à supposer que l'évolution des réseaux physiques est énergiquement plus facile. Dans cette zone, la gélification a été ralentie à cause de la diffusion contrôlée lorsque la viscosité devient trop importante.

Le gel obtenu à température élevée n'a été qu'en partie thermoréversible, lors d'un refroidissement jusqu'à 5°C, à cause de la subsistance de certaines associations moléculaires. Il a néanmoins montré une réversibilité complète en fonction du *pH*. La conformation devient cependant plus étendue après avoir atteint l'état sol.

Enfin, des cryogels ont été produits avec le système chitosane-GP à des températures inférieures à 0°C. La cryogélification a été très lente en comparaison avec la gélification induite par le chauffage. Encore une fois, elle a été favorisée en augmentation les concentrées de chitosane et de GP. Un phénomène de précipitation ou de séparation de phases a eu lieu après un mois, pour les solutions de chitosane conservées à température ambiante, due à l'absence d'une force de gélification suffisante pour former un gel homogène.

Abstract

Chitosan, a biopolymer extracted from crustaceans discarded in the seafood processing industry, have been attracting much attention because of its non-toxic, biodegradable and biocompatible characters. In addition, it has a variety of bioactivities such as antifungal, antitumor, antiallergic and an immune activating character. At the present time, many chitosan-based applications have been claimed in nutraceutic, medical, cosmetic and pharmaceutical industries. Recently, a homogenous thermoreversible chitosan gel system, an injectable *in-situ* hydrogel usable for loading with therapeutic materials, was prepared in the presence of β -glycerophosphate (Chenite *et al.*, 2001). The gelation mechanisms and nature of the gel produced have been under investigation. A broader analysis may however expand the applications of physical chitosan gels system in general. In this study, sol and gel behavior of chitosan-glycerophosphate based systems were extensively characterized using rheological and physicochemical measurements under various ionic strength, additives, polymer concentration and temperature.

Initially, the overlapping (C^*) and entanglement (C_e) concentrations were determined as a function of ionic strength. Both critical concentrations were exponentially proportional to ionic strength (I). The exponents were 2/9 for C^* and 1/15 for C_e . In the dilute regime ($C_C < C^*$), the intrinsic viscosity decreased with increasing ionic strength. Additionally, the molecular chain became more flexible and compacted at high ionic strength due to the reduction of the electrostatic repulsion. The persistence

length, calculated from the measured intrinsic viscosity data, decreased with increasing ionic strength and it was 24nm in a θ solvent. White-like precipitates formed when ionic strength was 0.7M.

In the concentrated regime ($C_C > C_e$), the dynamic mechanical properties of chitosan solutions were measured in terms of ionic strength, urea, GP and chitosan concentrations. When ionic strength decreased, the rheological properties and nonlinear behavior were lower due to the reduction of the electrostatic repulsion force by the salt screening effect. However, chitosan rheological properties were enhanced when chitosan concentration increased, due to the larger number of entanglements as well as polymer-polymer interactions. The stress relaxation mode was more complex at high chitosan concentration. The relaxation time (τ_H) and the zero-shear viscosity (η_0) also showed power-law relationships with chitosan concentration (C_C): $\tau_H \sim C_C^{3.1}$ and $\eta_0 \sim C_C^{4.1}$. The viscoelastic properties were greatly dependent on urea, GP and chitosan content. The flow activation energy (E_{af}) was reduced with decreasing GP content, but increased with chitosan concentration. At low temperature, urea lowered viscoelastic properties and shortened relaxation times of chitosan-GP solutions due to the reduction of polymer-polymer interactions. The relaxation behavior was also more simplified in the presence of urea.

The evolution of the rheological properties of chitosan-GP systems was characterized in terms of temperature. During the heat-induced gelation process, three regions were defined according to rheological properties: 1) a liquid-like behavior at low temperature ($G' < G''$), 2) a fast gelation process ($G' > G''$), and 3) a slow gelation

process ($G' > G''$). Physical gelation is generally achieved by several interactions such as ionic, hydrogen bonding and hydrophobic interactions. These interactions are very sensitive to temperature. We evaluated that the protonation of chitosan molecules (-NH_3^+) was lowered with increasing temperature. However, the ionization of divalent GP ($\text{-OP(O}^-\text{)}_2$) was larger, resulting in the increase of the ionic strength. Therefore, the ratio of both ions decreased in terms of temperature. It indicates that high temperature reduces the possibility of ionic interactions such as ionic bridging. In addition, the increase of ionic strength, mainly due to the elevated ionization of GP at high temperature, promoted polymer-polymer junctions through hydrophobic interactions. Increasing temperature also modifies hydrogen bonds distribution and favors polymer-polymer interactions over those of polymer-solvent. Thus, the main driving force of the chitosan-glycerophosphate heat-induced gelation may be hydrophobic interactions. This assumption was supported by the results obtained during the gelation tests performed in the presence of urea.

The gelation temperature (T_{gel}), determined as the crossover point of G' and G'' , decreased with increasing chitosan and GP concentrations. A synergetic effect was shown by a sudden drop of the gelation temperature at high chitosan and GP concentrations. The gelation process was accelerated when ionic strength increased in chitosan solutions, but retarded in the presence of urea.

The gelation activation energy (E_{ag}) was calculated from a nonisothermal kinetics model for each chitosan system. When chitosan concentration increased from 0.10 to 0.20M, it decreased from 3000 to 500kJ/mol in the second region. However, the

activation energy was independent on chitosan concentration in the last third regime. The content of GP was insignificant on E_{ag} , indicating that the gelation kinetics is independent on GP concentration. The lower gelation activation energy in the last zone suggested that the evolution of the physical networks was energetically easier, but the gelation was nevertheless strongly slowed down in that region since it was diffusion controlled due to the large viscosity increase.

The gel structure formed at high temperature was only partially thermoreversible upon cooling to 5°C due to the existence of remaining associations. The gel system however showed complete pH-reversibility, and molecular conformation becomes more extended after recovering the solution state from the gel.

Finally, cryogels were produced with the chitosan-glycerophosphate system below 0°C. The cryogelation process was very slow compared to that of the heated-induced gelation. Again, the gelation was more favourable at high chitosan and glycerophosphate concentrations. Precipitation or phase separation occurred after a month for chitosan solutions stored at room temperature due to the absence of sufficient driving forces to form a homogeneous gel.

Condensé en Français

Dans l'industrie de transformation des fruits de mer, de grandes quantités de carapaces de crustacés sont accumulées en raison de leur faible taux de biodégradation, causant ainsi un souci environnemental majeur. Ces carapaces peuvent être traitées chimiquement et réemployées afin de produire la chitine. Cette dernière constitue le composé organique le plus abondant dans la nature après la cellulose. La déacétylation de la chitine par un traitement alcalin donne un produit appelé chitosane qui a la propriété d'être soluble dans les solutions acidulées (Roberts, 1992). La chitine et le chitosane sont des hétéropolysaccharides composés de deux unités structurales : la glucosamine (2-amino-2-déoxy-D-glucopyranose) et l'acétylglucosamine (2-acétamido-2-déoxy-D-glucopyranose). La fraction d'unités de glucosamine définit le degré de déacétylation (DDA). Lorsque le DDA est supérieur à 50%, le polysaccharide est défini comme étant du chitosane (Burgnerotto et al., 2001a).

La solubilité du chitosane est liée principalement à la protonation de ses groupements amines libres, à *pH* supérieur à 6.2 (Park et al., 1983). La charge positive de ce polyélectrolyte lui a permis de trouver de nombreuses applications en tant que matériel non-toxique, biocompatible et biodégradable. Il a notamment été employé dans les industries nutraceutique, médicale, cosmétique et pharmaceutique. De nombreux brevets internationaux ont été déposés pour ces applications (Kasaai, 1999; Kumar, 2001; Singla et Chawla, 2001).

Le chitosane peut être étudié sous divers aspects physiques dépendant de la concentration du polymère, du *pH*, de la force ionique et de la température. Pour un *pH* inférieur à son *pKa* (*pH* < 6.2 (Roberts, 1992)), le chitosane est hydrosoluble et positivement chargé dû à la protonation de ses groupements amines ($-NH_2$), causant ainsi la répulsion électrostatique entre les chaînes moléculaires. Par l'ajout de sel, résultant en une augmentation de la force ionique de la solution, la répulsion électrostatique intramoléculaire peut éventuellement favoriser les interactions intermoléculaires par l'intermédiaire de liaisons hydrophobes via le groupe ($-CH_3$) et de

liaisons hydrogènes via les groupes (- OH, - NH et - C=O) (Roberts, 1992). Des gels de chitosane peuvent être obtenus en augmentant la concentration du polymère au-dessous du pH de 6.2 (Iverson et al., 1997) ou par contrôle du pH (Jackson, 1987). L'addition d'une base augmente logiquement le pH mais peut également réduire la répulsion électrostatique entre les molécules de chitosane et mener à la formation d'une structure colloïdale à pH supérieur à 6.2. Récemment, un système thermoréversible homogène de gel a été préparé en neutralisant des solutions semi-diluées et fortement déacétylées de chitosane avec une base faible, le β -glycérophosphate (β -GP) (Chenite et al. 2001). Le système demeure en solution à pH physiologique (= 7.2) et température ambiante, mais se transforme en gel lors du chauffage à la température physiologique (= 37°C). Lorsque la température décroît, le gel de chitosane redevient à l'état solution.

La gélification du système chitosane- β -GP peut impliquer plusieurs phénomènes tels que l'effet d'écrantage dû à la répulsion électrostatique, les interactions ioniques, les liaisons hydrophobes et hydrogènes. La base faible β -glycérophosphate ($pK_{a,2} = 6.65$ à 25°C) (Alberty, 1983; Goldberg et al., 2002) peut augmenter le pH des solutions de chitosane autour du point de neutralité. En solution, le β -GP négativement chargé peut sous sa forme monovalente masquer les répulsions électrostatiques entre les molécules de chitosane ou sous sa forme divalente, induire un pontage ionique. Grâce à la présence de groupements favorisant les liaisons hydrophobes et hydrogènes (Roberts, 1992), des réseaux tridimensionnels peuvent également se former. Bien que plusieurs travaux aient essayé de décrire les mécanismes d'interactions afin d'expliquer la gélification du système chitosane- β -GP (Chenite et al., 2001; Wang, 1999), les mécanismes exacts restent encore non établis. Ainsi, l'objectif de ce travail est d'améliorer la compréhension des mécanismes de gélification du système chitosane- β -GP, en aidant également au développement d'autres produits similaires. Pour cela, le travail consistera en la caractérisation rhéologique et physico-chimique des solutions de chitosane du régime dilué au régime concentré (ou régime d'enchevêtrement), et à l'état sol et gel.

Propriétés viscoélastiques de solutions de chitosane : Effet de la concentration et de la force ionique

Les propriétés rhéologiques dynamiques des solutions de chitosane ont été étudiées en terme de force ionique et de la concentration de chitosane pour les systèmes présentant des enchevêtrements. La concentration critique de croisement C^* et la concentration critique d'enchevêtrement C_e ont été déterminées initialement afin de délimiter les domaines du régime dilué, semi-dilué et concentré ou d'enchevêtrement. Pour les solutions diluées, l'effet de la force ionique (I) sur la viscosité intrinsèque ($[\eta]$) a été interprété en termes de longueur d'écran électrostatique de Debye. La viscosité intrinsèque, le rayon de giration et la longueur de persistance ont diminué suite à une augmentation de la force ionique, diminution attribuée à l'effet d'écrantage, généré par le sel, des charges électrostatiques présentes sur les chaînes de chitosane. Cela a entraîné une flexibilité accrue des chaînes. Pour les solutions concentrées, des mesures dynamiques ont été exécutées et les spectres de relaxation ont été calculés à partir du module élastique (G') et du module de perte (G'') qui ont été caractérisés dans le domaine de viscoélasticité linéaire. Pour toutes les concentrations de chitosane et toutes les forces ioniques les spectres de relaxation n'ont présenté qu'un seul pic. Cependant, la largeur des spectres s'est accrue avec l'augmentation de la concentration de polymères, indiquant une plus grande distribution des modes de relaxation dus à plus d'enchevêtrements et d'interactions intermoléculaires. Le temps moyen de relaxation (τ_H), relié à la reptation, et la viscosité plateau (η_0) ont montré une dépendance avec la concentration de chitosane selon une loi de type puissance, avec $\tau_H \sim C^{3.1}$ et $\eta_0 \sim C^{4.1}$ respectivement. Les valeurs élevées de ces exposants indiquent la tendance associative du polymère. La nature non-Newtonienne (propriétés élastiques et comportement rhéofluidifiant) des solutions de chitosane ont augmenté avec l'augmentation de la concentration de chitosane et la réduction de la force ionique.

Gélification physique du chitosane en présence de β - glycérophosphate : Effet de la température

En ajoutant du β -glycérophosphate à des solutions aqueuses de chitosane, le polymère demeure en solution à pH neutre et température ambiante, tandis qu'une gélification homogène de ce système peut être déclenchée par le chauffage. Ce système est donc un des rares vrais hydrogels physiques de chitosane. Dans cette étude, les propriétés physico-chimiques et rhéologiques de solutions de chitosane en présence d'acide acétique et de β -GP ont été étudiées en fonction de la température afin d'avoir une meilleure connaissance du mécanisme de gélification. La structure de gel formée à température élevée s'est avérée être seulement partiellement thermoréversible lors d'un refroidissement à $5^{\circ}C$ dû à des associations résiduelles dont l'existence a été confirmée par un rétablissement spontané du gel après sa dissociation à basse température. Une augmentation de la température n'a eu aucun effet sur le pH de ce système, tandis que sa conductivité (et sa force ionique calculée) s'est accrue. Les valeurs de pH ont été utilisées pour estimer le degré de protonation de chaque espèce en fonction de la température. Le rapport décroissant de $-NH_3^+$ sur les chaînes de chitosane et $-OPO(O^-)_2$ du β -GP a suggéré que la solubilité du chitosane décroît et que les interactions ioniques diminuent également suite à une augmentation de la température. D'autre part, l'augmentation de la force ionique en fonction de la température, en présence de β -GP, a augmenté l'écrantage de répulsions électrostatiques et l'effet hydrophobe, causant ainsi des conditions favorables à la formation de gel. Par conséquent, notre étude a suggéré que les interactions hydrophobes et la solubilité réduite sont les forces motrices du phénomène de gélification du chitosane à température élevée et en présence de β - GP.

Effet de l'urée sur le comportement en solution et gélification du système chitosane- β glycérophosphate provoquée par la chaleur

Dans cette autre étape de l'étude, nous avons étudié l'effet de l'urée sur les propriétés physico-chimiques (pH et conductivité) et rhéologiques du système chitosane- β -GP afin d'évaluer les interactions principales de type polymère-polymère à basse et à

haute température. Le pH des solutions a légèrement augmenté en raison de la consommation accrue de H^+ en solution par l'hydrolyse de l'urée. En outre, l'addition de l'urée a considérablement diminué la conductivité, et donc la force ionique de ces solutions, et cet effet était plus important à température élevée. Ce résultat indique que l'urée affecte fortement les interactions de type polymère-polymère en diminuant les ponts hydrogènes à basse température, mais qu'elle peut également réduire le comportement hydrophobe à température élevée, puisque la réduction de la force ionique résulte en une réduction de l'écrantage des répulsions électrostatiques entre les groupes protonés de la glucosamine. À $15^\circ C$, l'addition de l'urée à des solutions de chitosane- β -GP a diminué leur élasticité, leur temps de relaxation et a simplifié leur processus de relaxation puisque les ponts hydrogènes furent supprimés. La gélification induite thermiquement du système de chitosane en présence de l'urée a démontré une température de gélification (T_{gel}) plus élevée pour des essais non-isothermes et de plus long temps de gélation (t_{gel}) en conditions isothermes. L'énergie d'activation pour la gélification a également augmenté avec l'augmentation de la concentration d'urée. Nous avons conclu que l'effet retardateur de l'urée sur le processus de gélification est principalement lié à une diminution des interactions polymère-polymère par effet hydrophobe, appuyé par la diminution de la conductivité.

Influence de la concentration de glycérophosphate sur le comportement et le point de gélification du chitosane en solution lors d'un cisaillement oscillatoire de faible amplitude

Les propriétés viscoélastiques linéaires ont été étudiées, à l'état sol comme à l'état gel, en fonction de la concentration du glycérophosphate (GP) (C_{GPe}) et du polymère (C_C). Les solutions de chitosane ont présenté un comportement fluide à faibles concentrations de β -GP, mais se sont écartées de l'état de sol aux concentrations plus élevées. La viscosité complexe à 0.1 rad/s ($\eta_{*0.1\text{rad/s}}$) a montré un comportement en loi de puissance marqué avec la concentration en chitosane, i.e. $\eta_{*0.1\text{rad/s}} \sim C_C^{5.0}$. L'énergie d'activation pour l'écoulement (E_{af}), calculée à partir des courbes maîtresses des données

de viscoélasticité linéaire, a augmenté avec la diminution de C_{GP} et l'augmentation de C_C . Le comportement opposé a été expliqué en terme d'interactions hydrophobes favorisées aux hautes concentrations en glycérophosphate et à haute température, tel que confirmé par la force ionique calculée. Le suivi de la gélification induite par la chaleur a prouvé que les données obtenues à différentes concentrations en β -GP sont superposables en une seule courbe maîtresse, indiquant que le mécanisme de gélification et sa cinétique sont indépendants de la teneur en β -GP. Cependant, des mesures obtenues à différentes concentrations de chitosane n'ont pas pu être superposées sur une seule et même courbe maîtresse. De plus hautes C_C ont eu pour conséquence d'abaisser la température de gélification mais également de ralentir sa cinétique en raison de la viscosité élevée et de la diffusion moléculaire plus lente. Le diagramme de phase sol-gel en trois dimensions a été déduit des mesures rhéologiques pendant la gélification provoquée par l'augmentation de température. Un effet synergique aux plus hautes concentrations de β -GP et de polymère a conduit à une gélification aux limites des gélifications induites par la concentration et thermiquement.

Gélification en dessous de la température ambiante

Les systèmes chitosane-GP ont été stockés à trois températures différentes (0°C, 5°C, et température ambiante) et le changement de leur état physique a été étudié selon la température. À 0 et à 5°C, des systèmes gélifiés ont été formés aux concentrations élevées de chitosane et de GP. La gélification à basse température s'explique principalement par la formation de réseaux 3D par l'intermédiaire de liaisons hydrogène. Cependant, la séparation de phase a été observée pour la plupart des échantillons de chitosane conservés à température ambiante. Les deux forces principales, les liaisons hydrogènes et hydrophobes, sont considérablement fonction de la température. Les interactions entre les liaisons hydrogènes sont dominantes aux basses températures, mais sont réduites à des températures plus élevées. Les liaisons hydrophobes, quant à elles, augmentent à des températures élevées. Ainsi, la séparation de phase observée à

température ambiante peut être due à un nombre insuffisant d'interactions physiques entre les chaînes polymères.

Effets de la force ionique sur la température de gélification

À 80°C, des solutions de chitosane en l'absence de GP (de pH 4.2 – 4.3) ont été caractérisées selon leur force ionique en utilisant la rhéométrie. Quand la force ionique était inférieure à 0.1, la viscosité diminuait en fonction du temps pour ensuite se stabiliser. La diminution initiale de la viscosité peut être due à la dégradation thermomécanique et/ou au changement de conformation moléculaire résultant de la disparition des liaisons hydrogènes aux hautes températures. Cependant, les interactions hydrophobes peuvent former un réseau en trois dimensions pour les systèmes chitosane aux températures élevées. Ainsi, la viscosité constante est peut être due à l'équilibre de la dégradation thermomécanique et/ou à la disparition des liaisons hydrogènes et des interactions hydrophobes. Au-dessus d'une concentration ionique de 0.3M, la formation d'un réseau tridimensionnel par l'intermédiaire des interactions hydrophobes est dominante; ainsi, les propriétés mécaniques augmentent. Quand la concentration ionique a augmenté, le mécanisme de gélification a été accéléré et des systèmes gélifiés plus forts ont été formés. L'étude appuie également que les interactions hydrophobes sont les forces principales des réseaux en trois dimensions pendant la gélification induite thermiquement.

Contributions scientifiques originales

- 1) L'une des contributions scientifiques les plus originales de ce travail réside dans l'étude de l'influence de la force ionique à pH constant sur les propriétés rhéologiques linéaires et non-linéaires des solutions de chitosane en régime concentré. Le comportement en relaxation des solutions de chitosane a été caractérisé au moyen du calcul du spectre de relaxation continu et de l'utilisation

d'un diagramme de type Cole-Cole. Il a également été comparé pour la première fois avec les prédictions du modèle de reptation. Cette étude sur l'effet de la force ionique fournit les bases fondamentales du comportement du chitosane en solutions concentrés (chapitre 4).

2) Des mécanismes de gélification ont été proposés à partir du calcul de la force ionique et de l'ionisation de chacune des espèces du système chitosane - glycérophosphate en utilisant les valeurs de pH mesurées en terme de température. Cette approche, couplée à la rhéologie, s'est avérée suffisamment puissante pour explorer le processus de gélification tout en demeurant simple. Le calcul a permis de confirmer l'absence d'interactions ioniques, telles que le pontage ionique, et de déterminer les principales forces motrices de la formation du gel (chapitre 5).

3) Le diagramme de phases sol-gel du chitosane et du glycérophosphate a été généré pour la première fois. La température de gélification a été utilisée pour caractériser la structure des jonctions de polymère (chapitre 7).

4) Nous avons montré qu'il était possible d'induire la gélification du chitosane en l'absence de glycérophosphate par l'action de la chaleur. La gélification était alors observée pour des forces ioniques supérieures à 0.3M. Pour des forces ioniques élevées, le processus de gélification était accéléré et les gels formés étaient plus résistants. Cette étude montre l'importance des interactions

hydrophobiques sur la formation de structures de gel pour les systèmes à base de chitosane à haute température (chapitre 8).

5) Nous avons finalement montré la faisabilité de la cryo-gélification dans les systèmes chitosane – glycérophosphate. Les cryogels ont pu être formés sur une période d'un mois lorsque les solutions étaient stockées à des températures inférieures à 0°C. La cryo-gélification était accélérée pour des concentrations en chitosane et en glycérophosphate élevées (chapitre 8).

Table of Contents

Acknowledgments	iv
Résumé	v
Abstract	ix
Condensé en Français	xiii
Table of Contents	xxii
List of Figures	xxx
List of Tables	xxxvi
List of Appendices	xxxviii
List of Symbols and Abbreviations	xxxix
Chapter 1. Introduction and objectives	1
1.1. Introduction	1
1.2. Objectives	5
Chapter 2. Literature review	7
2. 1. Applications of chitosan	7
2.2. Physicochemistry of chitosan	8
2.2.1. <i>Preparation of chitosan</i>	8
2.2.2. <i>Determination of degree of deacetylation</i>	9
2.2.3. <i>Determination of molecular weight</i>	12
2.2.4. <i>Modification of degree of deacetylation and</i> <i>depolymerization</i>	16
2.3. Solubilization of chitosan	17
2.4. Characterization of chitosan solutions	21
2.4.1. <i>Determination of critical concentrations C^* and C_e</i>	21
2.4.2. <i>Solution behavior in dilute regime</i>	22

2.4.3. Characterization of dilute chitosan solutions	25
2.5. Chitosan solution behavior in concentrated regime	26
2.5.1. Concentration effect on viscosity	26
2.5.2. DDA effect on viscosity	28
2.5.3. Temperature effect on viscosity	28
2.5.4. Effect of various parameters on relaxation time	29
2.6. Gel systems	30
2.6.1. Classification of gels	31
2.6.2. Chitosan-based chemical gels	32
2.6.3. Physical chitosan gels	33
2.6.4. Secondary forces related to physical chitosan gelation	35
2.6.5. Temperature effect on chitosan physical gelation	35
2.6.6. Urea effect on the secondary forces of chitosan gel	36
Chapter 3. Presentation of the articles	38
Chapter 4. Viscoelastic Properties of Chitosan Solutions: Effect of Concentration and Ionic Strength	42
4.1. Abstract	43
4.2. Introduction	44
4.3. Literature review	45
4.3.1. Characterization of dilute chitosan solutions	45
4.3.2. Determination of the critical concentrations C^* and C_e	46
4.3.3. Characterization of concentrated chitosan solutions	47
4.4. Experiments	49
4.4.1. Materials	49
4.4.2. Solutions preparation and physicochemical characterization	50

4.4.3. <i>Intrinsic viscosity measurements</i>	51
4.4.4 <i>Dynamic and steady shear rheological tests</i>	52
4.5. Results and discussion	52
4.5.1. <i>Physicochemical characterization of chitosan solutions</i>	52
4.5.2. <i>Determination of overlapping C^* and entanglement C_e concentrations</i>	54
4.5.3. <i>Dynamic and steady shear rheological measurements in the entangled regime</i>	58
4. 6. Conclusions	64
4. 7. Acknowledgements	65
4. 8. References	65
Chapter 5. Physical Gelation of Chitosan in the Presence of	
β -Glycerophosphate: The Effect of Temperature	92
5.1. ABSTRACT	93
5.2. INTRODUCTION	94
5.3. THEORETICAL BACKGROUND	96
5.4. EXPERIMENTS	98
5.4.1 <i>Materials</i>	98
5.4.2. <i>Chitosan solutions preparation</i>	98
5.4.3. <i>pH and conductivity measurements</i>	99
5.4.4. <i>Rheological measurements</i>	100
5.5. RESULTS	101
5.5.1 <i>Heat-induced gelation and partial thermoreversibility</i>	101
5.5.2. <i>Non-isothermal kinetics of gelation</i>	103
5.5.3. <i>Characterization of the gel strength and recovery</i>	105
5.5.4. <i>Effects of temperature on pH and conductivity</i>	106

5.5.5. <i>Determination of the degree of ionization and solution ionic strength</i>	107
5.6. DISCUSSION	108
5.7. CONCLUSIONS	111
5.8. ACKNOWLEDGEMENTS	113
5.9. REFERENCES	113
Chapter 6. Effect of urea on solution behavior and heat-induced gelation of chitosan- β -glycerophosphate	127
6.1. Abstract	128
6.2. Introduction	129
6.3. Temperature and presence of urea effects on gelation of chitosan ...	131
6.3.1. <i>Temperature effect</i>	131
6.3.2. <i>Urea effect on hydrogen bonding interactions</i>	132
6.3.3. <i>Urea effect on hydrophobic interactions</i>	133
6.4. Experiments	134
6.4.1. <i>Materials</i>	134
6.4.2. <i>Preparation of chitosan solutions</i>	135
6.4.3. <i>pH and conductivity measurements</i>	136
6.4.4. <i>Rheological measurements</i>	137
6.5. Results	138
6.5.1. <i>Physiochemical measurements</i>	138
6.5.2. <i>Urea effect on solution behaviour</i>	140
6.5.3. <i>Urea concentration effect on gelation</i>	142
6.5.4. <i>Non-isothermal gelation kinetics</i>	143
6.5.5. <i>Partial thermoreversibility of the gels</i>	144
6.5.6. <i>Isothermal gelation</i>	145

6.6. Discussion	147
6.7. Conclusions	149
6.8. Acknowledgements	151
6.9. References	151
Chapter 7. Chitosan and glycerophosphate concentration dependence of solution behavior and gel point using small amplitude oscillatory rheometry	
	175
7.1. ABSTRACT	176
7.2. INTRODUCTION	177
7.3. THEORETICAL BACKGROUND	179
7.4. EXPERIMENTS	181
7.4.1. <i>Materials</i>	181
7.4.2. <i>Chitosan solutions preparation</i>	181
7.4.3. <i>Rheological measurements</i>	183
7.5. RESULTS	183
7.5.1. <i>Effect of β-GP and chitosan concentrations on solution behaviour</i>	183
7.5.2. <i>Effect of β-GP and chitosan concentrations on gelation</i>	186
7.5.3. <i>Non-isothermal gelation kinetics</i>	188
7.5.4. <i>Effect of GP type on sol and gel viscoelastic properties</i>	189
7.5.5. <i>Structure of physical junction zones formed in the chitosan-β-GP gel</i>	190
7.7. DISCUSSION	191
7.8. CONCLUSIONS	193
7.9. ACKNOWLEDGEMENTS	194
7.10 REFERENCES	194

8.5.1.2. Rheological measurements	227
8.5.2. Results and Discussion	227
8.5.2.1. Physicochemical properties of each chitosan solution	227
8.5.2.2. Rheological measurements	228
8.6. Summary	229
Chapter 9. General discussion	231
9.1. Determination of dilute and concentrated regimes	231
9.2. Solution behaviour in dilute regime	232
9.3. Solution behaviour in concentrated regime	232
9.3.1 Ionic strength effect	232
9.3.2. Urea effect on chitosan-GP solution behaviour	234
9.3.3. Effects of β -GP and chitosan concentrations on solution behaviour	235
9.4. Heat-induced gelation	236
9.4.1. Temperature effect on gelation	237
9.4.2. Urea effect on gelation	238
9.4.3. 3D sol-gel phase diagram for gelation	238
9.4.4. Gelation kinetics study	239
9.4.5. Reversibility of the gel structure formed	239
9.4.6. Gelation below room temperature	240
9.4.7. Effects of ionic strength and temperature on gelation	240
Chapter 10. Original scientific contributions	242
Chapter 11. Conclusions and perspectives	244
11.1. Conclusions	244
11.1.1. Solution behavior in dilute regime	244

<i>11.1.2. Solution behavior in concentrated regime</i>	244
<i>11.1.3. Chitosan gelation</i>	245
11.2. Perspectives	246
References	248
Appendices	261

List of Figures

Figure 2.1. The scheme of chitosan preparation of chitosan. (Roberts, 1992)...	9
Figure 2.2. Titration curve of chitosan dissolved in excess HCl (0.138N) and then titrated with NaOH (0.1018N). (Wang, 1999).	10
Figure 2.3. A typical plot of η_{sp}/c (circle) and $\ln \eta_{rel}/c$ (square) as a function of chitosan concentration for the determination of intrinsic viscosity $[\eta]$ (\overline{M}_w : 715 kDa). (Kasaai, 1999).	13
Figure 2.4. Dependence of specific viscosity as functions of (a) the overlap parameter, $C[\eta]$, and (b) the function $C[\eta] + k_H(C[\eta])^2$ for chitosan solutions (solvent: 0.3M AcOH/0.05 AcONa; temperature: 278K; $\eta_{solvent} = 1.58$ mPa.s; and $k_H = 0.45$). (Desbrières, 2002).....	22
Figure 2.5. Effect of the number average degree of polymerization (\overline{DP}_n) on the intrinsic viscosity, $[\eta]$, of chitosan solution at 0.1M ionic strength. (Anthonsen et al., 1993).....	24
Figure 4.1. Conductivity as functions of ionic strength (I) and chitosan concentration at 25°C.	75
Figure 4.2. Determination of the intrinsic viscosity for various ionic strengths at 25°C: (a) Huggins's representation.	76
Figure 4.2. Determination of the intrinsic viscosity for various ionic strengths at 25°C: (b) Kraemer's representation.	77
Figure 4.3. (a) Dependency of the specific viscosity (η_{sp}) on $C[\eta]$ and on $C[\eta] + k'(C[\eta])^2$ at various ionic strengths.	78
Figure 4.3. (b) Viscosity ratio (η/η_s) as functions of chitosan concentration (C) and ionic strength (I) at 25°C.	79
Figure 4.4. Effect of chitosan concentration at $I = 0.12$ M on (a) storage (G') and loss (G'') moduli as a function of frequency at 25°C. RS: relaxation spectrum.	80

Figure 4.4. Effect of chitosan concentration at $I = 0.12$ M on (b) $\tan\delta$ as a function of frequency at 25°C	81
Figure 4.5. Effect of ionic strength (I) for a 41.7 g/L chitosan solution on (a) storage (G') and loss (G'') moduli as a function of frequency at 25°C . RS: relaxation spectrum.	82
Figure 4.5. Effect of ionic strength (I) for a 41.7 g/L chitosan solution on (b) $\tan\delta$ as a function of frequency at 25°C	83
Figure 4.6. (a) Effect of chitosan concentration at $I = 0.12\text{M}$ on the time-weighted normalized stress relaxation spectrum.	84
Figure 4.6. (b) Effect of ionic strength (I) for a 41.7 g/L chitosan solution on the time-weighted normalized stress relaxation spectrum.	85
Figure 4.7. Effect of chitosan concentration (C) and ionic strength (I) on the mean relaxation time (τ_H).	86
Figure 4.8. Power-law index P from the log-log plot of G' and G'' as functions of chitosan concentration (C) and ionic strength (I).	87
Figure 4.9. Calculated stress relaxation modulus from the experimental derived relaxation spectra (Equation 4.6) and Doi-Edwards equation (Equation 4.20) for various chitosan concentrations and $I = 0.46$ M.	88
Figure 4.10. Comparison of the complex viscosity and steady shear viscosity data of a 41.7 g/L chitosan solution for various ionic strengths.	89
Figure 4.11. Shear-thinning power-law index (n) as functions of chitosan concentration (C) and ionic strength (I).	90
Figure 4.12. Effects of chitosan concentration (C) and ionic strength (I) on the zero-shear viscosity.	91
Figure 5.1. Evolution of (a) storage modulus G' and (b) loss modulus G'' of sample 10C-69GP-15Ac upon heating and cooling in small amplitude oscillatory shear ($\pm 1^\circ\text{C}/\text{min}$, $\omega = 6.28$ rad/s, $\gamma_0 = 0.01$).	119
Figure 5.2. Frequency sweeps before gelation (B.G.) and after gelation (A.G.) at 5°C ($\gamma_0 = 0.1$) (sample 10C-69GP-15Ac).	120

Figure 5.3. Nonisothermal kinetics of sample 10C-69GP-15Ac.	121
Figure 5.4. (a) Strain sweep resulting in gel break-up and (b) following recovery at 5°C ($\omega = 6.28$ rad/s, $\gamma_0 = 0.01$ for the recovery test) (sample 10C-69GP-15Ac).	122
Figure 5.5. (a) pH and (b) conductivity measurements as a function of temperature.	123
Figure 5.6. Calculated ionization degree (I_D) of each specie under various pH and temperature conditions: (a) acetic acid (AcOH), (b) chitosan, and (c) divalent GP ($ROPO(O^-)_2$ or GP(-2)).	124
Figure 5.7. Calculated ionic strength (I_s) of each solution as a function of temperature.	125
Figure 5.8. (a) Concentration C of selected ions and (b) ratio R of ions $-NH_3^+$ in chitosan and $-OPO(O^-)_2$ in GP as functions of temperature.	126
Figure 6. 1. Chemical structure of (a) chitosan and (b) β -glycerophosphate (β -GP).	162
Figure 6.2. Effects of urea content and temperature on the pH of various solutions.	163
Figure 6.3. Urea effect on (a) conductivity and (b) relative conductivity as a function of temperature.	164
Figure 6.4. Dynamic moduli G' and G'' of chitosan- β -GP solutions in the presence of urea at 15°C. Insert: $\tan\delta$ ($\gamma_0 = 0.1$).	165
Figure 6.5. Urea effect on the normalized time-weighted stress relaxation spectra.	166
Figure 6.6. Urea effect on the Cole-Cole plot. Insert: effect of urea on exponent P and plateau modulus G_e (Equation 6.5).	167
Figure 6.7. Urea effect on heat-induced gelation. Complex moduli G^* reported as a function of temperature ($\gamma_0 = 0.01$, $\omega = 6.28$ rad/s, heating rate = 1°C/min).	168

Figure 6.8. Effect of urea on gelation temperature (T_{gel}) and gel strength (G^* at 90°C).	169
Figure 6.9. Nonisothermal gelation kinetics under various urea concentrations. (a) Plot of $1/G'^2 \times dG'/dt$ vs. $1/T$ and (b) gelation activation energy as a function of urea content	170
Figure 6.10. Urea effect on the thermoreversibility of the gels. (a) Dynamic moduli G' and G'' and (b) $\tan\delta$ during the cooling process ($\gamma_0 = 0.01$, $\omega = 6.28$ rad/s, cooling rate = 1°C/min).	171
Figure 6.11. Dynamic moduli G' and G'' for gels cooled at 15°C, as a function of frequency. Insert: $\tan\delta$ ($\gamma_0 = 0.1$).	172
Figure 6.12. (a) Dynamic moduli G' and G'' as a function of time under various temperatures and urea concentrations. (b) Effects of urea and temperature on gelation time (t_{gel}). Concentration of chitosan = 0.14 M, pH at 25°C = 7 ($\gamma_0 = 0.01$, $\omega = 6.28$ rad/s).	173
Figure 6.13. Calculated relaxation moduli using Doi-Edwards equation (DE) and the relaxation spectra of Figure 6.4 (RS)	174
Figure 7.1. Model junction made up of S chains and ζ structural units bound together [20]	203
Figure 7.2. Chemical structure of the two glycerophosphates used in this study	204
Figure 7.3. Master curves of complex moduli obtained for three different GP concentrations: (a) sample 15-33, (b) sample 15-66, and (c) sample 15-83. Circles represent data obtained at 15°C (5°C for 15-83), triangles at 25°C; and squares at 45°C ($\gamma_0 = 0.1$).	205
Figure 7.4. Master curves of complex moduli obtained for three different chitosan concentrations: (a) sample 10-66, (b) sample 15-66, and (c) sample 20-66. Circles represent data obtained at 15°C, triangles at 25°C; and squares at 45°C ($\gamma_0 = 0.1$).	206

Figure 7.5. Effects of GP (C_{GP}) and chitosan (C_C) concentrations on the flow activation energy (E_{af}).	207
Figure 7.6. Effects of GP (C_{GP}) and chitosan (C_C) concentrations on the complex viscosity ($\eta^*_{0.1\text{rad/s}}$) at $\omega = 0.1\text{rad/s}$ and 25°C	208
Figure 7.7. Effects of (a) β -GP (C_{GP}) and (b) chitosan (C_C) concentrations on the heat-induced gelation process ($\gamma_0 = 0.01$, $\omega = 6.28\text{ rad/s}$). (c) Master curve obtained by shifting the data in (a) using the horizontal shift factor $S_F = T_{gel}(15 - 66) / T_{gel}(\text{sample})$ (from Table 7.2) with T in $^\circ\text{C}$	209
Figure 7.8. Phase diagram for T_{gel} under various β -GP (C_{GP}) and chitosan (C_C) concentrations	210
Figure 7.9. Effects of β -GP (C_{GP}) and chitosan (C_C) concentrations on the gelation activation energy (E_{ag}) in Regions 2 and 3 of Figure 7.7	211
Figure 7.10. Effect of GP type on (a) solution behaviour at 5°C ($\gamma_0 = 0.1$) and (b) heat-induced gelation using samples 5-69 (α) and 5-69 (β) ($\gamma_0 = 0.01$, $\omega = 6.28\text{ rad/s}$).	212
Figure 7.11. Semi-log plot of chitosan gel concentration (C_{gel}) vs. $1/T_{gel}$ for various β -GP (C_{GP}) concentrations.	213
Figure 7.12. Effect of GP concentration (samples 15-33, 15-66 and 15-83) on the calculated ionic strength (I_s) as a function of temperature.	214
Figure 8.1. Effects of cooking time and temperature on the zero shear viscosity (η_0) of the recovered chitosan solutions from the gel state.	218
Figure 8.2. Cooking time effect on the intrinsic viscosity $[\eta]$ of the dialyzed chitosan powders measured in 0.25M AcOH/0.25M AcONa at 25°C	219
Figure 8.3. The relationship between K and a determined under various temperatures and ionic strengths, pH , DDA and molecular weight ranges (data from Kasai, 1999; Chen and Tsaih, 1999).	220
Figure 8.4. Effect of cooking time on MHS constants a and K	221
Figure 8.5. Cooking time effect on the FTIR spectra	221

Figure 8.6. Effect of storage time on the zero shear viscosity (η_0) of sample 5-66 at 5°C	223
Figure 8.7. Effect of ionic strength (I_S) on the complex viscosity at $\omega = 6.28$ rad/s ($\eta^*_{6.28 \text{ rad/s}}$) at 80°C	228
Figure 8.8. The evolution of the complex modulus (G^*) during the gelation process at 80°C ($\gamma_0 = 0.01$ and $\omega = 6.28$ rad/s) under various ionic strength (I_S) ($pH = 4.2 \sim 4.3$ at room temperature)	229

List of Tables

Table 2.1. Published Mark-Houwink constants for chitosan (Kasaai et al., 2000).	15
Table 4.1. Intrinsic viscosity at 25°C.	71
Table 4.2. Overlap concentration (C^*) and entanglement concentration (C_e) as a function of ionic strength (I).	72
Table 4.3. Radius of gyration (R_G) and persistence length (l_p).	73
Table 5.1. pK_a and ΔG at 298.15 K.	116
Table 5.2. Nomenclature and solution compositions expressed in molarity. ...	117
Table 6.1. Nomenclature and solution compositions expressed in molarity. ...	159
Table 7.1. Composition, nomenclature and measured pH at room temperature of chitosan-GP solutions in 1 w/v% AcOH.	198
Table 7.2. Characteristic relaxation times τ_1 and τ_2	199
Table 7.3. Gelation temperature of selected chitosan-GP systems (Figure 7.7).	200
Table 8.1. Effect of cooking time on the molecular weight (\overline{M}_w) and polydispersity (PI) measured with GPC.	218
Table 8.2. Composition, nomenclature and measured pH at room temperature of chitosan-GP solutions in 1 w/v% AcOH.	222
Table 8.3. Physical state of the chitosan systems after 1 month storage at 0°C.	224
Table 8.4. Physical state of the chitosan solutions after 1 month storage at 5°C.	225
Table 8.5 Physical state of the chitosan solutions after 1 month storage at room temperature.	225
Table 8.6. Physical state of the chitosan solutions after 3 months storage at room temperature.	225
Table 8.7. Composition, nomenclature, ionic strength (I_s) and measured pH	

at room temperature of each chitosan solution.	227
Table 8.8. Effect of ionic strength (I_S) on gelation time (t_{gel}) at 80°C.	230

List of Appendices

Appendix I. Conference paper 1 – Rheological properties and gelation of chitosan/ β -glycerophosphate solutions	262
Appendix II. Conference paper 2 – Gelation study of chitosan/ β -glycerophosphate solutions by rheological measurements	274
Appendix III. Conference paper 3 – Concentrations effect on the gelation of chitosan and glycerophosphate	278
Appendix VI. Conference Paper 4 – Rheology of heat-induced gelation f chitosan solutions	281

List of Symbols and Abbreviations

a_T : a temperature shift factor	GP : glycerophosphate
b : Kuhn length	G'_c : the storage modulus at the critical strain γ_c
C : polymer or electrolyte concentration	G' : the storage modulus
C_C : chitosan concentration	G'' : the loss modulus
C_e : the entanglement concentration	G^* : the complex modulus
C_{gel} : the melting gel concentration	$G(t)$: the relaxation modulus
C_{GP} : glycerophosphate concentration	ΔG : the change in Gibbs free energy
c_i : the concentration of ion i	$H(\tau)$: the stress relaxation spectrum
C^* : the overlap concentration	I or I_S : Ionic strength
DDA: Degree of deacetylation	I_D : the ionization degree of a species
DP: the degree of polymerization	K and a : MHS constant
\overline{DP}_n : the number average degree of polymerization	K_a : Dissociation constant
e : the Coulomb electronic charge	k_B : Boltzmann constant
E_c : the cohesion energy	κ_T : the conductivity measured at a given temperature T
E_{af} : the flow activation energy	k_0 : the Arrhenius frequency factor
E_{ag} : the activation energy for gelation	k^{-1} : the Debye screening length
ϵ : the permittivity of water	κ_{25} : the conductivity referenced to 25°C
G_e : the plateau value of G' at high frequencies	k' : the Huggins constant

k'' : the Kraemer constant	S_F : a horizontal shift factor defined as
L : the sample thickness	the ratio of the gelation temperatures
l : the virtual bond length per monomer unit	$T_{gel}(15 - 66) / T_{gel}(sample)$
l_p : the persistence length ($b/2$)	t : time
$l_{p,0}$: the intrinsic persistence length ($l_{p,0}$)	t_{gel} : gelation time
$l_{p,e}$: the electrostatic persistence length	t_I : a characteristic time
M : the molecular weight of polymer	T : temperature
\overline{M}_n : Number-average molecular weight	T_{gel} : Gelation temperature
\overline{M}_v : Viscosity-average molecular weight	V_e : elution volume, V_e :
\overline{M}_w : Weight-average molecular weight	Z_i : the charge number of ion i
N : the polymer junction zone structure	η : viscosity
$(S \times \zeta)$	χ : the extent of neutralization ($1 - I_D$)
N_{Av} the Avogadro number	η : viscosity
N_i : the equivalent concentration (or normality) of ions i	η_e : the entanglement viscosity
PI: Polydispersity ($\overline{M}_w / \overline{M}_n$)	η_{red} : reduced viscosity
R : the ideal gas constant	η_s : the solvent viscosity
$\langle R_G \rangle$: the radius of gyration	η_{sp} specific viscosity
S : the junction multiplicity	η_0 : the zero shear viscosity
	$[\eta]$: the intrinsic viscosity
	η^* : the complex viscosity
	Φ : a universal constant ($2.1 \times 10^{23} \text{ mol}^{-1}$)

$\dot{\gamma}$: the steady shear rate	τ_R : relaxation time at the crossover point
γ_c : the critical strain at which a polymeric system begins to show non-linear viscoelastic behavior (in this case gel break-up)	of G' and G'' ($1/\omega^*$)
λ_i : the equivalent conductance of ions i	τ : the relaxation time
λ_i° : the equivalent conductance at infinite dilution	τ_m or τ_H : the mean relaxation time
μ , P and ν : power-law indexes	ω : frequency
	ζ : the junction zone lengths

Chapter 1

Introduction and objectives

1.1. Introduction

In the seafood processing industry, large quantities of crustaceans have been accumulated because of their lower degradation rate in nature so that their disposal has been a main concern. The discarded crustaceans can be used to produce chitin, the most abundant organic material after cellulose, by series of chemical treatments. Applications for chitin are limited due to its poor solubility. However, it becomes soluble in aqueous acid solutions after deacetylation in an alkaline environment that results in the product called chitosan. Chitin and chitosan are linearly binary heteropolysaccharides composed of 2-amino-2-deoxy-D-glucopyranose (glucosamine) and 2-acetamido-2-deoxy-D-glucopyranose (acetylglucosamine) units, and the two biopolymers are mainly distinguished from each other by their solubility in aqueous acidic solutions (Roberts, 1992). One important parameter of the molecular structure of these materials is degree of deacetylation (DDA), or number percentage of glucosamine in the chitosan molecule. The copolymer is generally accepted as chitosan when the DDA is larger than 50% (Burgnerotto et al., 2001a).

The increased solubility of chitosan with respect to that of chitin is related to its positively charged polyelectrolyte nature, due to the protonation of the free amine groups below a *pH* of 6.2 (Park et al., 1983). Positively charged chitosan has been attracting a great deal of attention because of its various bioactivities such as antifungal, antitumor, antiallergic and immune activating characters (Kasaai et al., 1999). In

addition, chitosan is a non-toxic, biocompatible and biodegradable material. It has been used in nutraceutical, medical, cosmetic and pharmaceutical industries, and numerous international patents have claimed the applications of chitosan in these areas (Kasaai, 1999; Kumar, 2001; Singla and Chawla, 2001)

These characteristics and related potential applications have driven many studies on chitosan. Several have been focusing on the investigation of the physical properties of dilute solutions (Anthonsen *et al.*, 1993; Chen and Tsaih, 2000; Tsaih and Chen, 1997, Wetton *et al.*, 1991), looking at the effect of *pH*, ionic strength, DDA and molecular weight on the conformation of the chitosan molecule. Other studies have dealt with the rheological properties of concentrated chitosan solutions (Desbrières, 2002; Mucha, 1997; Nystrom *et al.*, 1999; Wang and Xu, 1994). While the effect of ionic force on these solutions has been investigated through *pH* changes (Nystrom *et al.*, 1999), no studies have looked at the effect of ionic force by added salt at constant *pH* for concentrated solutions. Since *pH* controls the ionization of the chitosan molecule, it is interesting to isolate the effect of the solution ionic strength on a constant polymer charge density.

Chitosan can be studied under various physical states depending upon polymer concentration, *pH*, ionic strength and temperature. For *pH* below its *pKa* (*pH* < 6.7) (Roberts, 1992), chitosan is water-soluble and positively charged following the protonation of the free amine groups ($-NH_2$), causing electrostatic repulsion between the molecules. Adding salt, corresponding to increasing ionic strength, in chitosan solution screens the electrostatic repulsion, eventually providing a favorable environment to form

macromolecular interactions via hydrophobic ($-\text{CH}_3$) and hydrogen bonding favoring groups ($-\text{OH}$, $-\text{NH}$, and $-\text{C}=\text{O}$) in chitosan molecule (Roberts, 1992). Chitosan gels can be obtained by increasing polymer concentration (concentration-induced gelation) below a pH of 6.2 (Iverson *et al.*, 1997) or by control of the pH (Jackson, 1987). The addition of a base will obviously increase the pH but can also reduce the electrostatic repulsion between chitosan molecules and eventually lead to the formation of a gel-like structure above a pH of 6.2. Recently, a homogenous thermoreversible gel system was prepared by neutralizing highly deacetylated semi-dilute chitosan solutions with a weak base, β -glycerophosphate (β -GP) (Chenite *et al.*, 2001). The system remained in solution at physiological pH ($= 7.2$) and room temperature, but changed into a gel upon heating at physiological temperature, 37°C (heat-induced gelation). When the temperature decreased, the chitosan gel returned to the solution state under particular conditions.

The gelation of the chitosan- β -GP system may involve several interactions such as screening of electrostatic repulsion, “ionic” cross-linking, hydrophobic and hydrogen bonding interactions. β -glycerophosphate, a weak base ($\text{pK}_{\text{a},2} = 6.65$ at 25°C) (Alberty, 1983; Goldberg *et al.*, 2002) can increase the pH of chitosan solutions around neutrality. It is negatively charged in solution, and thus may screen the electrostatic repulsion between chitosan molecules in its monovalent form or induce ionic bridging in its divalent one. Since chitosan presents hydrophobic and hydrogen bonding favoring groups (Roberts, 1992), three-dimensional networks can also form by hydrogen bonding and/or hydrophobic interactions. Even though several possible interactions have been

proposed to explain the gelation of the chitosan- β -GP system (Chenite et al., 2001; Wang, 1999), the exact mechanisms have not been established.

Studying the effect of temperature may however help understanding which interactions predominate. For example, the ionization of chemical species in solution is very sensitive to temperature and the change in ionization will affect the ionic strength and consequently electrostatic repulsion between chitosan molecules. It will also play a role on the multivalent ionization of β -GP, and therefore on possible ionic bridging. In addition, temperature is related to the intensity of hydrogen bonding and hydrophobic interactions. By controlling the intensities of hydrogen bonding and hydrophobic interactions, we may understand which interactions are more dominant during gelation process. Furthermore, some additives can easily control the intensities of the interactions in solution. Urea is generally known as a hydrogen bonding disrupting agent (Hammes and Schimmel, 1967; Kim et al., 1996; Kjonisken et al., 2003; Kokufuta et al., 1998; McGrane et al., 2004), but it can also affect hydrophobic interactions (Philippova et al., 2001). The presence of urea on chitosan- β -GP solutions upon temperature increase can consequently reduce furthermore hydrogen bonds and decrease hydrophobic interactions. Finally, chitosan and β -GP concentrations are directly related to the number of polymer junction zones such as hydrophobic, hydrogen bonding and ionic strength. Thus, we may fully understand the gelation mechanisms by performing gelation tests under chitosan, β -GP, and urea concentrations as functions of temperature.

1.2. Objectives

Chenite *et al.* (Chenite *et al.*, 2001) have produced the new thermoreversible homogeneous chitosan- β -GP gel system applicable as an injectable *in-situ* hydrogel. The system can be loaded with some therapeutic materials (drug, protein, cells...) in the liquid state and then injected into the body to form gel implants *in-situ* (Wang, 1999). However, the formation and nature of the gel produced has not been fully investigated. A broader analysis may expand the applications of physical chitosan gels system. Thus, the initial motive of this work is to improve our understanding of the gelation mechanisms of the heat-induced chitosan- β -GP system in order to help the development of other products by providing knowledge of gel formation.

In order to reach the goal of this work, we will characterize chitosan solutions from dilute to concentrated (or entangled) regime in the sol state and during the gelation process, using rheological and physicochemical measurements under various conditions. The goal will be approached by using the four steps below:

- 1) To establish the effect of chitosan concentration and ionic force at constant pH on the physicochemical properties and dynamics of entangled chitosan solutions. The results will be analyzed in the light of simple rheological models and compared to theoretical scaling law predictions. This work will help to understand the effect of ionic strength at constant pH on the linear and non-linear rheological properties of chitosan solutions in the concentrated regimes. In addition, this study may provide the fundamental idea about the chitosan sol behavior in the concentrated regime.

- 2) To gain insight into the gelation mechanisms of chitosan in the presence of acetic acid and β -glycerophosphate. Rheological measurements and theoretical calculations will be used to propose a heat-induced gelation mechanism. These calculations combined with rheological tests can be used as powerful and simple methods to explore gelation behavior. Additionally, this calculate may provide a clue about the presence of ionic bridging between chitosan and glycerophosphate molecules and the main driving interactions to from gel structure.
- 3) To expand our understanding of the function of hydrogen bonding and hydrophobic interactions in the sol and gel states by characterizing the rheological and physicochemical of the chitosan- β -GP system in terms of temperature in the presence of urea. This study will help us to understand the hydrogen bonding and hydrophobic interactions in terms of temperature during the gelation processes.
- 4) To establish the sol-gel phase diagram for the heat-induced gelation. The gel temperature determined under various conditions will used to explain the structure of the physical junction zone at the gelation point by using the modified Eldridge-Ferry method. Additionally, effect of GP type will be investigated on the gelation process to verify the possible ionic bridging between chitosan and GP during the gelation. .

Chapter 2

Literature review

In this chapter, the general view of chitosan will be introduced. Applications of chitosan will be briefly presented in the section 2.1. In the following section 2.2, it will be described the precise methods to extract chitosan from the crustaceans discarded from seafood processing industry and to characterize and modify its molecular weight and degree of deacetylation (DDA). The solubilization of chitosans will be mentioned in the section 2.3. Chitosan solution behavior in dilute and concentrated regimes will be explained under various *pH*, ionic strength, molecular weight and DDA and temperature in the sections 2.4 and 2.5, respectively. Finally the general review related to gel systems will be introduced in the section 2.6.

2. 1. Applications of chitosan

Chitosan has cationic nature, biocompatibility, biodegradability and various bioactivities such as antifungal antitumor, antiallergic, and immune activating characters (Kasaai, 1999; Kumar, 2000). In addition, chitosan is very safe and non-toxic. It has been used in many areas such as food, medical, cosmetic and pharmaceutical industries (Imeri and Knorr, 1998; Kasaai, 1999; Kumar 2000; Singla and Chawla, 2001) and numerous international patents have claimed the applications of chitosan in these areas (Chaput and Chenite, 2001; Chenite et al., 2001; Mukherjee, 2001; Soto-Perlata et al., 1988).

In medical industry, gel-like structures with chitosan can be formed to apply for the preparation of controlled drug release formulations by several methods (Berth and Dauzenberg, 2002; Chenite et al., 2001, Jackson, 1987; Imeri and Knorr, 1998). Chitosan derivatives are used as antibacterial agents, blood anticoagulants, and anti-thrombogenic and haemostatic materials. Chitosan can form water-absorbent and biocompatible films, which can be used as wound dressing products. N-carboxylbutyl chitosan is effective in repairing wound tissue because of the similarity of its molecular

and biological characteristics to glycosaminoglycans (heparin) so that it can be used as skin replacement (Yong and Lovell, 1999). Kasaai mentioned that the antimicrobial and wound healing properties along with excellent film capability make chitosan suitable for the development of ocular bandage lenses and has been applied for the treatment of dermatitis, fungal infections and used in contact lenses (Kasaai, 1999).

Chitosan is approved as a food additive by the FDA since 1983 (Knorr, 1985). Chitosan is used as a food additive in some countries. In Japan, dietary cookies, potato chips, noodles enriched chitosan have been produced because of its hypocholesterolemic effect. The vinegar products containing chitinous materials have been manufactured due to cholesterol lowering ability (Hirano, 1989). Chitosan is also used as a fat trapper in stomach. Chitosan by itself is considered as a digestive fiber. Chitosan salt, which has a strong positive charge, is used to control acidity in fruit juices (Chen and Li, 1996). Chitosan is a clarifying agent for grapefruit juice (Roberts, 1995) and a highly effective fining agent for apple juice.

Finally, chitosan can be used to produce cosmetics due to its antifungal properties when dissolved in acidic solution (Soto-Perlata et al., 1988). For example, high DDA chitosan has a better antifungal activity than low DDA chitosan because of its high solubility due to the protonation of the amine groups on the molecular chain at pH 6.0. One possible mechanism of antifungal activity is explained in that interactions between protonated amine groups and negatively charged microbial cell membranes inhibit the growth of microorganisms. It is used to fabricate creams, lotions, and permanent waving lotions (Imeri and Knorr, 1998).

2.2. Physicochemistry of chitosan

2.2.1. Preparation of chitosan

Figure 2.1 shows the scheme of chitosan preparation. In general, chitin is commercially extracted from various crustaceans such as crab, shrimp, lobster, squid, oyster etc., from which residues are closely associated with impurities such as proteins, inorganic materials (mainly CaCO_3), pigments and lipids (Roberts, 1992). The

impurities can be removed by several chemical treatments: 1) demineralization, frequently performed in dilute HCl aqueous solution, 2) deproteination in dilute NaOH solution and 3) decolorization in 0.5% KMnO_4 and oxalic acid solutions. Chitin is generally obtained after these chemical treatments; however, its applications are limited due to low solubility. Solubility can be increased by the modification of the chemical structure through deacetylation, usually performed in 0.5M NaOH solution at high temperature. In general, the DDA and molecular weight values of chitosan obtained are dependent on production conditions (salt concentration, treatment temperature and processing steps) and natural resources (age, species, and environmental conditions).

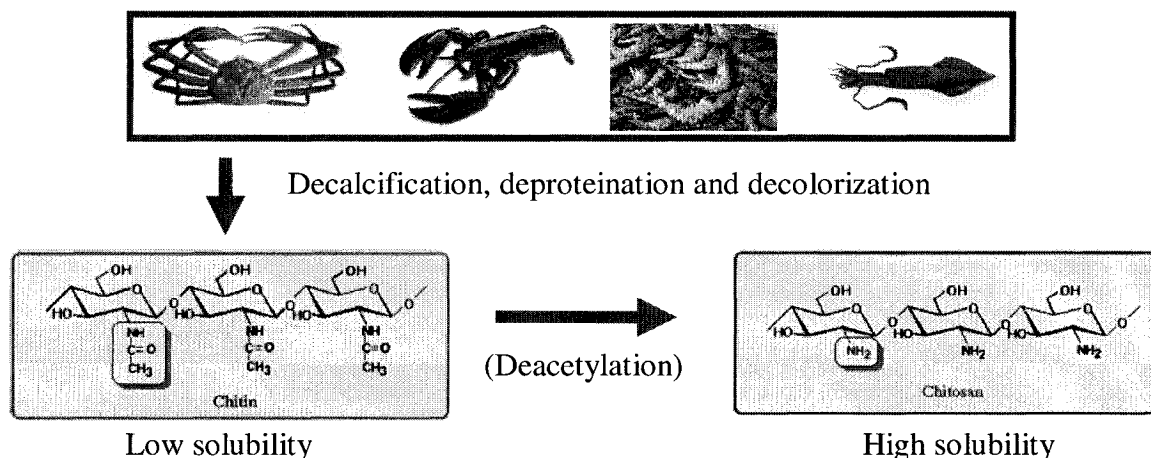


Figure 2.1. The scheme of chitosan preparation of chitosan (Roberts, 1992).

2.2.2. Determination of degree of deacetylation

There are several methods available to determine the degree of deacetylation (DDA) of chitosan. The methods used are element analysis (EA), infrared spectroscopy, near infrared spectroscopy, titration, NMR spectroscopy, UV absorbance spectroscopy, circular dichroism, equilibrium dye absorption, periodate oxidation, pyrolysis-mass spectroscopy, thermal analysis and enzymatic degradation, acid degradation followed by

analysis of the monomeric sugar units by high performance liquid chromatography, or colorimetric assays (Knaul, 1998; Kasaai, 1999).

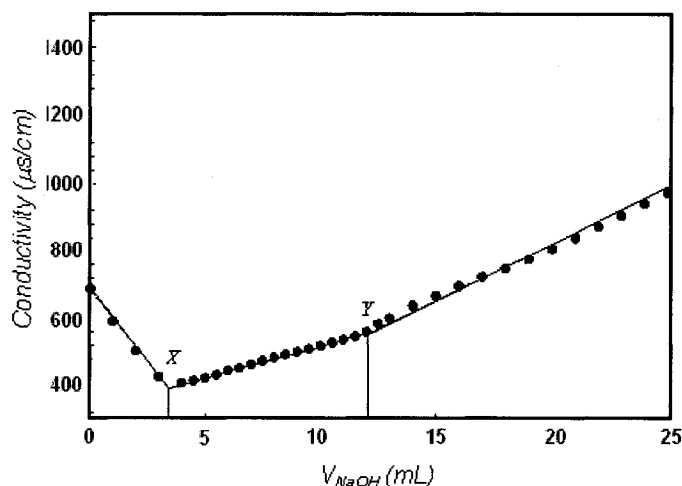


Figure 2.2. Titration curve of chitosan dissolved in excess HCl (0.138N) and then titrated with NaOH (0.1018N) (Wang, 1999).

Among many methods, the conductimetric titration method is easier and economical and also extensively used to determine DDA (Knaul, 1998; Raymond et al., 1993; Wang, 1999). In the process, chitosan is completely dissolved in excess HCl aqueous solution and then titrated with NaOH aqueous solution. The conductivity is measured in terms of the amount of the NaOH solution added as shown in Figure 2.2. In the figure, there are two inflections points (X and Y): the first inflection point (X) corresponds to the neutralization of the excess acid and the second one (Y) is related to the complete precipitation of chitosan sample. The volume difference between the two points is used to calculate the amount of free amine groups present in the sample. The mole number of chitosan ($C_{m, \text{chito}}$) and chitin ($C_{m, \text{chitin}}$) can be determined by Equation 2.1 and Equation 2.2, respectively.

$$C_{m, \text{Chito}} (\text{M}) = (Y - X) f / 1000 = \Delta n_{\text{NaOH}} \quad (2.1)$$

$$C_{m, \text{chitin}}(\text{M}) = \left[m - \frac{161(Y - X)f}{1000} \right] / 203 \quad (2.2)$$

where f is the molarity of the NaOH solution, m the amount of chitosan (g), 161 the molecular weight of chitin (acetylglucosamine) monomer and 203 the molecular weight of chitosan (glucosamine) unit. X and Y are equivalent volumes of NaOH solutions at each inflection point and Δn_{NaOH} is the mole number of NaOH. Thus, the DDA can be determined as follows:

$$\text{DDA}(\%) = \frac{C_{m, \text{chito}}}{C_{m, \text{chito}} + C_{m, \text{Chitin}}} \times 100 = \frac{203 \Delta n_{\text{NaOH}}}{m + 42 \Delta n_{\text{NaOH}}} \times 100 \quad (2.3)$$

With this method, DDA can be measured within the range of error $\pm 1\%$ if the titration process is carefully performed and given enough time to reach equilibrium (Knaul, 1998).

Elemental analysis (EA) is carried out by comparing the ratio of carbon to nitrogen in chitosan or chitin samples (Park et al., 1983). Lower DDA chitosan has more carbons due to the presence of more acetyl groups in the polymer molecule. This technique is very advantageous in that it is performed rapidly using automated elemental analyzers and requires only a few milligrams of the sample. However, the samples should be completely dried to remove the moisture content, which prevents the exact determination of their DDA. It is determined with the following equation:

$$\text{DDA}(\%) = 100 \left(1 - \frac{n_a}{n_n} \right) = 100 \left(\frac{0.5(n_c - 6n_n)}{n_n} \right) \quad (2.4)$$

where n_a , n_n and n_c are the moles of acetyl groups, nitrogen and carbon in the chitosan sample, respectively.

The use of UV absorbance spectroscopy involves making a calibration curve from absorbance data as a function of the content of acetylglucosamine, absorbing UV around 200 nm (Knaul, 1998). The calibration curve shows the relationship between amide absorbance and acetylglucosamine concentration (mg/100mL). It is very useful to determine the unknown DDA of a chitosan sample. The determination of DDA is calculated as follows:

$$DDA(\%) = 100 \left(1 - \frac{203(W_t - W_{ag})}{203W_t - W_{ag}(203 - 161)} \right) \quad (2.5)$$

where 203 is the molecular weight of acetylglucosamine monomer; 161 the molecular weight of glucosamine; W_t and W_{ag} the total weight (mg) of the chitosan sample and the total weight of the acetylglucosamine monomer in 100mL of 1% acetic acid. W_{ag} can be determined from the calibration curve.

2.2.3. Determination of molecular weight

Molecular weight of chitosan can be characterized with intrinsic viscosity measurement, light scattering (LS) and size exclusion chromatography (SEC).

The measurement of intrinsic viscosity is performed using dilute chitosan solutions, in which there is no interaction between individual macromolecules. This is a very useful tool to determine the molecular weight and hydrodynamic volume of a chitosan molecule in a given solvent. It is performed by measuring relative viscosity as a function of concentration. The relative viscosity (η_r) is the ratio of the times required for a given volume of fluid to flow through a bulb of a viscometer. The specific viscosity (η_{sp}) is given by Equation 2.6 (Carreau et al., 1997):

$$\eta_{sp} = \frac{\eta - \eta_s}{\eta_s} = \eta_r - 1 = \frac{t\rho_s}{t_s\rho} - 1 \approx \frac{t}{t_s} - 1 \quad (2.6)$$

where the subscript s symbolizes solvent; t flow time; and ρ density. The density of a very dilute solution is approximately similar to that of the solvent ($\rho = \rho_s$). As shown in Figure 2.3 for a chitosan sample, the intrinsic viscosity $[\eta]$ is determined by extrapolating η_{sp}/c or $\ln \eta_r/c$ to zero concentration (Carreau et al., 1997).

The relationship between the intrinsic viscosity and the molecular weight is expressed by the Mark-Houwink-Sakurada (MHS) equation as follows:

$$[\eta] = K \overline{M}_v^a \quad (2.7)$$

where K and a are empirical constants and \overline{M}_v is the viscosity average molecular weight. In general, the weight-average molecular weight \overline{M}_w is used instead of \overline{M}_v .

since \overline{M}_v is not experimentally accessible. The coefficients a and K measured with chitosan solutions are mainly dependent on solvent, temperature and DDA of chitosan as shown in Table 2.1 (Kasaai et al., 2000). Thus, the molecular weight of chitosan can be predicted by measuring $[\eta]$ if suitable K and a values are found from the literature.

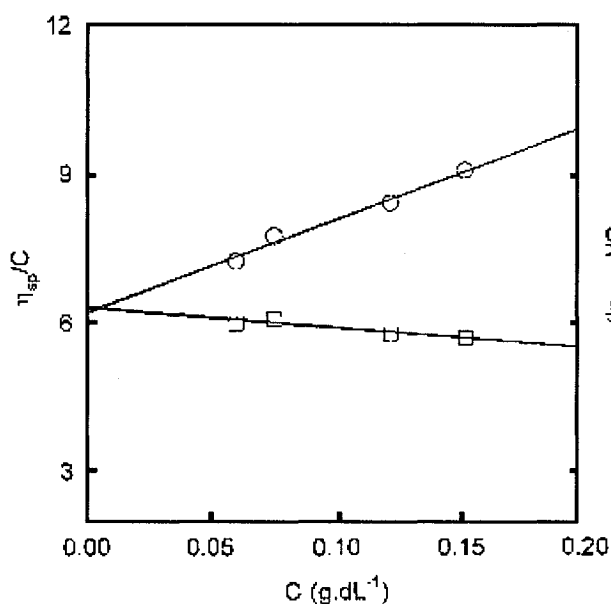


Figure 2.3. A typical plot of η_{sp}/c (circle) and $\ln \eta_{rel}/c$ (square) as a function of chitosan concentration for the determination of intrinsic viscosity $[\eta]$. (\overline{M}_w : 715 kDa) (Kasaai, 1999)

Size exclusion chromatography (SEC) is a column fractionation method in which solvated polymer molecules are separated according to their sizes. The technique is also known as gel permeation chromatography (GPC). The separation occurs as the solute molecules in a flowing liquid move through stationary bed of porous particles. Solute molecules of a given size are sterically excluded from some of the pores of the column packing, which itself has a distribution of pore sizes. Larger solute molecules can permeate a smaller proportion of the pores and thus elute from the column earlier than smaller molecules (Pa and Yu, 2001).

SEC is used to determine average molecular weight (\overline{M}_n , \overline{M}_w , and \overline{M}_z) and polydispersity ($\overline{M}_w/\overline{M}_n$). It is not a primary method as usually practiced, but it requires calibration in order to convert raw experiment data into molecular weight distribution.

For calibration of SEC columns, first of all, a series of commercially available polymers such as anionically polymerized polystyrene, pullulan, or dextran are particularly well suited. These polymers are available with a range of molecular weights and have relatively narrow molecular weight distribution. The chromatograms are obtained with a series of known molecular weight of standard sample. The intrinsic viscosity and GPC chromatograms can be used to construct a universal calibration curve of the hydrodynamic volume of the polymer as a function of the elution volume, V_e :

$$[\eta]M = f(V_e) \quad (2.8)$$

The conversion of a calibration curve for one polymer to that for another polymer can be established directly if the MHS equations are known for both species in the GPC solvent. From Equation 2.8, one can write

$$[\eta]_1 M_1 = [\eta]_2 M_2 = f(V_e) \quad (2.9)$$

where the subscript refers to the polymer type. Thus, at equal elution volumes, the molecular weight of polymer 2, which appears at the same elution volume as polymer 1 with molecular weight M_1 , is given by

$$\ln M_2 = \frac{1+a_1}{1+a_2} \ln M_1 + \frac{1}{1+a_2} \ln \left(\frac{K_1}{K_2} \right) \quad (2.10)$$

For 83% DDA chitosan solutions, the relationship between molecular weight (\overline{M}_w) and average elution volume (V_e) was as follows (Tsaih and Chen, 1999):

$$\text{Log}(\overline{M}_w) = -0.483V_e + 11.660 \quad (2.11)$$

In addition, the MHS constants K and a of 83% DDA chitosan solutions were greatly dependent on ionic strength. For example, a value decreased from 0.715 to 0.521 when ionic strength increased from 0.01 M to 0.30. In the same range of ionic strength, K increased from 5.48×10^{-4} to 2.04×10^{-3} . Chitosan behaves like a polyelectrolyte in aqueous solution. In other words, it is expanded due to electrostatic repulsion force exerted from protonated amine group in chitosan molecule. Thus, it is necessary to

choose the appropriate solvent system to eliminate ionic effect effects in order to measure correctly intrinsic viscosity and molecular weight (Yomota et al., 1993).

Table 2.1. Published Mark-Houwink constants for chitosan (Kasaai et al., 2000).

Solvent	\overline{M}_w (kDa)	DDA (%)	T (°C)	$K \times 10^5$ (dL/g)	a
0.02M AcOH/0.02M AcONa/0.1M NaCl	15-310	100	20	559	0.58
0.02M AcOH/0.02M AcONa/0.1M NaCl	35-245	85	20	58.5	0.78
0.5M AcOH/0.5M AcONa	115-1590	70.5	25	199	0.76
0.3M AcOH/0.2M AcONa	100-600	98	25	82	0.76
0.3M AcOH/0.2M AcONa	100-600	89.5	25	76	0.76
0.3M AcOH/0.2M AcONa	100-600	79	25	74	0.78
0.25M AcOH/0.25M AcONa	35-2220	74-79	25	15.7	0.79
0.2M AcOH/0.1M AcONa	194-937	100	30	16.8	0.81
2% AcOH/0.2M AcONa	61-150	82-88	25	13.8	0.85
0.2M AcOH/0.1M AcONa	211-1260	91	30	6.59	0.88
0.1M AcOH/0.2M NaCl	48-630	~80	25	1.81	0.93
0.2M AcOH/0.1M AcONa	536-1850	84	30	1.42	0.96
0.33 AcOH/0.3M NaCl	13-193	78-80	21	3.41	1.02
0.02M AcOH/0.02M AcONa/0.1M NaCl	15-164	40	20	2.18	1.06
0.2M AcOH/0.02M NaCl	477-2510	69	30	0.104	1.12
0.2M AcOH/0.1M NaCl/4M urea	163-492	91	20	89.3	0.71
1% AcOH	205-657		30	4.74	0.72

Recently, Brugnerotto et al. (Brugnerotto et al., 2001b) determined molecular weight by combining SEC and a multi angle laser light scattering detector without universal calibration procedure. The light scattering detector allows directly determination of the molar mass distribution and that of the dependence of the radius of gyration as a function of molecular weight in the solvent and conditions used. The authors successively determined the molecular weight of chitosan with different degrees of deacetylation (40 – 100%).

2.2.4. Modification of degree of deacetylation and depolymerization

Degree of deacetylation (DDA) and molecular weight of chitosan greatly influence the properties of solution, enzymatic degradability and biological activity (Yong and Lovell, 1991). Chitosan of molecular weight $10^3 \sim 10^5$ g/mol is used for medical and biological applications (Muzzarelli et al., 1994) and chitosan of $10^5 \sim 5 \times 10^5$ g/mol in cosmetic industry (Wachter and Stenberg, 1996). Solubility of chitosan is sensitive to its DDA and molecular weight. In general, solubility decreases with increasing molecular weight and decreasing DDA. In addition, DDA is directly related to the physical, chemical and biological properties (Anthonsen, et al., 1993; Kasaai, 1999; Wang, 1999) as well as chemical reaction and interactions with bifunctional compounds for gel formation. The alteration of DDA and molecular weight of chitosan without chemical structure modification is of great importance for certain applications and several modification methods will be presented in the following section.

DDA can be altered with deacetylation and/or reacetylation (Rinaudo *et al.*, 1999). In general, deacetylation process is performed in highly alkaline solution; however, the standard condition for the deacetylation has not been established yet. The deacetylation process is generally carried out in strong base, *i.e.* sodium hydroxide at elevated temperature. A study showed that during the deacetylation process, the increase in DDA occurred within 30 min and then the DDA was almost constant regardless of treatment time (Knaul, 1998). Thus, the desirable DDA of chitosan can be produced by several repeated deacetylation processes. Reacetylation can be done by adding different concentrations of acetic anhydride in the dissolved chitosan solution mixed with methanol. The use of different acetic anhydride concentration produces different DDA chitosans. To collect treated chitosan molecules, alkaline solutions such as NaOH or NH_4OH should be slowly added to precipitate chitosan molecules. The precipitants are washed with distilled water several times in order to remove some organic solvents in chitosan and dries in a convection oven at 50°C or in a freezing dryer.

The modification of molecular weight of chitosan is generally called as “depolymerization.” The depolymerization is performed with chemical reactions,

hydrolysis with diluted HCl solution and oxidation reaction with H₂O₂ and NaNO₂, physical treatments (ultrasound-induced fragmentation, microfluidization process and the use of intense femtosecond laser pulse), and the biological degradation with various enzymes. The precise processes and mechanisms about depolymerization are explained by Kasaai (Kasaai, 1999). In the fragmentation by chemical reactions (acid hydrolysis and oxidation), the degree of depolymerization is proportional to the concentration of chemical reagents, corresponding to the number of chain scission. Most of fragmentation occurs within 5 h with HCl hydrolysis, 24 h with H₂O₂ oxidation and 4 h with NaNO₂ oxidation. Oxidative fragmentation is more advantageous in that the process is performed at room temperature compared to the hydrolytic fragmentation carried out at 65°C. DDA is slightly increased after the hydrolytic and oxidative fragmentation processes. In physical fragmentation processes, the degree of depolymerization is mainly dependent on the power of ultrasound or laser pulse source and treatment time. The use of intense femtosecond laser pulse has a tendency to increase polydispersity ($\overline{M}_w/\overline{M}_n$) after fragmentation. The physical fragmentation is more favorable than chemical fragmentation in that no chemical reagent is needed to do fragmentation. Finally, the depolymerization with enzymes depends on the ratio of enzyme/chitosan concentration and treatment time.

2.3. Solubilization of chitosan

In general, solubility is strongly dependent on temperature since pK_a is a function of temperature. The effect of temperature on pK_a can be expressed by the following simple equation (Alberty and Silby, 1996):

$$\Delta G = -RT \ln K_a = 2.303RTpK_a = \text{const} \rightarrow pK_a(T) = \frac{\Delta G}{2.303RT} \quad (2.12)$$

where ΔG represents the change in Gibbs free energy; R is the ideal gas constant; and T is the absolute temperature. Thus, if the pK_a value and ΔG for a material are known at a certain temperature, we can calculate the pK_a of the material at another temperature.

Goldberg et al. (Lide, 2003/2004) proposed the compensation of temperature effect on pK_a value as follows:

$$pK_{a,T} = -(R \ln 10)^{-1} \left[- \left\{ \ln(10) \frac{RT pK_{a,\theta}}{\theta} \right\} + \Delta_r H_{\theta}^{\circ} \left\{ \left(\frac{1}{\theta} \right) - \left(\frac{1}{T} \right) \right\} + \Delta_r C_{p,\theta}^{\circ} \left\{ \left(\frac{\theta}{T} \right) - 1 + \ln \left(\frac{T}{\theta} \right) \right\} \right] \quad (2.13)$$

where R is the ideal gas constant; the subscripts T and θ denote the temperature to which a quantity pertains; the subscript P a constant pressure; and the subscript r the quantity to refer to a reaction. $pK_{a,\theta}$ is the pK_a value at the standard temperature θ (298.15 K), $\Delta_r H_{\theta}^{\circ}$ the enthalpy and $\Delta_r C_{p,\theta}^{\circ}$ the heat-capacity change at 298.15 K, $I = 0$ and $P = 0.1$ M Pa. The $pK_{a,\theta}$, $\Delta_r H_{\theta}^{\circ}$ and $\Delta_r C_{p,\theta}^{\circ}$ can be found in the literature (Goldberg *et al.*, 2002). Equation 2.16 can be used only between 274 and 350K and $I = 0$. To determine the effect of ionic strength on pK_a , the ionization reaction of a chemical should be known,



The thermodynamic equilibrium constant can be expressed as follows:

$$K_a = \frac{\alpha\{H^+(aq)\} \cdot \alpha\{A^-(aq)\}}{\alpha\{HA(aq)\}} \quad (2.15)$$

The above equilibrium constant has been defined in terms of activity α . The activity α is the multiplication of the molarities m and activity coefficients (molarity basis) γ_m of the solute species. Thus, Equation 2.15 can be rewritten as follows (Goldberg et al., 2002):

$$K_a = \frac{m\{H^+(aq)\} \cdot m\{A^-(aq)\}}{m\{HA(aq)\}} \cdot \frac{\gamma_m\{H^+(aq)\} \cdot \gamma_m\{A^-(aq)\}}{\gamma_m\{HA(aq)\}} \quad (2.16)$$

Using the Debye-Hückel equation 2.17 (Goldberg et al., 2002) or Davis equation 2.18, we can take into account effect of ionic strength on K_a :

$$\ln \gamma_i = \frac{-A_m Z_i^2 \sqrt{I}}{1 + B \sqrt{I}} \quad (2.17)$$

$$\ln \gamma_i = -A_m Z_i^2 \cdot \left\{ \left(\frac{\sqrt{I}}{1 + \sqrt{I}} \right) + 0.3I \right\} \quad (2.18)$$

where A_m is the Debye-Hückel constant, Z_i the charge number of the species; B an empirical constant. A_m and B are temperature-dependent. This extended Debye-Hückel (EDH) equation is valid only for dilute solutions ($\leq 5000\text{mg/L}$), while Davis equation is best at higher ionic strength up to $I = 0.5 \text{ M}$ (Morel and Hering, 1993).

The chemical structure of chitosan is shown in Figure 2.1. Chitosan can be dissolved in acidic medium. The chemical reaction for the protonation of chitosan is expressed as follows (Rinaudo *et al*, 1999):



where RNH_2 represent glucosamine monomers in the chitosan chain. The dissociation constant of the conjugate acid (Jones, 1999; Roberts, 1992) is obtained from the equilibrium:

$$K_a = \frac{[\text{RNH}_2][\text{H}_3\text{O}^+]}{[\text{RNH}_3^+]}; pK_a = -\log K_a \quad (2.20)$$

Equation 2.20 can be expressed as the form of Henderson-Hasselbalch equation (Alberty and Silbey, 1996):

$$pH = pK_a + \log \frac{[\text{RNH}_2]}{[\text{RNH}_3^+]} \quad (2.21)$$

If the pH and pK_a are known, we can estimate the protonation of chitosan as follows:

$$I_D = \frac{\text{Pronated amine number}}{\text{Total amine number in chitosan}} = \frac{1}{10^{pH-pK_a} + 1} \quad (2.22)$$

The pK_a of chitosan depends on the charge density of the polymer and hence depend on the extent of neutralization ($\chi = 1 - I_D$) of the charged groups and on its degree of deacetylation (DDA) having the same fraction of the $-\text{NH}_3^+$ groups neutralized (Roberts, 1992). Several studies have reported pK_a for chitosans. Without taking account into consideration of the effect of chain charge density, Doczi (Doczi, 1957) reported $pK_a \sim 6.2$; Noguchi *et al.* (Noguchi *et al.*, 1969) a pK_a of 6.3; and Muzzarelli *et al.* (Muzzarelli *et al.*, 1980) a pK_a of 6.8. Park *et al.* (Park *et al.*, 1983) firstly considered the charge density of chitosan chain and the measured pK_a values were dependent on the extent of neutralization (α). pK_a value was 6.2 when χ was smaller than 0.72, but 6.7 at $\chi > 0.72$.

Domard (Domard, 1987) investigated the effect of DDA and the extent of neutralization on the pK_a of chitosans in 0.1M $HClO_4$ aqueous solution. The pK_a value of chitosans having above 80% DDA rapidly increased with increasing χ from 0 to 0.5; however, the pK_a was almost constant when χ is larger than 0.5. In addition, the pK_a unchanged regardless of DDA and the magnitude of χ for chitosan having below DDA 80%. When $\chi = 1$, the obtained pK_a value (~ 6.5) was independent of DDA.

The solubility of chitosan is dependent on the type of acid used. According to Rinaudo *et al.* (Rinaudo *et al.*, 1993 and 1999), the solubilization of chitosan occurs in the range of a neutralization degree $\alpha \approx 0.5$ when the HCl concentration is nearly equal to that of the NH_2 group. The complete solubilization of chitosan in acetic acid is established at $\alpha \geq 0.5$ and a stoichiometric ratio $[acetic\ acid]/[-NH_2] = 0.6$. In addition, chitosan is dissolved in acidic solution at pH lower than 6.2 and it is completely soluble at pH 4.5. Chitosan is soluble in dilute HCl, HBr, HI, HNO_3 , but may be precipitated out of solution in HCl or HBr by increasing the concentration of acid in the system (Roberts, 1992) due to the screening effect of ionized Cl^- and Br^- . The solubility of chitosan is very sensitive to DDA and molecular weight. In general, higher DDA chitosan is more easily dissolved due to the protonation of amine groups. However, lower DDA chitosan is hard to dissolve in water-based solutions due to the hydrogen bonds mainly formed by the 2-acetyl group in the acetylglucosamine monomer (Wang, 1999). Lower DDA chitosan was dissolved in N,N-dimethylacetamide containing LiCl (DMAc/LiCl) and N-methyl-2-pyrrolidinone/LiCl (Austin, 1977 and Rutherford and Austin, 1977). Solubility decreases with increasing molecular weight of chitosan. In general, chitosan is in a more folded structure (or random coil conformation) at high molecular weight due to hydrogen bonding or hydrophobic intramolecular interactions so that this conformation hinders that amine groups contacts with acid aqueous solution.

2.4. Characterization of chitosan solutions

2.4.1. Determination of critical concentrations C^* and C_e

The physical properties of polymeric solutions are mainly dependent on their concentrations. In dilute solution, the polymeric molecules are completely separated from each other. Thus, the hydrodynamic volume and conformation of the macromolecular are important for their physical properties. However, in concentrated solutions the macromolecules are entangled and the chain dimensions are independent of concentration. The dilute and concentrated regimes are separated by the overlap concentration (C^*), which is the polymer concentration at which chains start overlapping, and the entanglement concentration C_e , above which the chain form entanglements. A dilute solution is for $C < C^*$, and a concentrated entangled solution is for $C > C_e$.

In a practical way, the overlap concentration C^* can be easily determined from the product $C^*[\eta] \approx 1$ (Carreau *et al.*, 1997; Nystrom *et al.*, 1999). Another criterion to identify the overlap concentration is to take it as the value for which the viscosity of a polymeric solution (η) is twice that of the solvent (η_s) (Dobrynin *et al.*, 1995, Rubinstein *et al.*, 1994). The dilute and concentrated regions can be determined from the log-log plot of specific viscosity (η_{sp}) vs. the overlap function ($C[\eta]$) and the function $C[\eta] + k_H(C[\eta])^2$ as shown in Figure 2.4 (Desbrières, 2002). According to the author, the overlap concentration (C^*) was calculated from the value at which the variation of the specific viscosity (η_{sp}) with $\{C[\eta] + k_H(C[\eta])^2\}$ deviates from the slope of 1 in the Huggins expression. The entanglement concentration C_e was determined as the concentration at which the terminal linear domain begins in the log-log plot of η_{sp} and $C[\eta] + k_H(C[\eta])^2$ as shown in Figure 2.4. Another criterion relates the entanglement viscosity, η_e , to that of the solvent. It has been proposed that at the onset of the entangled regime, each chain has to overlap with n others, where $5 \leq n \leq 10$, depending on the polymer species (Rubinstein *et al.*, 1994). Since the viscosity at the entanglement concentration is $\eta_e \approx n^2 \eta_s$, C_e is the concentration for which $\eta \approx 50 \eta_s$ (Dobrynin *et al.*, 1995).

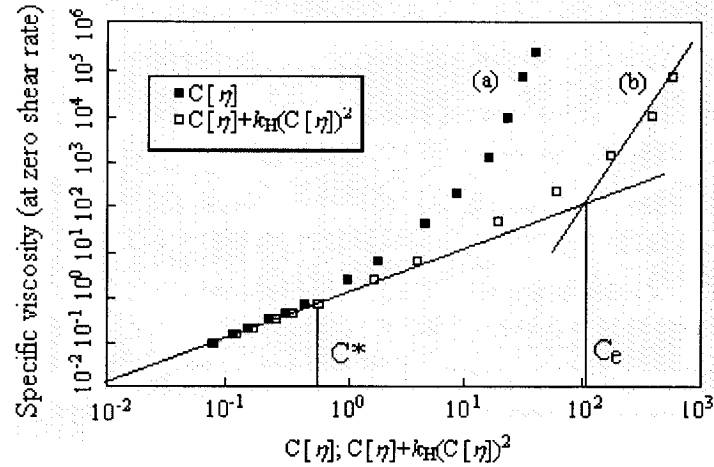


Figure 2.4. Dependence of specific viscosity as functions of (a) the overlap parameter, $C[\eta]$, and (b) the function $C[\eta] + k_H(C[\eta])^2$ for chitosan solutions (solvent 0.3M AcOH/0.05 AcONa; temperature, 278K; $\eta_{\text{solvent}} = 1.58 \text{ mPa.s}$; and $k_H = 0.45$) (Desbrières, 2002).

2.4.2. Solution behavior in dilute regime

In general, the rheological properties in dilute polymer solutions are investigated by measuring intrinsic viscosity, $[\eta]$. The properties are directly related to the conformation of polymeric molecules. The intrinsic viscosity of chitosan solution has been well explored under various conditions such as different molecular weight and DDA, ionic strength, pH and temperature.

The effects of molecular weight and DDA of chitosan molecule on the intrinsic viscosity were investigated extensively (Anthonsen et al., 1993; Kasaai et al., 2000; Pa and Yu, 2001; Tsaih and Chen, 1999). The intrinsic viscosity decreased with increasing molecular weight of chitosan (Yamota et al., 1993). Tsaih and Chen (Tsaih and Chen, 1997) reported that the MHS exponent a of chitosan value was between 0.65 and 1.01 under various ionic strength (0.01 – 0.30 M) below a molecular weight of $2.33 \times 10^5 \text{ g/mol}$; however, it was between 0.40 and 0.60 in the same range of ionic strength when the molecular weight of chitosan was greater than $2.33 \times 10^5 \text{ g/mol}$. The magnitude of

the MHS exponent a value is closely related to the conformation of polymeric molecules in solution. For example, values of a equal to 0, 0.5 – 0.8 and 1.8 indicate polymer chains in spherical, random coil and rod shapes, respectively (Chen and Tsaih, 1998). The change of the molecular weight-induced conformation may be caused by different spatial distribution of chain molecules and intramolecular hydrogen bonds and/or charge distribution according to molecular weight. In Figure 2.5, the effect of the number average degree of polymerization (\overline{DP}_n) on the intrinsic viscosity is shown for the condition of 0.1M ionic strength (Anthonsen et al., 1993) for different DDA chitosans. The intrinsic viscosity increased with increasing DDA for lower molecular weight chitosan samples; however, it decreased with increasing DDA for higher molecular weight chitosans. It indicates that electrostatic repulsion is detrimental for the hydrodynamic behavior of chitosan for lower molecular weight samples, but the number of acetylglucosamine is important on the hydrodynamic behavior for higher molecular weight chitosans. The MHS constant a related to molecular conformation decreased with increasing DDA of chitosans. In addition, the chain stiffness increased with decreasing DDA. Thus, in the range of higher molecular weights lower DDA chitosan showed larger intrinsic viscosities comparing to higher DDA ones.

pH and ionic strength are also significant for the intrinsic viscosity of chitosan, which behaves like a polyelectrolyte in acid aqueous solution. The intrinsic viscosity of chitosan in weak acetic acid aqueous solution increases with decreasing pH , suggesting a chain expansion molecule with increasing acetic acid concentration in aqueous solutions (Pa and Yu, 2001). The protonated amino group on the backbone of the chitosan makes the molecule unfold so that the hydrodynamic volume of chitosan increases and thus the viscosity increases. As pH increases, the electrostatic repulsion within the molecules decreases so that the hydrodynamic volume decreases and thus the viscosity decreases due to the reduction of the protonation of chitosan. From static light scattering (SLS) measurements, it was found that the chitosan molecules behave like rigid rod polymers due to higher intramolecular electrostatic charge repulsion at low pH , whereas, they are like flexible polymer at high pH . Chitosan solutions dissolved in bulkier exert higher

intrinsic viscosity due to steric effect at a same pH (Chen et al., 1994). When strong acids such as HCl and HBr are used to dissolve, it precipitated chitosan molecules due to the screening effect of ionized Cl^- and Br^- at low pH (Roberts, 1992). However, increasing pH with HCl, eventually resulting in the increase in ionic strength, decreases the intrinsic viscosity due to the reduction of the protonation degree of chitosan molecule.

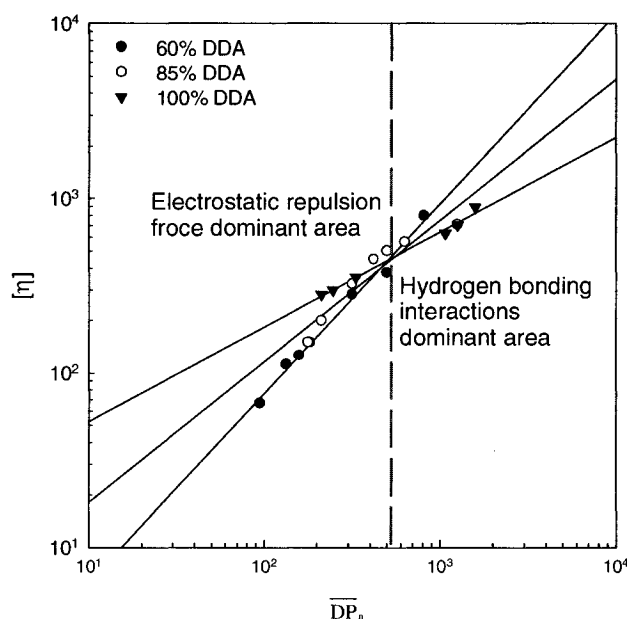


Figure 2.5. Effect of the number average degree of polymerization (\overline{DP}_n) on the intrinsic viscosity, $[\eta]$, of chitosan solution at 0.1M ionic strength (Anthonsen et al., 1993).

Temperature is one of the most important factors related to the conformation of polymeric molecules in aqueous solutions. In general, the intrinsic viscosity of chitosan decreases linearly with increasing solution temperature (Chen and Tsaih, 1998). Increasing temperature decreases the specific volume of the molecules due to the disruption of the structure of hydrogen bonded hydration water (Noguchi, 1981). The plot of the natural logarithmic intrinsic viscosity ($\ln[\eta]$) versus the inverse of absolute temperature ($1/T$) can be a useful tool to predict the stiffness of chitosan molecules because it relates to the activation energy for flow process (E_{af}). At the same DDA chitosan, the slope ($d\ln[\eta]/d(1/T)$) decreases with increasing weight-average molecular weight of chitosan. It indicates that larger molecular weight chitosan

molecules are more flexible than smaller molecular weight ones.

2.4.3. Characterization of dilute chitosan solutions

Intrinsic viscosity ($[\eta]$) can be often used to determine an approximation of the radius of gyration ($\langle R_G \rangle$) of a polymeric molecule in a solvent, by using the following equation (Carreau *et al.*, 1997):

$$[\eta] = \Phi \frac{\langle R_G \rangle^3}{\bar{M}_n} \quad (2.23)$$

where Φ is a universal constant ($2.1 \times 10^{23} \text{ mol}^{-1}$) and \bar{M}_n is the number-average molecular weight. $[\eta]$ is also useful to determine the Kuhn length (b), a statistical segment that describes the extension of the chain in a given direction of the initial bond and is closely related to the stiffness of the polymeric molecule in solution. The length can be calculated as follows (Anthonsen *et al.*, 1993):

$$b = \frac{6 \langle R_G \rangle^2}{IDP} \quad (2.24)$$

where l is the virtual bond length per monomer unit and DP is the degree of polymerization. In general, the persistence length is a half of the Kuhn length ($l_p = b/2$) for relatively stiff macromolecules or wormlike coils. The persistence length l_p is a characteristic of the local stiffness of a polymer; for example, the larger the l_p value, the larger the viscosity of a solution for a given molecular weight dissolved at a given concentration (Brugnerotto *et al.*, 2001b). For a polyelectrolyte, the persistence length l_p ($l_p = l_{p,0} + l_{p,e}$) is the contributions of two terms, the intrinsic persistence length ($l_{p,0}$) and the electrostatic persistence length ($l_{p,e}$). The intrinsic persistence length $l_{p,0}$ is determined for a neutral equivalent chain (θ conditions). On the other hand, for a charged molecule such as chitosan in acidic aqueous solution, $l_{p,e}$ increases with increasing charge density and is dependent on the Debye screening length (k^{-1}) for stiff polyelectrolytes and flexible chains (Ullner *et al.*, 1997). For example, $l_{p,e}$ shows a linear relationship ($l_{p,e} \sim k^{-1}$) for flexible polyelectrolyte.

In the dilute regime, the relationship between the viscosity and concentration for a polyelectrolyte solution can be expressed with Fuoss law as shown in Equation 2.25 (Fuoss, 1948 and 1949):

$$\eta_{red} = \frac{\eta_{sp}}{C} = \frac{A}{1 + BC^{1/2}} \quad (2.25)$$

where η_{red} is reduced viscosity; η_{sp} specific viscosity; C electrolyte concentration; and A and B empirical constants. As we can see from the equation, the viscosity of the polyelectrolyte solution is proportional to the square root of polymer concentration ($\eta \sim C^{1/2}$). However, the Fuoss law cannot describe the viscosity of polyelectrolyte solutions when the polyelectrolyte concentration approaches to zero (Jiang and Han, 1999). In the very dilute regime, the reduced viscosity decreases due to the expansion of the backbone caused by greater Coulombic repulsion between the charged point, which results from the decreased shielding of fixed charges on polyions (Chien et al., 1976; Kienzle-Sterzer et al., 1982). The concentration effect on the viscosity of polyelectrolyte solution in unentangled regime was theoretically derived by Dobrynin *et al.* (Dobrynin *et al.*, 1995). In the low salt limit, the viscosity increases as the square root of concentration $\eta \sim C^{1/2}$; however, in the high salt regime, $\eta \sim C^{5/4}$, which is the same scaling as semidilute unentangled neutral polymers in good solvent (Dobrynin et al., 1995).

2.5. Chitosan solution behavior in concentrated regime

2.5.1. Concentration effect on viscosity

Above the overlap concentration C^* , the physical properties of polymeric solutions have been mainly characterized with rheological measurements in steady simple shear mode or small amplitude oscillatory shear mode. The Cox-Merz rule (Cox and Merz, 1958) has been widely used for estimating the steady shear viscosity data from the more readily obtainable dynamic complex viscosity:

$$\eta(\dot{\gamma})|_{\dot{\gamma}=\omega} = |\eta^*(\omega)| \quad (2.2)$$

This rule has been shown to apply successfully for a number of polymer solutions and melts (Carreau et al., 1997), but with relative success for associating polymers (Kopperud and Nyström, 1998; Kulicke et al., 1998; Lauten and Nyström, 1999)

The behaviors of chitosan solutions have been characterized under various conditions with rheological measurements above the overlap concentration (C^*) (Desbrieres, 2002; Hwang and Shin, 2000; Iversen et al., 1997; Mucha, 1997; Wang and Xu, 1994). The shear rate dependency of viscosity was more clearly observed at higher chitosan concentration. The viscosity of chitosan solution increases with increasing concentration due to the larger number of entanglements of the macromolecular chains, which leads to a non-Newtonian flow pattern (Mucha, 1997). When chitosan concentration is increased, the viscosity was more dependent on shear rate in the power-law region (or lower power-law index) and also the length of the plateau zone decreases (Hwang and Shin, 2000). It can be explained in terms of the number of entanglements among macromolecules. As polymer concentration is increased, the movement of each chain is restricted due to the increased number of entanglements. It gives rise to an increase time required to form new entanglements to replace those disrupted by the externally imposed deformation.

The relationship between the viscosity and concentration shows a power-law relationship in concentrated regime: $\eta \sim C^v$ (Desbrières, 2002, Mucha, 1997; Nystrom et al., 1999; Wang and Xu, 1994). The theoretical scaling law predictions, based on the reptation concept for a polyelectrolyte in salt excess, are $\eta \sim C^{5/4}$ and $\eta \sim C^{15/4}$ for both semi-dilute unentangled and semi-dilute entangled solutions (Dobrynin et al., 1995). At low salt concentration, the dynamics of the chain is Rouse-like and $\eta \sim C^{1/2}$ and $\eta \sim C^{3/2}$ for both unentangled and entangled regimes (Dobrynin et al., 1995). On the experimental side, the specific viscosity of chitosan solutions was found to follow a power-law with respect to the chitosan concentration in 0.3M acetic acid (AcOH)/0.05M sodium acetate (AcONa) solvent at 25°C, i.e. $\eta_{sp} \sim C^{5.2}$ for entangled solutions (Desbrieres, 2002). Above the overlap concentration C^* , the relationship between the chitosan concentration and the specific viscosity was $\eta_{sp} \sim C^{3.94}$ (Hwang and Shin, 2000).

The value of this exponent is again slightly larger than the one found for most random-coil polysaccharides, i.e. 3.4 (Mitchell and Ledward, 1996; Ferry, 1980). This high exponent, compared to the theory (3.75), can be considered as the result of a larger number of contacts between macromolecular chains caused by intermolecular interactions.

2.5.2. DDA effect on viscosity

The effect of DDA on the viscosity is controversial. Wang and Xu (Wang and Xu, 1994) reported that the viscosity increased with increasing degree of deacetylation of chitosan in 0.2M acetic acid/0.1M sodium acetate solution. The charge density of chitosan increases with increasing DDA. Thus, it causes an increase of the entanglements by the expansion of the chitosan resulting from the intermolecular electrostatic forces. The non-Newtonian character increases with increasing DDA due to an increase of entanglements of chitosans in solution. However, Mucha (Mucha, 1997) reported that the shear viscosity decreased with increasing DDA. The author explained that low DDA chitosans are less soluble and form associates in acidic aqueous solution, resulting in increasing shear viscosity.

2.5.3. Temperature effect on viscosity

Polymeric solutions have been characterized under various temperatures with rheological measurements. In solution state, the storage (G') and loss (G'') moduli can be used to obtain a master curve by multiplying frequency by a temperature shift factor (a_T) described by (Carreau et al., 1997):

$$a_T = \frac{\eta^*(T)T_0\rho_0}{\eta^*(T_0)T\rho} \bigg|_{\omega} \quad (2.27)$$

where T , T_0 , ρ and ρ_0 are arbitrary temperature, reference temperature, sample density and reference density at arbitrary and reference temperatures, respectively. The estimated temperature shift factor (a_T) can be used to calculate the flow activation energy (E_{af}) with the Arrhenius relationship:

$$a_T = \exp\left\{\frac{E_{af}}{R}\left(\frac{1}{T} - \frac{1}{T_0}\right)\right\} \quad (2.28)$$

In general, the viscosity of chitosan solution decreases with increasing temperature. It is due to the loss of hydrogen bonding interactions and the increase of molecular mobility. The viscosity versus temperature relationship of chitosan solutions can be expressed in the form of an Arrhenius-type equation (equation 2.28). The magnitude of the energy of activation (E_{af}) determines the sensitivity of the solutions towards temperature and reflects the influence of the temperature on the intermolecular interaction of the chitosan macromolecules in the solvent. In the concept of free volume existence in the liquid (Frenkel, 1946), the activation energy of viscous flow is important when molecules have to move from one position to another through a barrier of activation energy reaching equilibrium level. Mucha (Mucha, 1997) measured the flow activation energy of chitosan solutions in terms of chitosan concentration, degree of deacetylation, and shear rate. Increasing chitosan concentration increased the energy, but increasing DDA and shear rate decreased E_{af} . According to the author, the activation energy was between 10 and 35 kJ/mol in all conditions. Wang and Xu (Wang and Xu, 1994) found that the flow activation energy was dependent on DDA. The energy was 25 kJ/mol for 91% DDA chitosan and 15 kJ for 75% DDA.

2.5.4. *Effect of various parameters on the relaxation time*

The relaxation time can be obtained from the inverse of frequency ($1/\omega^*$) at the crossover point of G' and G'' . The relaxation time (τ_R) is exponentially proportional to polymer concentration: $\tau_R \sim C^\nu$. For chitosan concentrations higher than 15g/L, the relationship between the relaxation time and concentration was $\tau_R \sim C^{3.7}$ (Desbrieres, 2002). The exponent 3.7 is quite large compared to the prediction of 1.5 for semidilute entangled solutions (de Gennes, 1976) and 2.08 predicted by the renormalization group theory for non-associating linear chains (Doi and Edward, 1986). A disagreement has been observed by different authors between theory and experiments either for polyelectrolytes (Boris and Colby, 1998; Krause et al., 1999) or uncharged polymers in

good solvents (Berry and Fox, 1968; Pearson, 1987; Takahashi et al., 1985; Berry and Fox, 1968). Higher exponents may be attributed to the interactions between macromolecular chains (Burchard, 2001).

For semidilute polyelectrolyte solutions, the polymer concentration dependency on the relaxation time increases with increasing salt concentration (or ionic strength) and the exponent at higher salinity approaches the value for nonionic polymer in good solvents (Yamaguchi et al., 1992). A very weak concentration dependency of the relaxation is shown in the low-salt limit of the semidilute entangled regime (Noda and Takahashi, 1996; Yamaguchi et al., 1992). The weak concentration dependency agrees with the theoretical prediction (Dobrynin et al., 1995; Rubinstein et al., 1994).

The relaxation time (τ_R) can be considered as the time required for a chain disentanglement of the network. τ_R shows a minimum value at a *pH* of 4.0; however, the relaxation time increased with *pH* lower or higher than 4.0 (Nystrom et al., 1999). It may be related to the formation of associates via hydrogen bonding and/or hydrophobic interactions. Around a *pH* of 4.0, the chitosan is completely protonated; thus, the electrostatic repulsion force hinders the formation of associations. However, weak base reduces the electrostatic repulsion so that chitosan molecules can associate with each other via physical hydrogen bonding and/or hydrophobic interactions. In addition, hydrochloric acid used to decrease the *pH* below 4.0 is completely dissociated in solution, resulting in the reduction of the electrostatic repulsion force by the neutralization effect of Cl^- ions.

2.6. Gel systems

A gel system is defined as a three-dimensional polymer network that is swollen in a liquid (Osada and Kajiware, 2000). The polymer network envelops the liquid and prevents the liquid from flowing out. In other words, the polymer network plays the role of a container that holds a large amount of solvent. Gels have both the characteristics of liquids and solids

2.6.1. *Classification of gels*

The classification of three-dimensional polymer networks is largely divided into those which are formed by a chemical reaction, sharing covalent bonds or crosslinking (chemical gels) and those which formed by aggregation caused by ionic, hydrogen bonding and hydrophobic interactions as well as entanglements between polymeric molecules (physical gels).

Chemical gels, or irreversible networks, are produced by the formation of covalent bonds between polymer molecules by chemical reactions (Osada and Kajiwara, 2000). Above the gel point, the average molecular weight of a material having a chemical network is infinite and it will have a finite equilibrium modulus. Chemical bonds are considered to be permanent while the physical junctions have finite lifetime, and in general the functionality of the chemical junctions is much lower than that of physical junctions. Typical examples of chemical gels systems are the vulcanized of linear polymer chains and the polycondensed multifunctional oligomeric species.

Physical gels are formed by the weak secondary forces such as van der Waals forces, hydrogen bonding and hydrophobic interactions. The network structure resulting from secondary forces is easy to create, but generally lacks stability due to sol-gel transition caused by changing temperature, ionic strength or *pH*. The sol-gel transitions refer to the status of the sol and gel being reversibly transferring form each other. For examples, agar and gelatin become gels when temperature decreases, but return into the original sol state at elevated temperature (Osada and Kajiwara, 2000).

Hydrogen bonding interaction is one of the crucial parameters to form physical gel structures. In general, the gelation via hydrogen bonding interactions occurs in cold environments below room temperature (cold-induced gelation) and the formed gel systems show excellent mechanical and water up-take properties. These gel structures are formed with various polysaccharides (Osada and Kajiwara, 2000). For example, gelatins, starches and carageenans can be transformed into three-dimensional physical networks below room temperature or during cooling process. The gel strength is dependent on polymer concentration, *pH* and cooling rate. For example, lower polymer

concentrations produces runny gels, but highly concentrated polymer solutions form stiff and rubbery gels. Soft gels are formed at low *pH* and fast cooling process.

For cellulose-based biopolymers, the gelation occurs via hydrophobic interactions. For example, methylcellulose (MC) solutions are changed into 3D networks at high temperature (heat-induced gelation) and then return to the original state at low temperature. The gel strength is proportional to the methyl concentration in the macromolecules. The most probable explanation for this heat-induced gelation may involve dehydration followed by hydrophobic association of the chain (Osada and Kajiwara, 2000). The vibration and rotation energy of water molecules increases at temperature greater than thermal gel point. The energy exceeds the ability of the weak hydrogen bonding to orient the dipolar water molecules around the polymer chain. The energized water molecules disengage from the fragile envelope of ordered water surrounding the chain. The dewatered hydrophobic polymers segments begin to associate with each other. As temperature or time spent at high temperature increases, the hydrophobic interactions increase in number, producing gels due to physical crosslinks being formed.

2.6.2. Chitosan-based chemical gels

Chemical chitosan gels can be formed by chemically reacting with glutaraldehyde (Argüelles-Mondal et al., 1998). Aldehyde groups in glutaraldehyde can react with amine groups in chitosan molecules. This reaction involves the formation of a Schiff base and is accompanied by color formation. The increase of the rate of color formation indicates the onset of gel formation. The three-dimensional networks can be established by polymer chains forming one or more crosslinks. For this system, the gelation rate can be affected by temperature, acetic acid concentration, electrolyte added and the overall concentration of amine and aldehyde functional groups. The viscosity is proportional to the chitosan and glutaraldehyde concentrations and temperature, but is inversely proportional to the concentration of acetic acid (Roberts, 1992). Chemical gels are also obtained by reacting chitosan with 1,1,3,3-tetramethoxypropane (TMP, a

“masked” dialdehyde) and then reducing the polymeric Schiff-base networks with an excess of cyanoborohydride (NaBH_3CN) (Capitani et al., 2001). The main drawback of the use of dialdehydes as crosslinkers is that they are generally considered toxic (Berger et al., 2003). In addition, some other alternatives are used as crosslinkers such as diethyl squarate (De Angelis et al., 1998), and genipin (Mi et al., 2000). Finally, chitosan can form chemical gels with functionalized biopolymers such as poly(ethylene glycol) (PEG) diacrylate (Kim et al., 1995), oxidised β -glycoldextrin (Crescenzi et al., 1997), and selerogulcan (Crescenzi, 1995).

2.6.3. *Physical chitosan gels*

Physical gelation of chitosan is greatly influenced by *pH*, temperature, polymer concentration, DDA and molecular weight of chitosan.

pH-induced gelation of chitosan was proposed by Jackson (Jackson, 1987). A chitosan-glycerol-water gel was prepared by dissolving chitosan in an acid-water-glycerol solution and by neutralizing the chitosan solution with 5N NaOH until *pH* 7. The resultant neutral solution unexpectedly turned into a gel upon standing. The gels apparently remained relatively stable and retained their three dimensional structures for long periods of time over wide variation in temperatures from 4 to 40°C, and were suitable for pharmaceutical use. The gel produced could be used as an excellent carrier for any medicament customarily administered in those forms e.g., antibacterial agents, silver sulfadiazine, quaterary ammonium agents, iodophors, vasodilators such as epinephrine and ketanserine, compounds which promote wound healing, analgesics, and anti-inflammatory agents. These medicaments can be added to the acid-water-glycerol-chitosan solution prior to neutralization with the base.

Thermoreversible chitosan gels can be categorized within two groups by thermal history during the gelation. One represents gels formed by cooling (cold-induced gelation) and the other gels formed by heating (heat-induced gelation). The gelation is mainly dependent on additives used for fabricating gel systems. For example, the chitosan solutions in 1.1M oxalic acid gradually gelled on standing at room temperature

(Hayes and Davies, 1978; Hirano, 1989). Roberts (Roberts, 1992) summarized the gelation behavior of chitosan-oxalic systems. The length of time required for gelation was considerable and depended on the chitosan concentration. Gels were melted on heating and gelled upon cooling, and the time required to gel after melting was considerably less than that required in the initial formation. The melting points were reasonably high and increased with increasing in chitosan concentration, being 88°C for the 50g/dm³ solution and 92°C for the 100g/dm³ one. Recently, Hamdine (Hamdine, 2004) produced cold-induced chitosan gel systems with phosphoric acid, oxalic acid, and sulfuric acid. The author investigated thermoreversibility by applying successive cooling-heating cycles on molten gels in the range of temperature 10 to 80°C. The gel systems recovered their original solution state during the first cycle; however, in subsequent cycles the gels became permanent, possibly due to the increased ionic crosslinks between chitosan molecules and divalent anions species. Finally, Chenite et al. (Chenite et al., 2000) prepared a thermally gelling chitosan system by neutralizing highly deacetylated chitosan solutions with β -glycerophosphate (β -GP) that remains in solution at physiological pH 7.2. The addition of β -GP increases the pH of chitosan solutions to the physiological level without immediate gelation at room temperature and induces gelation when temperature increases up to body temperature (37°C) or above (heat-induced gelation). When temperature decreases, the chitosan gels returns to the original sol state. The authors suggested various interactions occurring in aqueous solutions of the cationic polyelectrolyte chitosan and the divalent anionic base β -GP (Chenite et al., 2001) to explain the gelation: 1) electrostatic repulsion between charged chitosan in solution, 2) electrostatic attraction between oppositely charged chitosan and the phosphate moiety of β -GP, 3) attractive hydrophobic and hydrogen bonding between chains and 4) the hydrophobic or water-structuring character of the glycerol moiety of β -GP.

2.6.4. Secondary forces related to physical chitosan gelation

Chitosan has simultaneously hydrophobic ($-\text{CH}_3$) and hydrogen bonding interaction ($-\text{OH}$, $-\text{C}=\text{O}$, $-\text{NH}$) favoring groups (Roberts, 1992). From its hydrophobic and hydrogen bonding favoring parts, chitosan can self-associate in aqueous solutions (Roberts, 1992; Chenite et al., 2001; Philippova et al., 2001; Amiji, 1995; Nyström et al., 1999; Wang, 1999; Tsaih and Chen, 1997). These two types of junctions, along with ionic bridging in the presence of divalent species, are critical interactions involved in the formation of physical gel structures in chitosan-based systems. The balance between these interactions is critical to the formation of three-dimensional networks and can be controlled by temperature variation and/or in the presence of urea (Tako and Hanashiro, 1997). Urea has been extensively used to control the intensity of hydrogen bonding interactions in biomedical systems (Hammes and Schimmel, 1967; Kim et al., 1996; Kjøniksen et al., 2003; Kokufuta et al., 1998; McGrane et al., 2004; Tsaih and Chen, 1997) as well as to control hydrophobic interactions (Philippova et al., 2001). We briefly discuss below the general influence of temperature and urea on hydrogen bonds and hydrophobic interactions in the light of previous research.

2.6.5. Temperature effect on chitosan physical gelation

Water molecules are presumed to form enclosed structures that surround the polymer chain at low temperature (Li et al., 2001). Increasing temperature increases the mobility of polymer molecules and exceeds the ability of weak hydrogen bonds to orient dipolar water molecules around the polymer chains, causing the decrease of hydrogen bonding interactions. With increasing temperature, the energized water molecules enclosing the polymer chain are removed and the dewatered hydrophobic polymer segments start associating with each others. Thus, increasing temperature increases the number of hydrophobic interactions and results in physical networks formed by increased association (Desbrières et al., 1996).

2.6.6. Urea effect on the secondary forces of chitosan gels

Urea, known as a hydrogen breaking agent (Hammes and Schimmel, 1967; Kim et al., 1996; Kjønsken et al., 2003; Kokufuta et al., 1998; McGrane et al., 2004; Tsaih and Chen, 1997) can hinder the formation of macromolecular structures. However, there are two different views about the effect of urea on hydrogen bonding interactions. One is that urea is unable to disrupt intramolecular interactions (Cheetham and Tao, 1997; Kim et al., 1996; McGrane et al., 2004) and only have impact on the intermolecular ones, while the other suggests that adding urea breaks intramolecular hydrogen bonds and causes a change in the molecular conformation (Chen and Tsaih, 2000; Tsaih and Chen, 1997). Two mechanisms are proposed to explain the denaturing function of urea in aqueous media (Hammes and Swann, 1967). The first is the specific binding of urea to groups on the polymer chains, thereby weakening hydrogen bonding between polymer chains (intermolecular), and the other possible mechanism is the breakdown of the hydrogen-bonded structure of the solvent, or the “structuring breaking effect”. According to the literature (Hammes and Swann, 1967) both mechanisms concurrently produce the denaturing process.

Kjønsken et al. (Kjønsken et al., 2003) showed that the dynamic moduli (G' and G'') of pectin solutions exhibited weaker values in the presence of urea, and that gel formation at 25°C was hindered. High urea concentrations also prevented a network microstructure forming for proanthocyanidin (PA) polymer solutions and yielded nearly Newtonian characteristics of independent particles (Kim et al., 1996), while for amylase gels in a mixture of water and dimethyl sulfoxide (DMSO) the use of urea reduced gel strength significantly (Cheetham and Tao, 1997). The previous examples illustrate the effect of urea on intermolecular hydrogen bonds. On the other hand, Tsaih and Chen (Tsaih and Chen, 1997) reported that the addition of urea to chitosan solutions resulted in an increase of the intrinsic viscosity and persistence length, therefore in a less compact structure, due to the hindrance of intramolecular hydrogen bonds.

The influence of urea on hydrophobic interactions is controversial. Kokufuta et al. (Kokufuta et al., 1998) proposed that these interactions, involved in the formation of

gels of poly(ethyleneimine), were not affected by the addition of urea. Furthermore, recent neutron light scattering experiments showed that urea caused no apparent disruption of the water structure even at high concentration of urea (Finny and Soper, 1994), indicating no effect on hydrophobic interactions. However, Dubin and Stauss (Dubin and Stauss, 1973) reported that urea weakened hydrophobic interactions between solute molecules. Urea preferentially solvates hydrophobic residues by breaking the hydrogen-bonded structures of water (Alonso and Dill, 1991; Roseman and Jenks, 1975), and this leads to an effective reduction of hydrophobic interactions. Computer simulations based on energy minimization of clusters supported that urea directly participates in the solvation of hydrophobic solutes by replacing water molecules in the hydration shells of the solute (Christianziana, 1989). Wallqvist and Covell (Wallqvist and Covell, 1998) monitored the effect of urea on hydrophobic interactions by computing the potential of mean force in the ternary system methane-water-urea. Urea appeared to enhance hydrophobic interactions and act as a renaturant for the uncharged methane. However, it acted as a denaturant in the ternary charged methane-water-urea system by destabilizing the hydrophobic bonds between the solutes. Finally, Philippova et al. (Philippova et al., 2001) investigated the effect of urea on hydrophobic interactions in the association of chitosan molecules using fluorescence measurements. The authors showed reduced formation of hydrophobic domains in chitosan solutions in the presence of urea at a concentration of 7M.

Chapter 3

Presentation of the articles

The next four chapters (Chapter 4 – 7) contain the articles submitted in the scope of this thesis and Chapter 8 shows the results of several additional studies performed to understand the gelation mechanisms and behaviors more clearly. The first paper, presented in Chapter 4, *Viscoelastic Properties of Chitosan Solutions: Effect of Concentration and Ionic Strength*, concerns the investigation of the effect of chitosan concentration and ionic strength on the rheological solution behaviour in dilute and concentrated regimes. Different amounts of sodium chloride were used to control the ionic strength of the chitosan solutions. The overlap concentration C^* and the entanglement concentration C_e were determined to identify dilute, semidilute and concentrated regimes. In the dilute regime, the intrinsic viscosity was measured in terms of ionic strength. The results were interpreted in terms of the Debye electrostatic screening length. The measured intrinsic viscosity was used to calculate the molecular radius of gyration and the persistence length. In the concentrated regime, the small oscillatory and steady shear tests were performed in terms of chitosan concentration and ionic strength at 25°C. The measured properties were used to determine zero shear viscosity, relaxation spectra and nonlinearity using various rheological models.

Physical gel systems can be formed by the association of polymeric molecules via weak secondary forces such as ionic, hydrogen bonding, and hydrophobic interactions. However, these interactions are greatly dependent on temperature. In the second paper, presented in Chapter 5, *Physical Gelation of Chitosan in the Presence of*

β -Glycerophosphate: The Effect of Temperature, the temperature effect on each interaction was thus investigated during the heat-induced gelation process. The evolution of the physical properties was characterized using rheological measurements during the gelation process. In addition, the physicochemical properties, i.e. pH and conductivity, were measured in function of temperature. The measured pH values were used to calculate the change in the ionization of each species and the ionic strength of the chitosan- β -glycerophosphate solutions in function of temperature. The practical experimental results and calculations were effectively used to interpret the function of temperature on the chitosan-based gelation and to propose possible gelation mechanisms.

In the third paper in Chapter 6, *Effect of urea on solution behavior and heat-induced gelation of chitosan- β -glycerophosphate*, the effect of urea on the physicochemical properties pH and conductivity, and rheological properties of chitosan- β -glycerophosphate systems was investigated in order to identify the main polymer-polymer interactions at low and high temperature. Urea controls simultaneously the magnitude of hydrogen and hydrophobic interactions, two very important forces related to chitosan-based gelation. The change of the ionic strength of the chitosan solutions was evaluated by measuring the conductivity in function of temperature. The evolution of the physical properties of the chitosan systems were monitored during the gelation process in the presence of different concentrations of urea. The gelation temperature, gel strength and activation energy to form the gel structures (E_{ag}) were determined in function of urea concentration. In addition, the effect of urea on chitosan solution behaviors was studied at 5°C using rheological measurements in the linear viscoelastic

regime. The measured properties in solution were analyzed with rheological models and the zero shear viscosity, time-weighted relaxation spectra, power-law index in Cole-Cole plots were determined to interpret the effect of urea on the chitosan solution behavior.

The fourth and last paper in Chapter 7, *Chitosan and glycerophosphate concentration dependence of solution behavior and gel point using small amplitude oscillatory rheometry*, presents the linear viscoelastic properties of chitosan systems in the sol and gel states in functions of glycerophosphate and polymer concentrations. In this study, the effect of the molecular structure of glycerophosphate (α -type and β -type) was monitored in the sol and gel states. In the solution state, the effect of β -glycerophosphate and chitosan concentrations on rheological properties were investigated in the temperature range from 5 to 45°C. The flow activation energy was determined in functions of chitosan and glycerophosphate concentrations. The gelation temperature determined from the heat-induced gelation process was used to derive the 3D sol-gel phase diagram of the chitosan-GP system. Nonisothermal gelation kinetic studies were performed under various chitosan and glycerophosphate concentrations. With the modified Eldridge-Ferry method, the polymer junction zone structures were interpreted at the gelation point in function of glycerophosphate concentration.

Chapter 8 reported the results of several investigations performed in order to understand the gelation mechanisms of chitosan-GP systems. First, it was verified the occurrence of the possible ionic interactions between chitosan and GP. For this study, chitosan-GP gel systems were produced in terms of cooking time at 80°C and then they transformed into solution state by decreasing pH. The recovered chitosan solutions were

dialyzed and freezing-dried. Rheological, GPC and FTIR measurements were employed to characterize the dried chitosan powder solution. Second, the change in physical state of chitosan-GP systems reported in terms of storage time, storage temperature, chitosan and GP concentrations. Finally, in the absence of GP the rheological properties of chitosan solutions were characterized as a function of ionic strength at 80°C.

Chapter 4

Viscoelastic Properties of Chitosan Solutions: Effect of Concentration and Ionic Strength

Jaepyoung Cho¹, Marie-Claude Heuzey^{1*}, André Bégin² and Pierre J. Carreau¹

¹ *CRASP, Department of Chemical Engineering, Ecole Polytechnique, P.O. Box 6079,
Station Centre-Ville, Montreal, QC, H3C 3A7, CANADA*

² *Food Research and Development Centre, 3600 Casavant Blvd West, Saint-Hyacinthe,
QC, J2S 8E3, CANADA*

* *Corresponding author. E-mail: marie-claude.heuzey@polymtl.ca; tel.: +1-514-340-4711 ext. 5930; fax: +1-514-340-2994*

4.1. Abstract

The dynamic rheological properties of chitosan solutions have been investigated in terms of ionic strength and chitosan concentration for entangled systems. The overlap concentration C^* and the entanglement concentration C_e have first been determined to identify the dilute, semi-dilute and concentrated entangled regimes. In dilute solutions, the effect of ionic strength (I) on the intrinsic viscosity ($[\eta]$) has been interpreted in terms of the Debye electrostatic screening length. The intrinsic viscosity, the radius of gyration and the persistence length decreased with increasing ionic strength, due to the screening of the electrostatic charges on the chitosan chains by the salt resulting in increased chain flexibility. For concentrated solutions, dynamic measurements were performed and the relaxation spectra were calculated from the storage (G') and loss (G'') moduli characterized in the linear viscoelastic region. For all chitosan concentrations and ionic strengths, the time-weighted stress relaxation spectra showed only one peak. However, the width of the spectra increased with increasing polymer concentration, indicating a larger distribution of relaxation modes due to more entanglements and interchain interactions. The mean relaxation time (τ_H), related to reptation, and the zero-shear viscosity (η_0) were found to follow power-law expressions of the chitosan concentration, with $\tau_H \sim C^{3.1}$ and $\eta_0 \sim C^{4.1}$, respectively, with the high exponents indicating the associating character of the polymer. The non-Newtonian nature (elastic properties and shear-thinning behavior) of the chitosan solutions increased with increasing chitosan concentration and decreasing ionic strength.

Keywords: Chitosan solution, intrinsic viscosity, viscoelastic properties, relaxation spectrum, polyelectrolyte

4.2. Introduction

Chitin is the most abundant organic material after cellulose. It is extracted from the shells of crustaceans and the exoskeletons of arthropods. Applications for chitin are limited due to its poor solubility. However, it becomes soluble in aqueous acid solutions after deacetylation in an alkaline environment that results in the product called chitosan. Chitin and chitosan are linear binary heteropolysaccharides composed of 2-amino-2-deoxy-D-glucopyranose (glucosamine) and 2-acetamido-2-deoxy-D-glucopyranose (acetylglucosamine) units, and the two biopolymers are mainly distinguished from each other by their solubility in aqueous acidic solutions [1]. One important parameter of the molecular structure of these materials is the degree of deacetylation (DDA), or number percentage of glucosamine in the chitosan molecule. The copolymer is generally accepted as chitosan when the DDA is larger than 50% [2].

The increased solubility of chitosan with respect to that of chitin is related to its positively charged polyelectrolyte nature, due to the protonation of the free amine groups below a pH of 6.2 [3]. Positively charged chitosan has been attracting a great deal of attention because of its various bioactivities such as antifungal, antitumor, antiallergic and immune activating characters [4]. In addition, chitosan is a non-toxic, biocompatible and biodegradable material. It has been used in many industries such as food, medical, cosmetic and pharmaceutical industries, and numerous international patents have claimed the applications of chitosan in these areas [4,5,6,7].

These characteristics and related potential applications have driven many studies on chitosan. Several have been focusing on the investigation of the physical properties of diluted solutions [8,9,10,11], looking at the effect of pH, ionic strength, DDA and molecular weight on the conformation of the chitosan molecule. Other studies have dealt with the rheological properties of concentrated chitosan solutions [12,13,14,15]. While the effect of *pH* on these solutions has been investigated [15], no studies have looked at the effect of ionic force at constant *pH* for concentrated solutions. Since *pH* controls the ionization of the chitosan molecule, it is interesting to isolate the effect of the solution ionic strength on a constant polymer charge density.

This study aims at evaluating the effect of chitosan concentration and ionic force at constant pH on the evolutionary aspect of the viscoelastic properties of chitosan solutions, towards gelation by salting out. The results are analyzed in the light of simple rheological models and compared to theoretical scaling law predictions.

4.3. Literature review

4.3.1 Characterization of dilute chitosan solutions

In dilute solutions, the physical properties of chitosan solutions have been largely characterized by the intrinsic viscosity $[\eta]$. This property can be used to get an approximation of the radius of gyration ($\langle R_G \rangle$) of a polymeric molecule in a solvent. The relation between $[\eta]$ and $\langle R_G \rangle$ is given by [16]:

$$[\eta] = \Phi \frac{\langle R_G \rangle^3}{M_n} \quad (4.1)$$

where Φ is a universal constant ($2.1 \times 10^{23} \text{ mol}^{-1}$) and \overline{M}_n is the number-average molecular weight. In addition, the value of the intrinsic viscosity is useful to predict the stiffness of the polymeric molecules in solution by determining the Kuhn length (b). In general, the Kuhn length increases with increasing chain stiffness. This length can be determined by [8]:

$$b = \frac{6 \langle R_G \rangle^2}{l DP} \quad (4.2)$$

where l is the virtual bond length per monomer unit and DP is the degree of polymerization. The persistence length (l_p) is $b/2$ for relatively stiff molecules (wormlike coils).

In addition, the relationship between the viscosity of polyelectrolyte solutions at low concentration has been shown to be proportional to the square root of polymer concentration $\eta \sim C^{1/2}$ (Fuoss law [17], Equation 4.3), while for solutions of uncharged polymers at the same concentration, $\eta \sim C$.

$$\eta_{red} = \frac{\eta_{sp}}{C} = \frac{A}{1 + BC^{1/2}} \quad (4.3)$$

The empirical Fuoss model dependency on concentration has been theoretically proven by Dobrynin et al. [18].

4.3.2 Determination of the critical concentrations C^* and C_e

In general, the physical properties of a polymeric solution are greatly dependent on its concentration. In dilute solutions, the polymeric chains are isolated from each other in the solvent and the hydrodynamic volume and the conformation of the molecules are the most important parameters that determine the physical properties. In the concentrated regime, the macromolecules are entangled and the chain dimensions are independent of the polymeric concentration. The diluted and concentrated regimes are defined by the overlap concentration (C^*), which is the polymer concentration at which chains start overlapping, and the entanglement concentration C_e , above which the chain dimensions form entanglements and are independent of the polymer concentration. A dilute solution is for $C < C^*$, and a concentrated entangled solution is for $C > C_e$.

In a practical way, the overlap concentration C^* can be easily determined from the product $C^*[\eta] \approx 1$ [15,16]. Hwang et al. [19] measured the specific viscosity (η_{sp}) as a function of space occupancy $C[\eta]$ to determine the overlap concentration of a chitosan solution. They found that the overlap concentration was approximately 2.8 g/L. Argüelles-Monal et al. [20] reported that the onset of incipient contact and interpenetration occurred at $C[\eta] \approx 1.45$ for a chitosan of DDA 80% at 25°C. Desbrières [12] determined the overlap concentration as the value for which the variation of the specific viscosity (η_{sp}) with $\{C[\eta] + k_H(C[\eta])^2\}$ deviates from the slope of 1 in the Huggins expression. The overlap concentration was determined as 1.05 g/L ($C^*[\eta] \approx 1.07$ and $[\eta] = 1.013$ L/g at 5°C). Finally, another criterion to identify the overlap concentration is to take it as the value for which the viscosity of a polymeric solution (η) is twice that of the solvent (η_s) [18,21].

The entanglement concentration C_e can also be determined using different approaches. It has been designated by Desbrières as the concentration at which the terminal linear domain begins in the log-log plot of η_{sp} and $C[\eta] + k_H(C[\eta])^2$ [12]. Another criterion relates the entanglement viscosity, η_e , to that of the solvent. It has been proposed that at the onset of entangled regime, each chain has to overlap with n others, where $5 \leq n \leq 10$, depending on polymer species [18]. Since the viscosity at the entanglement concentration is $\eta_e \approx n^2 \eta_s$, C_e can be defined as the concentration at which the solution viscosity represents fifty times that of the solvent ($\eta \cong 50\eta_s$) [18]. These different approaches are compared in the results section of this work.

4.3.3. Characterization of concentrated chitosan solutions

Above the overlap concentration C^* , rheological properties of semi-dilute unentangled and concentrated entangled polymeric solutions have frequently been characterized in terms of steady simple shear and small amplitude oscillatory shear. The Cox-Merz rule [22] has been widely used for estimating the steady shear viscosity data from the more readily obtainable dynamic complex viscosity:

$$\eta(\dot{\gamma}) \Big|_{\dot{\gamma}=\omega} = |\eta^*(\omega)| \quad (4.4)$$

This rule has been shown to apply successfully for a number of polymer solutions and melts [16], but with relative success for associating polymers [23,24,25].

When the viscosity of polymer solutions is measured as a function of steady shear rate, two distinct viscosity regions are observed: a plateau region at low shear rate, the zero-shear viscosity (η_0), and a power-law regime at high shear rate. One model that can fit the viscosity on the entire shear rate interval is the three-parameter Carreau model [16]:

$$\eta = \frac{\eta_0}{\left[1 + (t_1 \dot{\gamma})^2\right]^{\frac{1-n}{2}}} \quad (4.5)$$

where t_1 is a characteristic time and n , that characterize the material shear-thinning behavior, is dimensionless. When the steady shear rate ($\dot{\gamma}$) tends towards zero, the

model predicts the zero-shear viscosity (η_0), and the slope in the high shear rate regime on a log-log scale is given by $n-1$. This model has been appropriately predicting the behavior of the chitosan solutions studied in this work.

Oscillatory shear flow has been extensively used to characterize polymeric solutions. In general, the oscillatory test is performed in the linear viscoelastic regime, where the storage (G') and loss (G'') moduli are independent of the strain amplitude. Both G' and G'' determined in the linear viscoelastic regime or the relaxation modulus ($G(t)$) can be used to calculate the stress relaxation spectrum ($H(\tau)$) [26] :

$$G(t) = \int_{-\infty}^{\infty} H(\tau) e^{-t/\tau} d(\ln \tau) \quad (4.6)$$

$$G^*(\omega) = \int_{-\infty}^{\infty} (\omega\tau + i) H(\tau) \frac{\omega\tau}{1 + (\omega\tau)^2} d(\ln \tau) \quad (4.7)$$

where ω is the frequency and τ a relaxation time, and with the complex modulus defined as $G^*(\omega) = \sqrt{G'(\omega)^2 + G''(\omega)^2}$. The validity of the calculated stress relaxation spectrum can be verified by comparing the zero-shear viscosity determined using the Carreau model [16] presented earlier (Equation 4.5) with that estimated from the area under the time-weighted relaxation spectrum curve:

$$\eta_0 = \int_{-\infty}^{\infty} \tau H(\tau) d(\ln \tau) \quad (4.8)$$

Mucha [13] reported that the shear stress and viscosity of chitosan solutions increased with increasing chitosan concentration, corresponding to a progressive increase of entanglements between the macromolecular chains. Wang et al. [14] also concluded that the non-Newtonian character increased with increasing DDA due to the chains expanded structure and the increase of entanglements. Hwang et al. [19] on their part observed that the more shear-thinning behavior was observed for large chitosan concentrations. In general, the motion of individual chains gets restricted with increasing number of entanglements as the polymer concentration increases. The chains disentangled by hydrodynamic forces cannot form new entanglements because of the lack of mobility.

For a highly concentrated solution, disentanglement becomes dominant at high shear rate and the non-Newtonian behavior more pronounced.

The dependency of the specific viscosity on chitosan concentration has also been investigated in the concentrated regime [12,13,14,15]. The theoretical scaling law predictions, based on the reptation concept for a polyelectrolyte in salt excess, are $\eta_{sp} \sim C^{5/4}$ and $\eta_{sp} \sim C^{15/4}$ for both semi-dilute unentangled and semi-dilute entangled solutions [18]. At low salt concentration, the dynamics of the chain is Rouse-like and $\eta_{sp} \sim C^{1/2}$ (Fuoss model) [18]. On the experimental side, the specific viscosity of chitosan solutions was found to follow a power-law with respect to the chitosan concentration in 0.3M acetic acid (AcOH)/0.05M sodium acetate (AcONa) solvent at 25°C, i.e. $\eta_{sp} \sim C^{5.2}$ for entangled solutions [12]. This high exponent, compared to the theory (15/4), can be considered as the result of a larger number of contacts between macromolecular chains caused by hydrophobic interactions, as proposed by Amiji [27]. For a chitosan dissolved in 0.1M AcOH/0.1M sodium chloride (NaCl), the specific viscosity was measured as a function of the chitosan concentration at 25°C [19]. Above the overlap concentration C^* , the relationship between the chitosan concentration and the specific viscosity was $\eta_{sp} \sim C^{3.94}$. The value of this exponent is again slightly larger than the one found for most random-coil polysaccharides, i.e. 3.4 [28,29].

4.4. Experiments

4.4.1. Materials

The chitosan used in this study was purchased from Marinard Biotech (QC, Canada). The degree of deacetylation of the chitosan is 93%, determined from colloidal titration, and the weight average molecular weight (\overline{M}_w), measured by gel permeation chromatography (GPC), is 8.5×10^5 g/mol ($\overline{M}_w / \overline{M}_n = 2.76$). The GPC measurements were conducted with a Ultrahydrogel™ 500 column (Waters Co., MA, USA) in 0.25M acetic acid / 0.25M sodium acetate using dextran standards. In this work, acetic acid (Assay: 99.7%, Aldrich, WI, USA) was used to dissolve the chitosan. Sodium acetate (Assay: 99.3%, Fisher Scientific, NJ, USA) was added to prepare the buffer solutions.

Ionic strength (I) was controlled with sodium chloride (NaCl, assay: 99%, Laboratoire Mat Inc., QC, Canada).

4.4.2. Solutions preparation and physicochemical characterization

A stock solution of chitosan (75 g/L) was first prepared by dissolving the polymer in 0.5M acetic acid by mildly stirring with a high torque stirrer (Caframo Ltd., ON, Canada) at 30 RPM for 72h at room temperature. During the stirring process, the container of the stock solution was covered with aluminum foil to prevent evaporation, and the slight weight difference before and after the stirring process was compensated by adding extra amount of solvent. Using the stock solution, a series of less concentrated solutions were prepared by adding the aqueous acetic acid solution. Sodium acetate of 0.1M was added to the chitosan solution to control pH . Different amounts of NaCl (0 – 0.6M) were incorporated to each chitosan solution to vary the ionic strength. All chitosan solutions were left to rest 3h for degassing without stirring at room temperature and then kept in a refrigerator ($T < 5^{\circ}C$) to prevent degradation of the macromolecules.

Each chitosan solution was characterized in terms of pH , conductivity and turbidity. The results of the pH measurements at room temperature (pH -meter from Hana Ltd, Portugal) were used to estimate the degree of protonation of the chitosan applying the method of Rinaudo et al. [30,31]. These results confirmed that the chitosan molecules dissolved in the acidic solution were protonated at 99%. The conductivity (conductance meter YSI model 35, YSI Inc., USA) was determined at room temperature. In addition, the conductivity was theoretically determined from [32]:

$$\text{Conductivity (mS/cm)} = \sum_i N_i \lambda_i \quad (4.9)$$

where N_i is the equivalent concentration (or normality) and λ_i the equivalent conductance of ions i . The equivalent conductance for any electrolyte of concentration (c) can be approximately calculated using the Debye-Hückel-Onsager equation written for a symmetrical (equal charge of cations and anions) electrolyte as [33]:

$$\lambda_i = \lambda_i^{\circ} - (A' + B' \lambda_i^{\circ}) c^{1/2} \quad (4.10)$$

For a solution at 25°C and both cations and anions of unit charge, the constants are $A' = 60.2$ and $B' = 0.229$. λ_i° is the equivalent conductance at infinite dilution and can be obtained from the literature [34]. The turbidity measurements were performed with a UV-visible spectrophotometer (Varian Cary 300 Bio, Varian, Inc., USA). The turbidity τ was determined according to Equation (4.11) [35]:

$$\tau = \left(-\frac{1}{L} \right) \ln \left(\frac{I}{I_0} \right) = \frac{2.303A}{L} \quad (4.11)$$

where L is the sample thickness (1 cm in this case), I_0 the input wavelength (600 nm), I the output wavelength and A the absorbance index.

The ionic strength was evaluated from Equation (4.12):

$$I = \frac{1}{2} \sum (c_i Z_i^2) \quad (4.12)$$

where c_i and Z_i are the concentration and the charge number of ion i , respectively. The ionic strength was expressed on a molarity basis (M).

4.4.3. Intrinsic viscosity measurements

The intrinsic viscosity of the chitosan solutions was measured using a Ubbelohde capillary viscometer ($\phi = 0.78$ mm, Fisher Scientific, Canada) in various solvents at 25°C, and was investigated as a function of the ionic strength. These data were also used to determine the different regime of concentrations of the chitosan solutions. Three different methods were used to determine the overlap concentration C^* at each ionic strength. Firstly, it was estimated from the product $C^*[\eta] \approx 1$ [15,16]. Secondly, C^* was obtained as the value for which the variation of η_{sp} with $C[\eta] + k'(C[\eta])^2$ deviates from the slope of 1 of Huggins law [12]. Finally, it was determined as the concentration at which the viscosity of the chitosan solution is twice that of the solvent [18,21]. The entanglement concentration C_e was estimated as the concentration at which the terminal linear domain begins in the log-log plot of η_{sp} and $C[\eta] + k_H(C[\eta])^2$ [12], and as the concentration for which $\eta \cong 50\eta_s$ for all ionic strengths [18].

4.4.4 Dynamic and steady shear rheological tests

Above C_e , the dynamic properties of the chitosan solutions were characterized in terms of the chitosan concentration and the ionic strength at 25°C. The rheometers used were a highly sensitive strain-controlled rheometer ARES (Rheometric Scientific, NJ, USA) with a double-Couette geometry for chitosan concentrations of 10.1 – 30.9 g/L, and a stress-controlled rheometer AR-2000 (TA Instruments, DE, USA) with a Couette geometry for the chitosan concentration of 41.7 g/L. The dynamic and steady shear tests were repeated three times with each solution. Low viscosity mineral oil covered the surface of the chitosan solutions in order to hinder evaporation during the measurements. The stability of the chitosan solutions was investigated as a function of time in oscillatory shear tests under a small deformation of 0.1 and a low frequency of 1 rad/s. Oscillatory shear measurements were performed in the linear viscoelastic region. The G' and G'' data obtained from the small amplitude oscillatory shear measurements were used to calculate the relaxation time spectrum using a commercial software (NLREG®) [36]. Finally, the shear viscosity was measured as a function of the steady shear rate. The zero-shear viscosity was determined from the shear data using the three-parameter Carreau model (Equation 4.5) and the time-weighted stress relaxation spectrum area calculations (Equation 4.8).

4.5. Results and discussion

4.5.1 Physicochemical characterization of chitosan solutions

The ionic strength (I) of each chitosan solution was determined from Equation (4.12). As presented in Table 4.1, the ionic strength increased from 9×10^{-4} to 0.46M by increasing the concentration of sodium acetate and NaCl. The Debye screening length (k^{-1}), related to the double layer thickness, can be calculated from the ionic strength. The Debye screening length is a measure of the distance over which an individual charged particle exerts an electrostatic effect. It can be determined by the following equation [37]:

$$k^{-1}(nm) = \left(\frac{1000\epsilon k_B T}{8\pi e^2 N_{Av} I} \right)^{0.5} = \frac{0.3043}{I^{0.5}} \quad (4.13)$$

where ϵ is the permittivity of water, k_B is Boltzmann constant, T the absolute temperature (K), e the Coulomb electronic charge and N_{Av} the Avogadro number. From this equation, the electrostatic double layer thickness decreases inversely as the square root of the ionic strength. We determined that the k^{-1} value decreased from ≈ 3 to 0.45 nm by increasing the ionic strength from 9×10^{-3} to 0.46M. This decrease is related to the screening of the positively charged amino groups by anions such as CH_3COO^- and Cl^- , and indicated a strong diminution of the repulsive potential. This repulsion reduction resulted in an increased risk of flocculation or precipitation, which was observed experimentally for our chitosan solutions at $I > 0.46\text{M}$ ($k^{-1} < 0.45$ nm). In effect, the addition of salt is frequently used to improve the recovery by precipitation of polysaccharides. Desbrières et al. [38] also reported that increasing the ionic strength results in enhanced polymer-polymer interactions over those of polymer-solvent.

The pH values of the chitosan solutions ($I = 0.12 - 0.46\text{M}$) in the presence of AcONa were 4.2 ± 0.2 , while for the 0.5M AcOH solution ($I = 9 \times 10^{-3}\text{M}$) it was 3.3 ± 0.5 . The pH was slightly dependent on the polymer concentration, due to the consumption of H^+ ions by the protonation of the free amine groups, and on the ionic strength. Rheological measurements were performed up to an ionic strength of 0.46M to avoid the two-phase systems. The observed precipitation at large salt concentration was confirmed by turbidity measurements (results not shown): the turbidity gradually increased up to an ionic strength of 0.46M; after, it underwent a rapid increase at an ionic strength of 0.76M. The abrupt increase of the turbidity was related to the appearance of the white-like precipitate observed during the pH measurements.

Figure 4.1 shows the effect of the ionic strength on the chitosan solutions conductivity. Both the experimental and calculated conductivities (from Equations 4.9 and 4.10) are quite similar. The limit conductivity of the protonated amine groups of chitosan was assumed negligible, which seems to be a reasonable assumption. The conductivity of the chitosan solutions was found to be approximately linear with the

ionic strength. Chitosan solutions of concentrations above 30.9 g/L were too viscous to allow the measurement of conductivity.

4.5.2 Determination of overlapping C^* and entanglement C_e concentrations

The intrinsic viscosity $[\eta]$ was evaluated in terms of ionic strength at 25°C. Figure 4.2 (a) and (b) shows the determination of the intrinsic viscosity by extrapolating η_{sp}/C and $\ln \eta_r/C$ to the chitosan zero concentration for various ionic forces. In addition, $[\eta]$ was determined from the Solomon-Gatesman equation [39] at $C = 0.3$ g/L (Table 4.1). The three different methods resulted in similar values, as shown in Table 1. As expected the intrinsic viscosity is found to be greatly dependent on the ionic strength. When I increased from 9×10^{-3} to 0.46M, $[\eta]$ decreased from 2.9 to 0.71 L/g. The slight reduction of the $[\eta]$ value in the presence of NaCl can be explained by the fact that sodium acetate already screens most of the electrostatic repulsion. In acidic conditions, chitosan takes an expanded conformation because of the electrostatic repulsion [40], and adding salt results in a more compact structure related to enhanced chain flexibility, as reported by Tsaih and Chen [10]. Thus the intrinsic viscosity, which is related to the macromolecule volume in solution, reduces with increasing ionic strength. We have also measured the intrinsic viscosity in a 0.25M AcOH/0.25M AcONa solvent at 25°C ($[\eta] = 9.1$ dL/g) to evaluate the molecular weight of our chitosan. The calculated value (1.1×10^6 g/mol) was in fair agreement with the molecular weight of 8.5×10^5 g/mol measured in GPC, using the Mark-Houwink-Sakurada (MHS) constants of $K = 1.49 \times 10^{-4}$ (dL/g) and $a = 0.79$ proposed by Kasaai et al. [41]. In the MHS equation, Kasaai et al. used the weight average molecular weight (\overline{M}_w) instead of the viscosity-average molecular weight (\overline{M}_v).

The dependency of the polymer concentration on the viscosity can be expressed by the Huggins and the Kraemer equations (Equations 4.14 [42] and 4.15 [43], respectively):

$$\frac{\eta_{sp}}{C} = [\eta] + k'[\eta]^2 C \quad (4.14)$$

$$\frac{\ln \eta_{rel}}{C} = [\eta] - k''[\eta]^2 C \quad (4.15)$$

where k' is the Huggins constant, k'' the Kraemer constant and $k' + k'' = 0.5$ [39]. The constant k' has been found to be 0.35 in a good solvent and approximately 2.0 for a solid particle [3]. The magnitude of k' can be related to the breadth of the molecular weight distribution or branching of the solute [39]. In this work (Figure 2 (a) and (b)), $k' + k''$ was determined to be between 0.40 and 0.67 in the various ranges of the ionic strength. This deviation from the value of 0.5 is believed to be caused by the use of truncated expressions for the Huggins and Kraemer expressions. The Huggins constant k' increased from 0.28 to 0.67 by increasing the ionic strength from 9×10^{-3} to 0.46M, in agreement with other observations [3,44,45]. This indicates that the solubility of the chitosan molecules gets lower as the ionic strength increases. In other words, the polymer-solvent interactions are decreasing, but the polymer-polymer interactions, or association, are increasing with the ionic strength. We also observed that the Fuoss model (Equation 4.3) fitted well our viscosity data, showing $\eta_{sp} \sim C^{1/2}$.

The value of the intrinsic viscosity could be used to determine the overlap concentration (C^*) that is inversely proportional to the molecular weight [46]. The overlap concentration C^* can be determined using three different criteria, as stated in section 2.2, i.e. from $1/[\eta]$, from the point at which the variation of η_{sp} with $\{C[\eta] + k'(C[\eta])^2\}$ deviates from slope = 1 in a log-log plot (Figure 4.3 (a)), and at the concentration where $\eta = 2\eta_s$ (Figure 4.3 (b)). In addition, the entanglement concentration C_e was determined as the concentration at which the final linear domain begins in the log-log plot of η_{sp} and $C[\eta] + k_H(C[\eta])^2$, and as the concentration for which $\eta = 50\eta_s$ (Figure 4.3 (a) and (b) respectively). The various determined concentrations are presented in Table 2. The two critical concentrations (C^* and C_e) increase with increasing ionic strength (I), except for the method proposed by Desbrières [12] (using $k_H = 0.44, 0.60$ and 0.67 for $I = 0.12, 0.24$ and 0.46 M, respectively), which gives nearly

constant values, nevertheless very similar to the ones determined with the other methods. However, a slight variation with ionic strength is expected because of the molecular change of conformation from expanded to collapse structure, therefore the Desbrières method is not considered for the determination of the C^* and C_e dependence on ionic strength. The unentangled-semidilute regime is quite small ($8 < C_e/C^* < 18$) in the presence of salt, and similar to that of uncharged polymers ($5 < C_e/C^* < 10$), while in opposition to the salt-free regime that can be three to four decades wide ($10^3 < C_e/C^* < 10^4$) [18]. Both critical concentrations show a power-law relationship with ionic strength, with $C^* \sim I^{1/3}$ and $C_e \sim I^{1/9}$, therefore the entanglement concentration shows a smaller ionic strength dependence than the overlap concentration.

From the determined $[\eta]$, the radius of gyration $\langle R_G \rangle$ was calculated in terms of the magnitude of the ionic strength (Equation 4.1). The results using $\overline{M}_n = 3.1 \times 10^5$ g/mol are presented in Table 4.3. The radius of gyration abruptly decreases from 162 to 113 nm when I is increased from 9×10^{-3} to 0.12M. The radius of gyration further decreases to 101 nm for the ionic strength of 0.46M. It is generally accepted that an ionic strength of 0.05M is sufficient to screen most of the repulsive electrostatic interactions within polyelectrolytes, so further addition of salt does not have a strong impact on the radius of gyration of the molecules, similarly to the effect observed on the Debye screening length. The intrinsic viscosity can also be used to predict the stiffness of the polymeric molecules by determining the Kuhn length (b) and the persistence length (l_p). The Kuhn length was calculated using Equation 4.2 [8]. For the determination of DP , or degree of polymerization, we use the following equation:

$$DP = \frac{\overline{M}_n}{xM_1 + (1-x)M_2} \quad (4.16)$$

where x and M_1 are respectively the molar fraction and the molecular weight (161 g/mol) of the glucosamine unit, and M_2 is the molecular weight of the acetylglucosamine unit (203 g/mol). The DP determined for our material is 1890. The virtual bond length in Equation 4.2 was calculated from the result of Anthonsen et al. [8] and is 0.51 nm for

chitosan, regardless of the molecular weight, DDA and ionic strength. Thus, Equation 4.2 simplifies to:

$$b = \frac{\langle R_G \rangle^2}{161} \quad (4.17)$$

where the Kuhn length is only dependent on $\langle R_G \rangle^2$. As mentioned earlier, the persistence length (l_p) is $b/2$ for relatively stiff (wormlike) molecules. The value of the persistence length is shown to decrease from 81 to 32 nm with increasing ionic strength from 9×10^{-3} to 0.46M in Table 4.3, and is 24 nm for $1/\sqrt{I} = 0$ or $I = \infty$, corresponding to θ conditions. This result shows a similar trend as observed for sodium carboxymethyl cellulose, where the value of b ($= 2 l_p$) gradually decreased with increasing ionic strength [1]. The reduction of the persistence length in terms of the ionic strength indicates that the chitosan chain become more flexible when the repulsive potential is weakened. The persistence length of 24 nm in θ conditions is very similar to the one reported by Terbojevich et al. [47], i.e. 20 ± 2 nm for chitosan with DDA between 60 and 85%. It is, however, larger than other values reported in the literature [2]. A persistence length of 12 nm was given by hydrodynamic experiments in large excess salt [48], while a very low value of 2.5 nm was reported by Anthonsen et al. [8]. Based on multidetector steric exclusion chromatography, l_p was found constant for DDAs between 80 and 100% for a molecular weight of 10^5 to 10^6 g/mol, and equal to 5 nm from the radius of gyration analysis and 8 nm from intrinsic viscosity measurements [49]. Molecular modelling [50] also allowed the determination of intrinsic persistence length equal to 9 nm for 0% N-acetylated chitosan. It is not clear at this point why our estimated l_p value in salt excess is much larger than those reported, except for that of Terbojevich et al. [47].

As mentioned before, the persistence length l_p is a characteristic of the local stiffness of a polymer; for example, the larger the l_p value, the larger the viscosity of a solution for a given molecular weight dissolved at a given concentration [2]. For a polyelectrolyte, the persistence length l_p ($l_p = l_{p,0} + l_{p,e}$) is the contributions of two terms, the intrinsic persistence length ($l_{p,0}$) and the electrostatic persistence length ($l_{p,e}$). The

intrinsic $l_{p,0}$ is determined for a neutral equivalent chain (θ conditions). On the other hand, for a charged molecule such as chitosan in acidic aqueous solution, $l_{p,e}$ increases with increasing charge density and is dependent on the Debye screening length (k^{-1}) for stiff polyelectrolytes and flexible chains [51]. For example, $l_{p,e}$ shows a linear relationship ($l_{p,e} \sim k^{-1}$) for flexible polyelectrolyte. In our results, $l_{p,e}$ did show a linear relationship with k^{-1} in the range of $I = 0.12 - 0.46\text{M}$. Dobrynin et al. [18] also reported that the electrostatic repulsion length of a polyelectrolyte is assumed to be proportional to the Debye screening length.

4.5.3. Dynamic and steady shear rheological measurements in the entangled regime

In this work, all dynamic and steady shear rheological properties were measured for $C > C_e$. We have initially investigated the stability of the chitosan solutions under small deformation (0.1) and for a frequency of 1 rad/s at 25°C. The largest decrease in the complex viscosity (η^*) was for the 41.7 g/L chitosan solution, which decreased by 4 % during 3h (maximum measurement time) compared to the initial viscosity. The slight viscosity decrease has been attributed to the mechanical degradation of the chitosan molecules. Negligible variation due to storage at low temperature has been observed for storage time as long as two months, and evaporation was prevented during measurements.

Small amplitude oscillatory shear tests were performed to investigate the effect of chitosan concentration and ionic strength on the dynamic rheological properties of concentrated chitosan solutions. Figure 4.4 (a) and (b) show respectively the complex moduli G' , G'' and $\tan\delta$ as functions of frequency, in terms of chitosan concentration. Both G' and G'' moduli increase with increasing chitosan concentration at $I = 0.12\text{M}$ as shown in Figure 4.4 (a). At low chitosan concentration, the G' and G'' follow the typical power relationships with frequency in the terminal zone, i.e. $G' \sim \omega^2$ and $G'' \sim \omega^1$. In Figure 4.4 (b), $\tan\delta$ decreases with increasing chitosan concentration, indicating that the elasticity is enhanced by increasing polymer concentration. Figure 4.5 (a) and (b) show the effect of the ionic strength on G' , G'' and $\tan\delta$ for the highest chitosan concentration

(41.7 g/L). Both G' and G'' decrease with increasing ionic strength. In addition, $\tan\delta$ increases with increasing ionic strength. The reduction of the elasticity may result from the decrease in the number of interactions and entanglements between the chitosan molecules, due to the increased chain flexibility and reduction of molecular size.

Both G' and G'' were used to calculate the stress relaxation spectrum ($H(\tau)$). In Figure 4.6 (a) and (b) we present the time-weighted relaxation spectra $\tau(H(\tau))$ normalized by the zero shear viscosity, in order to compare the spectra on similar scales. We observe in Figure 4.6 (a) that the mean relaxation time τ_H (time corresponding to the peak in the spectra) increases with increasing chitosan concentration. The calculated spectrum of the lowest chitosan concentration (10.1 g/L) is, however, questionable since the mean relaxation time is outside the experimental window. Figure 4.6 (b) shows the effect of the ionic strength on the time-weighted normalized relaxation spectra. In either case the relaxation spectra show only one peak and remained unchanged by the chitosan concentration and ionic strength, indicating that the main relaxation mechanism is unchanged. This aspect is discussed further. However, the width of the spectra increases with chitosan concentration and decreasing ionic strength, and this is related to extra modes of relaxation due to enhanced polymer-polymer interactions, including entanglements. We have also presented in Figures 4.4 (a) and 4.5 (a) the calculated values of the dynamic moduli (G' and G'') using the determined stress relaxation spectra, and an excellent agreement is found.

As shown in Figure 4.7, τ_H , the mean relaxation time corresponding to the peak in the relaxation spectra, is proportional to chitosan concentration with an exponent slightly larger than 3, i.e. $\tau_H \sim C^{3.1}$. A similar power-law exponent (2.6) has been reported for the longest relaxation time ($\tau = 1/2\pi\omega_c$, with ω_c the frequency of G' and G'' cross-over) of a cationic polyacrylamide of 45% charge density, while it was reported to be 0.8 for a 10% charge density [23]. For uncharged polymers, a dependence of reptation time with concentration $\tau_{rep} \sim C^{2.8}$ have been determined for semi-dilute polystyrene solutions under good solvent conditions [52], while lower values of 1.4-1.7 have been reported for the terminal relaxation time of entangled polymer solutions [29].

On the theoretical side [21], a concentration independent relaxation time is predicted for polyelectrolytes in salt-free solutions, which is highly unusual, while the theory proposes $\tau \sim C^{1.5}$ for entangled uncharged polymers in good solvents. We also found that the concentration dependence of the mean relaxation time slightly increased with increasing ionic strength, in agreement with other reported experimental findings [23,53], and therefore approaching the predictions for uncharged polymers in good solvents.

Complex moduli G' and G'' measured in the linear regime can be presented in a Cole-Cole plot, and different polymer systems will show a power-law relationship ($G'' \sim G'^P$) [23,54]. Exponent P is equal to 0.5 for a one-mode Maxwell fluid:

$$G''^2 = G' (G_e - G') \quad (4.18)$$

or $\log (G'') = \frac{1}{2} \log (G') + \frac{1}{2} \log (G_e - G'),$

where G_e represents the plateau value of G' at high frequencies. Therefore Cole-Cole plots can be used to characterize deviations from the one-mode Maxwell model [23,54], using the generalized equation:

$$\log (G'') = P \log (G') + (1-P) \log (G_e - G') \quad (4.19)$$

in analogy with Equation 4.18, provided that $G'^{2P} \ll G_e^{2P}$.

Figure 4.8 shows the effect of chitosan concentration (C) and ionic strength (I) on the magnitude of the power-law index P . For all solutions, P was between 0.55 – 0.71, indicating that the characterized chitosan solutions deviates from the single mode Maxwell element behavior, as shown from the dynamic data vs. frequency (Figures 4.4 (a) and 4.5 (a)). This deviation is often observed for cross-linked and entangled polymer systems. The power-law index P increased with increasing chitosan concentration, denoting that the stress relaxation becomes multimodal due to the enhancement of molecular interactions. Even though the ionic strength effect on the value of P is not clearly demonstrated in Figure 4.8, the highest values of P were found for $I = 0.46\text{M}$ at the lowest chitosan concentrations (10.1 and 20.4 g/L). Increasing ionic strength provides a favorable environment for association between chitosan molecules through hydrophobic interactions and hydrogen bonding, resulting in a more complex system to relax from external forces and therefore multimodal relaxation. The presence of

hydrogen bonding in the chitosan solutions have been investigated using urea, a hydrogen bonding agent decomposer [55].

In order to identify the main relaxation mechanism illustrated by the mean relaxation time τ_H in Figure 4.6 (a) and (b), we have also examined the stress relaxation modulus $G(t)$, calculated from the evaluated relaxation spectra using Equation 4.6. Considering that at high salt content the behavior of polyelectrolyte solutions becomes similar to that of uncharged polymers [18], we have compared the behavior of the relaxation modulus of the chitosan solutions at high ionic strength to that of entangled linear polymer solutions and presented by Rubinstein and Colby [56]. The relaxation of entangled uncharged linear polymer solutions is characterized by three zones that differ on the length scale observed. At very short times, topological interactions are unimportant and dynamics are Rouse-like. The Rouse model predicts that the relaxation modulus on these short time scales decayed as $G(t) \sim t^{-1/2}$. However our measurements were not performed at high enough frequency to observe this regime. At the Rouse time of an entanglement strand, τ_e , the chain motion is topologically hindered and free Rouse motion is no longer possible. The value of the stress relaxation modulus at τ_e is the plateau modulus G_e . This rubbery plateau can span many decades in time. Past the plateau modulus, i.e. at times larger than the reptation time τ_{rep} , $G(t)$ can be approximated by the Doi-Edwards equation [57]:

$$G(t) = \frac{8}{\pi^2} G_e \sum_{odd p} \frac{1}{p^2} \exp\left(-\frac{p^2 t}{\tau_{rep}}\right) \quad (4.20)$$

In this work, the Doi-Edwards equation was used to calculate the stress relaxation modulus $G(t)$ and to compare its predictions with the experimental derived moduli obtained from the relaxation spectra. The plateau modulus G_e was estimated from the Cole-Cole plots (not shown) and Equation 4.19 ($G_e = 50, 220, 410$ and 660 Pa for the $10.1, 20.4, 30.9$ and 41.7 g/L polymer concentrations, respectively, at $I = 0.46M$), while the reptation time τ_{rep} was taken as the mean relaxation time τ_H of Figure 4.7. We present in Figure 4.9 the comparison of the calculated stress relaxation moduli from the experimental derived relaxation spectra (Equation 4.6) and from Doi-Edwards equation

(Equation 4.20) for various chitosan concentrations at $I = 0.46\text{M}$. The main observation to be made is that the chitosan solutions, even under large ionic force conditions, do not relax as simply predicted by the Doi-Edwards model for entangled linear uncharged polymers. This is most probably due to the association phenomenon between chitosan molecules that slows down relaxation. The dynamics of entangled solutions of associating polymers has been examined by Rubinstein and Semenov [58] and they have shown that the associating groups (stickers) along the chains are controlling the dynamics, and this behavior has been referred to as “sticky reptation”. It is interesting to mention that their proposed reptation time has a high dependency on concentration, i.e. $\tau_{rep} \sim C^\nu$ with $\nu = 1.44 - 4.48$ in good solvents, depending on the length of the strands between stickers and the entangled strands. Our demonstration therefore seems to show that the mean relaxation time τ_H determined from the stress relaxation spectra is related to the reptation regime.

We have also measured the viscosity as a function of steady shear rate. Figure 4.10 compares the steady shear and complex viscosities for the highest chitosan concentration solution (41.7 g/L) at various ionic strengths, and shows that the Cox-Merz rule is not entirely valid. These viscosities show some differences at low frequency and shear rate, though within the uncertainties on the measurements, but the differences become negligible at high deformation rate. From the viscosity curve, the shear-thinning power-law index (n) was characterized in terms of polymer concentration and ionic strength. As presented in Figure 4.11, n moderately increased with increasing ionic strength, but decreased strongly with increasing chitosan concentration. These effects can again be explained in terms of number of interactions and entanglements, which increases with chitosan concentration and restricts the motion of individual chains. It results in a longer time required to form new entanglements replacing those disrupted by the flow. Thus, the Newtonian behavior is lost progressively and shear-thinning, or non-linear effects, increase with increasing polymer concentration [59]. On the other hand, the number of chain entanglements decreases with increasing ionic strength due to the reduction of chain stiffness. Hence, the non-linear behavior becomes less important.

We show in Figure 4.12 the zero-shear viscosity (η_0) values determined from the area under the time-weighted relaxation spectrum curves (Equation 4.8). These values were compared with those fitted with the Carreau model (Equation 4.5) and were found in excellent agreement, suggesting that the reported relaxation spectra were valid. As for the mean relaxation time, the zero-shear viscosity is proportional to the chitosan concentration but to a larger exponent, i.e. $\eta \sim C^{4.1}$. This exponent is related to the number of interactions or contacts between macromolecular chains. Thus, a higher exponent means a larger number of interactions. In the concentrated region ($C > C_e$), Hwang et al. [19] reported an exponent of 3.94 for chitosan ($\overline{M}_w = 1.71 \times 10^6$ g/mol and DDA = 91%) in 0.1M AcOH/0.1M NaCl, while Desbrières [12] determined an exponent of 5.2 ($\overline{M}_w = 1.93 \times 10^5$ g/mol and DDA = 88%) in 0.3M AcOH/0.05M AcONa. Muthukumar, using a theory of dynamics of dilute and semidilute polyelectrolyte in excess salt, derived a $\eta \sim C^{4.25}$ dependence, similar to our results [60]. An exponent of 15/4 was predicted by Drobynin et al. for the reptation of a polyelectrolyte in a semidilute entangled solution in the presence of excess salt [18]. The fact that we find a higher exponent than the reptation-based prediction is explained in terms of additional interactions such as hydrogen bonding and hydrophobic interactions. As mentioned earlier, Amiji [27] also reported the existence of hydrophobic interactions for chitosan, which are not considered in the reptation model. The disagreement with the reptation-based predictions is a confirmation of the observations made on the stress relaxation modulus in Figure 9. It is interesting to compare again our experimental finding with the proposed sticky-reptation model of Rubinstein and Semenov [58] for associating polymers, which predicts a dependence of the zero-shear viscosity with polymer concentration $\eta \sim C^\mu$, with $\mu = 3.75 - 8.52$ in good solvents, therefore much higher than that for polyelectrolytes in excess salt. Hence, it is an additional confirmation of the presence of association phenomena in the chitosan solutions.

4.6. Conclusions

In this study, dynamics of entangled chitosan solutions have been investigated as a function of polymer concentration and ionic strength. Initially we determined the overlapping (C^*) and entanglement (C_e) concentrations as a function of ionic strength, and observed power-law relationships with $C^* \sim I^{-1/3}$ and $C_e \sim I^{-1/9}$. For the dilute solutions ($C < C^*$), the intrinsic viscosity was shown to decrease with increasing ionic strength as the chain became more flexible and compact with a reduction of the repulsive potential. The derived Kuhn length (b) and persistence length ($l_p = b/2$) showed the effect of ionic strength on the stiffness of the macromolecule. The l_p value decreased from 81 to 32 nm with increasing I from 9×10^{-3} to 0.46M, and the calculated persistence length in a θ solvent ($1/\sqrt{I} = 0$ or $I = \infty$) was 24 nm. White-like precipitates formed above $I = 0.46$ M. This precipitation was the results of increased polymer-polymer interactions over those of polymer-solvent through hydrophobic interactions and hydrogen bonding, and the decrease of the electrostatic repulsion by salt screening effect.

Dynamic rheological measurements were performed in the concentrated ($C > C_e$) domain, i.e. for $C > 7.5$ g/L. The lower concentrated solution (10.1 g/L) showed a typical viscoelastic solution behavior, i.e. $G' \sim \omega^2$ and $G'' \sim \omega^1$ at low frequencies. In general, the G' and G'' moduli decreased with increasing ionic strength. In addition, $\tan \delta$ increased with increasing ionic force, indicating that the elasticity of the chitosan solution was reduced. The stress relaxation spectra were calculated from the storage (G') and loss (G'') moduli data. The relaxation spectra showed only one peak and their shape remained unchanged by the chitosan concentration and ionic strength, indicating that the main relaxation mechanism was unchanged. However, the width of the spectra increased with chitosan concentration and decreasing ionic strength and this augmentation was related to extra modes of relaxation due to enhanced interchain interactions, including entanglements. The mean relaxation time (τ_H) was found to be proportional to the chitosan concentration to a power larger than 3, i.e. $\tau_H \sim C^{3.1}$. In Cole-Cole plots, the power-law index P ($G'' \sim G'^P$) was larger than $1/2$ for all chitosan solutions, indicating a

deviation from the single-mode Maxwell element behavior. The P value increased with increasing chitosan concentration, suggesting that the relaxation was getting more complex and multimodal. Results from the Cole-Cole plots and relaxation spectra were used to estimate the stress relaxation modulus. A comparison with predictions of the Doi-Edwards equation suggested that the relaxation of the chitosan solutions was more complex than reptation alone, and that the mean relaxation time τ_H was related to a sticky-reptation regime [58], due to the association nature of the polymer. The zero-shear viscosity also showed a power-law relationship with chitosan concentration, i.e. $\eta_0 \sim C^{4.1}$. Non-linearity effects in the shear viscosity increased with chitosan concentration and decreasing ionic strength.

4.7. Acknowledgements

The authors gratefully acknowledge the financial support of Conseil de Recherches en Pêche et en Agroalimentaire du Québec (CORPAQ). They also thank Dr. Stéphane Costeux for providing the program to calculate the complex moduli from the stress relaxation spectra, and the reviewers for their useful comments.

4.8. References

1. Roberts, G.A. E. (1992). *Chitin Chemistry*, 1st Ed., The Macmillan Press, London.
2. Brugnerotto, J., Desbrières, J., Heuz, L., Mazeau, K., & Rinaudo, M. (2001). Overview in structural characterization of chitosan molecules in relation with their behavior in solution. *Macromolecular Symposia*, 168, 1 – 20.
3. Park, J. W., Choi, K.-H., & Park, K. K. (1983). Acid-base equilibria and related properties of chitosan. *Bulletin of Korean Chemistry Society*, 4(3), 68 – 72.
4. Kasaai, M. R. (1999). Depolymerization of chitosan. *Doctoral Thesis*, Université Laval, Quebec, Canada.
5. Jackson, D. S. (1987). USA Patent 4,659,700.
6. Chaput, C., & Chenite, A. (2001). WO 01/41822 A1.
7. Chenite, A., Chaput, C., Wang, D., & Selmani, A. (2001). WO 01/3600 A1.

-
8. Anthonsen, M. W., Vårum, K. M., & Smidstrød, O. (1993). Solution properties of chitosans: conformation and chain stiffness of chitosans with different degrees of *N*-acetylation. *Carbohydrate Polymers*, 22, 193 – 201.
 9. Chen, R. H., & Tsaih, M. L. (2000). Urea-induced conformational changes of chitosan molecules and the shift of break point of Mark-Houwink equation by increasing urea concentration. *Journal of Applied Polymer Science*, 75(3), 452 – 457.
 10. Tsaih, M. L., & Chen, R. H. (1997). Effect of molecular weight and urea on the conformation of chitosan molecules in dilute solutions. *International Journal of Biological Macromolecules*, 20, 233 – 240.
 11. Wetton, R. E., Marsh, R. D. L., & Ven-de-Velde, J. G. (1991). Theory and application of dynamic thermal analysis. *Thermochimica Acta*, 175, 1 – 11.
 12. Desbrières, J. (2002). Viscosity of semiflexible chitosan solution: influence of concentration, temperature, and role of intermolecular interactions. *Biomacromolecules*, 3, 342 – 349.
 13. Mucha, M. (1997). Rheological characteristics of semi-dilute chitosan solutions. *Macromolecular Chemistry and Physics*, 198, 471 – 484.
 14. Wang, W., & Xu, D. (1994). Viscosity and flow properties of concentrated solutions of chitosan with different degrees of deacetylation. *International Journal of Biological Macromolecules*, 16(3), 149 – 152.
 15. Nystrom, B., Kjøniksen, A.-L., & Iversen, C. (1999). Characterization of association phenomena in aqueous systems of chitosan of different hydrophobicity. *Advances in Colloid and Interface Science*, 79, 81 – 103.
 16. Carreau, P. J., De Kee, D. C. R., & Chabra, P. R. (1997). *Rheology of Polymeric Systems: Principles and Applications*, Hanser Publishers, Munich, Germany.
 17. Fuoss R.M. (1951). Polyelectrolytes. *Discuss. Faraday Soc.*, 11, 125-135.
 18. Dobrynin, A.V., Colby, R. H., & Rubinstein, M. (1995). Scaling theory of polyelectrolyte solutions. *Macromolecules*, 28, 1859 – 1871.
 19. Hwang, J. K., & Shin, H. H. (2000). Rheological properties of chitosan solutions. *Korea-Australia Rheology Journal*, 12(3/4), 175 – 179.

-
20. Argüelles-Monal, W., Goycoolea, F. M., Peniche, C., & Higuera-Ciapara, I. (1998). Rheological study of the chitosan/glutaraldehyde chemical gel system. *Polymer Gels and Networks*, 6, 429 – 440.
21. Rubinstein M., Colby R.H., Dobrynin A.V. (1994). Dynamics of Semidilute Polyelectrolyte Solutions. *Phys. Rev. Lett.*, 73(20), 2776-2779.
22. Cox, W., & Merz, E. (1958). Correlation of dynamic and steady flow viscosities. *Journal of Polymer Science*, 28, 619 – 622.
23. Lauten, R. A., & Nyström, B. (1999). Linear and nonlinear viscoelastic properties of aqueous solutions of cationic polyacrylamides. *Macromolecular Chemistry and Physics*, 201(6), 677 – 684.
24. Kopperud, H. M., Hansen, F. K., & Nyström, B. (1998). Effect of surfactant and temperature on the rheological properties of aqueous solutions of unmodified and hydrophobically modified polyacrylamide. *Macromolecular Chemistry and Physics*, 199, 2385 – 2394.
25. Kulicke, W.-M., Arendt, O., & Berger, M. (1998). Rheological characterization of the dilatant flow behavior of highly substituted hydroxypropylmethylcellulose solutions in the presence of sodium lauryl sulfate. *Colloid & Polymer Science*, 276(7), 617 – 626.
26. Roth, T., Maier, D., Friedrich, C., Marth, M., & Honerkamp, J. (2000). Determination of the relaxation time spectrum from dynamic moduli using an edge preserving regularization method. *Rheologica Acta*, 39, 163 – 173.
27. Amiji, M. M. (1995). Pyrene fluorescence study of chitosan self-association in aqueous solution. *Carbohydrate Polymers*, 26, 211 – 213.
28. Mitchell, J.R., & Ledward, D. A. (1996). *Functional properties of food macromolecules*, Elsevier Applied Science Publishers, New York.
29. Ferry, J.D. (1980). *Viscoelastic properties of polymers*, J. Willey & Sons, New York.
30. Rinaudo, M., Pavlov, G., & Desbrières, J. (1999). Influence of acetic concentration on the solubilization of chitosan. *Polymer*, 40, 7029 – 7032.

-
31. Rinaudo, M., Pavlov, G., & Desbrières, J. (1999). Solubilization of chitosan in strong acid medium. *International Journal of Polymer Analysis and Characterization*, 5, 267 – 276.
32. Savarmand, S., Carreau, P. J., Bertrand, F., & Vidal, D. J.-E. (2003). Rheological properties of concentrated aqueous silica suspensions: Effects of pH and ions content. *Journal of Rheology*, 47(5), 1133 – 1149.
33. Lide, D. R. (2002/2003). *CRC Handbook of Chemistry and Physics: A Ready-Reference Book of Chemical and Physical Data*, 83rd Ed., CRC Press, 5-94.
34. Harned, H.S., & Owen, B.B., *The physical chemistry of electrolytic solutions*, Reinhold, New York (1943).
35. Hu, H., Hale, T., Yang, X., & Wilson, L. J. (2001). A spectrophotometer-based method for crystallization induction time period measurement. *Journal of Crystal Growth*, 232, 86 – 92.
36. Honerkamp, J., & Weese, J. (1993). A nonlinear regularization method for the calculation of relaxation time. *Rheologica Acta*, 32, 65 – 83.
37. Heimenz, P. C. (1977). *Principles of colloid and surface chemistry*, Marcel Dekker Inc., New York.
38. Desbrières, J., Marinez, C., & Rinaudo, M. (1996). Hydrophobic derivatives of chitosan: characterization and rheological behaviour. *International Journal of Biological Macromolecules*, 19, 21 – 28.
39. Solomon, O. F., & Ciută, I. Z. (1962). Détermination de la viscosité intrinsèque de solutions de polymères par une simple détermination de la viscosité. *Journal of Applied Polymer Science*, 6(24), 683 – 686.
40. Chen, R. H., & Lin, J. H. (1994). Effects of pH, ionic strength, and type of anion on the rheological properties of chitosan solution. *Acta Polymerica*, 45, 41 – 46.
41. Kasaai, M.R., Arul, J., & Charlet, G. (2000). Intrinsic viscosity-molecular weight relationship for chitosan. *Journal of Polymer Science: B: Polymer Physics*, 38, 2591 – 2598.

-
42. Huggins, M. L. (1942). The viscosity of dilute solutions of long-chain molecules. IV. Dependence of concentration. *Journal of the American Chemical Society*, 64(11), 2716 – 2718.
43. Kraemer, E. O. (1938). Molecular weights of cellulose and cellulose derivatives. *Industrial and Engineering Chemistry*, 30(10), 1200 – 1203.
44. Signini, R., Desbrières, J., Campana Filho, S. P. (2000). On the stiffness of chitosan hydrochloride in acid-free aqueous solutions. *Carbohydrate Polymers*, 43, 351 – 357.
45. Kjoniksen A.L., Nyström B., Iversen C., Nakken T., Palmgren O., Tande T. (1997). Viscosity of dilute aqueous solutions of hydrophobically modified chitosan and its unmodified analogue at different conditions of salt and surfactant concentrations, *Langmuir*, 13, 4948-4952.
46. Burnard, W. (2001). Structure formation by polysaccharide in concentrated solutions. *Biomacromolecules*, 2, 342 – 353.
47. Terbojevich, J., Cosani, A., Coio, G., Marsano, E., & Bianchi, E. (1991). Chitosan: chain rigidity and mesophase formation. *Carbohydrate Research*, 209, 251 – 260.
48. Pavlov G.M. (1995). *Cellulose and Cellulose Derivatives*, Ed. J.F. Kennedy, G.O. Phillips, P.O.W. Williams, L. Picullel. Woodhead, Cambridge, UK.
49. Rinaudo, M., Milas, M., & Le Dung, P. (1993). Characterization of chitosan. Influence of ionic strength and degree of acetylation on chain expansion. *International Journal of Biological Macromolecules*, 15, 281 – 285.
50. Mazeau, K., Perez, S., & Rinaudo, M. (2000). Predicted influence of N-acetyl group content on the conformational extension of chitin and chitosan chains. *Journal of Carbohydrate Chemistry*, 19(9), 1269 - 1284.
51. Ullner, M., Jönsson, B., Peterson, C., Sommelius, O., Söderberg, B. (1997). The electrostatic persistence length calculated from Monte Carlo, variation and perturbation methods. *Journal of Chemical Physics*, 107(4), 1279 – 1284.
52. Adam M., Delsanti M. (1979) Viscosity and reptation time in polystyrene-benzene semidilute solutions. *Journal de Physique-Lettres*, 40, 523-526.

-
53. Yamaguchi M., Wakutsu M., Takahashi Y., Noda I (1992). Viscoelastic properties of polyelectrolyte solutions. 2. Steady-state compliance. *Macromolecules*, 25, 475-478.
54. Thuresson K., Lindman, B., and Nyström, B. (1997). Effect of hydrophobic modification of a nonionic cellulose derivative on the interaction with surfactants. Rheology. *Journal of Physics and Chemistry B*:, 101, 6450 – 6459.
55. Cho J, Heuzey M.C., Bégin A., Carreau P.J. (in preparation).
56. Rubinstein M., Colby R.H., *Polymer Physics*, Oxford University Press, New York, 2003.
57. Doi, M., & Edwards, S. F. (1978). Dynamics of concentrated polymer systems. I. Brownian motion in the equilibrium systems. II. Molecular motion under flow. III. The constitutive equation. *Journal of the Chemical Society Faraday Transactions II*, 74, 1787 – 1832.
58. Rubinstein M., Semenov A.N. (2001). Dynamics of entangled solutions of associating polymers, *Macromolecules*, 34, 1058-1068.
59. Kjønsken, A. L., Nyström, B., Nakken, T., Palmgren, O., & Tande, T. (1997). Effect of surfactant concentration, pH and shear rate on the rheological properties of aqueous of a hydrophobically modified chitosan and its unmodified analogue. *Polymer Bulletin*, 38, 71 – 79.
- 60 Muthukumar M. (1997). Dynamics of polyelectrolyte solutions, *J. Chem. Phys.* 107 (7), 2619-2635.

Table 4.1. Intrinsic viscosity at 25°C.

Composition	I (M)	$[\eta]_1^*$ (L/g)	$[\eta]_2^{**}$ (L/g)	$[\eta]_3^{***}$ (L/g)	k'	k''
0.5M AcOH	9×10^{-3}	3.0	2.8	2.9	0.28	0.12
0.5M AcOH/0.1M AcONa	0.12	0.97	0.98	1.0	0.44	0.11
0.5M AcOH/0.1M AcONa/0.1M NaCl	0.24	0.79	0.80	0.83	0.58	0.05
0.5M AcOH/0.1M AcONa/0.3M NaCl	0.46	0.69	0.71	0.73	0.66	0.01

* $[\eta]_1$ from $\eta_{sp}/C \rightarrow 0$ (Equation 14)

** $[\eta]_2$ from $\ln \eta_r / C \rightarrow 0$ (Equation 15)

*** $[\eta]_3$ from $\sqrt{2(\eta_{sp} - \ln \eta_r)} / C$ (Solomon-Gatesman equation) at $C = 0.3$ g/L

Table 4.2. Overlap concentration (C^*) and entanglement concentration (C_e) as a function of ionic strength (I).

I (M)	C^*_1 (g/L)	C^*_2 (g/L)	C^*_3 (g/L)	C_{e1} (g/L)	C_{e2} (g/L)
9×10^{-3}	0.28	-	0.34	5.0	-
0.12	0.78	1.0	1.0	7.0	7.4
0.24	0.90	1.0	1.3	7.2	7.4
0.46	0.98	1.0	1.5	7.5	6.6

C^*_1 : from $\eta = 2\eta_s$

C^*_2 : Desbrières method [12]

C^*_3 : from $1/[\eta]$

C_{e1} : from $\eta = 50\eta_s$

C_{e2} : Desbrières method [12].

Table 4.3. Radius of gyration (R_G) and persistence length (l_p).

I (M)	R_G (nm)	l_p (nm)
9×10^{-3}	162	81
0.12	113	40
0.24	105	35
0.46	101	32
∞	\times	24
$I = \infty$ represents θ conditions.		

List of figures

Figure 4.1. Conductivity as functions of ionic strength (I) and chitosan concentration at 25°C.

Figure 4.2. Determination of the intrinsic viscosity for various ionic strengths at 25°C: (a) Huggins's representation, (b) Kraemer's representation.

Figure 4.3. (a) Dependency of the specific viscosity (η_{sp}) on $C[\eta]$ and on $C[\eta] + k'(C[\eta])^2$ at various ionic strengths, (b) Viscosity ratio (η/η_s) as functions of chitosan concentration (C) and ionic strength (I) at 25°C.

Figure 4.4. Effect of chitosan concentration at $I = 0.12$ M on (a) storage (G') and loss (G'') moduli as functions of frequency at 25°C. RS: relaxation spectrum, and on (b) $\tan\delta$ as a function of frequency at 25°C.

Figure 4.5. Effect of ionic strength (I) for a 41.7 g/L chitosan solution on (a) storage (G') and loss (G'') moduli as a function of frequency at 25°C. RS: relaxation spectrum, and on (b) $\tan\delta$ as a function of frequency at 25°C.

Figure 4.6. (a) Effect of chitosan concentration at $I = 0.12$ M on the time-weighted normalized stress relaxation spectrum, (b) Effect of ionic strength (I) for a 41.7 g/L chitosan solution on the time-weighted normalized stress relaxation spectrum.

Figure 4.7. Effects of chitosan concentration (C) and ionic strength (I) on the mean relaxation time (τ_H).

Figure 4.8. Power-law index P from the log-log plot of G' and G'' as functions of chitosan concentration (C) and ionic strength (I).

Figure 4.9. Calculated stress relaxation modulus from the experimental derived relaxation spectra (Equation 4.6) and Doi-Edwards equation (Equation 4.20) for various chitosan concentrations and $I = 0.46$ M.

Figure 4.10. Comparison of the complex viscosity and steady shear viscosity data of a 41.7 g/L chitosan solution for various ionic strengths.

Figure 4.11. Shear-thinning power-law index (n) as functions of chitosan concentration (C) and ionic strength (I).

Figure 4.12. Effects of chitosan concentration (C) and ionic strength (I) on the zero-shear viscosity.

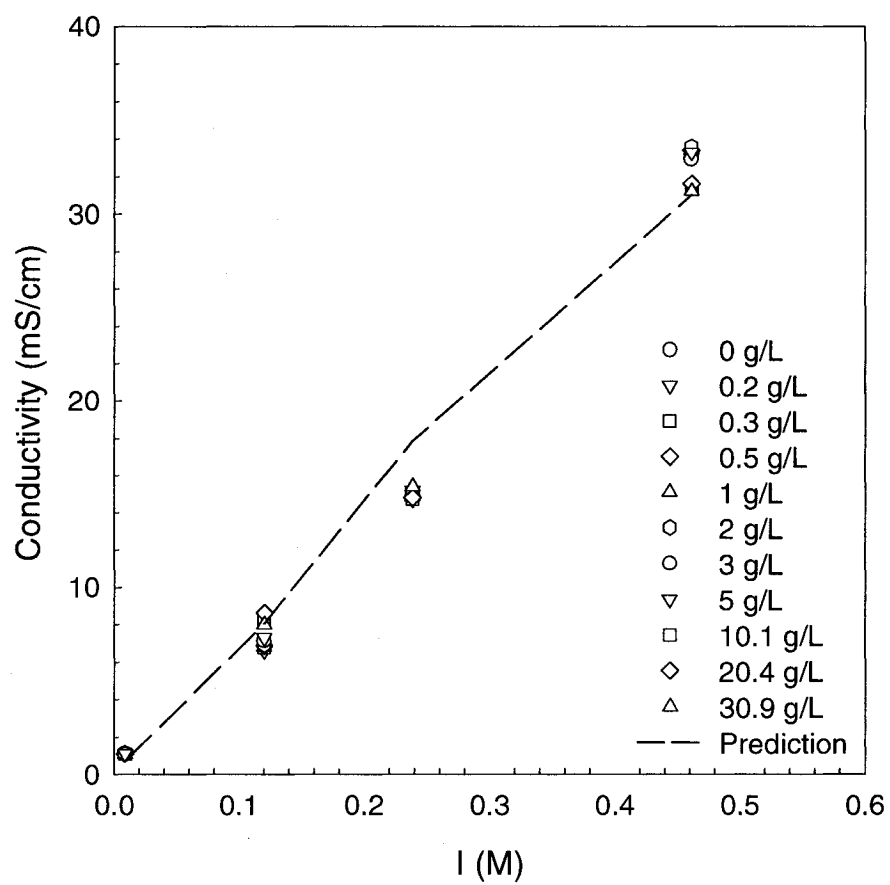


Figure 4.1. Conductivity as functions of ionic strength (I) and chitosan concentration at 25°C.

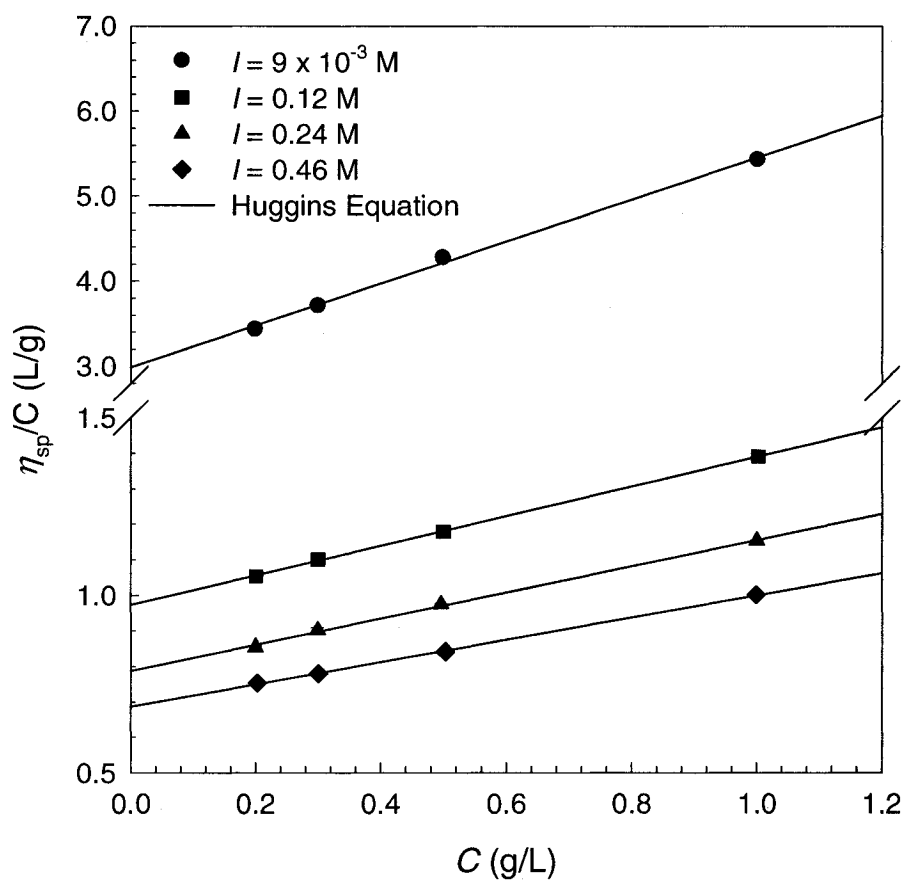


Figure 4.2. Determination of the intrinsic viscosity for various ionic strengths at 25°C: (a) Huggins's representation.

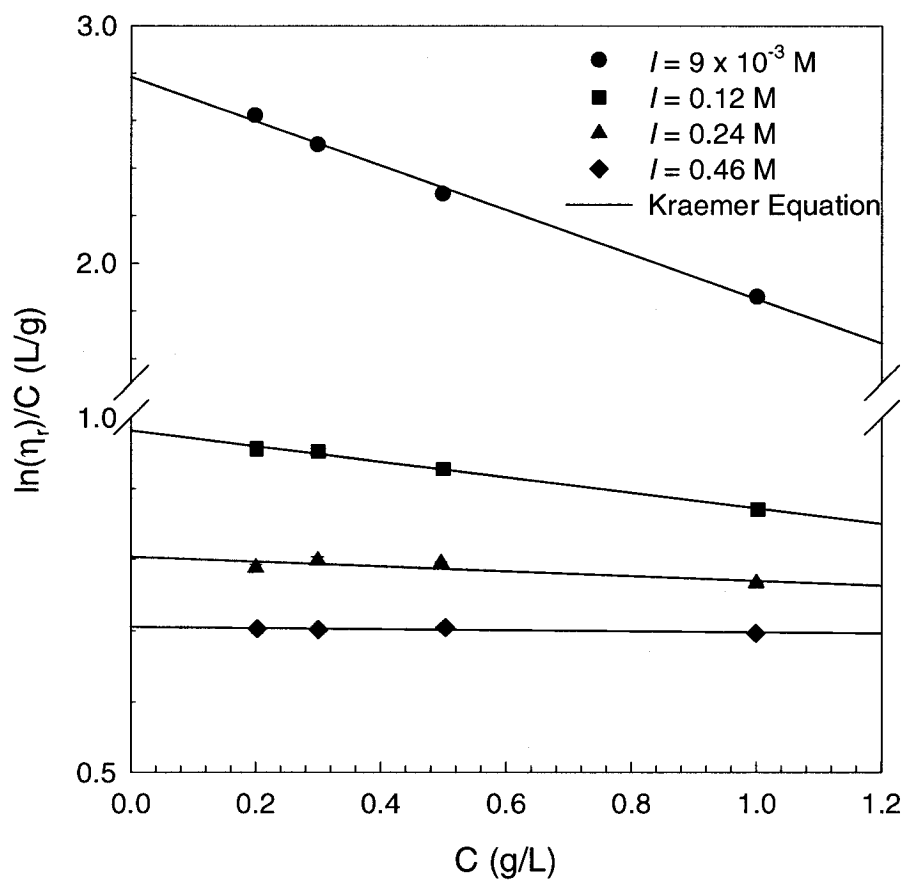


Figure 4.2. Determination of the intrinsic viscosity for various ionic strengths at 25°C:
(b) Kraemer's representation.

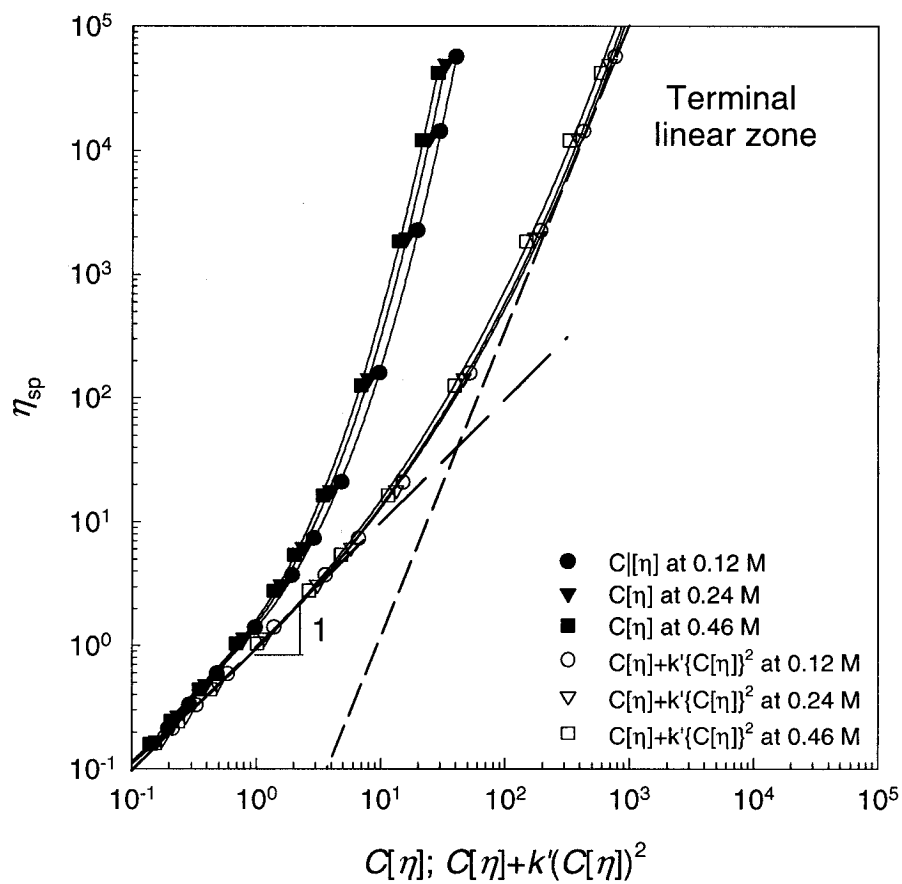


Figure 4.3. (a) Dependency of the specific viscosity (η_{sp}) on $C[\eta]$ and on $C[\eta] + k'(C[\eta])^2$ at various ionic strengths.

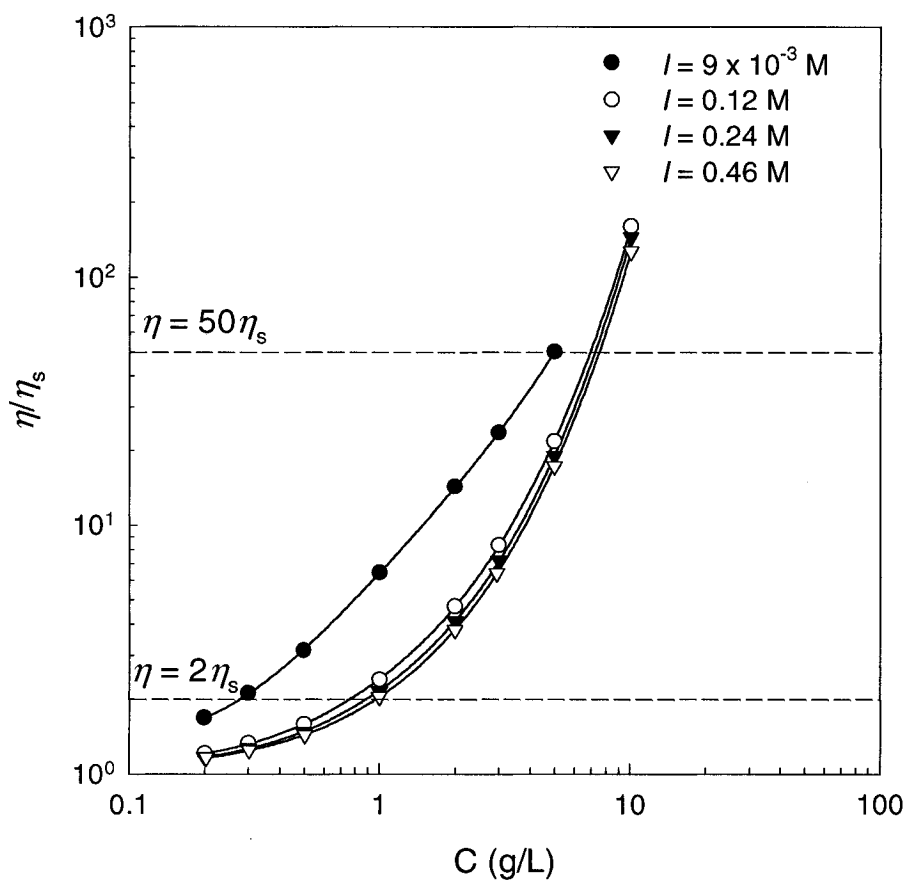


Figure 4.3. (b) Viscosity ratio (η/η_s) as functions of chitosan concentration (C) and ionic strength (I) at 25°C.

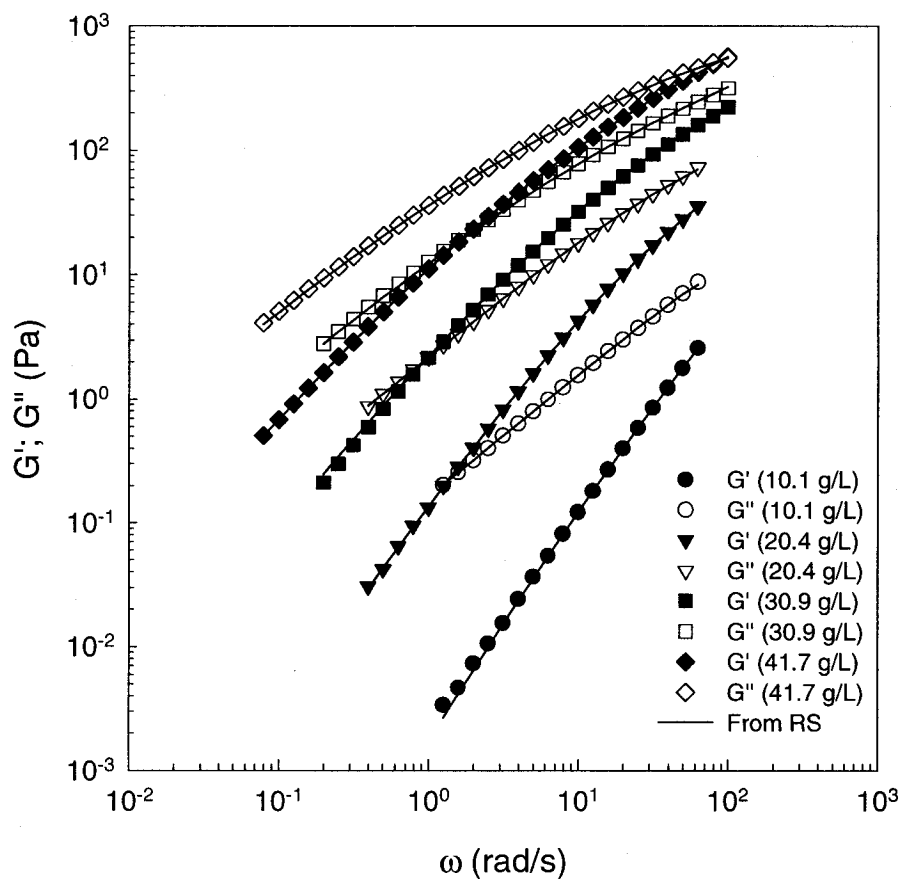


Figure 4.4. Effect of chitosan concentration at $I = 0.12$ M on (a) storage (G') and loss (G'') moduli as a function of frequency at 25°C . RS: relaxation spectrum.

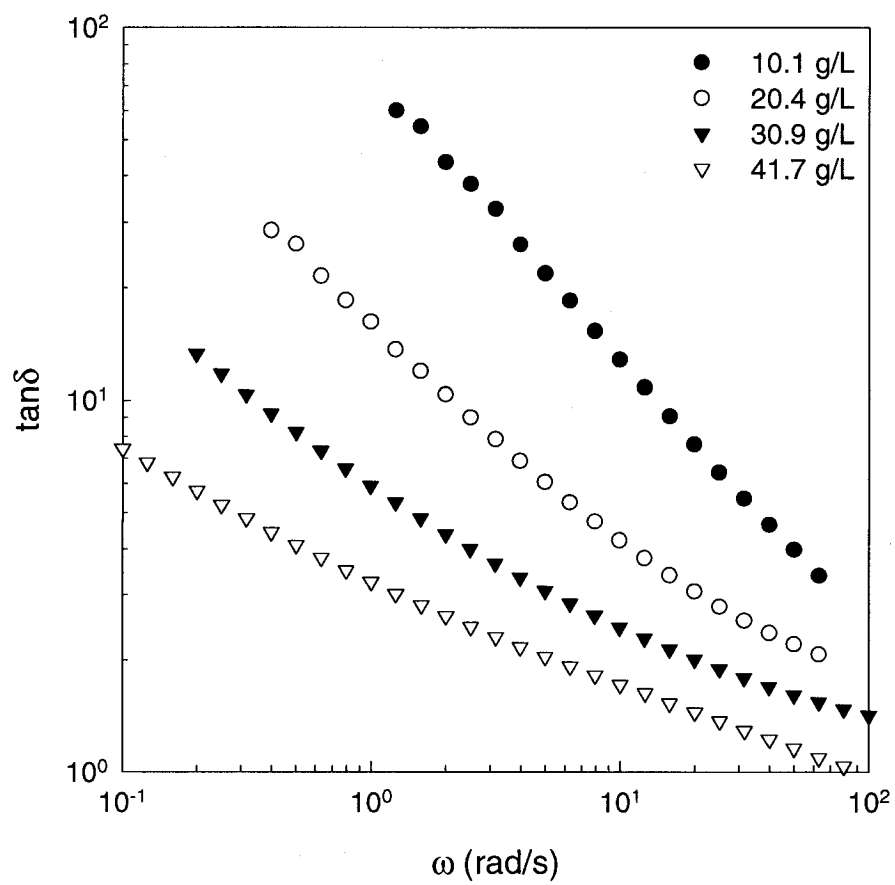


Figure 4.4. Effect of chitosan concentration at $I = 0.12$ M on (b) $\tan \delta$ as a function of frequency at 25°C .

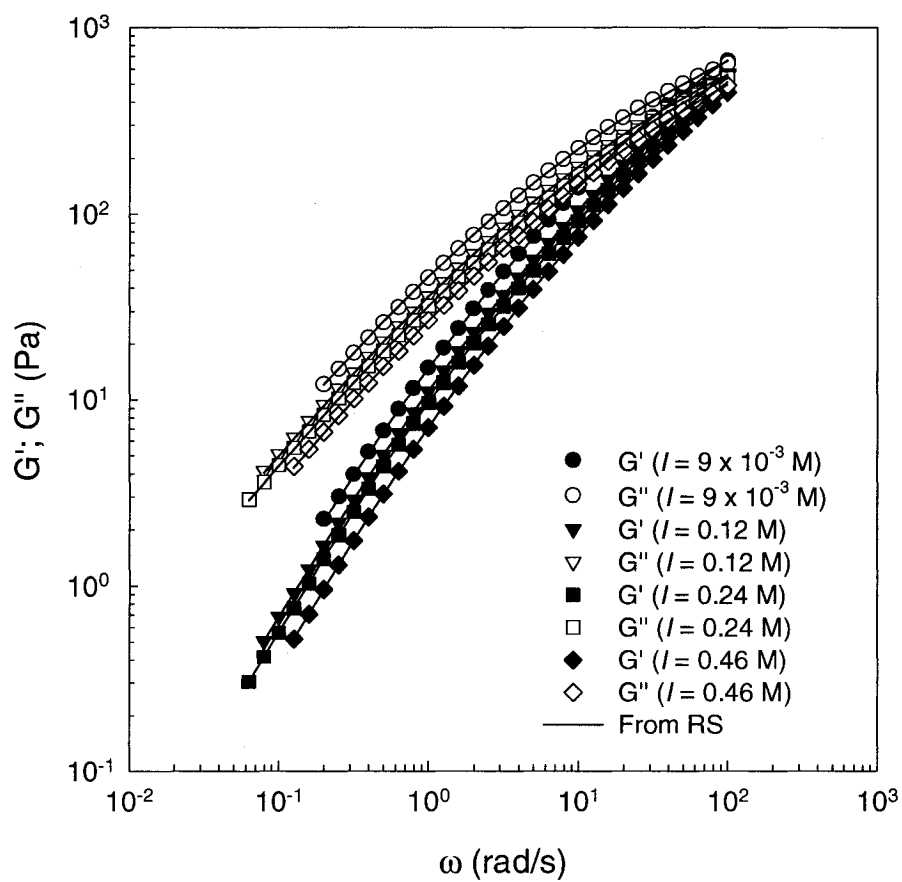


Figure 4.5. Effect of ionic strength (I) for a 41.7 g/L chitosan solution on (a) storage (G') and loss (G'') moduli as a function of frequency at 25°C. RS: relaxation spectrum.

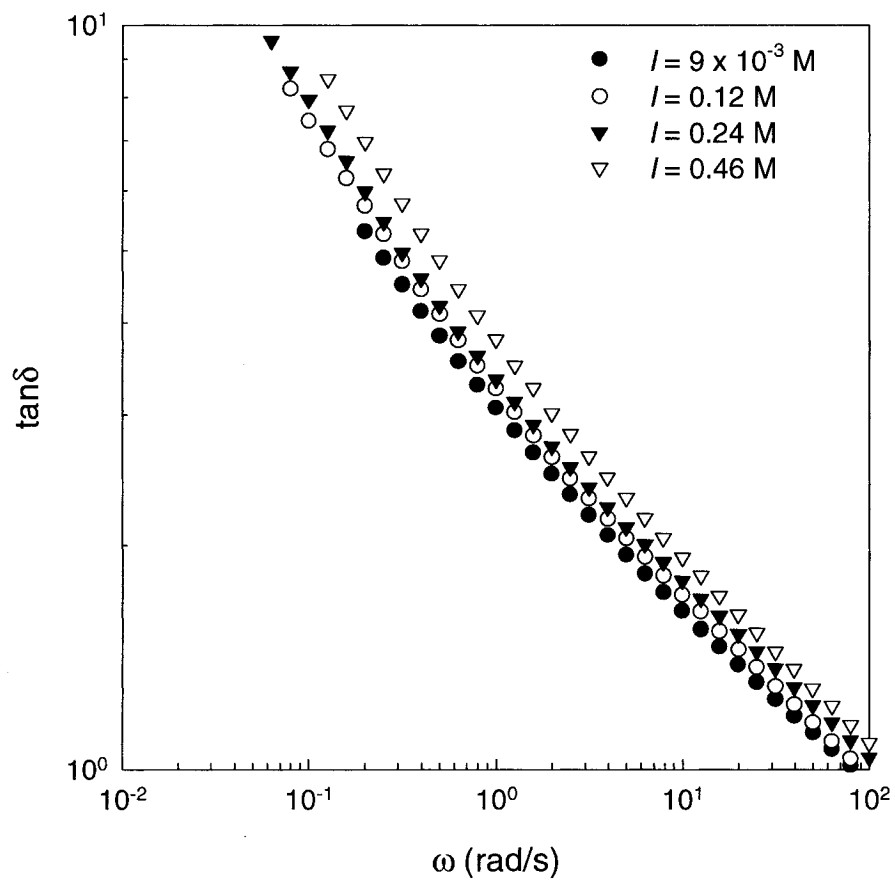


Figure 4.5. Effect of ionic strength (I) for a 41.7 g/L chitosan solution on (b) $\tan \delta$ as a function of frequency at 25°C.

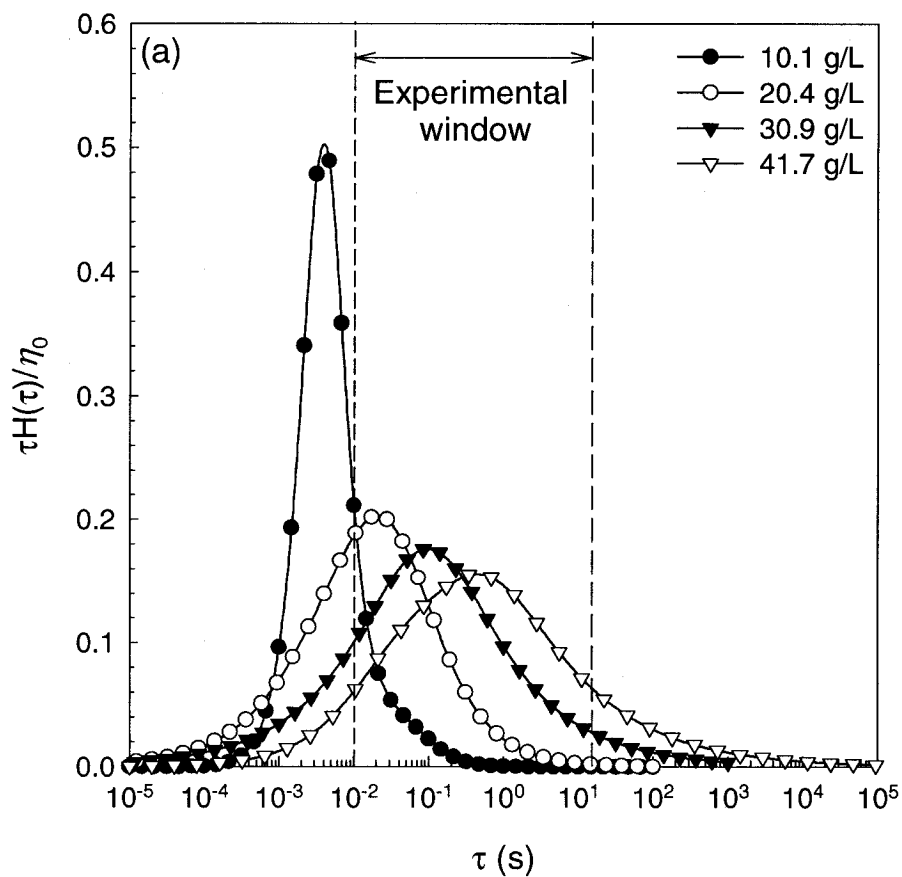


Figure 4.6. (a) Effect of chitosan concentration at $I = 0.12$ M on the time-weighted normalized stress relaxation spectrum.

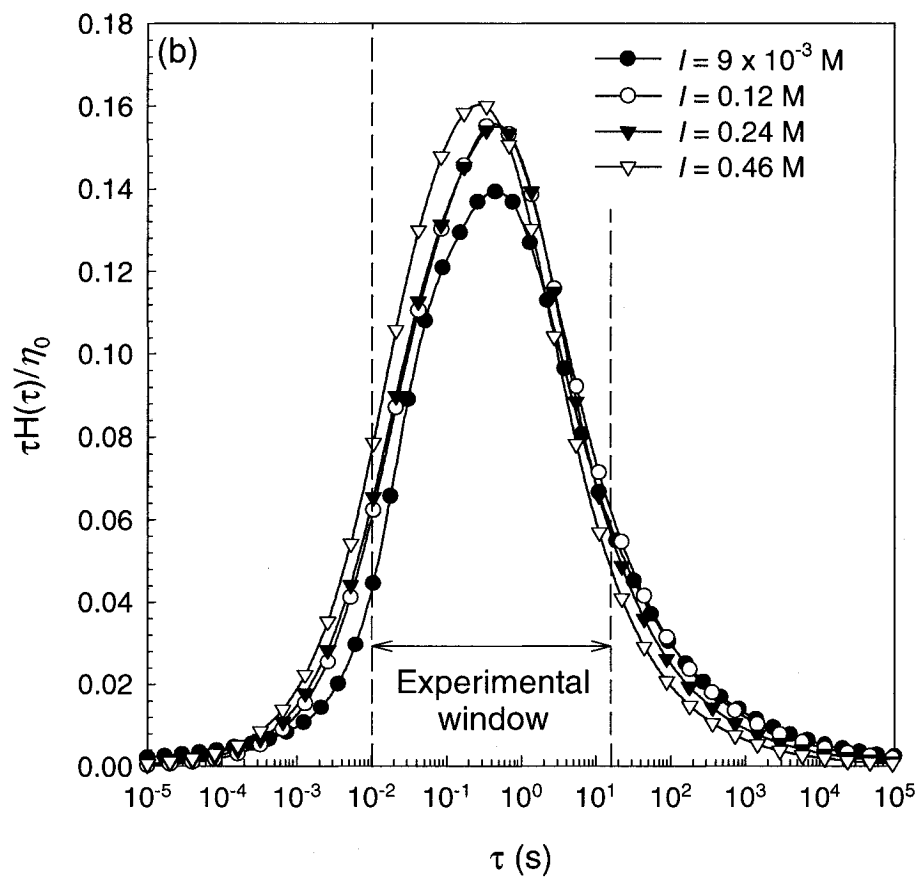


Figure 4.6. (b) Effects of ionic strength (I) for a 41.7 g/L chitosan solution on the time-weighted normalized stress relaxation spectrum.

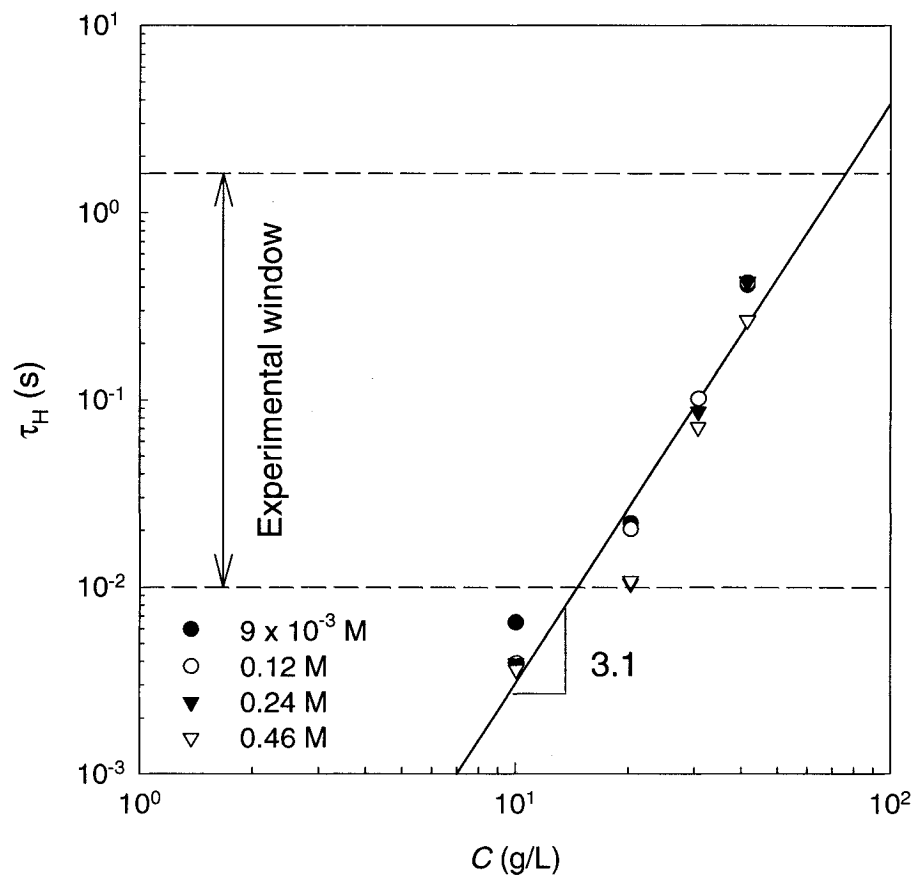


Figure 4.7. Effect of chitosan concentration (C) and ionic strength (I) on the mean relaxation time (τ_H).

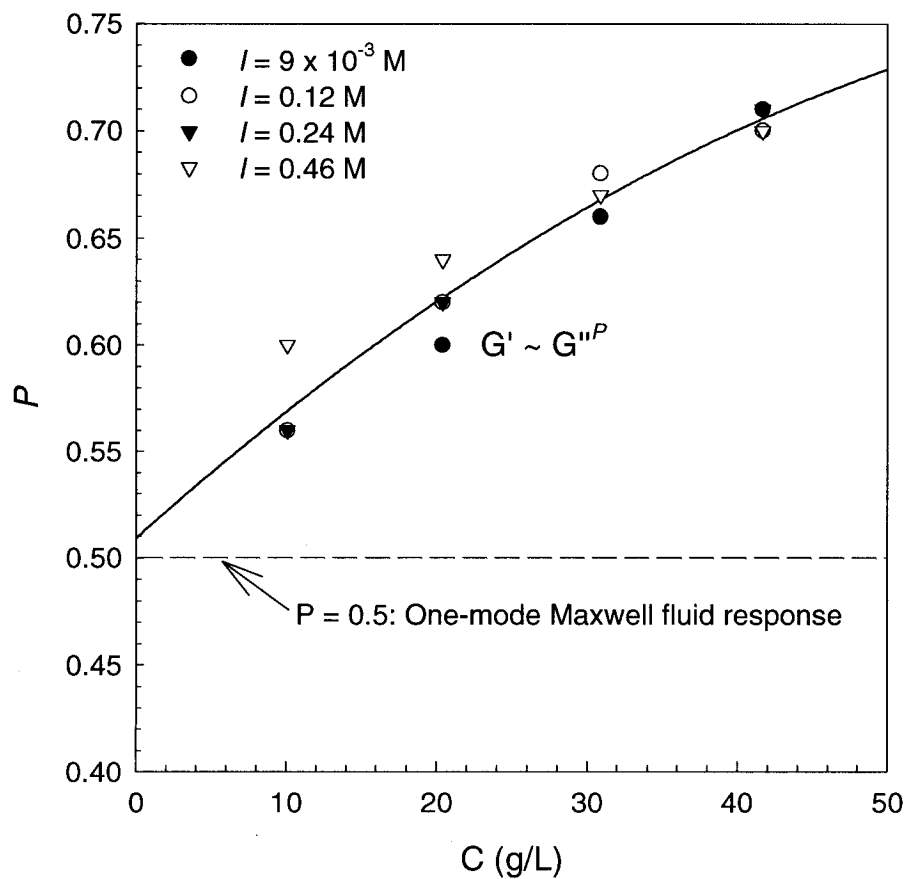


Figure 4.8. Power-law index P from the log-log plot of G' and G'' as functions of chitosan concentration (C) and ionic strength (I).

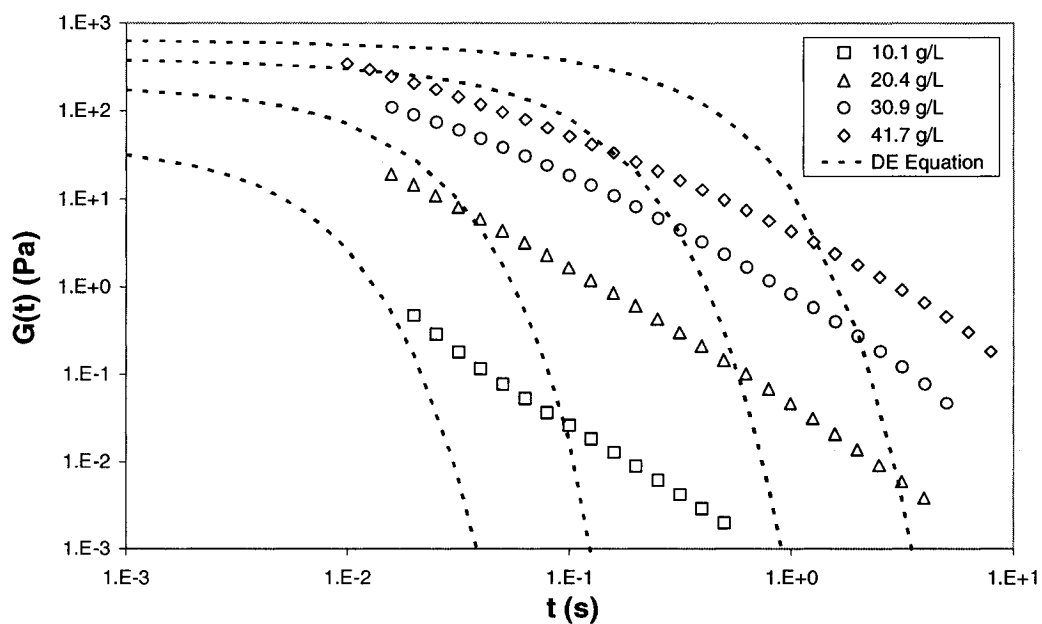


Figure 4.9. Calculated stress relaxation modulus from the experimental derived relaxation spectra (Equation 4.6) and Doi-Edwards equation (Equation 4.20) for various chitosan concentrations and $I = 0.46$ M.

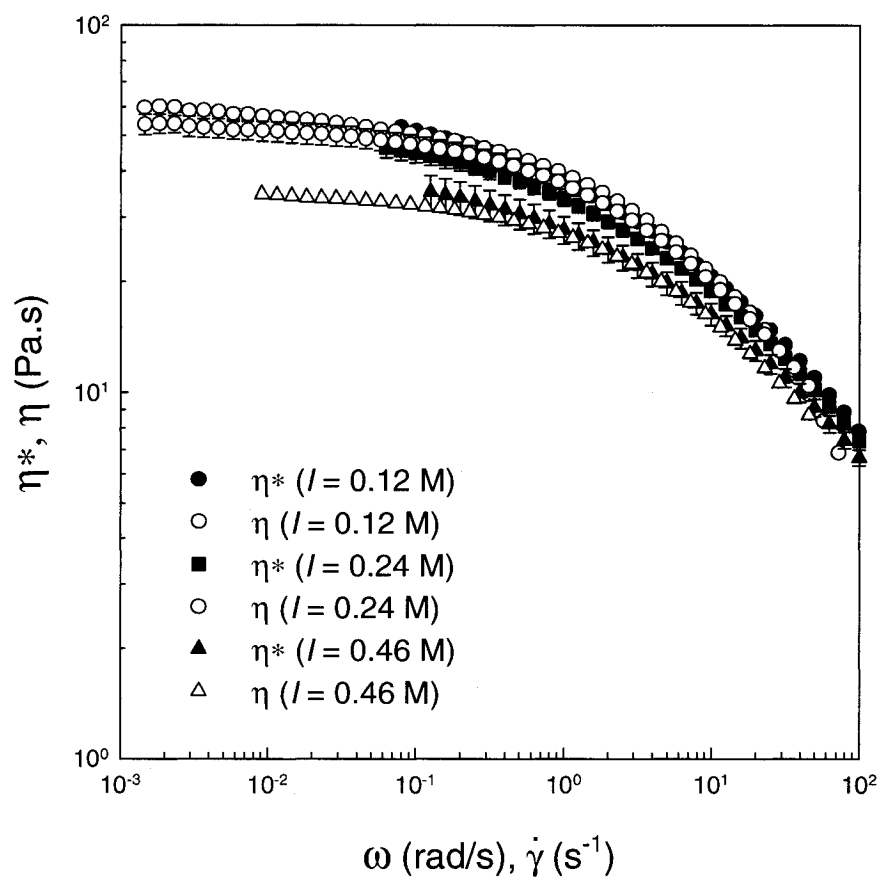


Figure 4.10. Comparison of the complex viscosity and steady shear viscosity data of a 41.7 g/L chitosan solution for various ionic strengths.

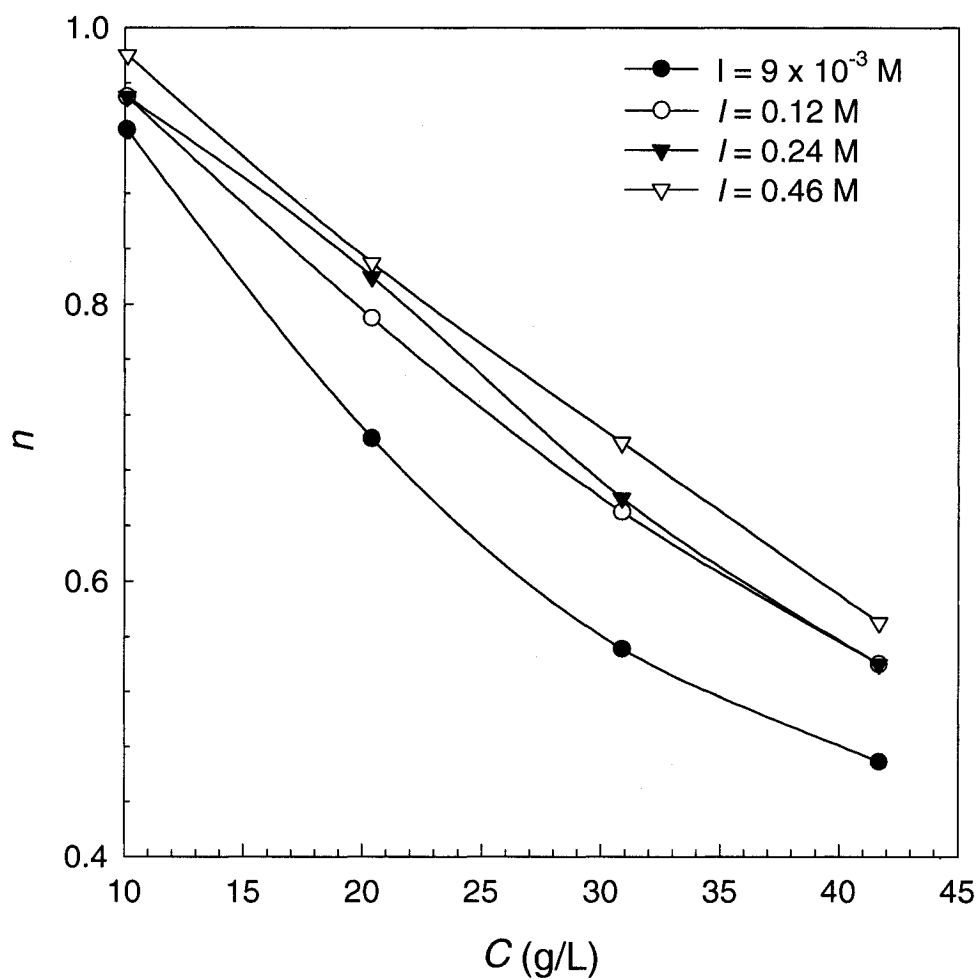


Figure 4.11. Shear-thinning power-law index (n) as functions of chitosan concentration (C) and ionic strength (I).

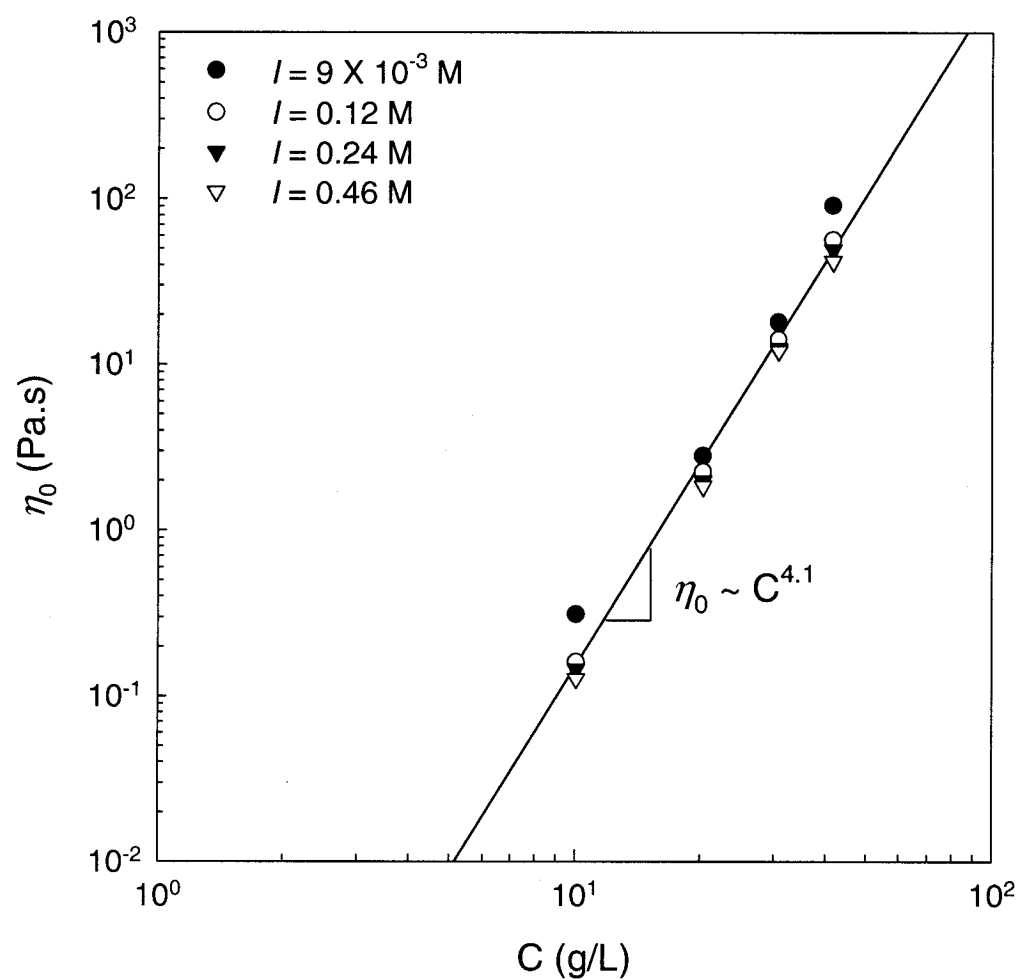


Figure 4.12. Effects of chitosan concentration (C) and ionic strength (I) on the zero-shear viscosity.

Chapter 5

Physical Gelation of Chitosan in the Presence of β -Glycerophosphate: The Effect of Temperature

Jaemyoung Cho¹, Marie-Claude Heuzey^{1*}, André Bégin² and Pierre J. Carreau¹

¹ CREPEQ, Department of Chemical Engineering, Ecole Polytechnique, P.O. Box 6079,
Station Centre-Ville, Montreal, QC, H3C 3A7, CANADA

² Food Research and Development Centre, 3600 Casavant Blvd West, Saint-Hyacinthe,
QC, J2S 8E3, CANADA

* Corresponding author. E-mail: marie-claude.heuzey@polymtl.ca; tel.: +1-514-340-4711 ext. 5930; fax: +1-514-340-2994

5.1. ABSTRACT

When adding β -glycerophosphate (β -GP), a weak base, to chitosan aqueous solutions the polymer remains in solution at neutral pH and room temperature while homogeneous gelation of this system can be triggered upon heating¹. It is therefore one of the rare true physical chitosan hydrogel. In this study, physicochemical and rheological properties of chitosan solutions in the presence of acetic acid and β -GP were investigated as a function of temperature in order to gain a better understanding of the gelation mechanisms. The gel structure formed at high temperature was only partially thermoreversible upon cooling to 5°C due to the existence of remaining associations, confirmed by the spontaneous recovery of the gel after break-up at low temperature. Increasing temperature had no effect on the pH values of this system, while conductivity (and calculated ionic strength) increased. Values from the pH measurements were used to estimate the degree of protonation of each species as a function of temperature. The decreasing ratio of $-NH_3^+$ in chitosan and $-OPO(O^-)_2$ in β -GP suggested reduced chitosan solubility along with a diminution of ionic interactions such as ionic bridging with increasing temperature. On the other hand the increased ionic strength as a function of temperature, in the presence of β -GP, enhanced screening of electrostatic repulsion and increased hydrophobic effect, resulting in favorable conditions for gel formation. Therefore, our study suggests that hydrophobic interactions and reduced solubility are the main driving force for chitosan gelation at high temperature in the presence of β -GP.

5.2. INTRODUCTION

Chitosan is a biopolymer prepared from crustaceans using a series of chemical treatments. As chitin, it belongs to the family of the linear copolymers of β -(1 \rightarrow 4)-2-amino-2-deoxy-D-glucan (GlcN or glucosamine units) and β -(1 \rightarrow 4)-2-acetamido-2-deoxy-D-glucan (GlcNAc or acetylglucosamine units). An important characteristic of the molecule is the degree of deacetylation (DDA), or the fraction of glucosamine units in the chemical structure². The copolymer is generally accepted as “chitosan” when the DDA is larger than 50%³. Chitosan is known to be non-toxic, biocompatible and biodegradable, and because of its various bioactivities has been used in nutraceutic, medical, cosmetic and pharmaceutical applications^{4,5,6}. Chitosan can be studied under various physical states depending upon polymer concentration, DDA, *pH*, ionic strength and temperature. For *pH* below its *pK_a* (*pH* < 6.2), chitosan is water-soluble and positively charged following the protonation of the free amine groups (-NH₂), causing electrostatic repulsion between the protonated amines and consequently between the molecules^{7,8}. Screening of the electrostatic repulsion by excess salt leads to the formation of white-like precipitates⁹. Chitosan gels can be obtained by increasing polymer concentration (concentration-induced gelation)^{10,11} or by control of the *pH*¹². The addition of a base will obviously increase the *pH* but can also reduce the electrostatic repulsion between chitosan molecules and eventually lead to the formation of a gel-like structure above a *pH* of 6.2. Recently, a homogenous thermoreversible gel system was prepared by neutralizing highly deacetylated semi-diluted chitosan solutions with a weak base, β -glycerophosphate (β -GP)¹. The system remained in solution at

physiological pH ($= 7.2$) and room temperature, but changed into a gel upon heating at physiological temperature ($= 37^{\circ}C$), undergoing therefore a heat-induced gelation. When the temperature decreased, the chitosan gel returned to the solution state under particular conditions. It is one of the rare true chitosan physical hydrogel, obtained without any cross-linking agent, in the same line as the one proposed very recently by Montembault et al.¹³

The gelation of the chitosan- β -GP system may involve several interactions such as screening of electrostatic repulsion, “ionic” cross-linking, hydrophobic effect and hydrogen bonding interactions. β -GP, a weak base ($pK_a = 6.65$ at $25^{\circ}C$)^{14,15} can increase the pH of chitosan solutions around neutrality. It is negatively charged in solution, and thus may screen the electrostatic repulsion between chitosan molecules in its monovalent form or induce ionic bridging in its divalent one. Since chitosan presents hydrophobic ($-CH_3$) and hydrogen bonding favoring groups ($-OH$, $-NH$, and $-C=O$)², three-dimensional networks can also form by hydrogen bonding and/or hydrophobic effect. Even though several possible interactions have been proposed to explain the gelation of the chitosan- β -GP system^{1,16}, the exact mechanisms have not been established. Studying the effect of temperature may help understanding which interactions predominate. For example, the ionization of chemical species in solution is very sensitive to temperature and the change in ionization will affect the ionic strength and consequently electrostatic repulsion between chitosan molecules. It will also play a role on the multivalent ionization of β -GP, and therefore on possible ionic bridging. In addition, temperature is related to the intensity of hydrogen bonding and hydrophobic effect. Therefore, the aim of this study is

to gain insight into the gel formation mechanisms of chitosan in the presence of acetic acid and β -GP. For this purpose, we have characterized key physicochemical and rheological properties of chitosan systems as a function of temperature. The measured pH and conductivity served to determine the degree of ionization of each species and to evaluate the systems ionic strength. Rheological measurements were also used to characterize the gelation process and to determine gel cohesion energy.

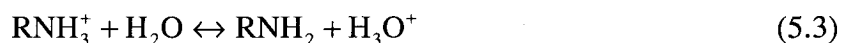
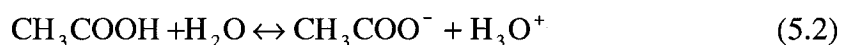
5.3. THEORETICAL BACKGROUND

Temperature controls acids dissociation constants K_a s ($pK_a = -\log K_a$). The dependence on temperature can be estimated by the following equation¹⁷:

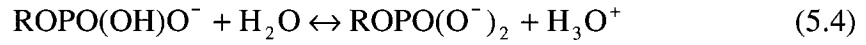
$$\Delta G = -RT \ln K_T = 2.303RTpK_T \quad (5.1)$$

where ΔG represents the change in Gibbs free energy of the equilibrium reaction of acid dissociation, R the gas constant ($8.314 \text{ J mol}^{-1} \text{ K}^{-1}$), T the absolute temperature and pK_T the pK_a at a given temperature. Thus, if the pK_a and ΔG values for a substance are known at some temperature, the pK_a can be estimated at another temperature. The pK_a and ΔG of the species used in this work, i.e. acetic acid, chitosan and β -GP, at a reference temperature of 298.15 K, are presented in Table 5.1^{2,14,15}.

To determine the degree of ionization of a substance under specific conditions, the chemical equilibrium reaction should be known. For acetic acid and chitosan, the acid-base equilibrium reactions¹⁸ are respectively:



Likewise, we can determine the ionization of β -glycerophosphoric acid $((\text{HOCH}_2)_2\text{CHOPO}(\text{OH})_2)$. At the $p\text{H}$ used in our study, β -GP is found either in monovalent or divalent form according to the equilibrium given by the pK_{a2} :



For a Brønsted acid, the ionization of each chemical species can be estimated from the Henderson-Hasselbalch equation¹⁹:

$$pH_T = pK_T + \log\left(\frac{[\text{Conjugate base}]}{[\text{Acid}]}\right) \quad (5.5)$$

where the pH_T and pK_T values are temperature-dependent, and the acid form for the glucosamine monomers is RNH_3^+ . From the above expressions, the degree of ionization (I_D) can be expressed as follows:

$$I_D = \frac{10^{pH_T - pK_T}}{10^{pH_T - pK_T} + 1} \quad \text{for acetic acid and } \beta\text{-GP} \quad (5.6)$$

$$I_D = \frac{1}{10^{pH_T - pK_T} + 1} \quad \text{for chitosan} \quad (5.7)$$

The concentration C of the ionized species is determined from the following equation:

$$C = I_D C_A \quad (5.8)$$

where C_A represents the total concentration of the dissociated and undissociated forms of each species in solution. Finally, the ionic strength of the sample (I_s)²⁰ can be evaluated as followed:

$$I_s = \frac{1}{2} \sum_i \{C_i Z_i^2 + 10^{-pH_T}\} \quad (5.9)$$

where C_i and Z_i are the concentration and charge number of ion i , respectively. In this expression, the contribution of the protons H^+ is accounted in the separate term on the right-end side. We note that the contribution of the glucosamine units is included in Equation 5.9. The ionic strength is expressed in a molarity basis.

5.4. EXPERIMENTS

5.4.1. *Materials*

The chitosan used in this study was purchased from Marinard Biotech (Rivière-aux-Renards, QC). Its degree of deacetylation is 93% and weight-average molar mass (\overline{M}_w) 8.54×10^5 g/mol ($\overline{M}_w / \overline{M}_n = 2.76$). The degree of deacetylation (DDA), or fraction of glucosamine units, was obtained from colloidal titration with polyvinyl sulfate potassium, initially standardized with cethylpyridinium chloride. For determining the molecular weight, size exclusion chromatography measurements were conducted with an Ultrahydrogel™ 500 Column (Waters Co., Milford, MA) in 0.25M acetic acid / 0.25M sodium acetate using dextran standards. Acetic acid (99.7%, Sigma-Aldrich Canada Ltd, Oakville, ON) was used to dissolve the chitosan, while disodium- β -GP (Glycerol 2-phosphate disodium salt hydrate: $C_3H_7Na_2O_6P \cdot xH_2O$: FW: 216.04, Sigma-Aldrich Canada Ltd, Oakville, ON) was used to adjust the pH of the chitosan solutions.

5.4.2. *Chitosan solutions preparation*

Chitosan (2g) was dissolved in 1 w/v% acetic acid aqueous solution (98mL) using a laboratory magnetic stirrer (PC-420 Corning® Stirrer/Hot Plate, Corning Inc.,

MA) at 50 RPM for 4h at room temperature. Then, β -GP (16g) was added very slowly under rapid stirring to increase the pH of the chitosan solution up to 6.9 without causing immediate precipitation or gelation at room temperature. The concentration of the final solution was recalculated in molarity taking into account the increased volume due to the addition of β -GP. The compositions of the successive solutions are summarized in Table 5.2, along with the nomenclature adopted for the various samples. During the stirring process, the containers of the solutions were covered with aluminum foil to prevent evaporation. After mixing, the chitosan solutions were left for 3h to degas without stirring at room temperature and stored in a refrigerator ($T \sim 5^{\circ}\text{C}$) overnight before the gelation tests. All samples were used within one week in order to avoid degradation effects.

5.4.3. *pH and conductivity measurements*

All solutions were characterized in terms of pH and conductivity as a function of temperature. A water bath (model BT-15, Cole-Parmer, IL, USA) was used to control temperature at a constant heating rate ($0.8^{\circ}\text{C}/\text{min}$) and all measurements were recorded in a continuous manner in order to simulate the heat-induced gelation process. The temperature range used was $0\text{-}55^{\circ}\text{C}$ for pH measurements (pH -meter, Hanna Ltd., Àrvore - Vila do Conde, Portugal) and $0\text{-}75^{\circ}\text{C}$ for conductivity (conductance meter, model 35, YSI Inc., Yellow Springs, OH). Since the conductance meter used was linearly temperature compensated (referenced to 25°C), we applied the following equation to recover the conductivity at a given temperature:

$$\kappa_T = \kappa_{25}[1 + \alpha(T - 25)] \quad (5.10)$$

with κ_{25} the conductivity referenced to 25°C, κ_T the conductivity measured at a given temperature T , and α the temperature coefficient of variation²¹. The choice of different temperature ranges was a consequence of the different limitations of the respective electrodes. The pH values were used to estimate the ionization of each chemical species (Equations 5.6 and 5.7) and the ionic strength of the various solutions (Equation 5.9) in terms of temperature. The conductivity measurements as a function of temperature were used to corroborate the estimated evolution of the ionic strength.

5.4.4. Rheological measurements

The rotational rheometer used in this study is a stress-controlled instrument (AR-2000, TA Instruments, New Castle, DE) with a Couette geometry. Mineral oil covered the surface of the chitosan solutions and gels in order to prevent evaporation during the tests. The effect of the mineral oil on the measurements was shown to be negligible. The dynamic mechanical properties of the chitosan- β -GP (10C-69GP-15Ac) system were characterized in the solution and gel states by small amplitude oscillatory shear. During the gelation process, the evolution of the rheological properties was investigated as a function of temperature by oscillatory shear measurements. Gelation tests were carried out by increasing the temperature from 5 to 90°C with a constant heating rate (1°C/min). Small deformation (γ_o) of 0.01 and low frequency (ω) of 6.28 rad/s were used in order not to disturb the gel formation during these tests. The gelation temperature (T_{gel}) was determined as the crossover point of the storage (G') and loss (G'') moduli ($\tan\delta = 1$),

despite of the slight dependency on the frequency. The thermoreversibility of the gels was investigated by decreasing the temperature from 90 to 5°C at the same rate (1°C/min). After the cooling cycle, the resulting system was characterized using frequency sweeps at 5°C. The effect of high deformation causing breakage of the gels was also investigated, along with the following recovery.

5.5. RESULTS

5.5.1. Heat-induced gelation and partial thermoreversibility

The evolution of the storage (G') and loss (G'') moduli upon temperature increase and decrease is shown in Figure 5.1 (a) and (b) for G' and G'' , respectively, for the 10C-69GP-15Ac system. The resulting curves can be divided into three regions according to the temperature range during the heating process. In Region 1, the chitosan- β -GP sample showed a viscoelastic fluid-like behavior ($G' < G''$), and both G' and G'' moduli decreased with increasing temperature. This is the common behavior of a polymer solution²². In the case of a polyelectrolyte such as chitosan, the chain flexibility and compactness of polymer molecules in solution increases with increasing temperature, causing the reduction of the molecular volume²³. In addition, increasing temperature generally decreases the volume of a molecule due to decreasing hydrogen-bonded hydration water²⁴, and results in a decrease of the rheological parameters. The chitosan- β -GP system could show a fluid-like behavior at a pH above its pK_a in this temperature range owing to the mild alkalinity of GP. The minima in G' and G'' values were preceded by very sharp decreases. This phenomenon was also reported by Sarkar²⁵. He

interpreted it as the precipitation of a small fraction of the polymer. Region 2 represents the temperature range where both storage (G') and loss (G'') moduli abruptly increased upon heating due to the fast formation of the three-dimensional network. However, the growth rate of G' was much larger than that of G'' in this region, indicating that the evolution of the gel structure mainly contributed to the increases of the elasticity in the system²⁶. The gelation temperature was determined at 72°C ($\pm 1^\circ\text{C}$) from the crossover point of storage (G') and loss (G'') moduli. In the last zone (Region 3), the much slower gelation was caused by the lower diffusivity that resulted from the viscosity increase during the network formation.^{27,28}

By the cooling process, the thermoreversibility of the gel was investigated. As shown in Figure 5.1, both G' and G'' moduli gradually decreased with decreasing temperature. However, the crossover between G' and G'' was not observed and the G' modulus remained larger than G'' , even at the lowest temperature (5°C). Figure 5.2 clearly illustrates the difference in the rheological behavior before gelation and after gelation at 5°C. The chitosan solution (before gelation) showed a typical fluid-like behavior with $G' \ll G''$, and $G' \sim \omega^2$ and $G'' \sim \omega^1$ in the terminal zone, i.e. at low frequency. However, after heat-induced gelation and cooling to 5°C, the elastic modulus remained larger than G'' and the dependency on frequency of both moduli ($G' \sim \omega^{0.11}$ and $G'' \sim \omega^{0.27}$) was much smaller than before gelation. This indicated that the gel formed was not completely thermoreversible to the original solution state. The hysteresis in the dynamic moduli between the heating and cooling processes may be due to the existence of some associated aggregates or weak connections that have not completely

disassociated^{22,29,30,31}. While the chitosan gel formed during the heating process was found to be opaque and hard, it became transparent, sticky and elastic-like upon cooling. The change in the turbidity of the chitosan- β -GP gel upon cooling was related to the reduction of the size of the junction zones in the network.

5.5.2. Non-isothermal kinetics of gelation

The kinetics of the nonisothermal gelation of chitosan were modeled using the data of the elastic modulus G' along with a combination of the Arrhenius equation and a time-temperature relationship, initially proposed in the scope of polymer crystallization and adapted for the case of cold-induced gelation^{32,33,34}:

$$\ln\left(\frac{1}{G'^n} \frac{dG'}{dt}\right) = \ln k_0 - \left(\frac{E_{ag}}{RT}\right) \quad (5.11)$$

For heat-induced gelation, the equation is rewritten as:

$$\ln\left(\frac{1}{G'^n} \frac{dG'}{dt}\right) = \ln k_0 + \left(\frac{E_{ag}}{RT}\right) \quad (5.12)$$

in order to account for a positive activation energy. In this equation n is the reaction rate or Avrami exponent, t the time, k_0 the Arrhenius frequency factor, E_{ag} the activation energy for gelation, and RT have their usual significance as in Equation 5.1. The Avrami exponent n represents both the dimension r of the growing crystallites and the type of nucleation s ($n = r + s$)³⁵. Parameter r is 1 for rods, 2 for discs and 3 for spheres, while s is either 0 for predetermined (nuclei already present) or 1 for sporadic nucleation (nuclei arise and their number increases linearly with time).^{35,36}. To evaluate the activation

energy for gelation from this equation, one needs to guess first the value of the Avrami exponent n , a complex and difficult task because of n dependency on temperature. Thus, in this work we have assumed that the Avrami exponent n was 2, as frequently proposed for gelation^{32,33,34}.

To determine the derivative term in Equation 5.12, the storage modulus was plotted as a function of time and fitted using a polynomial regression, and this polynomial was differentiated. Figure 5.3 shows the semi-log plot of $1/G'^2 dG'/dt$ vs. $1/T$. Two regions clearly appear according to the gelation rate, as seen previously in Figure 5.1 (a). We determined the activation energy for gelation from the slope of Regions 2 and 3, obtaining 3080 and 170 kJ/mol ($k_0 \approx 0$ (Pa.s)⁻¹), respectively. The very large activation energy calculated for chitosan in Region 2 indicates that the development of intermolecular interactions is not favoured energetically and is only possible when enough thermal energy is added to the system. In the slow gelation regime (Region 3), the evolution of the three-dimensional physical network is energetically easier, i.e. that it requires less thermal activation. However, viscosity increase eventually hinders the diffusion of the molecules and remarkably slows down the gelation process. In order to compare these values with other polysaccharides systems, we examined the work of Lopes da Silva et al.³² and Fu et al.³³ who studied nonisothermal cold-induced gelation kinetics of HMP (high-methoxyl pectin) and LMP (low-methoxyl pectin), respectively, with a cooling rate of 0.5°C/min. For 1% HMP/ 60% sucrose, the activation energy was 132 kJ/mol ($k_0 = 5 \times 10^{14}$ (Pa.s)⁻¹) between 90 and 62°C, and 27.6 kJ/mol ($k_0 = 1.8 \times 10^{-2}$ (Pa.s)⁻¹), between 50 and 20°C³². For LMP, the gelation could also be described by a

two-step process corresponding to temperature ranges of 70-50°C in the first region ($E_{ag} = 111-311$ kJ/mol) and 50-20°C in the second one ($E_{ag} = 39-67$ kJ/mol)³³. These reported values are much lower than the ones determined for the chitosan- β -GP system. This disparity may be explained by the different gelation modes considered, i.e. cold-induced and heat-induced, and the different interactions involved. Gelation at low temperature is generally related to hydrogen bonding, which becomes negligible at high temperature.

5.5.3. Characterization of the gel strength and recovery

The effect of strain on the gel obtained after the cooling process is shown in Figure 5.4 (a). The complex modulus G' remained constant at low strain, but abruptly decreased at strain larger than 0.65 where break-up occurred. However, the loss modulus G'' was constant in the whole range of strain. The decrease in G' can be explained in terms of disruption of interactions. Links between particles can be stretched up to a certain maximum. Once this limit is reached, the network is destroyed, though not necessarily irreversibly as seen below (Figure 5.4 (b)). The critical strain (γ_c) at which a polymeric system begins to show non-linear viscoelastic behavior (in this case gel break-up) can be used to calculate the gel cohesion energy³⁷:

$$E_c = \int_0^{\gamma_c} G'_c \gamma_c d\gamma_c = \frac{1}{2} \gamma_c^2 G'_c \quad (5.13)$$

where E_c is the cohesion energy and G'_c the storage modulus at the critical strain. The cohesion energy is related to the energy involved in the formation of physical crosslinks between the polymer chains. In this study, G'_c was evaluated as 225 Pa, and E_c

calculated as 48 J/m^3 . This value is extremely high compared to that obtained for a 5% wt aqueous solution of poly(N,N-diethylacrylamide) in water ($5 \times 10^{-3} \text{ J/m}^3$)³⁵, and this denotes much stronger physical crosslinks between the polymer chains. If we convert the cohesion energy in kJ/mol using a density of 1 g/cm^3 for the polymer, we obtain $\sim 4 \text{ kJ/mol}$ to break the crosslinks, a value that is almost three orders of magnitude smaller than the energy initially required to form the gel.

Following the strain sweep experiment of Figure 5.4 (a), oscillatory shear flow at a strain amplitude of 0.01 was imposed on the sample. Figure 5.4 (b) presents the recovery of the storage (G') and loss (G'') moduli at 5°C after the gel break-up. Recovery of the gel was instantaneous, and the storage modulus was shown to continuously increase (even after a day, no equilibrium value was observed), while the loss modulus increased only in the initial stage of the recovery test and then slightly decreased. In the whole time range, G' was larger than G'' and $\tan \delta$ gradually decreased during the recovery test, indicating increased elasticity due to the evolution of the gel structure. This evolution is due to the reformation and rearrangement of the junctions, showing the spontaneous nature of the gelation process once the system has been heated once.

5.5.4. Effect of temperature on pH and conductivity

The pH and conductivity of the various solutions were simultaneously measured as functions of temperature. Figure 5.5 (a) shows the effect of temperature on pH. Adding the polymer to the acetic acid aqueous solution resulted in a pH increase from

3.2 to 4.5 at 25°C, due to the protonation of the free amine groups in the chitosan molecules. Wang¹⁶ reported that the addition of β -GP to chitosan solution increased the pH value to a physiologically acceptable level around 6.8, as observed in Figure 5.5 (a), due to the high buffering capacity of β -GP in this range of pH. Temperature affected pH differently depending upon the chemical composition of the solutions (Figure 5.5 (a)). For 15Ac and 10C-15Ac, the pH values decreased with increasing temperature, since the dissociation of acetic acid and chitosan (Equations 5.2 and 5.3) increased with temperature (section 5.5.5). However, the pH of 10C-69GP-15Ac was nearly independent of temperature because of the high buffering capacity of β -GP at this pH. Figure 5.5 (b) presents the variation of the conductivity of each solution as a function of temperature. The strongest temperature-dependency was shown with the solution containing β -GP, with a strong conductivity increase as a function of temperature. This result is compared with the evolution of the ionic strength in the following section.

5.5.5. Determination of the degree of ionization and solution ionic strength

The degree of ionization of each species was calculated in terms of temperature and pH. For this calculation, the pK_a values were evaluated at various temperatures using Equation 5.1. Then, an arbitrary pH was chosen and the ionization was estimated using Equations 5.5 - 5.9. The results of these calculations are shown in Figure 5.6. For AcOH and β -GP, the ionization increased with increasing pH and temperature. Regardless of temperature, the estimated ionization was fully achieved above a pH of 7 for AcOH (Figure 5.6 (a)) and a pH of 9 for GP(-2) (divalent β -GP) (Figure 5.6 (c)).

However, the ionization approached zero for $pH < 2$. The ionization was also more sensitive to pH than to temperature. Chitosan showed an opposite behavior, as seen in Figure 5.6 (b). The degree of ionization of the polymer decreased with increasing temperature and pH . The chitosan was fully ionized below a pH of 3 and fully neutral above a pH of 9, with the effect of pH being more significant than that of temperature, similarly to acetic acid and β -GP. The effect of temperature on the ionization of chitosan and the acids was however slightly higher when the pH of the solution was at the pK_a of the compounds, as observed in Figure 5.6.

To evaluate the ionic strength of the solutions, the ionization of each substance was calculated using the experimental temperature and pH values, and the ionic strength was computed using Equation 5.9. Figure 5.7 shows the calculated ionic strength as a function of temperature. For solutions 15Ac and 10C-15Ac, the temperature almost did not affect the ionic strength. However, the ionic strength of solution 10C-69GP-15Ac was strongly temperature-dependent. These results are in agreement with the conductivity measurements shown in Figure 5.5 (b).

5.6. DISCUSSION

For chitosan-based systems, gelation can occur by a combination of charge neutralization along with ionic, hydrogen bonding and hydrophobic interactions. Chenite et al.¹ suggested that the chitosan gel in the presence of β -glycerophosphate may be formed by screening of the electrostatic repulsion and possible ionic interactions between $-NH_3^+$ in chitosan and $-O^-$ in glycerophosphate. Mi et al.^{38,39} reported the

occurrence of ionic interactions between positively charged chitosan molecules and negatively charged tripolyphosphates using FTIR spectra analysis. Even though a different kind of phosphate was used in our study, a large quantity of $\text{ROPO}(\text{O}^-)_2$ was present in solution, similarly to tripolyphosphate. Therefore, ionic interactions between chitosan and β -GP may be considered as a possible contribution to the gel structure. The effect of temperature on ionic interactions can be investigated more specifically by comparing the ratio (R) of positively charged glucosamine units in the chitosan molecules and divalent β -GP anions ($\text{GP}(-2)$). As shown in Figures 5.8 (a) and (b), even though the divalent ionization of β -glycerophosphate strongly increased as a function of temperature, the protonation of chitosan decreased and the ratio of the two was a decreasing function, indicating a reduction of possible ionic interactions at high temperature. Consequently the contribution of ionic cross-linking did not seem to be the main driving force for gelation.

Chitosan possesses hydrophobic ($-\text{CH}_3$) and hydrogen bonding favoring groups ($-\text{OH}$, $-\text{NH}$, and $-\text{C}=\text{O}$)². Amiji⁴⁰ stated that chitosan could be associated by intermolecular hydrophobic interactions between acetylglucosamine groups. In addition, Philippova et al.⁴¹ showed using pyrene fluorescence the existence of intermolecular hydrophobic aggregates both in chitosan and in hydrophobically modified chitosan. Chenite et al.¹ also commented that adding β -GP could control hydrophobic effect and hydrogen bonding interactions. It is well known that increasing ionic strength and temperature increases hydrophobic effect⁴². We showed that the addition of β -GP increased $p\text{H}$ and ionic strength in Figures 5.5 and 5.7, establishing therefore a favorable

environment to form a gel structure by the screening of electrostatic repulsion and enhanced hydrophobic interactions.

On the other hand, increasing temperature decreases hydrogen bonding interactions⁴³. At low temperature (room temperature or below), water molecules are presumed to form enclosed structures that surrounds the polymer chains²². Increasing temperature enhances the vibration and rotation energy of water, exceeding the ability of weak hydrogen bonds to orient the dipolar water molecules around the polymer chains⁴⁴. As a consequence, the energized water molecules surrounding the polymer are removed and the dewatered hydrophobic polymer segments begin to associate with each other. Finally, the reduction of hydrogen bonding interactions at high temperature may also cause a change in the chitosan molecular conformation. At low temperature, chitosan adopts a compact conformation due to intramolecular hydrogen bonds, and the physical junctions that could form a gel are confined inside the coil. It is therefore a poor conformation to build-up a 3D structure due to the difficulty of creating contacts between the junction zones. Increasing temperature reduces the number of intramolecular hydrogen bonds so that the chitosan molecules can unfold freely, thus making gelation more favorable.

Finally, the examination of Figure 5.6 (b) shows that at *pH* around 6 – 7, the ionization of chitosan decreases from values above 50% to values below 40%. At these low levels of protonation, the solubility of chitosan would decrease drastically² and contribute to gelation with increasing temperature.

In summary, the increase in ionic strength observed at high temperature for the system chitosan-acetic acid- β -glycerophosphate (10C-69GP-15Ac) provides a favorable environment to form a gel structure through the following mechanisms: a) the reduction of chitosan solubility, b) the diminution of the electrostatic repulsion forces by a screening effect, and c) the enhancement of polymer-polymer interactions over those of polymer-solvent via hydrophobic effect. Therefore, hydrophobic interactions are assumed to be the main driving force to form the gel consisting of chitosan and β -glycerophosphate at high temperature. In a subsequent paper⁴⁵, we investigate further the effect of temperature on hydrogen bonding interactions using urea, presumably a hydrogen bonding disrupting agent⁴⁶.

5.7. CONCLUSIONS

In this work, physicochemical and rheological properties of chitosan aqueous solutions in the presence of acetic acid and β -glycerophosphate were investigated as a function of temperature. The evolution of these properties during the gelation process revealed information regarding the mechanisms of gel formation.

During rheological measurements, the chitosan-acetic acid- β -glycerophosphate system showed typical viscoelastic solution behavior at 5°C. Upon temperature increase, three regions were defined according to mechanical properties: 1) a liquid-like behavior at low temperature, 2) a fast gelation process, and 3) a slow gelation process. The gelation temperature was determined at 72°C ($\pm 1^\circ\text{C}$) from the crossover point of storage (G') and loss (G'') moduli. Studies of the nonisothermal gelation kinetics revealed two

very different activation energies for gelation in Regions 2 and 3, i.e. 3080 and 170 kJ/mol, respectively. Though the gelation was energetically favored in Region 3 (lower activation energy), the viscosity increase eventually hindered the diffusion of the molecules and slowed down the gelation. The gel structure formed at high temperature was only partially thermoreversible upon cooling to 5°C due to the existence of remaining associations. Spontaneous recovery of the gel after high deformation gel break-up at low temperature confirmed this statement.

Increasing temperature decreased the *pH* values while conductivity remained almost constant for solutions 15Ac and 10C-15Ac. In the presence of β -GP, a very different behavior was observed, i.e. the *pH* was temperature-independent and the conductivity (and calculated ionic strength) increased with temperature. The measured *pH* values enabled us to establish the degree of protonation of each species as a function of temperature. Examining the decreasing ratio of -NH_3^+ in chitosan and $\text{-OPO(O}^-\text{)}_2$ in β -GP with temperature increase suggested a reduction of chitosan solubility and of possible ionic interactions such as ionic bridging. However the increased ionic strength, in the presence of β -glycerophosphate, involved enhanced screening of electrostatic repulsion and therefore increasing hydrophobic effect, resulting in favorable conditions to form a gel structure. Furthermore, increasing temperature most probably modified hydrogen bonds distribution and favored polymer-polymer interactions over those of polymer-solvent. Therefore, our study indicates that hydrophobic interactions are the main driving forces to form a chitosan gel at high temperature in the presence of β -glycerophosphate.

5.8. ACKNOWLEDGEMENTS

The authors gratefully acknowledge the financial support of Conseil de Recherches en Pêche et en Agroalimentaire du Québec (CORPAQ). They would also like to thank the reviewers for their very useful comments.

5.9. REFERENCES

- ¹ Chenite, A.; Buschmann, M.; Wang, D.; Chaput, C.; Kandani, N. *Carbohydr. Polym.* 2001, 46, 39.
- ² Roberts, G. A. F. *Chitin Chemistry*; Macmillan Press Ltd: London, 1992.
- ³ Brugnerotto, J.; Desbrières, J.; Heux, L.; Mazeau, K.; Rinaudo, M. *Macromol. Symp.* 2001, 168, 1.
- ⁴ Kasaai, M. R. Ph. D. Thesis, Université Laval, Québec, QC 1999.
- ⁵ Singla, A. K.; Chawla, M. J. *Pharma. Pharmacol.* 2001, 53, 1047.
- ⁶ Ravi Kumar, M. N. V. *React. Funct. Polym.* 2000, 46, 1.
- ⁷ Park, J. W.; Choi, K.-H.; Park, K. K. *Bull. Korean Chem. Soc.* 1983, 14, 68.
- ⁸ Vachoud, L.; Zydowicz, N.; Domard, A. *Carbohydr. Res.* 1997, 302, 169.
- ⁹ Cho, J.; Heuzey, M.C.; Bégin, A.; Carreau, P. J. *J. Food Eng.* In press.
- ¹⁰ Hamdine, M.; Heuzey, M.C.; Bégin, A. *Rheol. Acta.* In press.
- ¹¹ Iversen, C.; Kjoniksen, A.L.; Nystrom, B.; Nakken, T.; Palmgren, O.; Tande T. *Polym. Bul.* 1997, 39, 747.
- ¹² Jackson, D. S. US Patent 4659700, 1987.
- ¹³ Montembault, A.; Viton, C.; Domard, A. (2005). *Biomacromolecules* 2005, 6, 653-662.
- ¹⁴ Alberty, R. A. *Physical chemistry*; 6th Ed.; John Wiley & Sons Inc.: Toronto; 1983, chapter 7, p 238.
- ¹⁵ Goldberg, R. N.; Kishore, N.; Lennen, R. M. *J. Phys. Chem. Ref. Data.* 2002, 31, 231.
- ¹⁶ Wang, D. M. Sc. A. Thesis, École Polytechnique, Montréal, QC 1999.
- ¹⁷ Lide, D. R. (2003/2004). In *CRC Handbook of Chemistry and Physics: A Ready-Reference Book of Chemical and Physical Data*; 84th Ed.; CRC Press; 2003/2004, p 7 - 9.
- ¹⁸ Rinaudo, M.; Pavlov, G.; Desbrières, J. *Polymer* 1999, 40, 7029.

-
- ¹⁹ Ullman, G. M., *J. Phys. Chem. B* 2000, 104, 6293.
- ²⁰ Segel, I. H. *Biochemical calculation: how to solve mathematical problems in general biochemistry*; J. Wiley & Sons: New York, 1976.
- ²¹ Barron J.J.; Ashton C. *Technical Service Paper*, Issue 2, Reagecon Diagnostics Ltd: Shannon, Ireland
- ²² Li, L.; Thangamathesvaran, P. M.; Yue, C. Y.; Tam, K. C.; Hu, X.; Lam, Y. C. *Langmuir* 2001, 17, 8062.
- ²³ Launay, B.; Doublier, J. L.; Cuvelier, G. In *Functional Properties of Food macromolecules*, Michell J. R.; Ledward, D. A. Eds.; Elsevier Applied Science: London; 1986, p 1 – 78.
- ²⁴ Noguchi, H. Hydration around hydrophobic groups. In *Water activity: Influences on food quality*; Rocklan, L. B.; Stewart, G. F. Eds.; Academic Press: London; 1981, p 281.
- ²⁵ Sarkar, N. *Carbohydr. Polym.* 1995, 3, 195.
- ²⁶ Kobayashi, K.; Huang, C.-I.; Lodge, T. P. *Macromolecules* 1999, 32, 70.
- ²⁷ Ginde, R. M.; Myerson, A. S. *AIChE Symposium Series* 1991, 87, 284.
- ²⁸ Tao, H.; Lodge, T. P. *Macromolecules* 2000, 33, 1747.
- ²⁹ Ferry, J. D. *Viscoelastic properties of Polymers*. John Wiley & Sons; New York; 1980; Chapter 15, Page 496.
- ³⁰ Walter, A. T. *J. Polym. Sci.* 1954, 13, 207.
- ³¹ Bisschops, J. *J. Polym. Sci.* 1955, 27, 89.
- ³² Lopes da Silva, J. A.; Gonçalves, M. P.; Rao, M. A. *Int. J. Biol. Macromol.* 1995, 17, 25.
- ³³ Fu, J.-T.; Rao, M. A. *Food Hydrocolloids* 2001, 15, 93.
- ³⁴ Ross-Murphy, S. B. *Carbohydr. Polym.* 1991, 14, 281.
- ³⁵ Böhm, N.; Kulicke, W.-M. *Carbohydr. Res.* 1999, 315, 302.
- ³⁶ McIver, R. G.; Axford, D. W. E.; Colwell, K. H.; Elton, G. A. H. *J. Sci. Food Agric.* 1968, 19, 560.
- ³⁷ Lessard, D. G.; Ousalem, M.; Zhu, X. X.; Eisenberg, A.; Carreau, P. J. *J. Polym. Sci. Part B* 2003, 41, 1627.
- ³⁸ Mi, F.-L.; Shyu, S.-S.; Kuan, C.-Y.; Lee, S.-T.; Jang, S.-F. *J. Appl. Polym. Sci.* 1999, 74, 1868.
- ³⁹ Mi, F.-L.; Shyu, S.-S.; Lee, S.-T.; Wong, T.-B. *J. Polym. Sci. Part B* 1999, 37, 1551.
- ⁴⁰ Amiji, M. M. (1995). *Carbohydr. Polym.* 1995, 26, 211.

-
- ⁴¹ Philippova, O. E.; Volkov, E. V.; Sitnikova, N. L.; Khokhlov, A. R. *Biomacromolecules* 2001, 2, 483.
- ⁴² Desbrières, J.; Martinez, C.; Rinaudo, M. *Int. J. Biol. Macromol.* 1996, 19, 21.
- ⁴³ Kasaai, M. R.; Charlet, G.; Arul, J. *Food Res. Int.* 2000, 33, 63.
- ⁴⁴ Osada, Y.; Kajiware, K. *Gels Handbook* Academic Press: London; 2000.
- ⁴⁵ Cho, J.; Heuzey, M. C.; Bégin, A.; Carreau, P. J. *Carbohydr. Polym.* In revision.
- ⁴⁶ McGrane, S. J.; Mainwaring, D. E.; Cornell, H. J.; Rix, C. J. *Starch/Stärke* 2004, 56, 122.

Table 5.1. pK_a and ΔG at 298.15 K

Chemical	pK_a	ΔG (kJ/mol)
AcOH ^{13,14}	4.76	27.1
Chitosan	6.5 ^a	37.1 ^b
β -GP ^{13,14}	1.33	7.6
	6.65	38.0

^a Value at low protonation²^b Estimated from Equation 1.

Table 5.2. Nomenclature and solution compositions expressed in molarity

Sample	Chitosan	GP	AcOH
15Ac	0	0	0.15
10C-15Ac	0.10*	0	0.15
10C-69GP-15Ac	0.10*	0.69	0.15

* Concentration of glucosamine units or monomol/L

Figure captions

Figure 5.1. Evolution of (a) storage modulus G' and (b) loss modulus G'' of sample 10C-69GP-15Ac upon heating and cooling in small amplitude oscillatory shear ($\pm 1^\circ\text{C}/\text{min}$, $\omega = 6.28 \text{ rad/s}$, $\gamma_0 = 0.01$).

Figure 5.2. Frequency sweeps before gelation (B.G.) and after gelation (A.G.) at 5°C ($\gamma_0 = 0.1$) (sample 10C-69GP-15Ac).

Figure 5.3. Nonisothermal kinetics of sample 10C-69GP-15Ac.

Figure 5.4. (a) Strain sweep resulting in gel break-up and (b) following recovery at 5°C ($\omega = 6.28 \text{ rad/s}$, $\gamma_0 = 0.01$ for the recovery test) (sample 10C-69GP-15Ac).

Figure 5.5. (a) $p\text{H}$ and (b) conductivity measurements as a function of temperature.

Figure 5.6. Calculated ionization degree (I_D) of each specie under various $p\text{H}$ and temperature conditions: (a) acetic acid (AcOH), (b) chitosan and (c) divalent GP ($\text{ROPO}(\text{O}^-)_2$; or $\text{GP}(-2)$).

Figure 5.7. Calculated ionic strength (I_s) of each solution as a function of temperature.

Figure 5.8. (a) Concentration C of selected ions and (b) ratio R of ions $-\text{NH}_3^+$ in chitosan and $-\text{OPO}(\text{O}^-)_2$ in GP as a function of temperature.

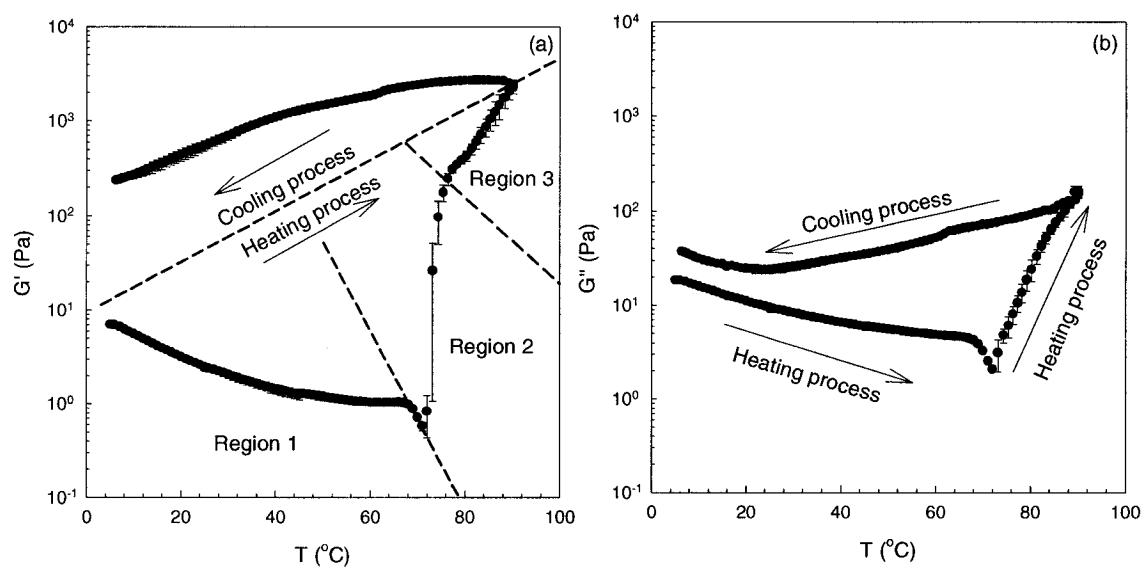


Figure 5.1. Evolution of (a) storage modulus G' and (b) loss modulus G'' of sample 10C-69GP-15Ac upon heating and cooling in small amplitude oscillatory shear (± 1 °C/min, $\omega = 6.28$ rad/s, $\gamma_0 = 0.01$).

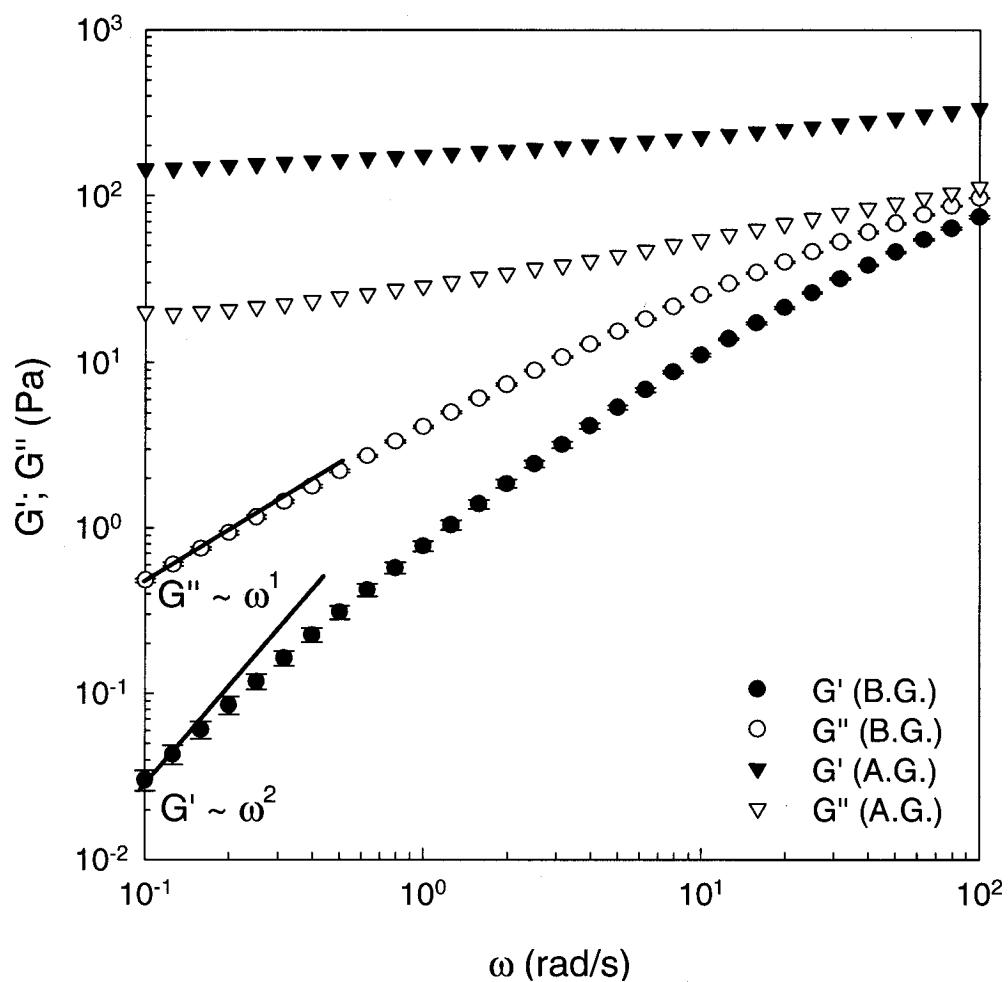


Figure 5.2. Frequency sweeps before gelation (B.G.) and after gelation (A.G.) at 5°C ($\gamma_0 = 0.1$) (sample 10C-69GP-15Ac).

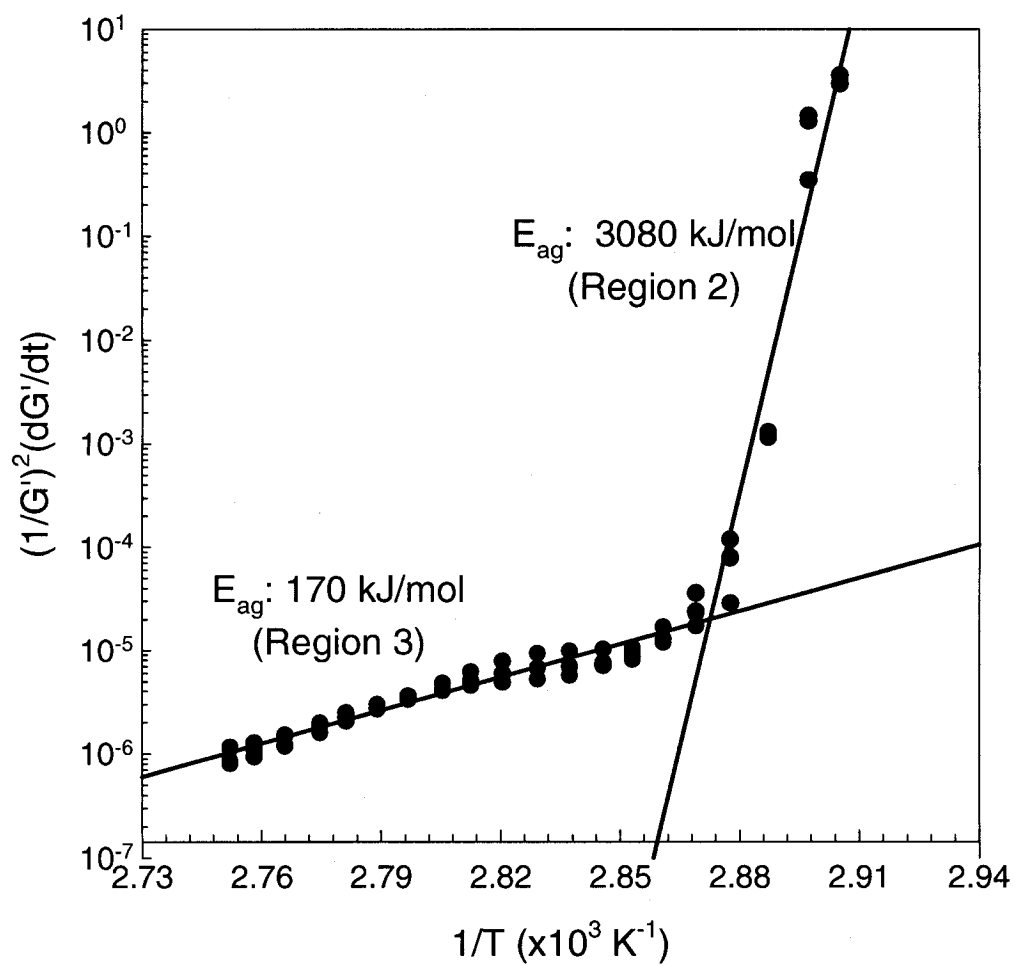


Figure 5.3. Nonisothermal kinetics of sample 10C-69GP-15Ac.

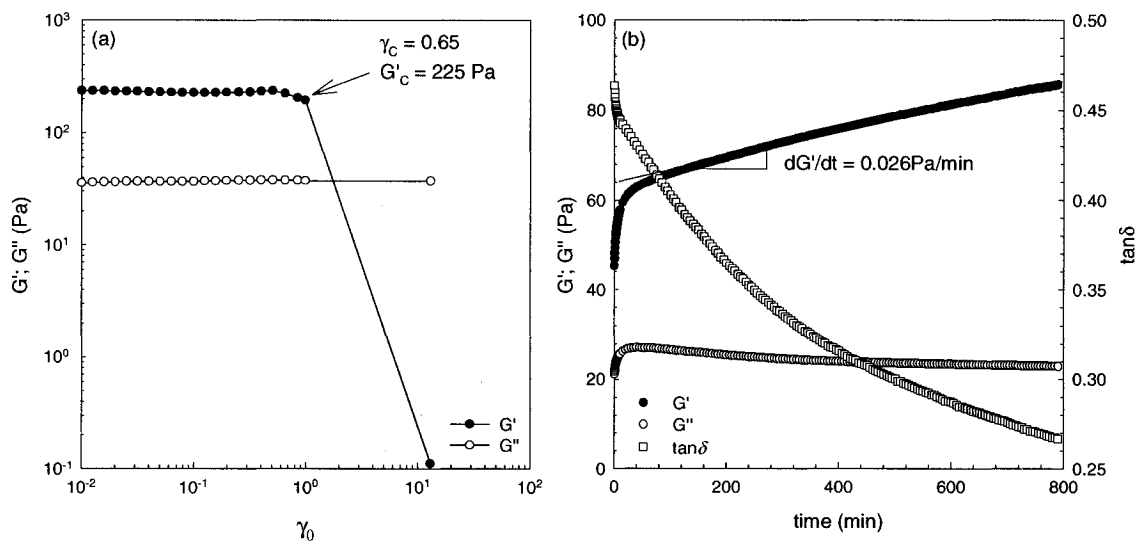


Figure 5.4. (a) Strain sweep resulting in gel break-up and (b) following recovery at 5°C ($\omega = 6.28$ rad/s, $\gamma_0 = 0.01$ for the recovery test) (sample 10C-69GP-15Ac).

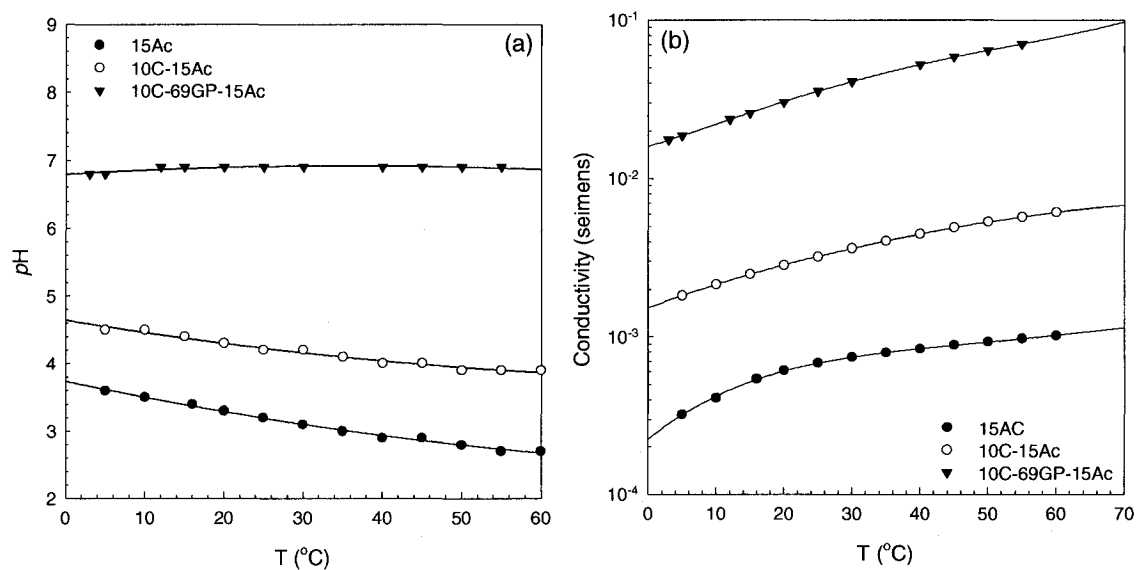


Figure 5.5. (a) pH and (b) conductivity measurements as a function of temperature.

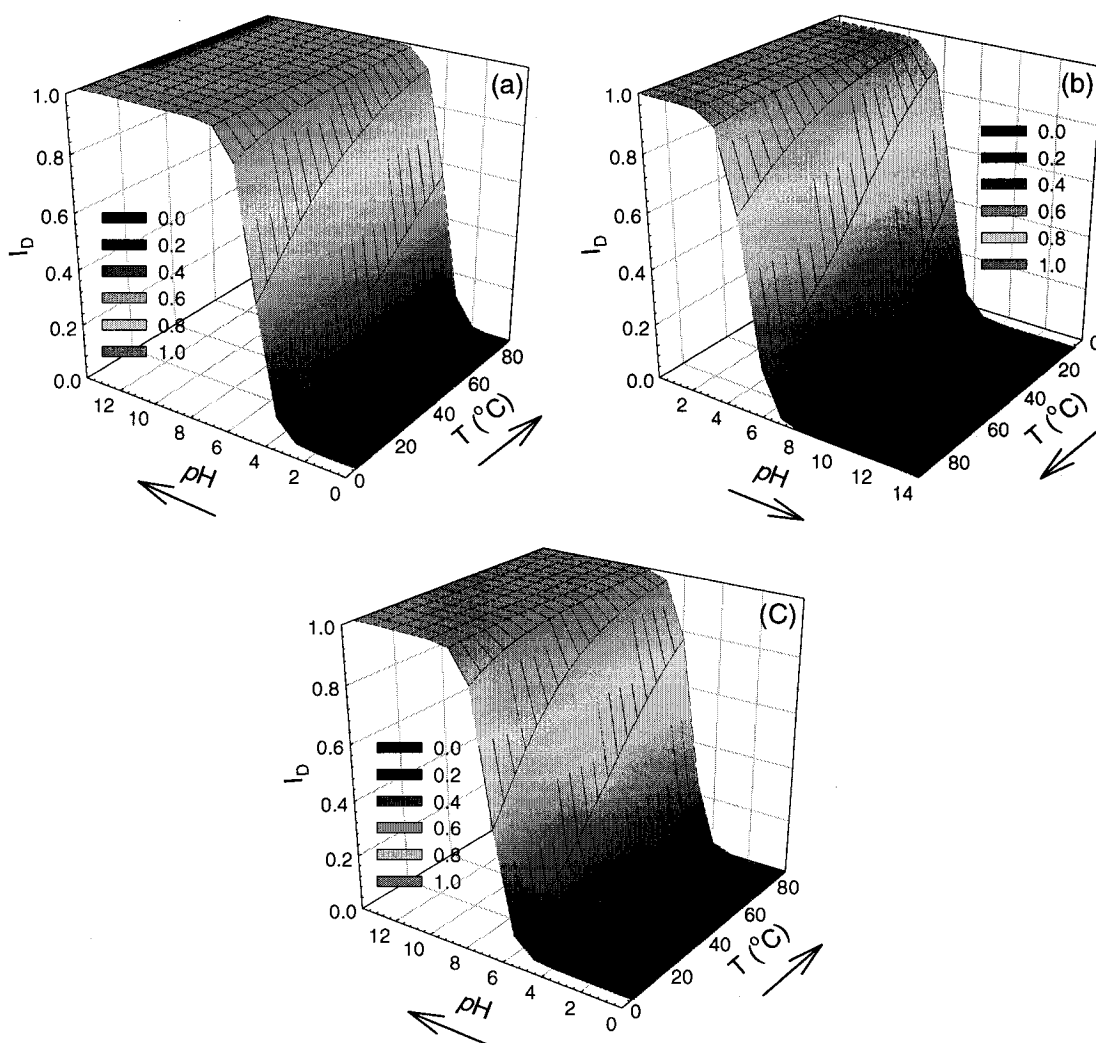


Figure 5.6. Calculated ionization degree (I_D) of each specie under various pH and temperature conditions: (a) acetic acid (AcOH), (b) chitosan and (c) divalent GP (ROPO(O $^{-}$) $_2$ or GP(-2)).

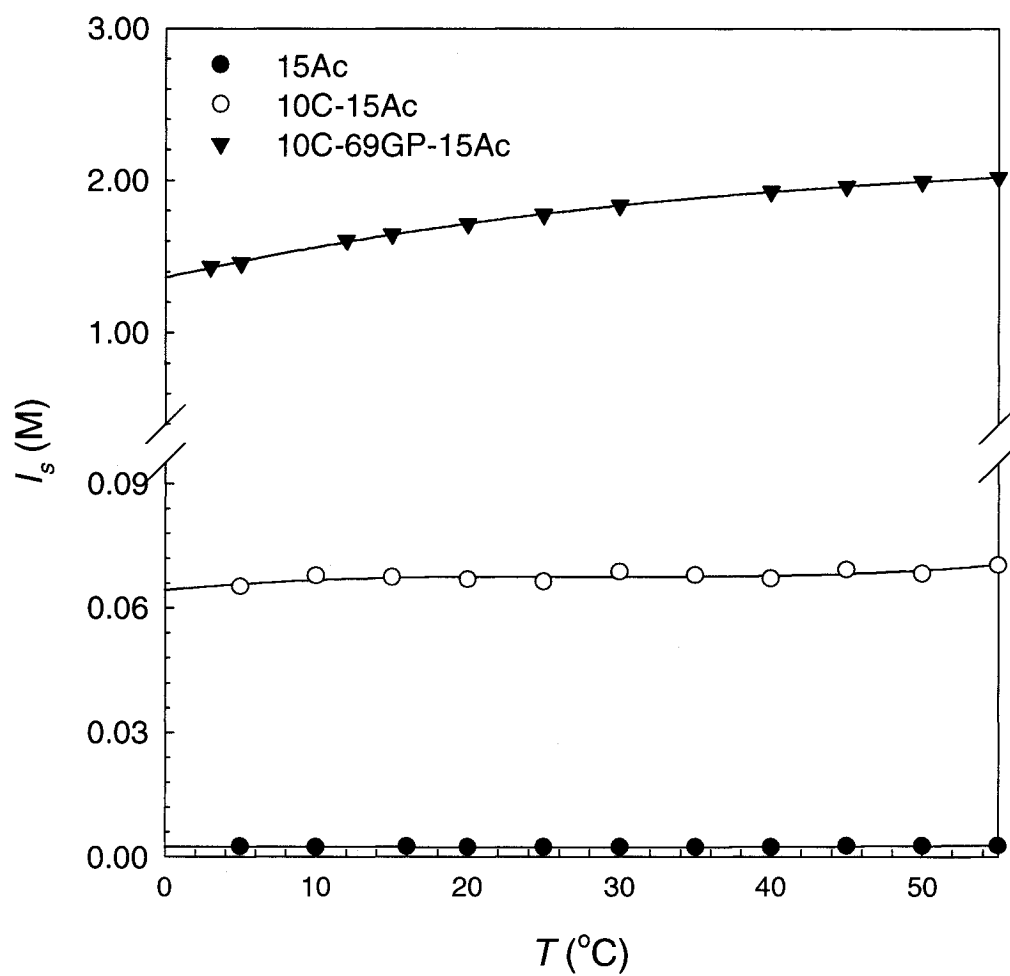


Figure 5.7. Calculated ionic strength (I_s) of each solution as a function of temperature.

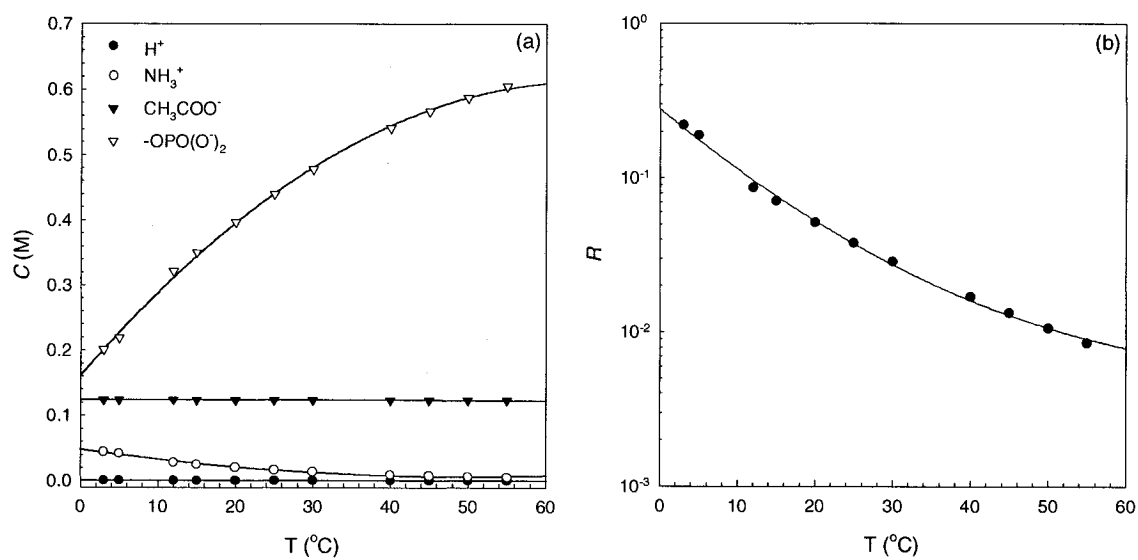


Figure 5.8. (a) Concentration C of selected ions and (b) ratio R of ions $-\text{NH}_3^+$ in chitosan and $-\text{OPO}(\text{O}^-)_2$ in GP as a function of temperature.

Chapter 6

Effect of urea on solution behavior and heat-induced gelation of chitosan- β -glycerophosphate

Jaepyoung Cho¹, Marie-Claude Heuzey^{1*}, André Bégin² and Pierre J. Carreau¹

¹ CREPEQ, Department of Chemical Engineering, Ecole Polytechnique, P.O. Box 6079,
Station Centre-Ville, Montreal, QC, H3C 3A7, CANADA

² Food Research and Development Centre, 3600 Casavant Blvd West, Saint-Hyacinthe,
QC, J2S 8E3, CANADA

* Corresponding author. E-mail: marie-claude.heuzey@polymtl.ca; tel.: +1-514-340-4711 ext. 5930; fax: +1-514-340-2994

6.1. Abstract

In this study, we have investigated the effect of urea on the physicochemical (*pH* and conductivity) and rheological properties of the chitosan- β -GP system in order to assess the main polymer-polymer interactions at low and high temperature. The *pH* of the solutions was slightly increased due to the consumption of H^+ in solution through the hydrolysis of urea. Furthermore, the addition of urea considerably decreased the conductivity, and therefore the ionic strength of the solutions, and this effect was more important at high temperature. It indicated that urea strongly affects polymer-polymer interactions by weakening hydrogen bonds at low temperature, but in addition can hinder hydrophobic effect at high temperature since the reduction of ionic strength results in less screening of electrostatic repulsion between protonated glucosamine groups. At 15°C, the addition of urea to chitosan- β -GP solutions decreased their elasticity, shortened relaxation times and simplified the relaxation process due to the disruption of hydrogen bonds. Heat-induced gelation of the chitosan system in the presence of urea showed higher gelation temperature (T_{gel}) in non-isothermal tests and longer gelation time (t_{gel}) in isothermal conditions. The activation energy for gelation also increased with increasing urea concentration. We concluded that the detrimental effect of urea on the gelation process was mainly related to a decrease in polymer-polymer hydrophobic effect, as shown by the decrease in conductivity.

6.2. Introduction

Chitosan is a biopolymer derived through a series of chemical treatments from the chitin components of the shells of crustaceans. It is a copolymer of 2-amino-2-deoxy-D-glucose (glucosamine) and 2-acetamido-2-deoxy-D-glucopyranose (acetylglucosamine) [1]. An important chemical characteristic of the molecule is its degree of deacetylation (DDA), or the fraction of glucosamine units in the chemical structure. The copolymer is generally considered as “chitosan” when the DDA is greater than 50% [2]. Chitosan is a non-toxic, biocompatible and biodegradable material and has been used in many industries such as nutraceutical, medical, cosmetic and pharmaceutical [3,4,5,6,7,8].

Chitosan contains hydrophobic ($-\text{CH}_3$) and hydrogen bonding favoring groups ($-\text{OH}$, $-\text{NH}_2$ and $-\text{C}=\text{O}$) [1]. However, since the copolymer becomes positively charged due to the protonation of the free amine groups below a $p\text{H}$ of 6.2, corresponding to the pK_a of chitosan at high protonation [9, 10], polymer-polymer interactions via hydrophobic effect and/or hydrogen bonding junctions can be hindered due to electrostatic repulsion. For example, it is known that phase separation is triggered by the use of high salt concentration [11]. Likewise, gels can be formed by controlling the $p\text{H}$. Chenite et al. [12] obtained a homogenous gel system by neutralizing chitosan solutions using a weak base, β -glycerophosphate ($\beta\text{-GP}$: $pK_{a,2} = 6.65$ at 25°C [13,14]) and controlling temperature. The system remained in solution at physiological $p\text{H}$ ($=7$) and room temperature and changed into a gel upon heating at physiological temperature ($=37^\circ\text{C}$).

We have investigated rheological and physicochemical properties of the chitosan- β -GP system in terms of temperature in a previous publication [15]. According to the evolution of the rheological properties under non-isothermal conditions, three regions were defined: 1) a liquid-like behavior at low temperature, 2) a fast gelation process near the gel point, and 3) a slow gelation beyond. The gel structure formed at high temperature was only partially thermoreversible upon cooling to 5°C. Increasing temperature had no effect on the pH value of the chitosan- β -GP system, while conductivity (and calculated ionic strength) increased. With values from the pH measurements, we have shown that the estimated protonation of chitosan decreased with increasing temperature, but that of β -GP increased. It indicated a reduction of the ratio of $-\text{NH}_3^+$ in chitosan and $-\text{OPO}(\text{O}^-)^2$ in β -GP at high temperature, resulting in a decrease of potential ionic interactions such as ionic bridging. On the other hand, increased ionic strength as a function of temperature involved enhanced screening of electrostatic repulsion forces and hence more polymer-polymer hydrophobic interactions, resulting in favorable conditions for gel formation. Since it is generally assumed that hydrogen bonding interactions are not predominant at high temperature, we suggested that hydrophobic effect was the main driving force for the chitosan- β -GP gelation at high temperature.

In this work we investigate physicochemical and rheological properties of the chitosan- β -GP system in the presence of urea in order to expand our understanding of the role of hydrogen bonding and hydrophobic effect. Urea is generally known as a hydrogen bonding disrupting agent [16,17,18,19,20] but it can also affect hydrophobic

interactions [21]. The presence of urea on chitosan- β -GP solutions when the temperature is increased can consequently reduce furthermore hydrogen bonds and decrease the hydrophobic effect. In this study, the variations of pH and conductivity of the polymer system are measured as functions of urea concentration and temperature, and the solution and gelation behaviors are characterized through rheological measurements.

6.3. Temperature and presence of urea effects on gelation of chitosan

From its hydrophobic and hydrogen bonding favoring parts, chitosan can self-associate in aqueous solutions [1,12,21,22,23, 24,25]. These two types of junctions, along with ionic bridging in the presence of divalent species [26], are critical interactions involved in the formation of physical gel structures in chitosan-based systems. The balance between these interactions is critical to the formation of three-dimensional networks and can be controlled by temperature variation and/or in the presence of urea [16,17,18,19,20,21,27,28]. Urea has been extensively used to control the intensity of hydrogen bonding interactions in biomedical systems [16,17,18,19,20,25] as well as to control hydrophobic effect [21]. We briefly discuss below the general influence of temperature and urea on hydrogen bonds and hydrophobic interactions in the light of previous research.

6.3.1. Temperature effect

Water molecules are presumed to form enclosed structures that surround the polymer chain at low temperature [29]. Increasing temperature enhances the vibrational

and rotational energy of water molecules and inhibits weak hydrogen bonds to orient dipolar water molecules around the polymer chains, causing the decrease of hydrogen bonding interactions. With increasing temperature, the energized water molecules enclosing the polymer chain are removed and the dewatered hydrophobic polymer segments start associating with each others. Thus, increasing temperature increases the hydrophobic effect and results in physical networks formed by enhanced association [30].

6.3.2. Urea effect on hydrogen bonding interactions

Urea, known as a hydrogen breaking agent [16,17,18,19,20], can hinder the formation of macromolecular structures. However, there are two different views about the effect of urea on hydrogen bonding interactions. One is that urea is unable to disrupt intramolecular interactions [19,20,31] and only have impact on the intermolecular ones, while the other suggests that adding urea breaks intramolecular hydrogen bonds and causes a change in the molecular conformation [25,32]. Two mechanisms are proposed to explain the denaturing function of urea in aqueous media [33]. The first is the binding of urea to specific groups on the polymer chains, thereby weakening hydrogen bonding between polymer chains (intermolecular), while the other possible mechanism is the breakdown of the hydrogen-bonded structure of the solvent, or the “structuring breaking effect”. According to the literature [33], both mechanisms concurrently produce the denaturing process.

Kjønnsken et al. [17] showed that the dynamic moduli (G' and G'') of pectin solutions exhibited weaker values in the presence of urea, and that gel formation at 25°C was hindered. High urea concentrations also prevented a network microstructure forming for proanthocyanidin (PA) polymer solutions and yielded nearly Newtonian characteristics of independent particle motions [19], while for amylase gels in a mixture of water and dimethyl sulfoxide (DMSO), the use of urea reduced the gel strength significantly [20]. The previous examples illustrate the effect of urea on intermolecular hydrogen bonds. On the other hand, Tsaih and Chen [25] reported that the addition of urea to chitosan solutions resulted in an increase of the intrinsic viscosity and persistence length, therefore in a less compact structure, due to the hindrance of intramolecular hydrogen bonds.

6.3.3. Urea effect on hydrophobic interactions

The influence of urea on hydrophobic interactions is controversial. Kokufuta et al. [18] proposed that these interactions, involved in the formation of gels of poly(ethyleneimine), were not affected by the addition of urea. Furthermore, recent neutron light scattering experiments showed that urea caused no apparent disruption of the water structure even at high concentration of urea [34], indicating no effect on hydrophobic interactions. However, Dubin and Stauss [35] reported that urea weakened hydrophobic interactions between solute molecules. Urea preferentially solvates hydrophobic residues by breaking the hydrogen-bonded structures of water [36,37], and this leads to an effective reduction of hydrophobic interactions. Computer simulations

based on energy minimization of clusters supported that urea directly participates in the solvation of hydrophobic solutes by replacing water molecules in the hydration shells of the solute [38]. Wallqvist and Covell [39] monitored the effect of urea on hydrophobic interactions by computing the potential of mean force in the ternary system methane-water-urea. Urea appeared to enhance hydrophobic interactions and to act as a renaturant for the uncharged methane. However, it acted as a denaturant in the ternary charged methane-water-urea system by destabilizing the hydrophobic bonds between the solutes. Finally, Philippova et al. [21] investigated the influence of urea on hydrophobic effect in the association of chitosan molecules using fluorescence measurements. The authors showed reduced formation of hydrophobic domains in chitosan solutions in the presence of urea at a concentration of 7M.

6.4. Experiments

6.4.1. Materials

The chitosan used in this study was purchased from Marinard Biotech (Rivière-aux-Renards, QC). The chemical structure of chitosan is shown in Figure 6.1(a). The degree of deacetylation (DDA), or fraction of glucosamine units, was obtained from colloidal titration with polyvinyl sulfate potassium, initially standardized with cetylpyridinium chloride. Gel permeation chromatography measurements were conducted in order to characterize the molecular weight using an UltrahydrogelTM 500 Column (Waters Co., Milford, MA) and dextran standards. The determined weight-average molecular weight (\overline{M}_w) was 8.5×10^5 g/mol ($\overline{M}_w / \overline{M}_n = 2.76$) in a solvent of

0.25M acetic acid/0.25M sodium acetate. For the solutions preparation, acetic acid (AcOH) (99.7%, Sigma-Aldrich Canada Ltd., Oakville, ON) was used to dissolve the chitosan. Also disodium- β -GP (glycerol-2-phosphate disodium salt hydrate: $C_3H_7Na_2O_6P \cdot xH_2O$, FW 216.04, Sigma-Aldrich Canada Ltd., Oakville, ON) (chemical structure shown in Figure 6.1(b)) was used to adjust the *pH* of the solutions. Lastly, urea (99.5%, Sigma-Aldrich Canada Ltd., Oakville, ON) was added in order to control the various interactions at low and high temperature.

6.4.2. Preparation of chitosan solutions

Two different chitosan quantities were added to 1w/v% acetic acid aqueous solution. The solutions were mixed for 4h in order to achieve complete solubilization of chitosan. The mixing was performed at room temperature at a rate of 50 RPM using a laboratory magnetic stirrer (PC-420 Corning[®] Stirrer/Hot Plate, Corning Inc., MA, USA). The β -GP was slowly added to the chitosan solutions in order to increase the *pH* around 7. A mixing time of 0.5h was used to homogeneously disperse the β -GP and to avoid forming local precipitates. Finally, various amounts of urea (0 - 5M) were added to the chitosan- β -GP solutions and mixed for 1h. The volume difference caused by the addition of β -GP and urea was compensated in other solutions by adding deionized water. The final total volume of each solution was 60 mL. The composition in molarity and the nomenclature of the chitosan solutions are presented in Table 6.1. During the stirring process, the containers were covered with aluminium foil to prevent evaporation. The prepared chitosan- β -GP-urea solutions were left to rest 3h for degassing at room

temperature and kept in a refrigerator overnight at 5°C. It was found that this overnight storage was essential to obtain reproducible results, possibly because of the presence of small remaining bubbles. All the samples were stored at 5°C and used within one week in order to avoid aging effect due to polymer degradation.

6.4.3. *pH and conductivity measurements*

All solutions were characterized in terms of *pH* and conductivity as a function of temperature. A water bath (model BT-15, Cole-Parmer, IL, USA) was used to control temperature at a constant heating rate (0.8°C/min) and all measurements were recorded in a continuous manner in order to simulate the heat-induced gelation process. The temperature range used was 0-55°C for *pH* measurements (*pH*-meter, Hanna Ltd., Àrvore - Vila do Conde, Portugal) and 0-75°C for conductivity (conductance meter, model 35, YSI Inc., Yellow Springs, OH). Since the conductance meter used was linearly temperature compensated (referenced to 25°C), we applied the following equation to recover the conductivity at a given temperature:

$$\kappa_T = \kappa_{25}[1 + \alpha(T - 25)] \quad (6.1)$$

with κ_{25} the conductivity referenced to 25°C, κ_T the conductivity measured at a given temperature T , and α the temperature coefficient of variation [40]. The choice of different temperature ranges was a consequence of the different limitations of the respective electrodes.

6.4.4. Rheological measurements

The rotational rheometer used in this study was a stress-controlled device (AR-2000, TA Instruments, New Castle, DE) with a Couette geometry. Mineral oil covered the surface of the chitosan solutions to prevent evaporation during the tests. The effect of the mineral oil on the measurements was shown to be negligible. The chitosan concentration of 0.08 M was used to study the solution behavior and the gelation under non-isothermal conditions. The dynamic rheological properties of chitosan- β -GP solutions were characterized in terms of urea concentration at 15°C. The oscillatory shear measurements were performed in the linear viscoelastic regime. The stress relaxation spectra were calculated from the obtained G' and G'' data, using a commercial software (NLREG[®]) [40]. The chitosan solutions zero shear viscosity (η_0) was determined from small amplitude oscillatory data using the Carreau-Yasuda model [41], assuming validity of the Cox-Merz rule [11], and from the time-weighted stress relaxation spectra area.

During the gelation process in non-isothermal conditions, the evolution of rheological properties was monitored between 15 and 90°C using a constant heating rate (1°C/min). Small amplitude deformation γ_0 (0.01) and relatively low frequency ω (6.28 rad/s) were applied in order not to disturb the gel formation. The gelation temperature (T_{gel}) was determined as the crossover point of the storage (G') and loss (G'') moduli ($\tan \delta = 1$), despite of the slight dependency on frequency. The thermoreversibility of the gels was investigated by decreasing the temperature from 90 to 15°C at the same rate

(1°C/min). After the cooling cycle, the resulting system was characterized by a frequency sweep at 15°C.

For the isothermal gelation tests, the rheological properties of the chitosan- β -GP system were also investigated in the absence and presence of urea (3M). A chitosan concentration of 0.14 M was used since the lower one (0.08 M) resulted in too large inertial effects. The moduli G' and G'' were reported as functions of time under various temperatures (40 - 60°C). As for non-isothermal tests, a small deformation ($\gamma_0 = 0.01$) and frequency ($\omega = 6.28$ rad/s) were applied. The gelation time (t_{gel}) was also determined as the crossover of G' and G'' , and the gelation activation energy was calculated from these specific times at various temperatures using an Arrhenius type relationship.

6.5. Results

6.5.1. Physiochemical measurements

The pH of various solutions was measured as a function of temperature and urea concentration (Figure 6.2). The pH of a 0.15M acetic acid aqueous solution was very sensitive to temperature due to the increased ionization of AcOH. Adding the polymer to the acetic acid solution (0.10M chitosan - 0.15M AcOH) resulted in a pH increase from 3.2 to 4.2 at 25°C, due to the protonation of the free amine groups in the chitosan molecules. For this chitosan-AcOH solution, the decrease in pH at high temperature resulted from the deprotonation of chitosan and the increased ionization of AcOH [15]. Upon the addition of β -GP (solution U0), the pH was increased around neutrality. Wang [24] also reported that the addition of β -GP to chitosan solution increased the pH value

to a physiologically acceptable level, from 6.8 to 7.2, due to the high buffering capacity of β -GP in this range of pH . In the presence of β -GP, the pH was nearly independent of temperature, most probably because of its buffering capacity. It can also be observed in Figure 6.2 that the pH slightly increased in terms of urea concentration (solutions U1, U3 and U5). The hydrolysis of urea causes the consumption of H^+ ions in solution [42], resulting in increasing pH value.

The conductivity of the chitosan- β -GP solutions was measured as a function of temperature in the presence of urea. Figure 6.3(a) presents the evolution of the conductivity of each solution. We may interpret the effect of urea on the conductivity of solutions U1, U3 and U5 from the interaction of urea with the carboxylic groups ($-COOH$) of acetic acid by hydrogen bonding and/or possibly by the formation of ureanium ions [43]. It is known that higher ionic strength decreases electrostatic repulsion between chitosan protonated amines, therefore enhancing the hydrophobic effect [30]. Consequently, the observed decrease of the conductivity (or ionic strength) was directly correlated to lower polymer-polymer interactions, and this result agreed with that of Philippova et al [21]. Figure 6.3(b) shows the relative conductivity ratio (i.e solutions conductivity normalized by that of solution U0) as a function of temperature. Adding urea decreased the relative ratio, and this effect was more pronounced at high temperature. Thus the use of urea in the chitosan- β -GP system can affect polymer-polymer interactions by mainly weakening hydrogen bonds at low temperature (solution behavior), and predominantly hydrophobic interactions at high temperature [30] (gel behavior). In the next sections, we look more closely at these two different regimes.

6.5.2. Urea effect on solution behavior

The effect of urea on the rheological properties of chitosan- β -GP solutions at 15°C is shown in Figure 6.4 in terms of the dynamic moduli (G' and G'') and $\tan \delta$ (insert of Figure 6.4) as functions of frequency (ω). The behavior is typical of a concentrated entangled polymer solution. The entanglement concentration C_e of this chitosan sample in acetic acid has been determined previously to be approximately 7 g/L [11]. Therefore, the concentration used in this work (0.08M, corresponding to 14 g/L) is way into the entangled regime. The storage modulus (G') and loss modulus (G'') showed different responses to the addition of urea in solution. G' decreased with increasing urea concentration while G'' slightly increased. This dissimilar behavior caused a decrease of the elasticity of the polymeric solutions, as shown by $\tan \delta$ in the insert of Figure 6.4. This decline has been related to the urea breaking intra- and/or intermolecular hydrogen bonding interactions [25,32,33].

The complex moduli G^* , defined as $G^*(\omega) = \sqrt{G'(\omega)^2 + G''(\omega)^2}$, was used to calculate the stress relaxation spectrum ($H(\tau)$) according to [44]:

$$G^*(\omega) = \int_{-\infty}^{\infty} (\omega\tau + i)H(\tau) \frac{\omega\tau}{1 + (\omega\tau)^2} d(\ln \tau) \quad (6.2)$$

with τ the relaxation time. The various spectra were normalized using the zero shear viscosity (η_0), corresponding to the area under the spectra curves:

$$\eta_0 = \int_{-\infty}^{\infty} \tau H(\tau) d(\ln \tau) \quad (6.3)$$

in order to compare them on similar scales. Figure 6.5 shows the normalized time-weighted stress relaxation spectra for various urea contents. All the solutions spectra are

monomodal, and most of the relaxation process of the urea-containing solutions was completed within $10^2 \sim 10^3$ s, while that of U0 was much slower, as expected for a more elastic system. In Figure 6.4, we report the calculated values of the dynamic moduli using the relaxation spectra (solid lines). The agreement is excellent.

The dynamic moduli G' and G'' measured in the linear viscoelastic regime can be presented in a Cole-Cole plot, and most polymer systems will show a power-law relationship ($G'' \sim G'^P$) [45,46]. The exponent P is equal to $1/2$ for a one-mode Maxwell fluid:

$$G''^2 = G' (G_e - G') \quad (6.4)$$

or $\log (G'') = 1/2 \log (G') + 1/2 \log (G_e - G')$,

where G_e represents the plateau value of G' at high frequencies. Therefore, Cole-Cole plots can be used to characterize deviations from the one-mode Maxwell model [45,46], using the generalized equation:

$$\log (G'') = P \log (G') + (1-P) \log (G_e - G') \quad (6.5)$$

in analogy with Equation 6.4, provided that $G'^{2P} \ll G_e^{2P}$. Figure 6.6 shows the Cole-Cole plots for solutions with various urea contents. For all solutions, the exponent P was larger than $1/2$ (between 0.63 and 0.75) (insert of Figure 6.6), indicating that the solutions deviated from the single mode Maxwell element simple relaxation, as observed from the dynamic data of Figure 6.4. This deviation is often observed for cross-linked and entangled polymers that exhibit a spectrum of relaxation times. The exponent P decreases with increasing urea concentration, denoting that the stresses relaxed faster due to the reduction of molecular interactions. The plateau modulus G_e was also

estimated from the Cole-Cole plots; it decreased from 2060 to 400 Pa when urea was added to the chitosan- β -GP solutions (solutions U0 and U5, respectively).

6.5.3. Urea concentration effect on gelation

The gelation behavior under non-isothermal conditions was investigated in the presence of urea. As mentioned before, the gelation of chitosan- β -GP solutions proceeded in three stages, and this behavior was unchanged by the presence of urea (Figure 6.7). In Region 1, the behavior was liquid-like. We are showing the complex modulus G^* since the storage modulus was extremely small below the gel point and interpreted as negative values by the rheometer software. G^* showed a very sharp decrease near Region 2 for all samples, and this phenomenon has been attributed to some polymer precipitation [47]. In Region 2, the complex modulus rapidly increased with increasing temperature due to the formation of a three-dimensional network. In the last zone (Region 3), the much slower gelation was caused by the lower diffusivity that resulted from the viscosity increase after gelation. The gelation temperature (T_{gel}) and the gel strength (G^* at 90°C) were examined in terms of urea concentration (Figure 6.8). While T_{gel} increased, denoting that urea retarded gelation, the gel strength decreased. As shown from our conductivity measurements, urea was detrimental to hydrophobic interactions and resulted in weaker gels.

6.5.4. Non-isothermal gelation kinetics

We investigated the non-isothermal gelation kinetics of the heat-induced gelation in order to quantify the negative effect of urea. We used a kinetic model that is a combination of Arrhenius and time-temperature relationships [48,49,50], yielding:

$$\ln\left(\frac{1}{G'^n} \frac{dG'}{dt}\right) = \ln k_o - \left(\frac{E_{ag}}{RT}\right) \quad (6.6)$$

For heat-induced gelation, the equation is rewritten as:

$$\ln\left(\frac{1}{G'^n} \frac{dG'}{dt}\right) = \ln k_o + \left(\frac{E_{ag}}{RT}\right) \quad (6.7)$$

in order to account for a positive activation energy. In this equation n is the reaction rate, t the time, k_o the Arrhenius frequency factor, E_{ag} the activation energy for gelation, and RT have their usual significance. The exponent n represents both the dimension r of the growing crystallites and the type of nucleation s ($n = r + s$) [51]. Parameter r is 1 for rods, 2 for discs and 3 for spheres, while s is either 0 for predetermined nucleation (nuclei already present) or 1 for sporadic nucleation (nuclei arise and their number increases linearly with time) [51,52]. We assumed that the reaction rate n was 2, as proposed by Lopes da Silva et al. [48,49,50] for gelation.

The derivative term in Equation 6.7 was obtained through the differentiation of a polynomial regression fitted to the kinetics data of Figure 6.7. Figure 6.9(a) shows the semi-log plot of $1/G'^2 dG'/dt$ vs. $1/T$. Gelation regions 2 and 3 were again clearly delimited. The activation energy for gelation determined from the slope of each zone is shown in Figure 6.9(b) as a function of urea concentration. The energy increased from

2800 to 5000 kJ/mol in the fast gelation region in the presence of urea, indicating that the development of intermolecular interactions was not favored energetically. In Region 3, E_{ag} was much lower (about 170 kJ/mol), and consequently the evolution of the physical network was energetically easier, however hindered because of the large viscosity increase. The activation energy for gelation was also nearly constant regardless of urea concentration in this last region, most probably because gelation was diffusion controlled.

6.5.5. *Partial thermoreversibility of the gels*

Physical networks are generally thermoreversible; therefore, the resulting gels were cooled down in order to evaluate their reversibility by examining the variations of the dynamic moduli with temperature. As shown in Figure 6.10 (a), G' gradually decreased with decreasing temperature while G'' showed a minimum and then increased during the cooling process. The temperature at the minimum was higher for larger urea concentration, i.e. from 24°C for U0 to 37°C for U5. As shown in Figure 6.10 (b), $\tan \delta$ rapidly increased below that critical temperature. Two competing effects resulted in the minimum observed for G'' : the destruction of the network junctions as the temperature was lowered, and the usual rheological properties increase with decreasing temperature due to reduced molecular mobility. This interpretation is in agreement with the variation of the critical temperature with urea concentration, as the second mechanism takes over earlier since there are fewer junctions to be destroyed. A minimum was not observed for G' , probably because the continuous reduction of junctions overcame the impact of the

decreased chain mobility at lower temperature. The gels were only partially thermoreversible since G' remained larger than G'' , and this partial thermoreversibility was most probably due to the existence of remaining weak associations [29].

The systems, cooled down at 15°C, were characterized using small amplitude oscillatory shear (Figure 6.11) in order to compare them with the initial solution state (Figure 6.4). This time, all the systems showed a typical solid-like behavior ($G' > G''$) with a very slight frequency dependency ($G' \sim \omega^{0.03-0.15}$ and $G'' \sim \omega^{0.07-0.33}$), illustrating their non complete thermo-reversibility, and showing a striking contrast with the data obtained before the heating-cooling cycle (Figure 6.4). As expected, the gel strength (G') and the elasticity ($\tan \delta$, insert of Figure 6.11) of the cooled gels were decreased in the presence of urea.

6.5.6. Isothermal gelation

We also investigated isothermal gelation in order to compare the activation energy with that obtained under non-isothermal conditions. For instances, it is often reported that there is large difference between the crystallization activation energies obtained in isothermal and non-isothermal conditions. For the crystallization of poly(3-hydroxybutyrate) (PHB), the reported activation energy was 170-220 kJ/mol from a non-isothermal kinetics study, while it was much lower, 9.8-10.8 kJ/mol for isothermal conditions [53]. Li et al. [54] reported that the activation energy for crystallization was 2000 and 240 kJ/mol for Nylon 1012, a newly industrialized engineering plastic, in non-isothermal and isothermal conditions respectively. Therefore, the crystallization

activation energy evaluated in non-isothermal conditions can be one order of magnitude higher than that obtained under isothermal studies. Since we were using gelation kinetics models derived from those used in crystallization, we expected to observe a similar difference.

As mentioned in the methodology part, solutions with larger chitosan concentrations (solutions 14CU0 and 14CU3) were used for these isothermal tests, and the evolution of G' and G'' was recorded as a function of time at various temperatures (Figure 6.12(a)). The gelation time (t_{gel}) was longer in the presence of urea, illustrating again the retarding effect of the substance, and this time was also longer at higher temperature. The gelation time was used to estimate the activation energy for gelation in isothermal conditions, by plotting it as a function of $1/T$ (Figure 6.12(b)). As observed for the non-isothermal data, urea had again a detrimental effect on gelation, requiring higher energy to proceed (170 and 200 kJ/mol for solutions 14CU0 and 14CU3, respectively) and resulting in lower modulus values. And as expected, the activation energy determined from isothermal kinetics was fairly small compared to that obtained in Region 2 of the non-isothermal kinetics (one order of magnitude smaller). It was, however, very similar to that obtained in Region 3, but this may be coincidental. Obviously, the energy required to achieve network formation in non-isothermal conditions is much larger since the sample is never at thermal equilibrium.

6.6. Discussion

The effect of urea on the solution and gel states of the chitosan- β -GP system has been widely illustrated by the previous data. Urea had a strong impact on the solution behavior, making the stresses relax considerably faster and the viscoelastic properties lower. Leibler et al. [55] presented a model for the dynamics of entangled polymer networks made up of linear chains and temporary physical cross-links. Using a simplified assumption, i.e. that entanglement and physical cross-link contributions are additive and do not show any synergetic effects; they proposed the following equation for the plateau modulus:

$$G_e \cong cRT \left[\frac{p}{N_s} + \frac{1}{N_e} \right] \quad (6.8)$$

where c is the number concentration of monomers, p the fraction of physical cross-links (or “stickers”), N_s the average number of monomers along the chains between stickers, and N_e the number of monomers in an entanglement. If we reasonably assume that N_s and N_e are unchanged by urea concentration, the decrease in the plateau modulus reported in the insert of Figure 6.6 is directly related to a decrease of temporary junctions in the presence of urea.

The model proposed by Leibler et al. is a modified reptation model that considers a slower diffusion in the presence of reversible cross-links. This hindered reptation results in a delayed relaxation; however, the terminal relaxation of the modulus remained that of a reptation model as shown schematically in Reference 55. Since

Leibler et al. did not propose a predictive equation for $G(t)$, we have used the Doi-Edwards model [56]:

$$G(t) = \frac{8}{\pi^2} G_e \sum_{\text{odd } k} \frac{1}{k^2} \exp\left(-\frac{k^2 t}{\tau_{rep}}\right) \quad (6.9)$$

in order to compare the relaxation moduli calculated from the stress relaxation spectra of our various solutions (Figure 6.5). The plateau modulus G_e used in this equation was that estimated from the Cole-Cole plots (insert in Figure 6.6), while the reptation time τ_{rep} was taken as the mean relaxation time τ_m of Figure 6.5 (or time at the maximum). It can be observed in Figure 6.13 that even though urea had a “simplifying” effect on the solutions relaxation by disrupting hydrogen bonds and hydrophobic interactions, as confirmed by the decreased exponent P of the Cole-Cole plot (insert in Figure 6.6), the spectrum of relaxation times remained much broader than that predicted by reptation. “Sticky” or hindered reptation would only delay the occurrence of the terminal relaxation, but still not result in an appropriate representation of the modulus behavior. Obviously, additional relaxation mechanisms such as fluctuations in tube length and constraint release, known to be important for ordinary linear polymers, may also have to be accounted for. Likhtman and McLeish [57] presented a model that combines self-consistently contour length fluctuations, constraint release and reptation for monodisperse linear polymers. Therefore, a combination of these mechanisms along with hindered reptation may improve the prediction of reversible networks relaxation such as that observed in Figure 6.13. However, this is beyond the scope of the present work.

The large influence of urea on the gelation process was demonstrated according to different characteristics: 1) higher gelation temperature in non-isothermal conditions, 2) longer gelation time in isothermal ones, and in both cases 3) larger gelation activation energies and 4) lower mechanical properties. The heat-induced gelation of the chitosan- β -GP system can be the result of hydrogen bonding, hydrophobic and/or ionic interactions. Our previous work [15] showed that among the three types of junctions, hydrophobic interactions were dominant since hydrogen bonds are known to weaken rapidly with temperature, and our ionization calculations showed that ionic interactions also decreased with increasing temperature [15]. Therefore, the effect of urea in the heat-induced gelation process was mostly related to a decrease of polymer-polymer hydrophobic interactions, as shown by the decreased conductivity as a function of temperature (Figure 6.3). Lower ionic strength involves less screening of electrostatic repulsion between protonated chitosan glucosamine groups, and hence reduced possible hydrophobic effect, resulting in detrimental conditions for gel formation. Therefore, the present results strengthen our suggestion that hydrophobic interactions are the main driving force for chitosan- β -GP gelation at high temperature [15].

6.7. Conclusions

In this study, physicochemical and rheological properties of chitosan- β -GP solutions and gels were investigated in terms of urea concentration and temperature. Though the presence of urea is not mandatory for the chitosan- β -GP-acetic acid gel

system, these properties provided information related to the function of hydrophobic and hydrogen bonding interactions.

In terms of physicochemical properties, the pH values of the chitosan- β -GP solutions slightly increased in the presence of urea due to the consumption of H^+ ions in solution through urea hydrolysis process, but they were constant regardless of temperature increase due to the buffering capacity of β -GP. The measured conductivity decreased with increasing urea concentration and temperature, most probably resulting from ionic interactions between ammonium ions and monovalent and divalent β -GP anions. Thus, the use of urea in the chitosan- β -GP system mainly affected polymer-polymer interactions by weakening hydrogen bonds at low temperature (solution behavior), and predominantly decreasing hydrophobic effect at high temperature (gel behavior).

In the solution state, urea resulted in lower elastic properties and shorter relaxation times. The relaxation process was also simplified (narrower spectrum of relaxation times) due to the disruption of hydrogen bonds and hydrophobic interactions.

For the heat-induced gelation, urea increased the gelation temperature in non-isothermal tests and the gelation time in isothermal conditions. From the non-isothermal and isothermal gelation kinetics, the activation energy to form the gel structure increased in the presence of urea, indicating a detrimental effect. Upon cooling all gel systems presented partial thermoreversibility, most probably due to the existence of remaining weak associations.

Our previous results on the gelation of the chitosan- β -GP system illustrated that hydrophobic interactions were dominant since hydrogen bonds are known to weaken rapidly with temperature and ionization calculations showed that ionic interactions also decreased with increasing temperature [15]. Therefore, the detrimental effect of urea in the heat-induced gelation process studied in this work was mostly related to a decrease of hydrophobic effect, as confirmed by the decrease in the measured conductivity (or ionic strength) in the presence of urea and at high temperature. Therefore, the present results confirm that hydrophobic effect is the main driving force for the chitosan- β -GP heat-induced gelation.

6.8. Acknowledgements

The authors gratefully acknowledge the financial support of the Conseil de Recherches en Pêche et en Agroalimentaire du Québec (CORPAQ).

6.9. References

- ¹ Roberts, G. A. F. (1992). Chitin Chemistry. London, The Macmillan Press Ltd.
- ² Brugnerotto, J., Desbrières, J., Heux, L., Mazeau, K., & Rinaudo, M. (2001). Overview on structural characterization of chitosan molecules in relation with their behavior in solution. *Macromolecular Symposia*, 168(1), 1-20.
- ³ Kassai, M. R. (1999). Depolymerization of chitosan. Ph. D. Dissertation, Université Laval, Quebec, Canada.

-
- ⁴ Singla, A. K. & Chawla, M. (2001) Chitosan: some pharmaceutical and biological aspects – an update, *Journal of Pharmacy and Pharmacology*, 53, 1047 – 1067.
- ⁵ Kumar, M. N. V. R. (2000). A review of chitosan and chitosan applications. *Reactive & Functional Polymers*, 46, 1 – 27 (2000)
- ⁶ Jackson, D. S. (1987) Chitosan-Glycerol-Water Gel, USA Patent 4.659,700.
- ⁷ Chenite, A.; Chaput, C.; Wang, D.; Slemani, A. (2001). Temperature-controlled and pH-dependent self-gelling biopolymeric aqueous solutions, WO 01/36000 A1.
- ⁸ Chaput, C.; Chenite, A. (2001). Mineral-polymer hybrid composition, WO 01/41822.
- ⁹ Park, J. W., Choi, K.-H., & Park, K. K. (1983). Acid-base equilibria and related properties of chitosan. *Bulletin of Korean Chemistry Society*, 14(2), 68-72.
- ¹⁰ Vachoud, L., Zydowicz, N., & Domard, A. (1997). Formation and characterisation of a physical chitin gel. *Carbohydrate Research*, 302(3-4), 169-177.
- ¹¹ Cho, J., Heuzey, M.-C., Bégin, A., Carreau, P. J. Viscoelastic Properties of Chitosan Solutions: Effect of Concentration and Ionic Strength. *Journal of Food Engineering* (In press).
- ¹² Chenite, A., Buschmann, M., Wang, D., Chaput, C. & Kandani, N. (2001). Rheological characterisation of thermogelling chitosan/glycerol-phosphate solutions. *Carbohydrate Polymers*, 46(1), 39-47.
- ¹³ Alberty, R. A., & Silbey, R. J. (1996). *Physical chemistry*, 2nd Ed. John Wiley & Sons, Inc.
- ¹⁴ Golberg, R. N., Kishore, N., Lennen, R. M. (2002). Thermodynamic Quantities for the ionization Reactions of Buffers, *J. Phys. Chem. Ref. Data.*, 31, 231 – 370.

-
- ¹⁵ Cho, J.; Heuzey, M.-C., Begin, A., Carreau, P. J. Physical gelation of chitosan in the presence of β -glycerophosphate: The effect of temperature. *Biomacromolecules* (In press).
- ¹⁶ Hammes, G. G., Schimmel, P. R. (1967). An Investigation of Water-Urea and Water-Urea-Polyethylene Glycol Interactions. *J. Am. Chem. Soc.* 89, 442.
- ¹⁷ Kjønsken, A.-L., Hiorth, M., Roots, J., Nystrom, B. (2003). Shear-induced Association and Gelation of Aqueous Solutions of Pectin. *J. Phys. Chem. B.* 107, 6324-6328.
- ¹⁸ Kokufuta, E., Suzuki, H., Yashida, R., Yamada, K., Hirata, M., Kaneko, R. (1998). Role of Hydrogen Bonding and Hydrophobic Interactions in the volume Collapse of a Poly(ethylenimine) Gel. *Langmuir*, 14, 788
- ¹⁹ Kim, S., Sarathchandra, D., Mainwaring, D. E. (1996). Effect of Urea on Molecular and Colloid Aggregation of Proanthocyanidin Polymers from *Pinus radiata*. *Journal of Applied Polymer Science*, 59, 1979 – 1986.
- ²⁰ McGrane, S., Mainwaring, D. E., Cornell, H. J., Rix, C. J. (2004). The Role of Hydrogen Bonding in Amylose Gelation. *Starch/Stärke*, 56, 122 – 131.
- ²¹ Philippova, O. E., Volkov, E. V., Sitnikova, N. L., Khokhlov, A., Desbrieres, J., Rinaudo, M. Two Types of Hydrophobic Aggregates in Aqueous Solution of Chitosan and Its Hydrophobic Derivative. *Biomacromolecules*, 2, 483 – 490 (2001).
- ²² Amiji, M. M. (1995). Pyrene fluorescence study of chitosan self-association in aqueous solution. *Carbohydrate Polymers*, 26, 211-213.

-
- ²³ Nyström, B., Kjøniksen, A.-L. & Iverson, C. (1999). Characterization of association phenomena in aqueous systems of chitosan of different hydrophobicity. *Advances in Colloid and Interface Science*. 79, 81 – 103.
- ²⁴ Wang, D. (1999). Characterization of thermoreversible PH-sensitive physical gels of chitosan, Master's Thesis, Ecole Polytechnique de Montreal, Quebec, Canada.
- ²⁵ Tsaih, M.L.; Chen, R. H. (1997). Effect of molecular weight and urea on the conformational of chitosan molecules in dilute solutions. *International Journal of Biological Macromolecules*, 20, 233 – 240
- ²⁶ Hamdine, M.; Heuzey, M.C.; Bégin A. (2005) Effect of organic and inorganic acids on concentrated chitosan solutions and gels. *International Journal of Biological Macromolecules*. (In revision).
- ²⁷ Cheng, Y., Prud'homme, R. K., Chik, J. & Rau, D. C. (2002). Measurement of Forces between Galactomannan Polymer Chains: Effect of hydrogen bonding. *Macromolecules*, 35, 10155 – 10161.
- ²⁸ Tako, M., & Hanashiro, I. (1997). Evidence for a conformational transition in curdlan.. *Polymer Gels and Networks*, 5, 241 – 250.
- ²⁹ Li, L., Thangamathesvaran, P. M., Yue, C. Y., Tam, K. C., Hu, X., & Lam, Y. C. Gel Network Structure of Methylcellulose in Water. *Langmuir*, 17(26), 8062-8068.
- ³⁰ Desbrieres, J., Martinez, C., & Rinaudo, M. (1996). Hydrophobic derivatives of chitosan: Characterization and rheological behaviour. *International Journal of Biological Macromolecules*, 19(1), 21-28.

-
- ³¹ Cheetham, N. W. H., Tao, L. (1997). Amylose conformational transition in binary DMSO/water mixtures. *Starch/Stärke*, 49, 407 – 415.
- ³² Chen, R. H., Tsaih, M. L. (2000). Urea-induced conformational changes of chitosan molecules and the shift of breaking point of Mark-Houwink equation by increasing urea concentration. *Journal of Applied Polymer Science*, 75, 452-457
- ³³ Hammes, G. G., Swann, J. C. (1967). Influence of denaturing agents on solvent structure. *Biochemistry*, 6, 1591 – 1596.
- ³⁴ Finny, J. L., Soper, A. K. (1994). Solvent structure and perturbations in solutions of chemical and biological importance. *Chem Soc. Rev.*, 23, 1 – 10.
- ³⁵ Dubin, P., & Stauss, U. P. (1973). Conformational transitions of hydrophobic polyacids in denaturant solutions. Effect of urea. *J. Phys. Chem.*, 11, 1427 - 1431..
- ³⁶ Roseman, M., Jenks, W. P. (1975). Interactions of urea and other polar compounds in water. *J. Am. Chem. Soc.*, 97, 631 - 640.
- ³⁷ Alonso, D. O. V., Dill, K. A. (1991). Solvent denaturation and stabilization of globular proteins. *Biochemistry*, 30, 5974 - 5985.
- ³⁸ Christianziana, P., Lelj, F., Amodeo, P., Barone, G., Barone, V. (1989). *J. Chem. Soc. Faraday. Trans. 2*, 85, 621.
- ³⁹ Wallqvist, A., & Covell, D. G. (1998). Hydrophobic Interactions in Aqueous Urea Solutions with Implications for the Mechanism of Protein Denaturation, *J. Am. Chem. Soc.*, 120, 427 – 428.
- ⁴⁰ HonerKamp, J., & Weese, J., (1993). A nonlinear regularization method for the calculation of relaxation time, *Rheological Acta*, 32, 65 – 83.

-
- ⁴¹ Carreau, P. J., De Kee, D. C. R., & Chabra, P. R. (1997). *Rheology of Polymeric Systems : Principles and Applications*, Hanser Publishers, Munich, Germany.
- ⁴² Shaw, W. H. R., & Bordeaux, J. J. (1995). The decomposition of urea in aqueous media. *Journal of the American Chemical Society*, 77, 4729 – 4733.
- ⁴³ Jana P.K., Moulik S.P. (1993). Interaction of amino acids and gelation with urea. *Indian Journal of Biochemistry and Biophysics*, 30(5), 297 – 305.
- ⁴⁴ Roth, T., Maier, D., Friedrich, C., Marth, M., & Honerkamp, J. (2000). Determination of the relaxation time spectrum from dynamic moduli using an edge preserving regularization method. *Rheologica Acta*, 39, 163 – 173.
- ⁴⁵ Lauten, R. A., & Nyström, B. (1999). Linear and nonlinear viscoelastic properties of aqueous solutions of cationic polyacrylamides. *Macromolecular Chemistry and Physics*, 201(6), 677 - 684
- ⁴⁶ Thuresson K., Lindman, B., and Nyström, B. (1997). Effect of hydrophobic modification of a nonionic cellulose derivative on the interaction with surfactants. *Rheology. Journal of Physics and Chemistry B*, 101, 6450 – 6459.
- ⁴⁷ Sarkar, N. (1995). Kinetics of thermal gelation of methylcellulose and hydroxypropylmethylcellulose in aqueous solutions. *Carbohydrate Polymers*, 26(3), 195-203.
- ⁴⁸ Lopes da Silva, J. A.; Gonçalves, M. P.; Rao, M. A. (1995). Kinetics and thermal behavior of the structure formation process in HMP/sucrose gelation. *International Journal of Biological Macromolecules*, 17(1), 25 – 32.

-
- ⁴⁹ Fu, J.-T.; Rao, M. A. (2001). Rheology and structure development during gelation of low-methoxyl pectin gels: the effect of sucrose. *Food Hydrocolloids*, 15(1), 93 – 100.
- ⁵⁰ Ross-Murphy, S. B. (1991). The estimation of junction zone size from geltime measurements. *Carbohydrate Polymers*, 14, 281 – 294.
- ⁵¹ Böhm, N., Kulicke, W.-M. (1999). Rheological studies of barley (1→3)(1→4)-β-glucan in concentrated solution: mechanistic and kinetic investigation of the gel formation, *Carbohydrate Research*, 315, 302 – 311.
- ⁵² McIver, R. G., Axford, D. W. E., Colwell, K. H., Elton, G. A. H. (1968). Kinetic study of the retrogradation of gelatinized starch. *J. Sci. Food Agric.*, 19(10), 560 – 563.
- ⁵³ Ahmed Mohamed El-Hadi Abdel Ghaffar (2000). Development of A Biodegradable Material Based on Poly(3-HydroxyButyrate) PHB. Ph. D. Dissertation. Martin-Luther Universität Halle-Wittenberg, Germany.
- ⁵⁴ Li, Y. Zhang, G., Zhu, X., & Yan, D. (2003). Isothermal and Nonisothermal Crystallization Kinetics of Partially Melting Nylon 10 12. *Journal of Applied Polymer Science*, 88, 1311 – 1319.
- ⁵⁵ Leibler, L., Rubinstein M., Colby R.H. (1991) Dynamics of reversible networks. *Macromolecules*, 24, 4701 – 4707.
- ⁵⁶ Doi, M., & Edwards, S. F. (1978). Dynamics of concentrated polymer systems. I. Brownian motion in the equilibrium systems. II. Molecular motion under flow. III. The constitutive equation. *Journal of the Chemical Society Faraday Transactions II*, 74, 1787 – 1832.

⁵⁷ Likhtman AE, McLeish TCB. (2002) Quantitative Theory for Linear Dynamics of Linear Entangled Polymers. *Macromolecules*, 35, 6332 – 6343.

Table 6.1. Nomenclature and solution compositions expressed in molarity

Sample	AcOH	Chitosan*	β -GP	Urea
U0	0.12	0.08	0.53	0
U1	0.12	0.08	0.53	1
U3	0.12	0.08	0.53	3
U5	0.12	0.08	0.53	5
14CU0	0.12	0.14	0.53	0
14CU3	0.12	0.14	0.53	3

* Concentration of glucosamine units or monomol/L

Figures caption

Figure 6.1. Chemical structure of (a) chitosan and (b) β -glycerophosphate (β -GP).

Figure 6.2. Effects of urea content and temperature on the pH of various solutions.

Figure 6.3. Urea effect on (a) conductivity and (b) relative conductivity as a function of temperature.

Figure 6.4. Dynamic moduli G' and G'' of chitosan- β -GP solutions in the presence of urea at 15°C. Insert: $\tan \delta$ ($\gamma_0 = 0.1$).

Figure 6.5. Urea effect on the normalized time-weighted stress relaxation spectra.

Figure 6.6. Urea effect on the Cole-Cole plot. Insert: effect of urea on exponent P and plateau modulus G_e (Equation 6.5).

Figure 6.7. Urea effect on heat-induced gelation. Complex modulus, G^* , reported as a function of temperature ($\gamma_0 = 0.01$, $\omega = 6.28$ rad/s, heating rate = 1°C/min).

Figure 6.8. Effect of urea on gelation temperature (T_{gel}) and gel strength (G^* at 90°C).

Figure 6.9. Nonisothermal gelation kinetics under various urea concentrations. (a) Plot of $1/G'^2 \times dG'/dt$ vs. $1/T$ and (b) gelation activation energy as a function of urea content.

Figure 6.10. Urea effect on the thermoreversibility of the gels. (a) Dynamic moduli G' and G'' and (b) $\tan \delta$ during the cooling process ($\gamma_0 = 0.01$, $\omega = 6.28$ rad/s, cooling rate = 1°C/min).

Figure 6.11. Dynamic moduli G' and G'' for gels cooled at 15°C, as a function of frequency. Insert: $\tan \delta$ ($\gamma_0 = 0.1$).

Figure 6.12. (a) Dynamic moduli G' and G'' as a function of time under various temperatures and urea concentrations. (b) Effects of urea and temperature on gelation

time (t_{gel}). Concentration of chitosan = 0.14 M, pH at 25°C = 7 ($\gamma_0 = 0.01$, $\omega = 6.28$ rad/s).

Figure 6.13. Calculated relaxation moduli using Doi-Edwards equation (DE) and the relaxation spectra of Figure 6.4 (RS).

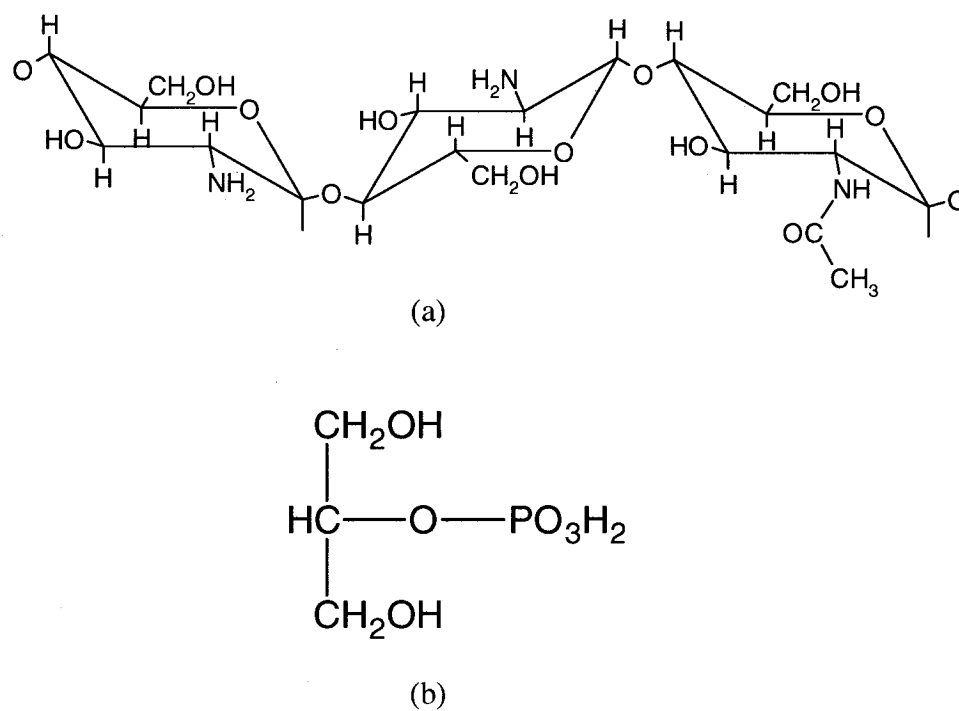


Figure 6.1. Chemical structure of (a) chitosan and (b) β -glycerophosphate (β -GP).

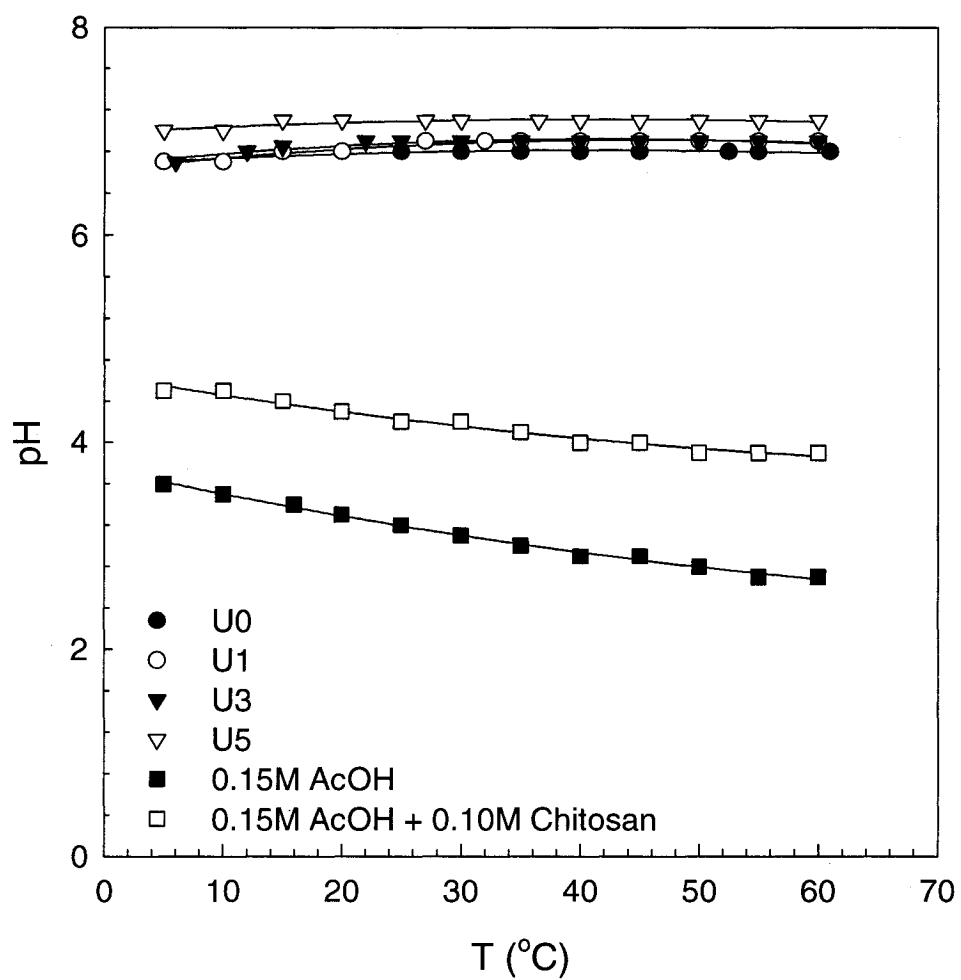


Figure 6.2. Effects of urea content and temperature on the pH of various solutions.

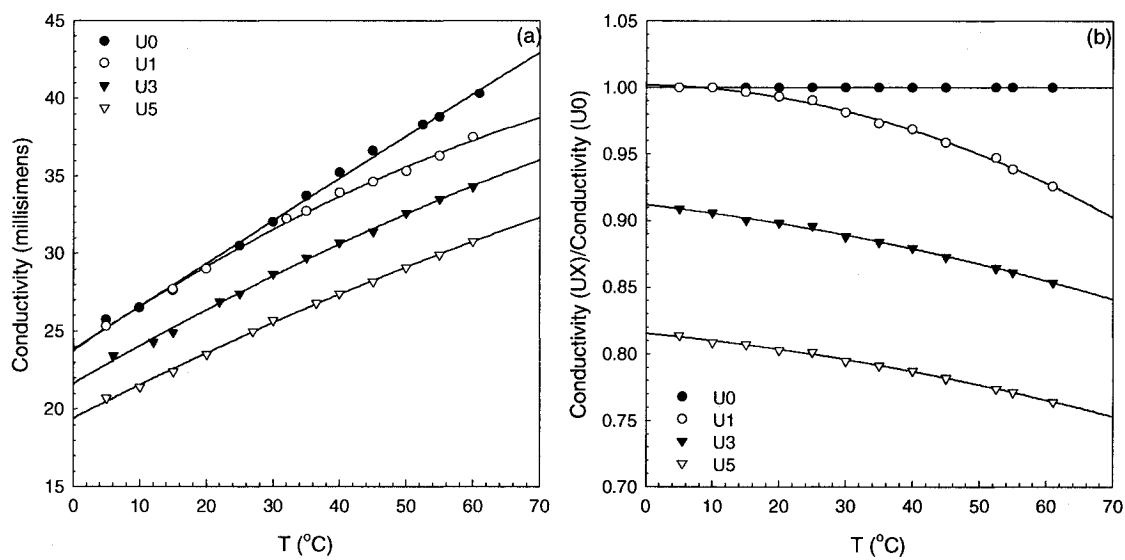


Figure 6.3. Urea effect on (a) conductivity and (b) relative conductivity as a function of temperature.

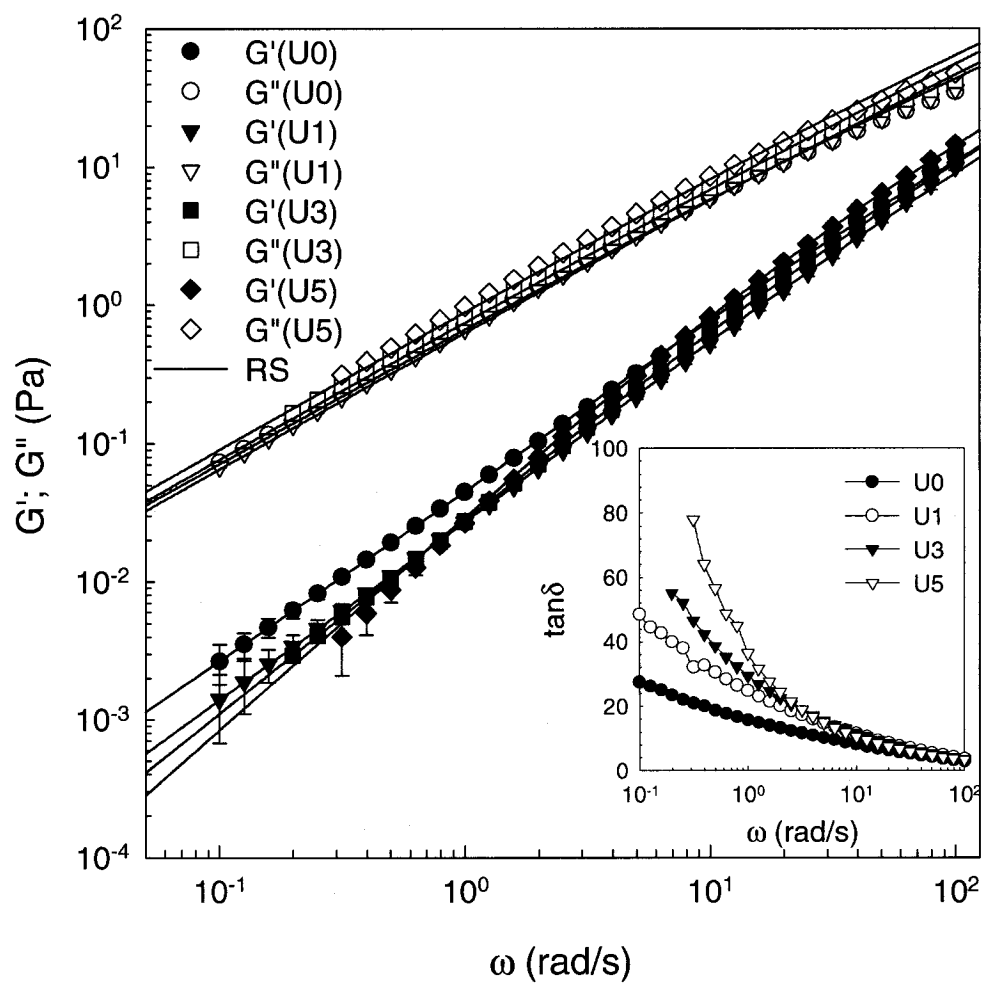


Figure 6.4. Dynamic moduli G' and G'' of chitosan- β -GP solutions in the presence of urea at 15°C. Insert: $\tan \delta$ ($\gamma_0 = 0.1$).

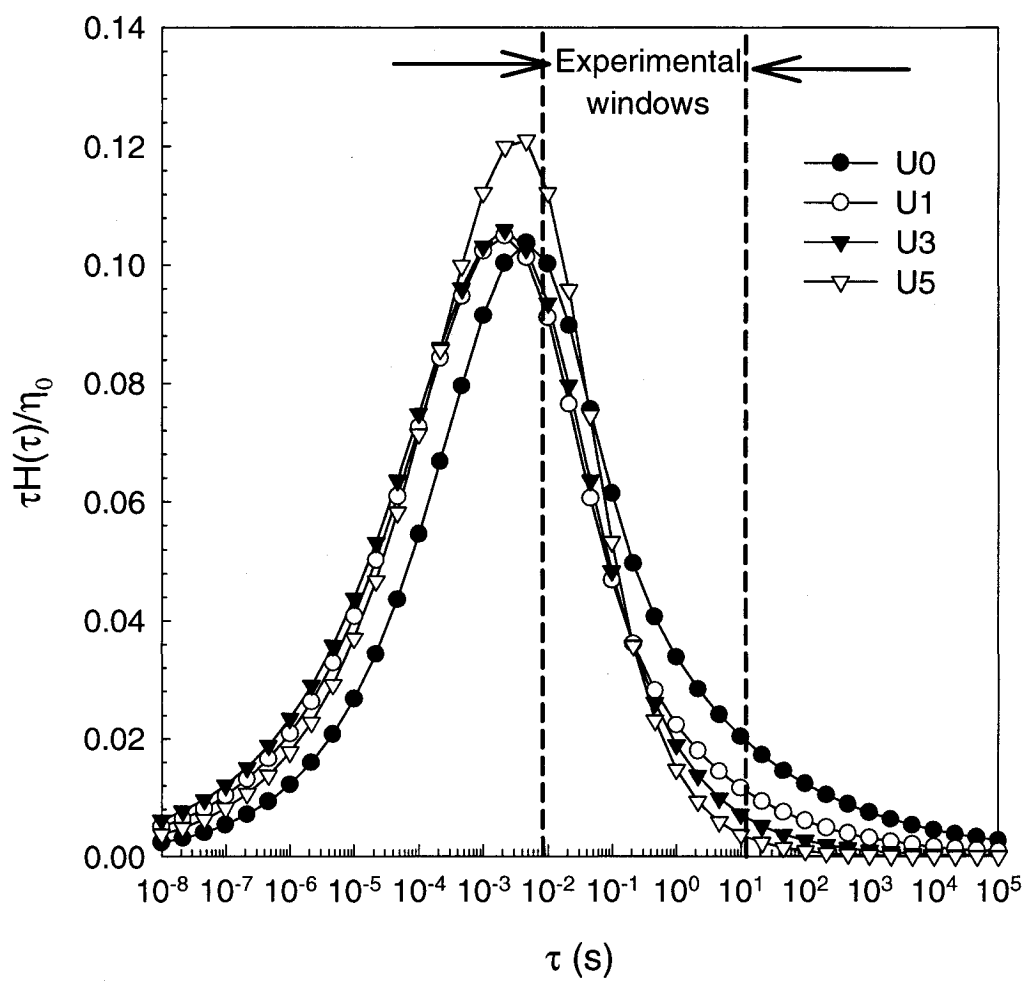


Figure 6.5. Urea effect on the normalized time-weighted stress relaxation spectra.

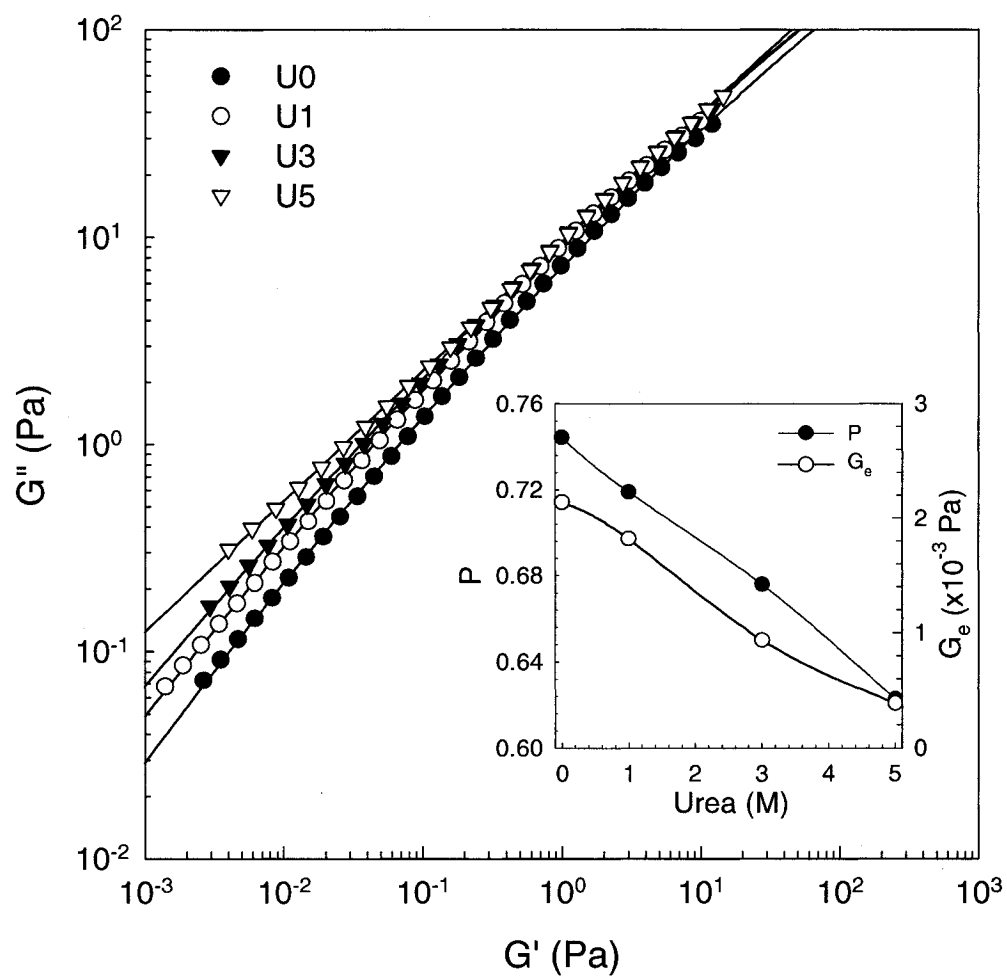


Figure 6.6. Urea effect on the Cole-Cole plot. Insert: effect of urea on exponent P and plateau modulus G_e (Equation 6.5).

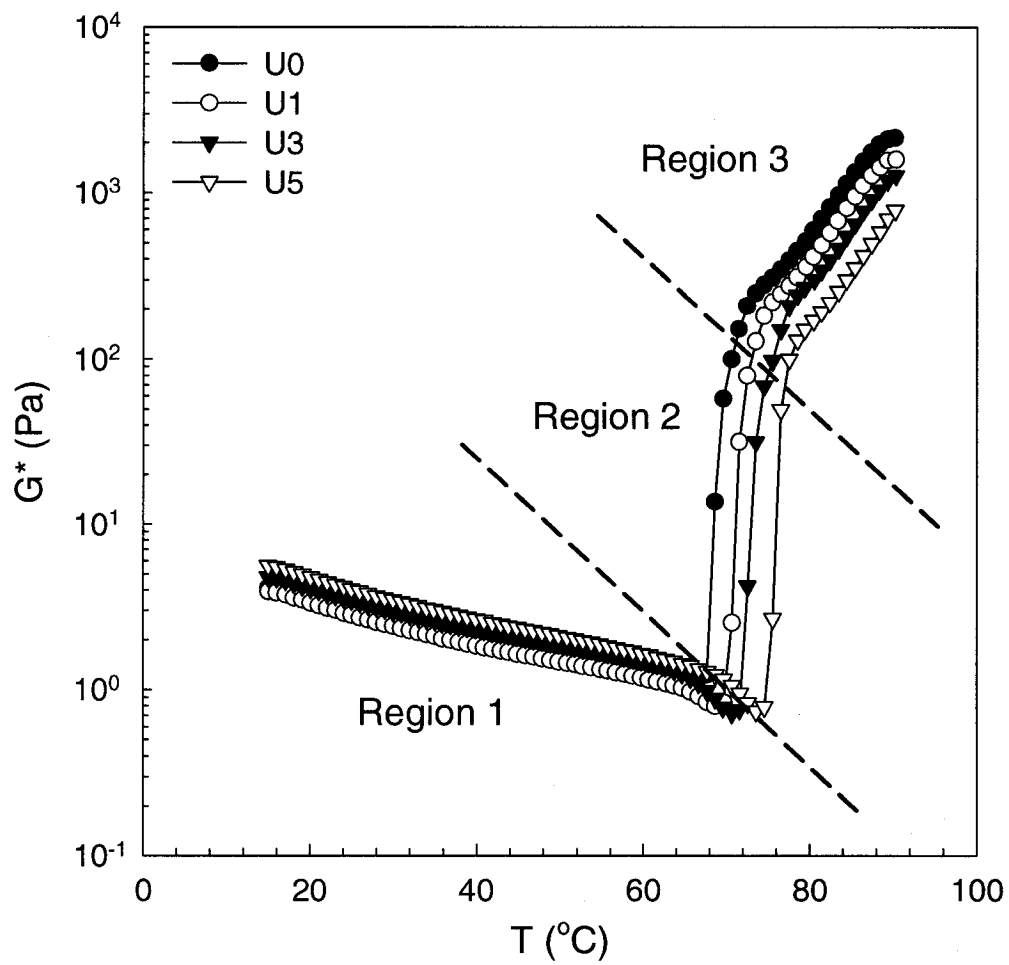


Figure 6.7. Urea effect on heat-induced gelation. Complex modulus G^* reported as a function of temperature ($\gamma_0 = 0.01$, $\omega = 6.28$ rad/s, heating rate = $1^{\circ}\text{C}/\text{min}$).

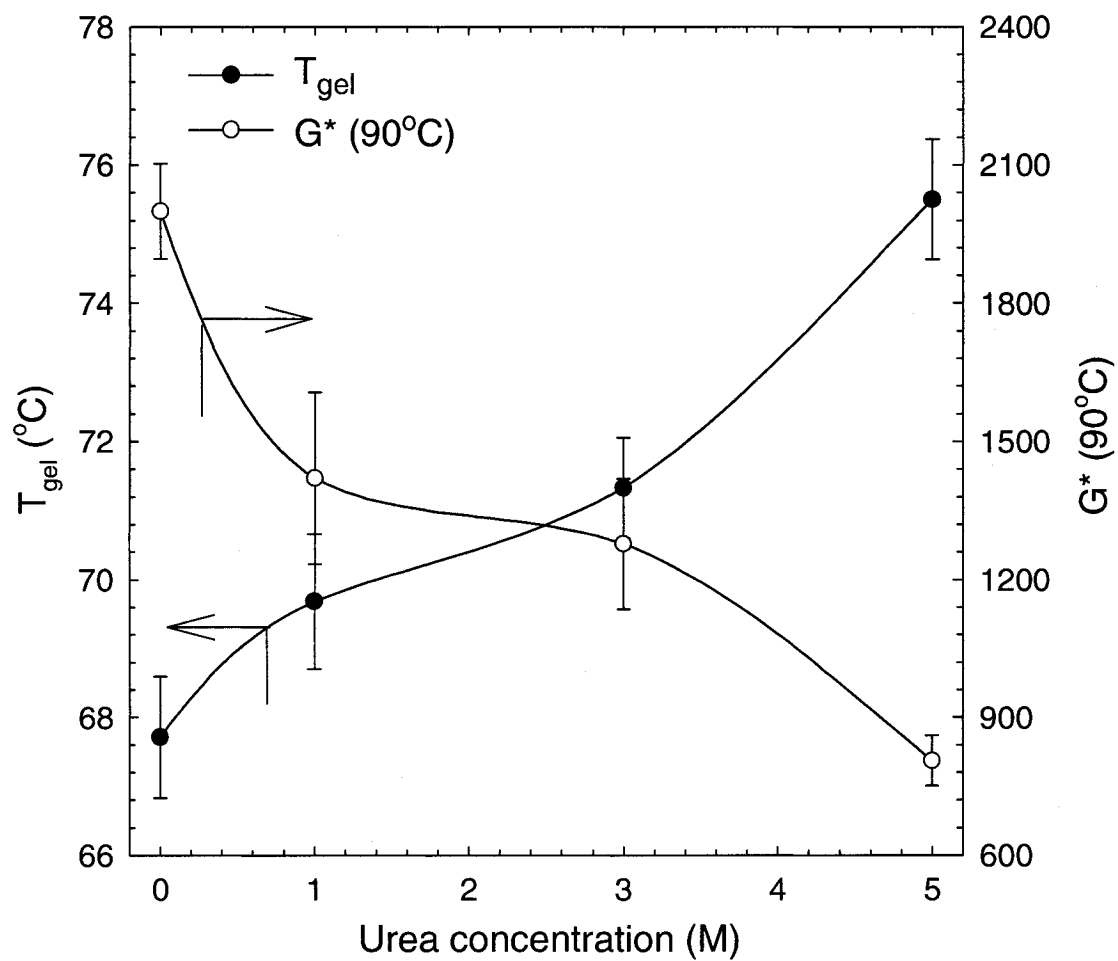


Figure 6.8. Effect of urea on gelation temperature (T_{gel}) and gel strength (G^* at 90°C).

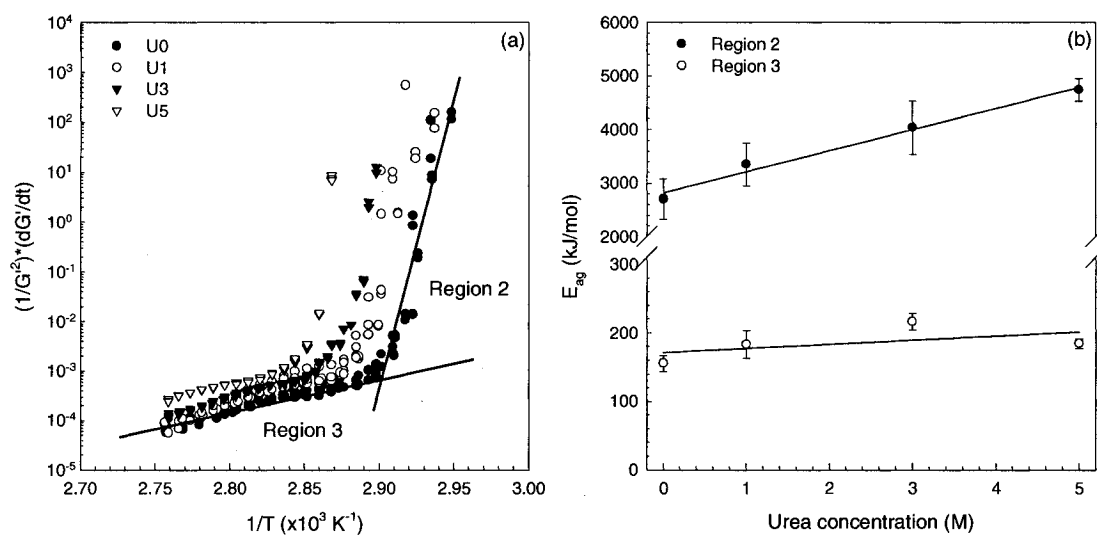


Figure 6.9. Nonisothermal gelation kinetics under various urea concentrations. (a) Plot of $1/G^2 \times dG/dt$ vs. $1/T$ and (b) gelation activation energy as a function of urea content.

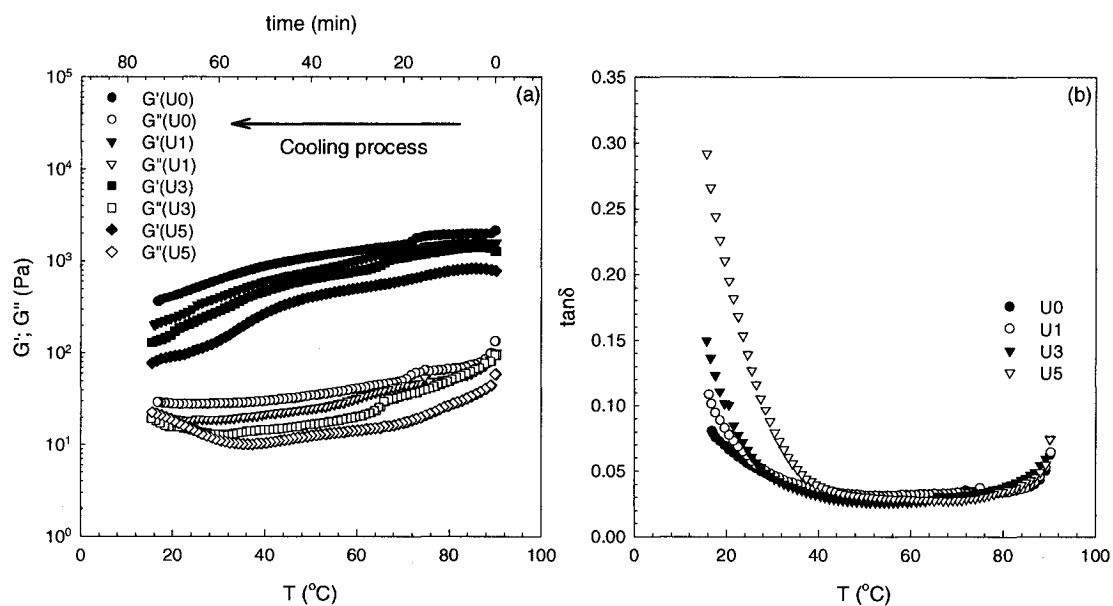


Figure 6.10. Urea effect on the thermoreversibility of the gels. (a) Dynamic moduli G' and G'' and (b) $\tan \delta$ during the cooling process ($\gamma_0 = 0.01$, $\omega = 6.28$ rad/s, cooling rate = $1^{\circ}\text{C}/\text{min}$).

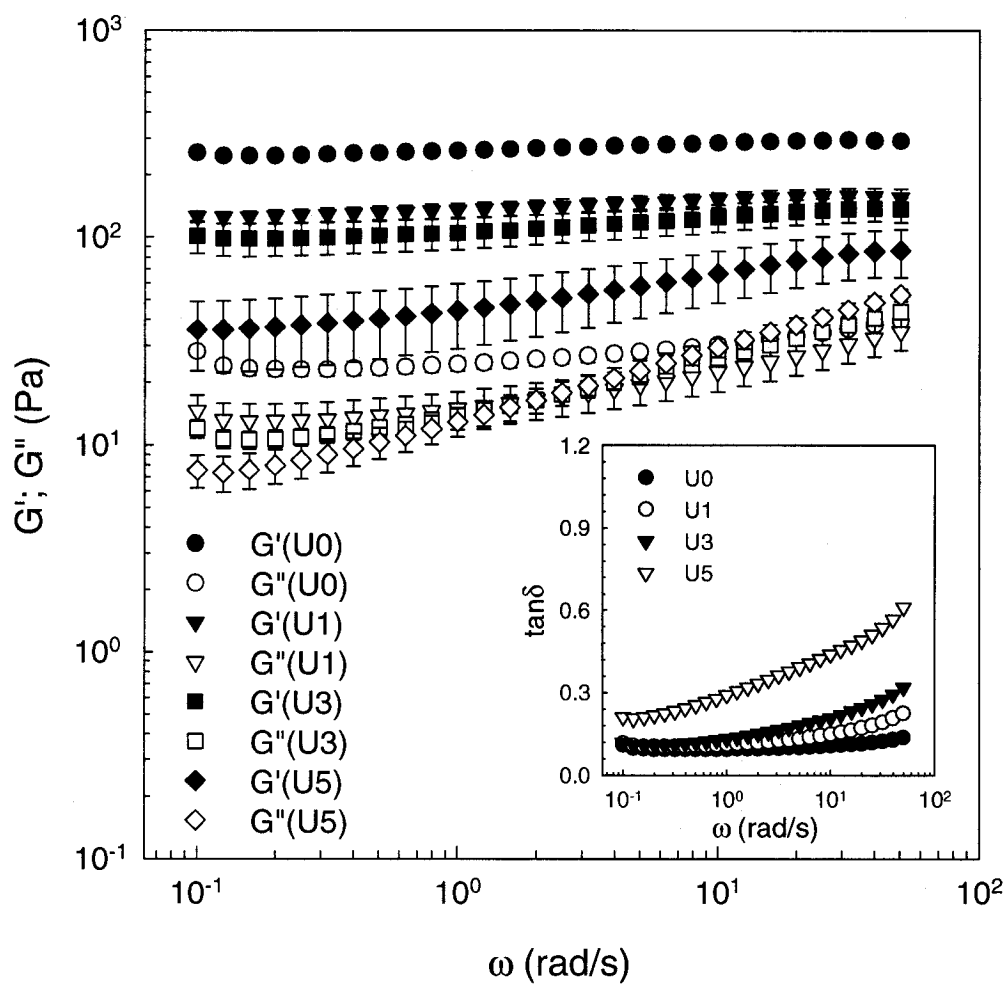


Figure 6.11. Dynamic moduli G' and G'' for gels cooled at 15°C, as a function of frequency. Insert: $\tan \delta$. ($\gamma_0 = 0.1$).

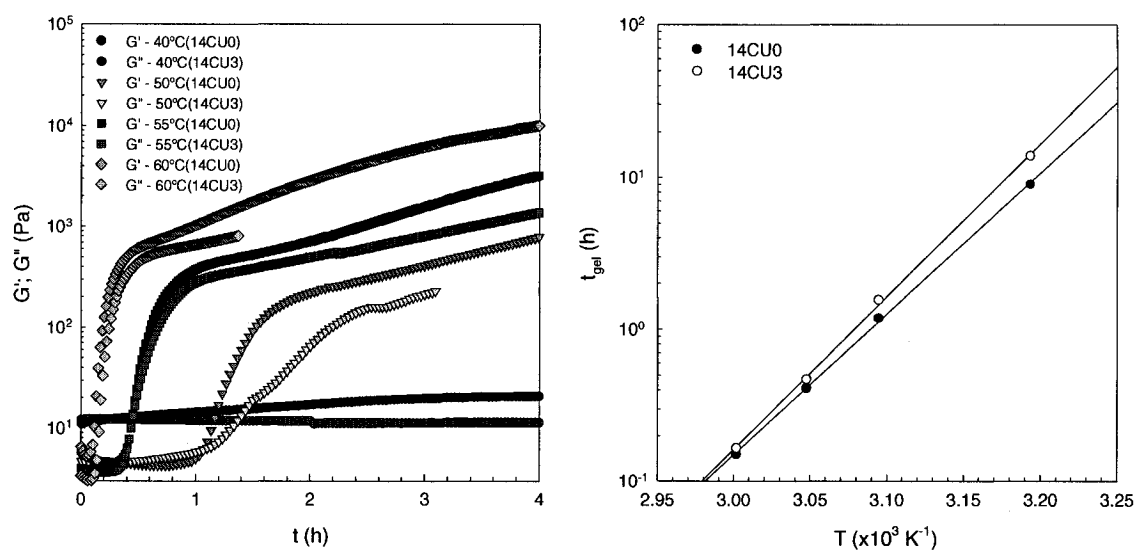


Figure 6.12. (a) Dynamic moduli G' and G'' as a function of time under various temperatures and urea concentrations. (b) Effects of urea content and temperature on gelation time (t_{gel}). Concentration of chitosan = 0.14 M, pH at $25^\circ\text{C} = 7$ ($\gamma_0 = 0.01$, $\omega = 6.28$ rad/s).

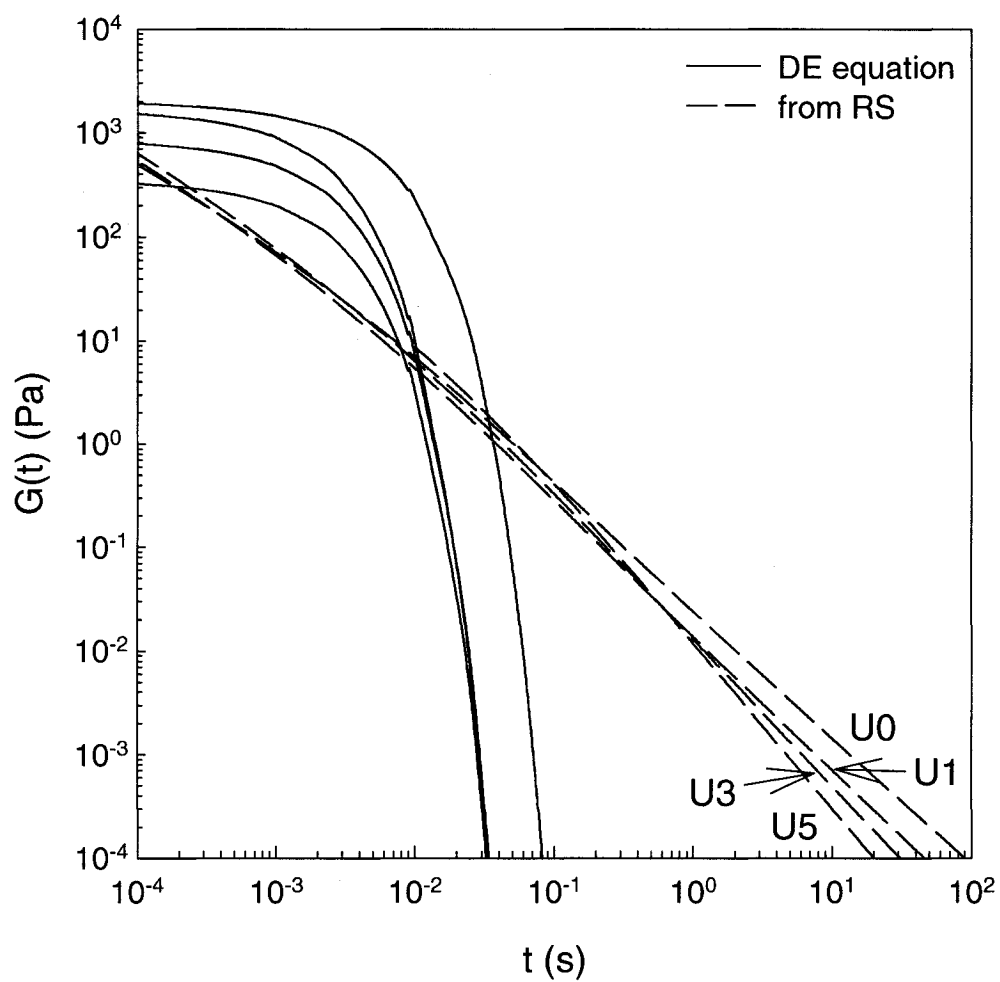


Figure 6.13. Calculated relaxation moduli using Doi-Edwards equation (DE) and the relaxation spectra of Figure 6.4 (RS).

Chapter 7

Chitosan and glycerophosphate concentration dependence of solution behavior and gel point using small amplitude oscillatory rheometry

Jaepyoung Cho¹, Marie-Claude Heuzey^{1*}, André Bégin² and Pierre J. Carreau¹

¹ CREPEQ, Department of Chemical Engineering, Ecole Polytechnique, P.O. Box 6079,
Station Centre-Ville, Montreal, QC, H3C 3A7, CANADA

² Food Research and Development Centre, 3600 Casavant Blvd West, Saint-Hyacinthe,
QC, J2S 8E3, CANADA

* Corresponding author. E-mail: marie-claude.heuzey@polymtl.ca; tel.: +1-514-340-4711 ext. 5930; fax: +1-514-340-2994

7.1. ABSTRACT

In this study, linear viscoelastic properties of a chitosan system were investigated in the sol and gel states in terms of glycerophosphate (GP) (C_{GP}) and polymer (C_C) concentrations. The chitosan solutions showed a liquid-like behaviour at low β -GP and chitosan content, but deviated from the sol state at higher concentrations. The complex viscosity at 0.1 rad/s ($\eta^*_{0.1\text{rad/s}}$) presented a strong power-law relationship with chitosan concentration, i.e. $\eta^*_{0.1\text{rad/s}} \sim C_C^{5.0}$. The flow activation energy (E_{af}) calculated from the master curves of the linear viscoelastic data increased with decreasing C_{GP} and increasing C_C . The opposite behaviour was explained in terms of enhanced hydrophobic interactions at high glycerophosphate concentration and high temperature, confirmed by the calculated ionic strength. Monitoring of the heat-induced gelation showed that the data obtained at different β -GP concentrations could be superposed in a single master curve in the gel state, indicating that the gelation process and kinetics were identical regardless of β -GP content. However, measurements obtained at different chitosan concentrations could not be shifted onto a single curve. Higher C_C resulted in lower gelation temperature but slower kinetics due to the high viscosity and slower molecular diffusion. The 3D sol-gel phase diagram was derived from the rheological measurements during the heat-induced gelation. A synergistic effect at high β -GP and polymer concentrations resulted in a gelation on the edge of concentration-induced and heat-induced gelation.

7.2. INTRODUCTION

Chitosan is a hydrophilic cationic copolymer produced by the deacetylation of chitin and composed of glucosamine and acetylglucosamine units [1]. The designation “chitosan” applies when the degree of deacetylation (DDA), or the fraction of glucosamine units in the chemical structure, is above 50% [2]. The increased solubility of chitosan with respect to that of chitin is related to its positively charged polyelectrolyte nature due to the protonation of the free amine groups below a pH of 6.2 [3]. It is a non-toxic, biocompatible and biodegradable material that has found many applications in industries such as nutraceutic, medical, cosmetic and pharmaceutical [4,5,6,7,8,9]. While chitosan has been mainly chemically cross-linked, it has been observed more recently to undergo polymer concentration-induced and heat-induced physical gelation. Concentration-induced physical gelation has been reported in acetic acid at chitosan concentration above 39 g/L [10], and in phosphoric and oxalic acid at polymer concentrations above 40 and 50 g/L, respectively [11]. Recently, a homogenous thermoreversible gel system was prepared by neutralizing highly deacetylated semi-diluted chitosan solutions with a weak base, β -glycerophosphate (β -GP) [8,9]. The system remained in solution at physiological pH (=7) and room temperature, but changed into a gel upon heating at physiological temperature (37°C), manifesting therefore heat-induced gelation. When the temperature decreased, the chitosan gel returned to the solution state under certain conditions.

In our previous studies we have investigated rheological and physicochemical properties of chitosan in the presence of β -glycerophosphate, mainly exploring the effect

of temperature and urea concentration in order to gain understanding of the gelation mechanisms [12,13]. While monitoring the evolution of the viscoelastic properties during the heat-induced gelation, three regions were observed: 1) a liquid-like behavior at low temperature ($G' < G''$), 2) a fast gelation in the vicinity of the gel point, followed by 3) a slow gelation process at higher temperature. The gel structure formed was only partially thermoreversible upon cooling to 5°C. Physicochemical properties such as pH and conductivity were also recorded upon temperature increase. It was found that temperature had no effect on the pH value of the chitosan- β -GP system, most probably because of the buffering capacity of the glycerophosphate, while conductivity (and calculated ionic strength) increased. Our calculations showed that the estimated protonation of chitosan decreased with increasing temperature, but that of β -GP increased. The reduction of the ratio of $-\text{NH}_3^+$ in chitosan and $-\text{OPO}(\text{O}^-)^2$ in β -GP at high temperature indicated a decrease of potential ionic interactions in the gel formed. On the other hand, increased ionic strength as a function of temperature involved enhanced screening of electrostatic repulsion between amine protonated groups, and hence more hydrophobic interactions. Since it is generally assumed that hydrogen bonding interactions are not predominant at high temperature, we suggested that hydrophobic interactions were the main driving force for the chitosan- β -GP gelation upon temperature increase [12].

In this work, we continue our in-depth study of the chitosan-GP system, looking specifically this time at the effect of polymer and glycerophosphate concentrations on solution and gelation behavior, using small amplitude oscillatory rheometry. Results

from the gelation tests are used to establish the 3D sol-gel phase diagram. Sol and gel behaviour are also investigated using two types of glycerophosphate (α -GP and β -GP) with different chemical architecture, in order to confirm our assumption that ionic bridging is of minor importance in the gelation process. Finally, the structure of the physical junction zones at the gelation point is characterized using a modified Eldridge-Ferry method [14].

7.3. THEORETICAL BACKGROUND

Most physical gels involve complex network junctions made of polymer segments belonging to several chains. Tanaka and Nishinari [14] proposed the notion of junction multiplicity S , representing the number of chains involved in a single junction (Figure 1), in order to characterize these complex structures. Simple cross-links made of pairs such as those described by the classical gelation theory from Flory [15] have a multiplicity of 2. In this case, the conventional Eldridge-Ferry procedure [16] can be used to determine the number of structural units ζ involved in a junction (Figure 7.1). The Eldridge-Ferry method [16] plots either the logarithm of the melting gel concentration C_{gel} or molecular weight M of polymer against reciprocal temperature to determine the bonding enthalpy ΔH_0 :

$$\ln C_{gel} = \frac{\Delta H_0}{k_B T} + \text{constant} \quad (7.1)$$

$$\ln M = \frac{\Delta H_0}{k_B T} + \text{constant} \quad (7.2)$$

with T the absolute temperature and k_B the Boltzmann constant. The bonding enthalpy determined by this method is expected to be proportional to the number of structural

units ζ involved in a junction, but independent of the junction multiplicity S . Hence, this assumption incorrectly characterizes physical gels involving complex junctions. Physical gels can present large S values, and Tanaka and Nishinari [14], following their lattice-theoretical description of network-forming polymer solutions, have proposed a new procedure to characterize junction multiplicity in thermoreversible gelation, referred to as the modified Eldridge-Ferry method. For homopolymer gelation, the resulting equation is expressed as:

$$\ln C_{gel} = \zeta \frac{\Delta h_0}{k_B T} - \frac{1}{S-1} \ln M + \text{constant} \quad (7.3)$$

with Δh_0 the bonding enthalpy per molecule of structural unit in the junction. The two parameters characterizing the multiple junctions, i.e. ζ and S , can be estimated from the slope of the semi-log plot of $\ln C_{gel}$ versus $(1/T + \ln M)$ [17]. According to Equation (7.3), the slope of the plot at a constant molecular weight M can be used to estimate the number of structural units ζ in a junction [14]:

$$\zeta = \frac{k_B}{|\Delta h_0|} * slope = \frac{R}{|\Delta h_0|_{mol}} * slope \quad (7.4)$$

with R the ideal gas constant. This procedure was used in our work to determine the bonding enthalpy per mole of structural unit in a junction of the chitosan-glycerophosphate system.

7.4. EXPERIMENTS

7.4.1. Materials

The chitosan used in this study was purchased from Marinard Biotech (Rivière-aux-Renards, QC). The degree of deacetylation (DDA), or fraction of glucosamine units, was 93% as determined from colloidal titration with polyvinyl sulfate potassium, initially standardized with cethylpyridinium chloride. Gel permeation chromatography (GPC) was used to characterize the polymer molecular weight. The GPC measurements were conducted with an Ultrahydrogel™ 500 Column (Waters Co., Milford, MA) in 0.25M acetic acid / 0.25M sodium acetate using dextran standards. The weight-average molecular weight (\overline{M}_w) was 8.5×10^5 g/mol ($\overline{M}_w / \overline{M}_n = 2.76$). Aqueous solutions of acetic acid (99.7%, Sigma-Aldrich Canada Ltd., Oakville, ON) were used to dissolve the chitosan. The two glycerophosphates, disodium- α -GP and disodium- β -GP (Sigma-Aldrich Canada Ltd., Oakville, ON) were used to control the pH values of the chitosan solutions and promote heat-induced gelation. Figure 7.2 shows the chemical structures of the two glycerophosphates. While the α -type has a linear structure, the β -type is more compact.

7.4.2. Chitosan solutions preparation

A stock solution of chitosan (5% w/v) was prepared by dissolving the biopolymer in 1% w/v acetic acid aqueous solution and mildly stirring with a high torque stirrer (Caframo Ltd., Wiarton, ON) at 30 RPM for 12h at room temperature. During the stirring process, the container of the stock solution was covered with

aluminium foil to prevent evaporation, and the slight weight difference before and after the stirring process was compensated by adding extra amount of solvent. With the stock solution, a series of less concentrated solutions were prepared by adding the acetic acid solution. Then, glycerophosphate was added very slowly to raise the pH of the chitosan solutions above a pH of 6.5, the pK_a of chitosan at low protonation [1]. For mixing the chitosan-GP solutions, we used a laboratory magnetic stirrer (PC-420 Corning® Stirrer/Hot Plate, Corning Inc., MA, USA). A mixing time of 0.5h was used to homogeneously disperse GP and to avoid the formation of local precipitates. The volume difference caused by the addition of GP was compensated in other solutions by adding deionized water. The final total volume of each solution was 80 mL. The composition (in molarity) and nomenclature of the chitosan solutions are presented in Table 7.1. After mixing, the chitosan solutions were left for 3h to degas without stirring at room temperature and stored overnight in a refrigerator ($T \sim 5^{\circ}C$) to stabilize the solutions before rheological measurements. It was found that this overnight storage was essential to the reproducibility of the results, possibly because of the presence of small remaining bubbles. If not used the following day, the samples were stored at $5^{\circ}C$ and characterized within one week to avoid minor aging related to polymer degradation. The pH (pH -meter, Hanna Ltd., Àrvore - Vila do Conde, Portugal) of each chitosan sample was measured at room temperature before the rheological measurements.

7.4.3. Rheological measurements

The rotational rheometer used in this study was a stress-controlled device (AR-2000, TA Instruments, DE, USA) with a Couette geometry. Mineral oil covered the surface of the chitosan solutions to prevent evaporation during the tests. The effect of the mineral oil on the measurements was shown to be negligible. The dynamic mechanical properties of the solutions were measured at various temperatures (5 - 45°C) in terms of polymer and GP concentrations. The oscillatory shear measurements were performed in the linear viscoelastic regime, and master curves were obtained from the oscillatory data.

During the gelation process in non-isothermal conditions, the evolution of rheological properties was investigated between 45 and 90°C using a constant heating rate (1°C/min). Small amplitude deformation γ_0 (0.01) and low frequency ω (6.28 rad/s) were applied in order not to disturb the gel formation. The gelation temperature (T_{gel}) was determined as the crossover of the storage and loss moduli ($\tan \delta = 1$), despite of the slight dependence on frequency. The rheological properties measured during the heat-induced gelation were used to evaluate the gelation activation energy (E_{ag}) using a non-isothermal kinetics model presented later.

7.5. RESULTS

7.5.1. Effect of β -GP and chitosan concentrations on solution behaviour

The pH values measured at room temperature for the various chitosan solutions are reported in Table 7.1. Increasing β -GP concentration slightly raised the pH due to the neutralizing effect of the phosphate groups of this weak base ($pK_{a,2}(\beta\text{-GP}) = 6.65$ at

25°C [18]). The small *pH* increase with polymer concentration, previously reported [12,19], was due to the consumption of H^+ ions in solution by the protonation of the free amine groups.

The effect of glycerophosphate and polymer concentrations on small amplitude oscillatory rheometry data is shown in Figures 7.3 and 7.4, respectively. The master curves have been obtained by the superposition of the complex moduli measured between 5 and 45°C using a temperature shift factor (a_T) related to a flow activation energy (E_{af}) in an Arrhenius-type relationship:

$$a_T = \exp \left\{ \frac{E_{af}}{R} \left(\frac{1}{T} - \frac{1}{T_0} \right) \right\} \quad (7.5)$$

with T_0 the reference temperature (298K). In Figure 7.3, the master curves of G' and G'' for samples 15-33, 15-66 and 15-83 showed increased values with higher C_{GP} content, while $\tan \delta$ (not shown) decreased, corresponding to an enhancement of elasticity due to the increase of specific interactions at high β -GP concentration. In the low frequency region, the chitosan solutions showed a terminal slope larger than 2 for G' , with values of 1.5 and 1.2 at the lowest and highest β -GP concentrations, respectively. The elastic modulus even manifested a slight inflexion in its slope and the onset of a small plateau at the lowest frequencies. Measurements at much lower frequencies would have been necessary to see the true solution terminal zone. The crossover of G' and G'' gradually moved to lower frequencies with increasing β -GP content. While the reciprocal of the cross-over frequency can be related to the characteristic relaxation time τ_1 , or longest reptation time, a characteristic relaxation time can also be associated with the frequency

where the change of slope is seen. This relaxation time, τ_2 , was related to specific molecular interactions that could be precursors of the junction zones in the subsequent gelation. It can be observed from Table 7.2 that τ_2 is three orders of magnitude longer than τ_1 , indicating that the relaxation process associated with these molecular interactions is much slower than reptation. Both times were also shown to slightly decrease with decreasing β -GP concentration (Table 7.2).

A similar behaviour was observed for the effect of chitosan concentration C_C on the complex moduli master curves, shown in Figure 7.4. At higher chitosan concentration, both moduli increased and the terminal slopes became smaller. For sample 20-66, the slopes of G' and G'' were as low as 0.8 ($G' \sim G'' \sim \omega^{0.8}$), while $\tan\delta$ was approximately 2.5 in the terminal zone (not shown). The moduli crossover frequency was also considerably moved to lower frequency as chitosan concentration increased, resulting in very large differences in τ_1 (Table 2), due to the increased number of entanglements at higher polymer content. Surprisingly, the characteristic relaxation time related to specific molecular interactions τ_2 was not a function of β -GP concentration, but this can be related to the uncertainty in evaluating the frequency where the change of slope is observed.

The effect of β -GP and chitosan concentrations on the calculated flow activation energies E_{af} can be seen in Figure 7.5. E_{af} decreased with increasing C_{GP} but increased with C_C . These opposite effects are examined further in the discussion section. Finally, Figure 7.6 presents the influence of C_C on the complex viscosity at $\omega = 0.1$ rad/s and 25°C ($\eta^*_{0.1\text{rad/s}}$). As expected, the complex viscosity increased with polymer content.

The viscosity presented a power-law relationship with chitosan concentrations, i.e. $\eta^*_{0.1\text{rad/s}} \sim C_C^5$, but was almost independent of β -GP concentration. The exponent value of the log-log plot of $\eta^*_{0.1\text{rad/s}}$ and C_C was also found to be 5 at 5 and 45°C (results not shown.).

7.5.2. Effect of β -GP and chitosan concentrations on gelation

The evolution of the complex moduli was investigated in terms of β -GP and chitosan concentrations during the heat-induced gelation, using a temperature ramp of 1°C/min. Figure 7.7 (a) shows the gelation behaviour of a 0.15M chitosan solution under three β -GP concentrations, while Figure 7.7 (b) illustrates that of solutions of various chitosan concentrations at a single β -GP content (0.66M). In either case, the heat-induced gelation could be divided into three regions, as reported in our previous work [12]: Region 1) solution behaviour ($G' < G''$), Region 2) fast gelation, Region 3) slow gelation. Gelation point T_{gel} , was determined as the temperature at the cross-over of the complex moduli. This method has been shown to give an appropriate value of the gel point, with a deviation of $\pm 1^\circ\text{C}$ compared to a frequency independent determination method and large-amplitude oscillatory shear technique [20]. The gelation temperature decreased with increasing β -GP and polymer content (Table 7.3), while moduli values increased, corresponding to an enhancement of gelation due to an increase of intermolecular interactions and entanglements. While the complex moduli curves were very similar regardless of glycerophosphate concentration (Figure 7.7 (a)), the slopes dG'/dT in Regions 2 and 3 were shown to decrease with C_C (Figure 7.7 (b)) due to the

low diffusivity at high polymer concentration, consequence of the high viscosity. Spontaneous or concentration-induced gelation at low temperature (5°C) was also observed when chitosan concentration was increased above $C_C = 0.20$ M. Since entanglements can be considered as nanometric gel precursors [21], high molecular weight chitosan at high concentration could result in gelation without the use of an external agent.

Considering the very similar behaviour of the heat-induced gelation in Regions 2 and 3 in the presence of various β -GP concentrations (Figure 7.7 (a)), we constructed a master curve presented in Figure 7.7 (c), using a horizontal shift factor defined as the ratio of the gelation temperatures, i.e. $S_F = T_{gel}(15-66)/T_{gel}(sample)$, with T in °C. While the behaviour differed in the sol state (Region 1), as discussed in the previous section, the shifted data superposed quite well in a single master curve in the gelation zone (Regions 2 and 3), indicating that the gelation process and kinetics were nearly identical, regardless of β -GP concentration.

From the gel point determined from the previous experiments it was possible to draw the 3D (T° , C_{GP} , C_C) sol-gel phase diagram for the chitosan- β -GP system, presented in Figure 7.8. The illustrated 2D surface represents gelation temperature as a function of glycerophosphate and polymer concentrations. The region below the surface is the sol state, while that above is a gel. Increasing C_{GP} and C_C gradually decreased T_{gel} , however a synergetic effect at high C_{GP} and C_C resulted in a sudden drop of the gelation temperature. The synergetic effect resulted in a phase transition that is on the edge between concentration-induced and heat-induced gelation.

7.5.3. Non-isothermal gelation kinetics

We investigated nonisothermal kinetics of the heat-induced gelation in order to quantify the beneficial effect of increased C_{GP} and C_C . Temperature rise was converted to time evolution using the temperature ramp value of 1°C/min. We used a model derived from polymer crystallization kinetics that is a combination of the Arrhenius equation and a time-temperature relationship [22,23,24], yielding:

$$\ln\left(\frac{1}{G'^n} \frac{dG'}{dt}\right) = \ln k_o - \left(\frac{E_{ag}}{RT}\right) \quad (7.6)$$

with n the reaction rate, t the time, k_o the Arrhenius frequency factor, E_{ag} the activation energy for gelation, and where RT have their usual significance. The exponent n represents both the dimension r of the growing crystallites and the type of nucleation s ($n = r + s$) [25]. Parameter r is 1 for rods, 2 for discs and 3 for spheres, while s is either 0 for predetermined nucleation (nuclei already present) or 1 for sporadic nucleation (nuclei arise and their number increases linearly with time) [26]. We assumed that the reaction rate n was 2, as proposed by Lopes da Silva et al. for gelation [22].

The derivative term (dG'/dt) in Equation 7.6 was obtained through the differentiation of a polynomial regression fitted to the kinetics data of Figure 7.7. The calculated activation energy for gelation (E_{ag}) was determined from the slope in Regions 2 and 3, with the slope in Region 3 evaluated in the linear part of the curve, away from the transition zone. The determined activation energies for gelation are shown in Figure 7.9 in terms of β -GP and chitosan concentrations. For the low chitosan concentrations, i.e. $C_C < 0.10\text{M}$, E_{ag} could not be determined due to insufficient experimental data.

Gelation activation energy E_{ag} decreased from ~3000 to 500 kJ/mol in Region 2 when chitosan concentration increased from 0.10M to 0.20M, indicating that the development of intermolecular junctions was more favourable energetically at high polymer content. However, the activation energy was nearly constant in Region 3. The lower E_{ag} in Region (3) suggested that the evolution of the physical networks was also energetically easier, however as shown previously in Figure 7.7, the gelation was nevertheless strongly slowed down in that region since it was diffusion controlled due to the large viscosity increase. And as expected from previous observations (Figure 7.7 (a) and (c)), gelation activation energy was not influenced by glycerophosphate concentration. Finally, it is interesting to compare the values of the activation energies for flow and gelation: E_{af} was found to be approximately 30 kJ/mol (Figure 5), therefore one and two orders of magnitude lower than E_{ag} in Regions 3 and 2, respectively.

7.5.4. Effect of GP type on sol and gel viscoelastic properties

Solution properties at 5°C and evolution of heat-induced gelation of a 0.05 M chitosan solution were investigated in the presence of 0.69 M glycerophosphate using α and β -GP. Regardless of the GP type, the solutions pH values were about 6.7 at room temperature (Table 7.1), indicating that both systems presented the same ionic strength and number of protonated glucosamine groups. Solution behaviour was also nearly similar (Figure 7.10 (a)), except for the elastic modulus of the β -GP type that was slightly higher than that of the α -type, mostly at low frequency. However, the very low value of G' for the α -GP solution, resulting in a slope higher than 2 in the terminal zone,

was related to experimental uncertainty due to the very low solution viscosity. During the gelation process (Figure 7.10 (b)), the complex modulus G^* of β -GP was also slightly higher than that of α -GP, but the difference was within the error range, and the gelation temperature was identically 78°C ($\pm 1^\circ\text{C}$), regardless of GP type. Thus the chemical structure of the glycerophosphate did not seem to influence the gelation process, supporting our assumption that ionic bridging is not an important contribution to the gelation mechanisms [12].

7.5.5. Structure of physical junction zones formed in the chitosan- β -GP gel

As stated previously, the modified Eldridge-Ferry method [14] (Equation 7.3) was used to have insight at the network structures of our systems. Figure 7.11 shows the semi-log plot of the chitosan gel concentration (C_{gel}) as a function of $1/T_{gel}$ used to determine the bonding enthalpy per mole of structural unit ($\Delta h_{0,mol}$) in a junction of the chitosan-GP system. The data at high chitosan concentration was not used for this calculation because of the gelation on the edge of concentration-induced and heat-induced gelation at high polymer content, as discussed previously. The slope was found to be 5420 mol.K/J.

Takahashi and Shimazaki [27] determined the number of structural units ζ for methylcellulose gels from the measured radius of gyration, using small angle neutron scattering (SANS), and obtained $\zeta = 2$ to 8. Using this range of structural units in Equation 7.4, we found $\Delta h_{0,mol}$ values that varied between 5.6 and 22.5 kJ/mol for the chitosan-GP system. The second value was closer to that determined for methylcellulose

gels by Takahashi and Shimazaki [27], i.e. 25 kJ/mol. Therefore, it is possible that chitosan-GP network junctions are made of multiple structural units. Unfortunately, since we did not have chitosan samples of different molecular weights and identical DDA and polydispersity to that of the parent sample, we could not evaluate the junction multiplicity S shown in Equation 7.3.

7.6. DISCUSSION

In the solution state, it was seen that increasing GP and polymer concentrations enhanced viscoelastic properties and caused them to deviate from the sol behaviour at low frequencies. The effect of increased polymer concentration is well known and easily explained in terms of enhanced physical interactions for associative polymers, including entanglements. However the effect of β -GP on viscoelastic properties required inspection of pH and ionic strength I_s . Examining the pH values of Table 1, it was reasonable to assume that increasing pH with increasing C_{GP} decreased chitosan protonation, therefore promoting polymer-polymer contacts via hydrophobic and/or hydrogen bonding interactions. We also calculated the ionic strength of solutions at various β -GP concentrations using the approach described previously [12] and a pK_a of 6.5 for chitosan [1]. As expected, the calculated ionic strength (shown in Figure 7.12 for a chitosan concentration of 0.15 M) was larger at higher C_{GP} , confirming enhanced screening of electrostatic repulsion between glucosamine groups in the presence of GP.

The effect of β -GP on flow activation energy (E_{af}) observed in Figure 7.5 could also be related to intermolecular interactions. Decreased activation energy indicates that

rheological properties are less sensitive to temperature changes. Molecular mobility and polymer-polymer interactions are all functions of temperature, with mobility and hydrophobic interactions increasing and hydrogen bonds decreasing. The expected lowering of viscosity due to increased mobility and decreased hydrogen bonds at higher temperature was hindered by increased hydrophobic interactions in the presence of GP, as shown by the decreasing activation energy. This is also illustrated in Figure 7.12 where the slope dI_S/dT below 45°C increased with increasing C_{GP} . It implied that polymer-polymer interactions via hydrophobic interactions increased more rapidly at high C_{GP} .

The complex viscosity at 0.1 rad/s ($\eta^*_{0.1\text{rad/s}}$) was exponentially proportional to the chitosan content regardless of the GP concentration: $\eta^*_{0.1\text{rad/s}} \sim C_C^{5.0}$. It indicated that the viscosity was mainly affected by the number of entanglements between macromolecules in the system. The large dependence on polymer concentration was also observed in our previous work on chitosan in 0.5M acetic acid / 0.1M sodium acetate aqueous solution with $\eta_0 \sim C_C^{4.1}$ [28]. The present power-law exponent of 5 is most probably higher because of enhanced associations in the presence of GP. It is nevertheless very similar to that of 5.2 reported for entangled chitosan solutions in 0.3M acetic acid / 0.05M sodium acetate at 25°C [29].

In the heat-induced gelation experiments, the effect of glycerophosphate could furthermore be explained by examining the ionic strength as a function of temperature (Figure 7.12). In our previous work [12], we found that increasing temperature decreased the protonation of chitosan and increased the ionic strength mainly by

increasing the ionization of GP, favouring therefore hydrophobic effect and polymer-polymer interactions and eventually leading to gelation. Finally, the use of GP with different chemical structures, i.e. α -type that has a linear structure and β -type that is more compact, supported our assumption that ionic bridging is not an important contribution to the gelation mechanisms [12].

7.7. CONCLUSIONS

In this study, the rheological properties of chitosan systems were characterized in the sol and gel states in terms of chitosan and glycerophosphate concentrations. In solution, the linear viscoelastic properties were greatly affected by β -GP and chitosan content. The flow activation energy, determined from the temperature shift factor used in the complex moduli master curves, decreased with decreasing β -GP content and increased with chitosan concentration. The opposite behavior was interpreted in terms of competing effects between increased mobility and enhanced hydrophobic interactions in the presence of glycerophosphate, as suggested by the calculated ionic strength.

In terms of heat-induced gelation, increasing chitosan and β -GP concentrations accelerated gelation and enhanced mechanical properties. At high polymer content ($C_C > 0.20$ M), concentration-induced gelation was observed at low temperature (5°C). While heat-induced gelation kinetics was a function of chitosan concentration, it was nearly independent of glycerophosphate content and the data could be shifted into a single master curve, showing that the gelation process and kinetics were identical regardless of β -GP content. In addition, two glycerophosphate with different chemical structures were

used in order to verify our previous assumption that ionic interactions (bridging) was negligible in the heat-induced gelation process. It was shown that the sol and gel behaviour and the sol-gel transition were unaffected by the GP type, confirming our supposition. Finally, using the modified Eldridge-Ferry method [14], we determined a value for the bonding enthalpy per mole of structural unit ($\Delta h_{0,\text{mol}}$) in a junction of the chitosan-GP system.

7.8. ACKNOWLEDGEMENTS

The authors gratefully acknowledge the financial support of the Conseil de Recherches en Pêche et en Agroalimentaire du Québec (CORPAQ). We are also thankful to Prof. Michel Moan for helpful discussions during the revision of this manuscript, and to the reviewers for their useful comments.

7.9. REFERENCES

-
- ¹ Roberts, G. A. F. (1992). *Chitin Chemistry*. London, The Macmillan Press Ltd.
 - ² Brugnerotto, J., Desbrières, J., Heux, L., Mazeau, K., & Rinaudo, M. (2001). Overview on structural characterization of chitosan molecules in relation with their behavior in solution. *Macromolecular Symposia*, 168, 1 – 20.
 - ³ Park, J. W., Choi, K.-H., & Park, K. K. (1983). Acid-base equilibria and related properties of chitosan. *Bulletin of Korean Chemistry Society*, 4(3), 68 – 72.
 - ⁴ Kassai, M. R. (1999). *Depolymerization of chitosan*. Ph. D. Dissertation, Université Laval, Quebec, Canada.

-
- ⁵ Singla, A. K., & Chawla, M. (2001). Chitosan: some pharmaceutical and biological aspects – an update. *Journal of Pharmacy and Pharmacology*, 53, 1047 – 1067.
- ⁶ Kumar, M. N. V. R. (2000). A review of chitosan and chitosan applications. *Reactive & Functional Polymers*, 46, 1 – 27.
- ⁷ Jackson, D. S. (1987). *Chitosan-Glycerol-Water Gel*. USA Patent 4.659,700.
- ⁸ Chenite, A., Chaput, C., Wang, D., Slemani, A. (2001). *Temperature-controlled and pH-dependent self-gelling biopolymeric aqueous solutions*. WO 01/36000 A1.
- ⁹ Chaput, C., & Chenite, A. (2001). *Mineral-polymer hybrid composition*. WO 01/41822.
- ¹⁰ Nyström, B., Kjoniksen, A.-L., & Iversen, C. (1999). Characterization of association phenomena in aqueous systems of chitosan of different hydrophobicity. *Advances in Colloid and interface Science*, 79, 81 – 103.
- ¹¹ Hamdine, M., Heuzey, M.-C., & Bégin, A. (2005). Viscoelastic properties of phosphoric and oxalic acid-based chitosan hydrogels. *Rheologica Acta*, 37, 1-17.
- ¹² Cho, J.; Heuzey, M.-C., Begin, A., & Carreau, P. J. (In press). Physical gelation of chitosan in the presence of β -glycerophosphate: The effect of temperature. *Biomacromolecules*.
- ¹³ Cho, J., Heuzey, M.-C., Begin, A., & Carreau, P. J. (In revision). Effect of urea on solution behavior and heat-induced gelation of chitosan- β -glycerophosphate. *Carbohydrate Polymers*.
- ¹⁴ Tanaka, F., & Nishinari (1996). Junction Multiplicity in Thermoreversible Gelation. *Macromolecules*, 29, 3625 – 3628.

-
- ¹⁵ Flory P.J. (1953). *Principles of Polymer Chemistry*, Cornell University Press, Ithaca, NY, Chap. 9.
- ¹⁶ Eldridge, J. E., & Ferry, J. D. (1954). Studies of the Cross-linking Process in Gelatin Gels. III. Dependence on Melting Point on Concentration and Molecular weight. *The Journal of Physical Chemistry*, 58, 992 – 995.
- ¹⁷ Aoki, Y., Li, L., & Kakiuchi, K. (1998). Rheological Images of Poly(vinyl) Gels. 6. Effect of Temperature. *Macromolecules*, 31, 8117 – 8123.
- ¹⁸ Goldberg, R. N., Kishore, N., & Lennen, R. M. (2002). Thermodynamic Quantities for the ionization Reaction of Buffers. *Journal of Physical and Chemical Reference Data*, 31, 231 – 370.
- ¹⁹ Hamdine, M., Heuzey, M.C., & Bégin A (In revision). Effect of organic and inorganic acids on concentrated chitosan solutions and gels. *International Journal of Biological Macromolecules*.
- ²⁰ Cho J., Heuzey M.C., Bégin A., Carreau P.J. (2005). Gelation point determination using fast Fourier transform rheometry. The Society of Rheology 77th Annual Meeting, Vancouver, BC, Canada.
- ²¹ Montembault, A., Viton, C., & Domard, A. (2005). Rheometric study of the gelation of chitosan in aqueous solution without cross-linking agent. *Biomacromolecules*, 6, 653 – 662.
- ²² Lopes da Silva, J. A., Gonçalves, M. P., & Rao, M. A. (1995). Kinetics and thermal behaviour of the structure formation process in HMP/sucrose gelation. *International Journal of Biological Macromolecules*, 17, 25 – 32.

-
- ²³ Fu, J.-T., & Rao, M. A. (2001). Rheology and structure development during gelation of low-methoxyl pectin gels: the effect of sucrose. *Food Hydrocolloids*, 15, 93 – 100.
- ²⁴ Ross-Murphy, S. B. (1991). The estimation of junction zone size from geltime measurements. *Carbohydrate Polymers*, 14, 281 – 294.
- ²⁵ Bohm, N., & Kulicke, W.-M. (1999). Rheological studies of barley (1→3)(1→4)- β -glucan in concentrated solution: mechanistic and kinetic investigation of the gel formation. *Carbohydrate Research*, 315, 302 – 311.
- ²⁶ McIver, R. G., Axford, D. W. E., Colwell, K. H., & Elton, G. A. H. (1968). Kinetic Study of the retrogradation of gelatinized starch. *Journal of the Science Food and Agriculture*, 19, 560 – 563.
- ²⁷ Takahashi, M., & Shimazaki, M. (2001). Formation of Junction Zones in Thermoreversible Methylcellulose Gels. *Journal of Polymer Science: Part B: Polymer Physics*, 39, 943 – 946.
- ²⁸ Cho, J.; Heuzey, M.-C., Begin, A., Carreau, P. J. (In press). Viscoelastic Properties of Chitosan Solutions: Effect of Concentration and Ionic Strength. *Journal of Food Engineering*.
- ²⁹ Desbrières, J. (2002). Viscosity of semiflexible chitosan solution: influence of concentration, temperature, and role of intermolecular interactions. *Biomacromolecules*, 3, 342 – 349.

Table 7.1. Composition, nomenclature and measured *pH* at room temperature of chitosan-GP solutions in 1%w/v AcOH

Sample	C _C (M) ¹	C _{GP} (M)	<i>pH</i>	Sample	C _C (M) ¹	C _{GP} (M)	<i>pH</i>
5-33	0.05	0.33	6.3	10-66	0.10	0.66	6.9
10-33	0.10	0.33	6.4	15-66	0.15	0.66	7.0
15-33	0.15	0.33	6.5	20-66	0.20	0.66	7.2
20-33	0.20	0.33	6.6	5-83	0.05	0.83	7.0
5-69 (α)	0.05	0.69	6.7	10-83	0.10	0.83	7.1
5-69 (β)	0.05	0.69	6.7	15-83	0.15	0.83	7.2
5-66	0.05	0.66	6.7	20-83	0.20	0.83	7.4

¹ Concentration of 2-amino-2-deoxy-D-glucose (glucosamine) units.

Table 7.2. Characteristic relaxation times τ_1 and τ_2

Sample	τ_1 (s)	τ_2 (s)
15-33	0.005	7
15-66	0.007	10
15-83	0.01	11
10-66	< 0.005 ¹	10
20-66	0.02	10

¹ Not observed in the experimental range of frequency used.

Table 7.3. Gelation temperature of selected chitosan-GP systems (Figure 7.7)

Sample	T _{gel} (°C)	Sample	T _{gel} (°C)
15-33	79	10-66	70
15-66	64	15-66	64
15-83	58	20-66	58

FIGURE CAPTIONS

Figure 7.1. Model junction made up of S chains and ζ structural units bound together [20].

Figure 7.2. Chemical structures of the two glycerophosphates used in this study.

Figure 7.3. Master curves of complex moduli obtained for three different GP concentrations: (a) sample 15-33, (b) sample 15-66, and (c) sample 15-83. Circles represent data obtained at 15°C (5°C for 15-83), triangles at 25°C; and squares at 45°C ($\gamma_0 = 0.1$).

Figure 7.4. Master curves of complex moduli obtained for three different chitosan concentrations: (a) sample 10-66, (b) sample 15-66, and (c) sample 20-66. Circles represent data obtained at 15°C, triangles at 25°C; and squares at 45°C ($\gamma_0 = 0.1$).

Figure 7.5. Effects of GP (C_{GP}) and chitosan (C_C) concentrations on the flow activation energy (E_{af}).

Figure 7.6. Effects of GP (C_{GP}) and chitosan (C_C) concentrations on the complex viscosity ($\eta^*_{0.1\text{rad/s}}$) at $\omega = 0.1$ rad/s and 25°C.

Figure 7.7. Effects of (a) β -GP (C_{GP}) and (b) chitosan (C_C) concentrations on the heat-induced gelation process ($\gamma_0 = 0.01$, $\omega = 6.28$ rad/s). (c) Master curve obtained by shifting the data in (a) using the horizontal shift factor $S_F = T_{gel}(15-66)/T_{gel}(\text{sample})$ (from Table 7.2) with T in °C.

Figure 7.8. Phase diagram for T_{gel} under various β -GP (C_{GP}) and chitosan (C_C) concentrations.

Figure 7.9. Effects of β -GP (C_{GP}) and chitosan (C_C) concentrations on the gelation activation energy (E_{ag}) in Regions 2 and 3 of Figure 7.7.

Figure 7.10. Effect of GP type on (a) solution behaviour at 5°C ($\gamma_0 = 0.1$) and (b) heat-induced gelation using samples 5-69 (α) and 5-69 (β) ($\gamma_0 = 0.01$ and $\omega = 6.28$ rad/s).

Figure 7.11. Semi-log plot of chitosan gel concentration (C_{gel}) vs. $1/T_{gel}$ for various β -GP (C_{GP}) concentrations.

Figure 7.12. Effect of GP concentration (samples 15-33, 15-66 and 15-83) on the calculated ionic strength (I_S) as a function of temperature.

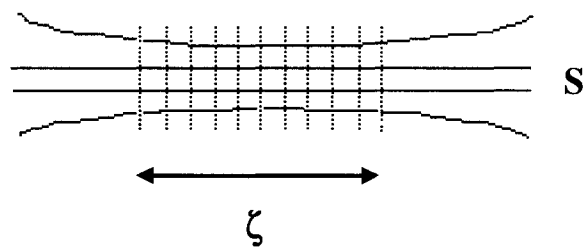
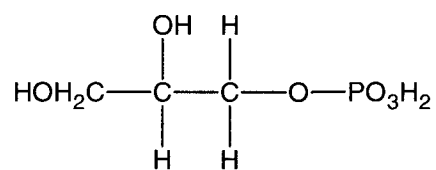
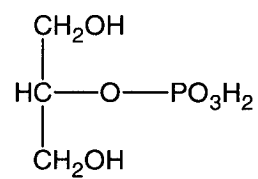


Figure 7.1. Model junction made up of S chains and ζ structural units bound together [20].



α -glycerophosphate (α -GP)



β -glycerophosphate (β -GP)

Figure 7.2. Chemical structures of the two glycerophosphates used in this study.

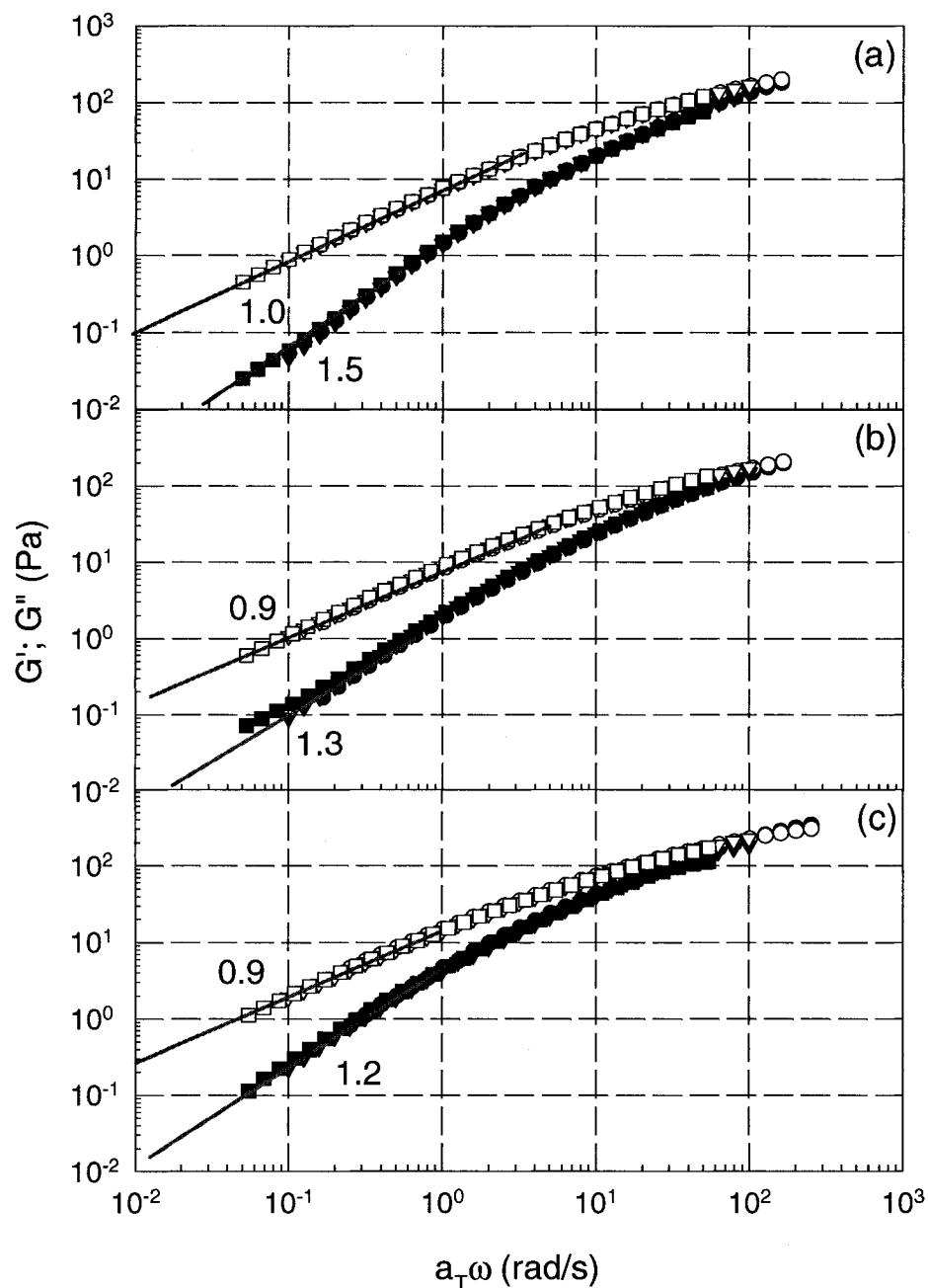


Figure 7.3. Master curves of complex moduli obtained for three different GP concentrations: (a) sample 15-33, (b) sample 15-66, and (c) sample 15-83. Circles represent data obtained at 15°C (5°C for 15-83), triangles at 25°C; and squares at 45°C ($\gamma_0 = 0.1$).

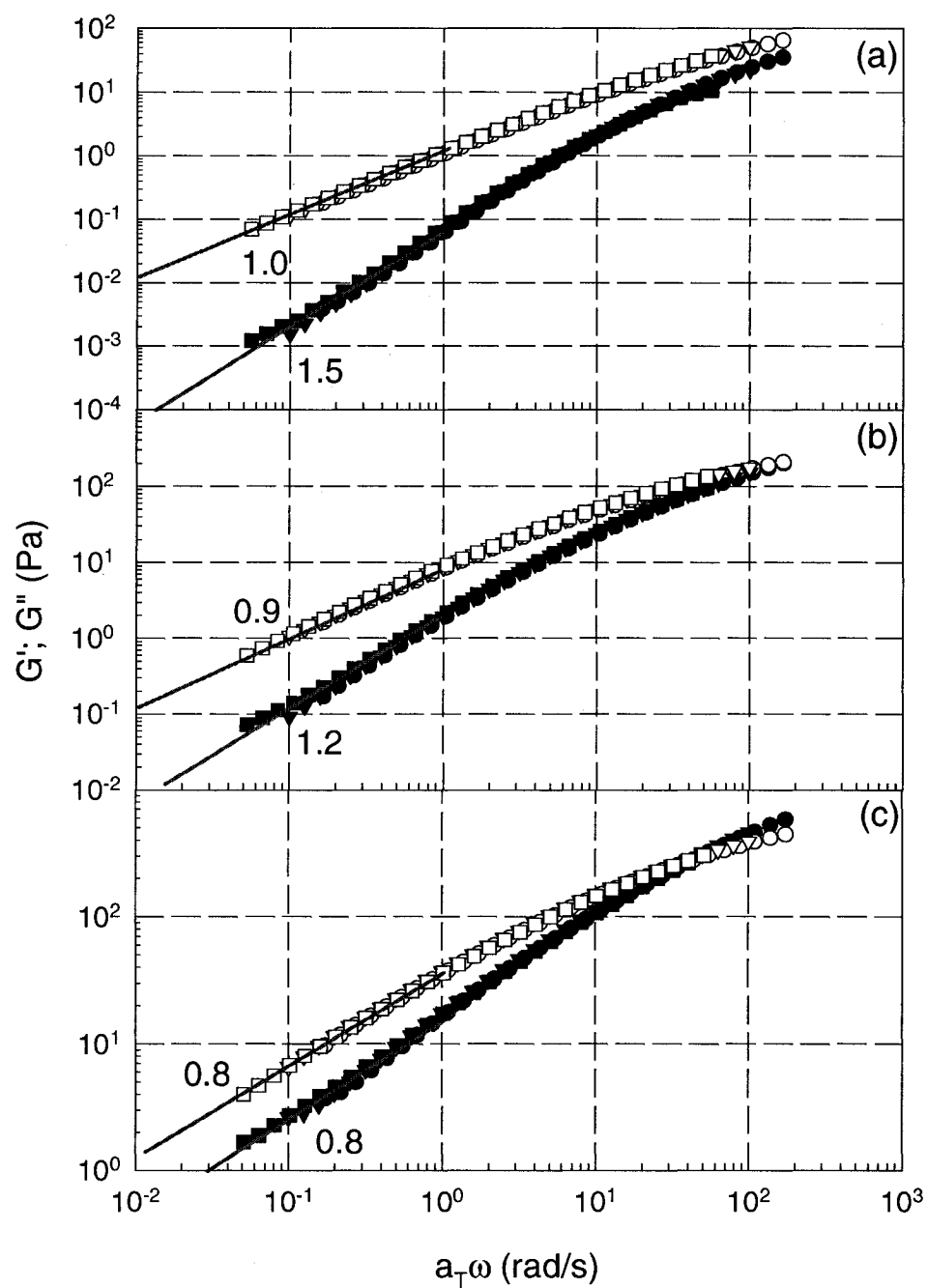


Figure 7.4. Master curves of complex moduli obtained for three different chitosan concentrations: (a) sample 10-66, (b) sample 15-66, and (c) sample 20-66. Circles represent data obtained at 15°C, triangles at 25°C; and squares at 45°C ($\gamma_0 = 0.1$).

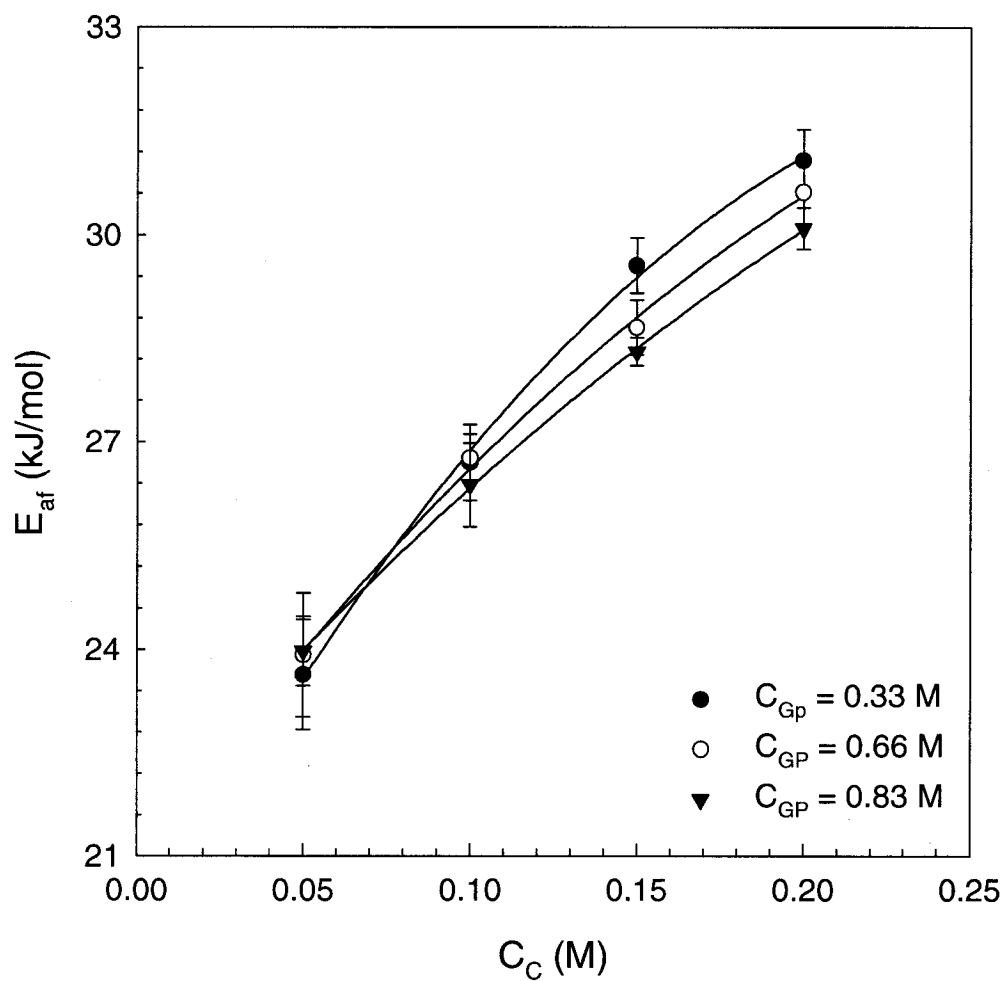


Figure 7.5. Effects of GP (C_{GP}) and chitosan (C_C) concentrations on the flow activation energy (E_{af}).

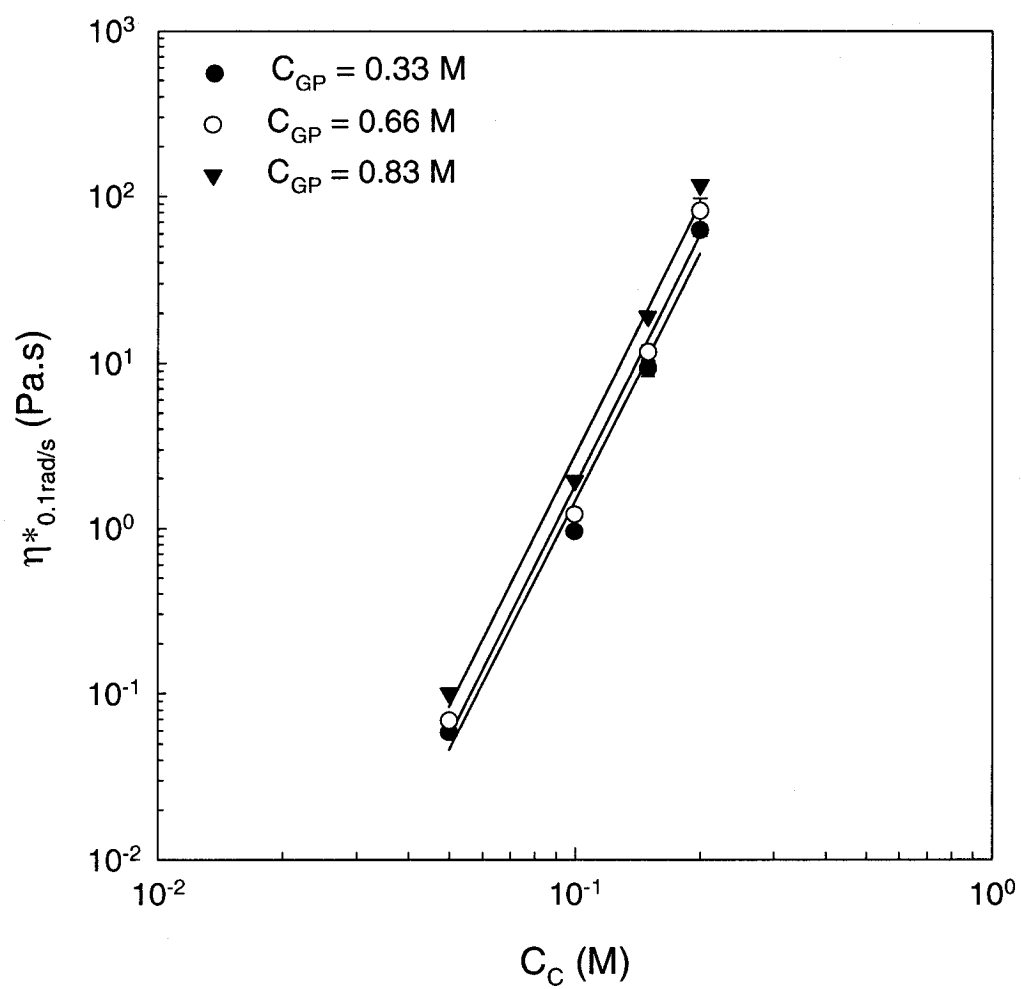


Figure 7.6. Effects of GP (C_{GP}) and chitosan (C_C) concentrations on the complex viscosity ($\eta^*_{0.1\text{rad/s}}$) at $\omega = 0.1$ rad/s and 25°C .

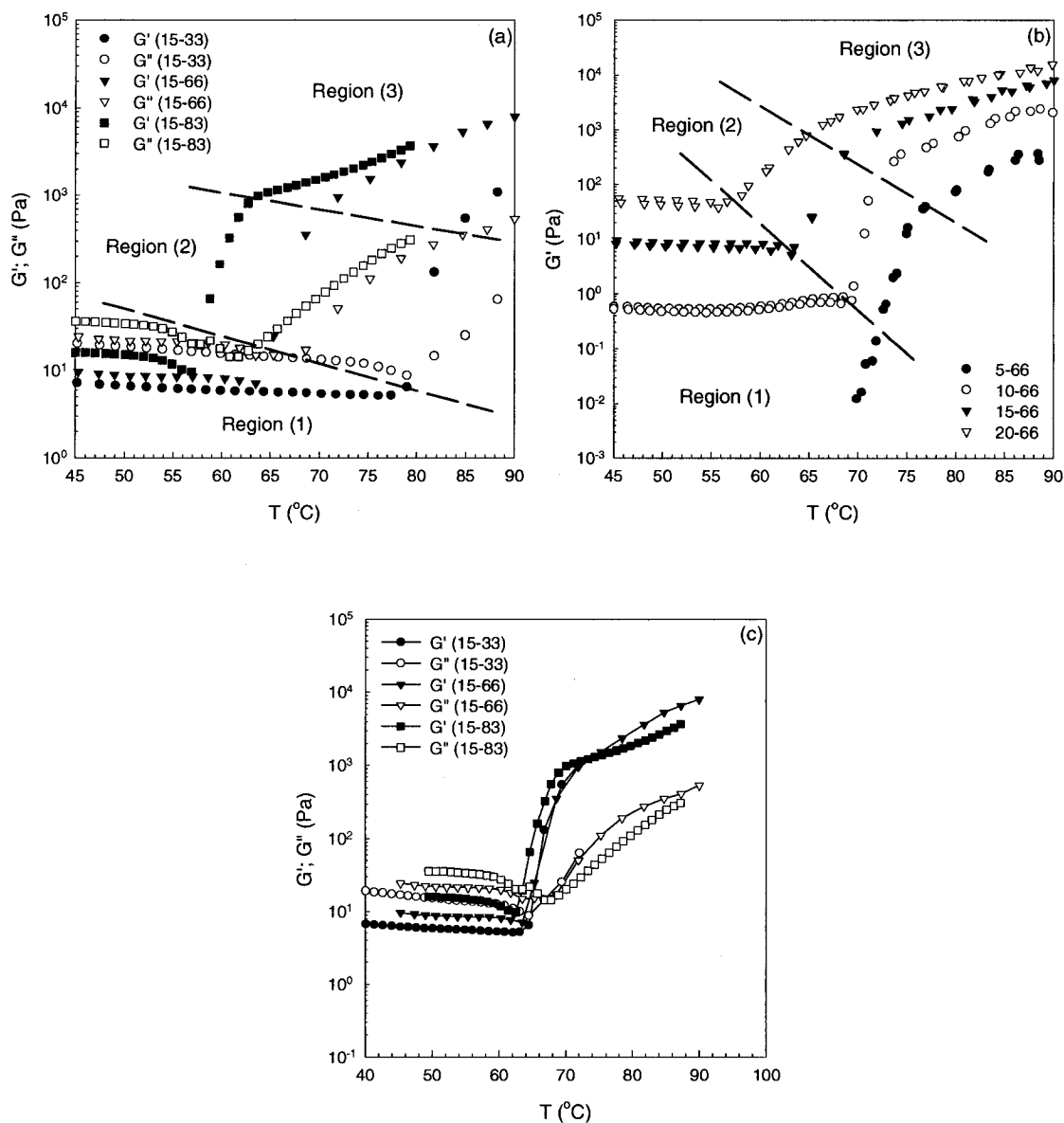


Figure 7.7. Effects of (a) β -GP (C_{GP}) and (b) chitosan (C_C) concentrations on the heat-induced gelation process ($\gamma_0 = 0.01$, $\omega = 6.28$ rad/s). (c) Master curve obtained by shifting the data in (a) using the horizontal shift factor $S_F = T_{gel}(15-66)/T_{gel}(sample)$

(from Table 7.2) with T in $^{\circ}\text{C}$.

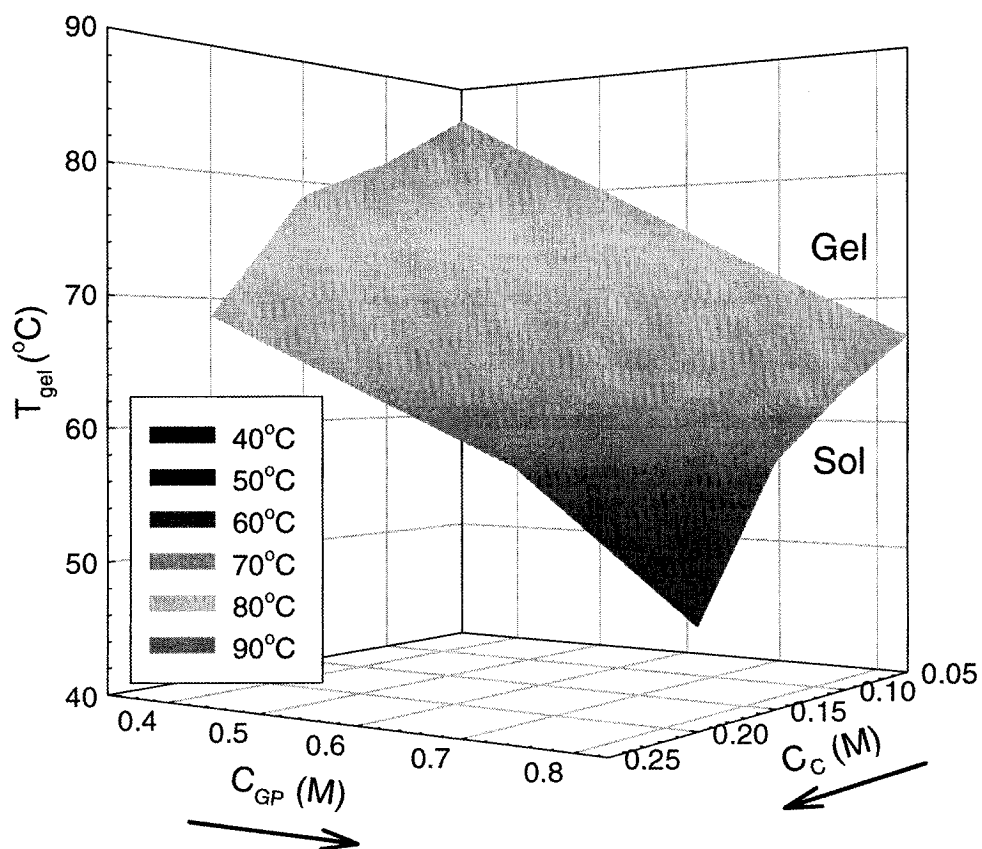


Figure 7.8. Phase diagram for T_{gel} under various β -GP (C_{GP}) and chitosan (C_C) concentrations.

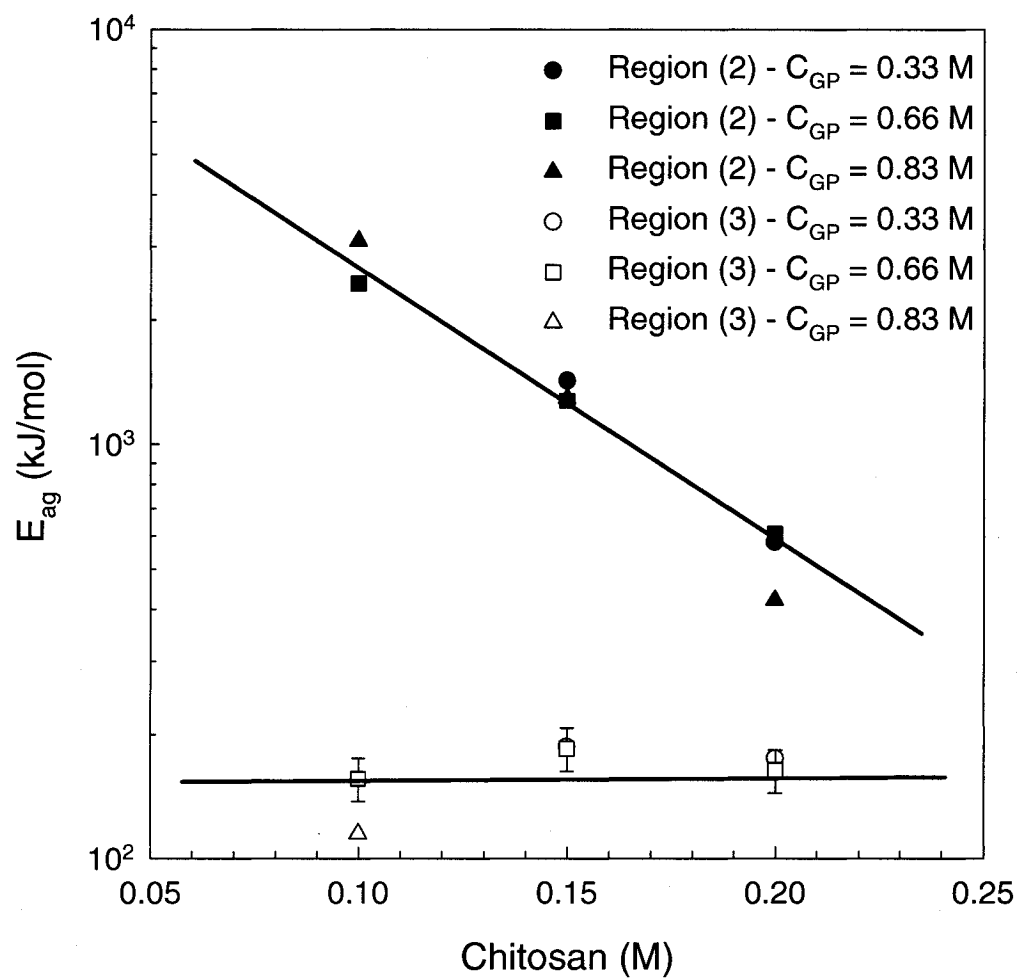


Figure 7.9. Effects of β -GP (C_{GP}) and chitosan (C_C) concentrations on the gelation activation energy (E_{ag}) in Regions 2 and 3 of Figure 7.7.

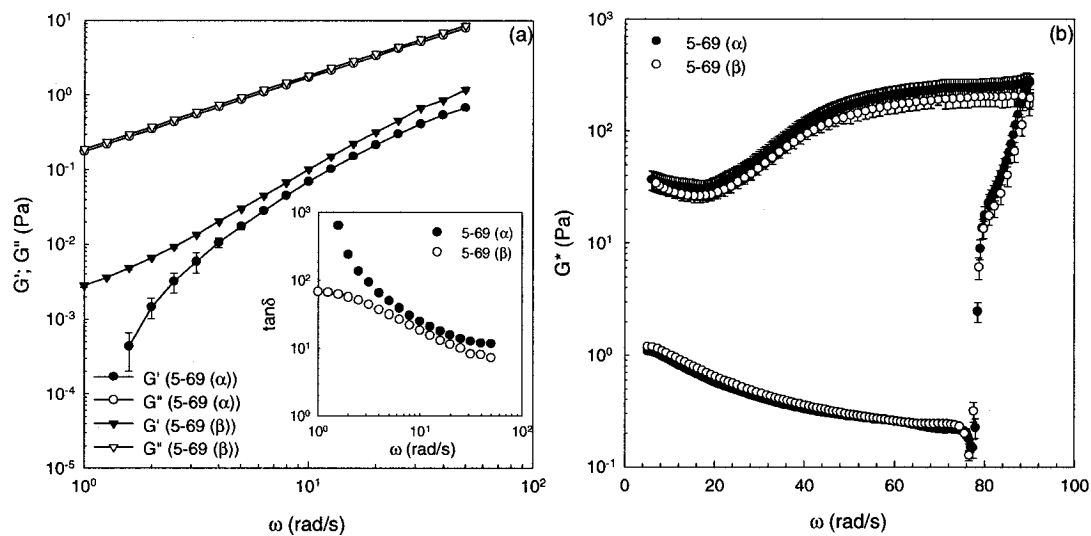


Figure 7.10. Effect of GP type on (a) solution behaviour at 5°C ($\gamma_0 = 0.1$) and (b) heat-induced gelation using samples 5-69 (α) and 5-69 (β) ($\gamma_0 = 0.01$ and $\omega = 6.28$ rad/s).

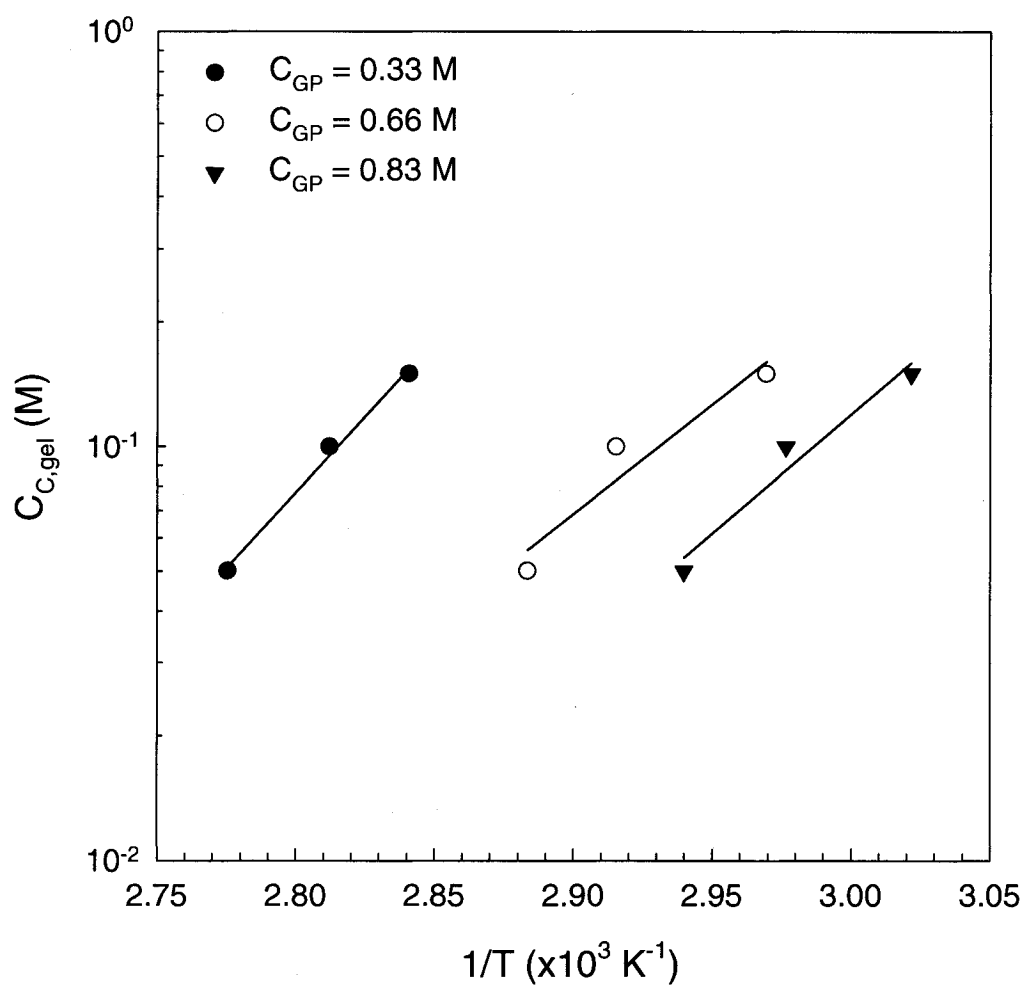


Figure 7.11. Semi-log plot of chitosan gel concentration (C_{gel}) vs. $1/T_{gel}$ for various β -GP (C_{GP}) concentrations.

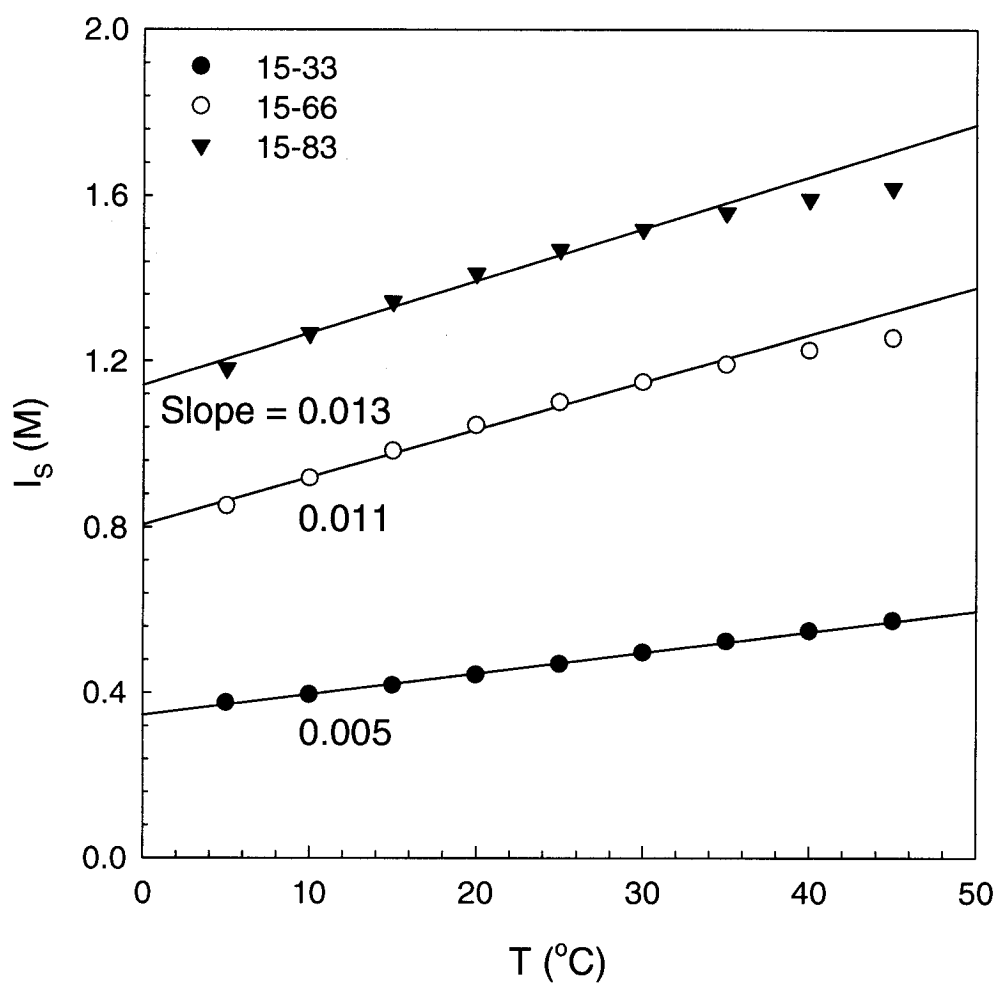


Figure 7.12. Effect of GP concentration (samples 15-33, 15-66 and 15-83) on the calculated ionic strength (I_s) as a function of temperature.

Chapter 8

Chitosan gels

8.1. Introduction

Several additional studies were performed to understand the gelation mechanisms and behaviours more clearly. First of all, rheological and physicochemical properties of chitosan- β -glycerophosphate (β -GP) systems were performed to verify the possible occurrence of a chemical reaction during the heat-induced gelation process. Second, the physical changes of chitosan- β -GP systems were investigated in terms of storage time and storage temperature. Finally, in the absence of β -GP the effect of the ionic strength on the chitosan solutions was investigated with rheological measurements at 80°C to understand the function of hydrophobic interactions on the chitosan gelation.

8.2. Materials

The chitosan used in this study was purchased from Marinard Biotech (QC, Canada). Its degree of deacetylation is 93% and weight-average molecular weight (\overline{M}_w) 8.54×10^5 g/mol ($\overline{M}_w / \overline{M}_n = 2.76$). For determining the molecular weight, gel permeation chromatography (GPC) measurements were conducted with an Ultrahydrogel™ 500 Column (Waters Co., MA, USA) in 0.25M acetic acid / 0.25M sodium acetate using dextran standards. Acetic acid (AcOH, 99.7%, Sigma-Aldrich, ON, Canada) was used to dissolve the chitosan, while β -GP (Sigma-Aldrich, ON, Canada) was used to adjust the pH of the chitosan solutions. Hydrochloric acid (HCl, 37%, Sigma-Aldrich, ON, Canada) was to decrease the pH of the chitosan systems. Sodium acetate (AcONa, 99.3%, Fisher Scientific, NJ, USA) was added to adjust the ionic strength of the chitosan solutions.

8.3. pH-reversible gels

8.3.1. Experiments

8.3.1.1. Chitosan solutions preparation

1g of chitosan was dissolved in 1w/v acetic acid aqueous solution (99mL) using a laboratory magnetic stirrer (PC-420 Corning® Stirrer/Hot Plate, Corning Inc., MA, USA) with a mild stirring rate of 50 RPM for 4h at room temperature. The pH of the prepared chitosan solution was 4.0. Then, 16g of β -GP was added very slowly under rapid stirring to increase the pH of the chitosan solution up to 6.7 without causing immediate precipitation at room temperature. During the stirring process, the containers of the solutions were covered with aluminum foil to prevent evaporation. After mixing, the chitosan solutions were left for 3h to degas without stirring at room temperature and stored in a refrigerator ($T \sim 5^{\circ}\text{C}$) overnight before the gelation processes.

The chitosan- β -GP solutions enclosed in sealed glass bottles were placed into hot water at 80°C , corresponding to gelation temperature of the chitosan- β -GP system in this study (Chapter 5), to form gel structures. Different cooking times (0 – 6h) were given in order to control the degree of gelation. To bring back each formed gel structure to the sol state, a 37wt% HCl solution (2.5mL) was added very slowly with a strong stirring rate in order not to prevent localized precipitation or phase separation. The pH was about 4.3 after adding the HCl aqueous solution.

8.3.1.2. Dialysis of the recovered chitosan samples

The dialysis process was performed in order to remove unreacted β -GP molecules with chitosan molecules. Dialysis tubing regenerated cellulose (MWCO 8000 Spectra/Por Spectrum, Spectrum Laboratories, Inc., USA) was used for the process. Deionized water was employed as a dialysis buffer solution. The total volume of the chitosan solution used was 100 mL for the dialysis process. The dialysis buffer was continuously stirred with a laboratory magnetic stirrer (PC-420 Corning® Stirrer/Hot Plate, Corning Inc., MA, USA). The progress of the dialysis was monitored by measuring the conductivity of the dialysis buffer. The dialysis buffer was replaced with

1000mL of fresh buffer when the increase of conductivity was slowed down. The dialysis process was considered as completed when the conductivity of the buffer remained essentially unchanged after stirring for 1 h. The dialyzed chitosan solutions were finally freeze-dried.

8.3.1.3. Characterization of the freeze-dried chitosan powders

The weighted-average molecular weights of the freeze-dried chitosan powders were characterized using GPC measurements. The intrinsic viscosity was measured using a Ubbelohde capillary viscometer ($\phi = 0.78\text{mm}$, Fisher Scientific, Canada) in 0.25M acetic acid (AcOH)/0.25M sodium acetate (AcONa) at 25°C, and was investigated as a function of cooking time. The determined intrinsic viscosities and molecular weights were used to calculate the MHS constants a and K . FTIR measurements were performed to detect the interactions between the protonated amine groups in chitosan molecules and negatively charged phosphate groups in β -GP molecules at 25°C. Potassium bromide (KBr) pellets mixed with the dried powders were used for the FTIR measurements.

8.3.3.4. Dynamic mechanical tests

The rheometer used was a stress-controlled instrument (AR-2000, TA Instruments, DE, USA) with a Couette geometry. The dynamic properties of the recovered chitosan solutions were characterized under various temperatures (5 - 45°C). The dynamic mechanical tests were repeated at least three times with each solution. Low viscosity mineral oil covered the surface of the chitosan solutions in order to hinder evaporation during the measurements. Oscillatory shear measurements were performed in the linear viscoelastic region. The complex viscosity (η^*) data obtained from the small amplitude oscillatory shear measurements were used to calculate the zero-shear viscosity using the three-parameter Carreau model (Carreau et al., 1997), assuming validity of the Cox-Merz rule (Cox and Merz, 1958).

8.3.2. Results and Discussion

8.3.2.1. Characterization of the recovered solutions from gel structures

The zero shear viscosity (η_0) increased with decreasing temperature and increasing cooking time as shown in Figure 8.1. The increase of the viscosity may be possibly related to the change in the molecular conformation during the cooking process. To verify this assumption, the change of the conformation was investigated by performing intrinsic viscosity and molecular weight measurements with the freeze-dried chitosan powders. The results are shown in the following section. However, the flow activation energy (E_{af}) was almost constant (34 kJ/mol) regardless of the cooking time except for the chitosan solution ($E_{af} \sim 37$ kJ/mol) recovered gel cooked for 6h.

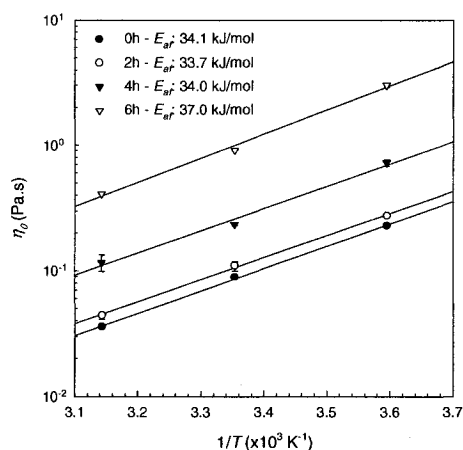


Figure 8.1. Effects of cooking time and temperature on the zero shear viscosity (η_0) of the recovered chitosan solutions from the gel state.

Table 8.1. Effect of cooking time on the molecular weight (\overline{M}_w) and polydispersity (PI) measured with GPC

Cooking time (h)	\overline{M}_w ($\times 10^{-5}$ g/mol)	PI*
0	8.34	2.91
2	8.26	2.98
4	7.99	3.09
6	7.82	3.14

* Polydispersity ($\overline{M}_w / \overline{M}_n$)

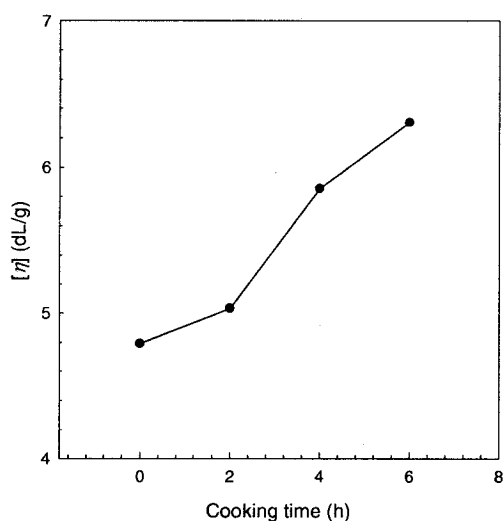


Figure 8.2. Cooking time effect on the intrinsic viscosity $[\eta]$ of the dialyzed chitosan powders measured in 0.25M AcOH/0.25M AcONa at 25°C.

8.3.2.2. Molecular weight and intrinsic viscosity measurements

GPC measurements were used to characterize the weight-average molecular weight (\overline{M}_w) and polydispersity ($PI = \overline{M}_w / \overline{M}_n$) of the chitosan powders in terms of the cooking time. As shown in Table 8.1, the molecular weight was slightly decreased with increasing cooking time, while polydispersity slightly increased. However, the intrinsic viscosity gradually increased with increasing cooking time presented in Figure 8.2. To study molecular conformation, we collected MHS constants K and a values measured under various temperatures, ionic strengths, pH , DDA and molecular weight ranges (Kasaai, 1999; Tsaih and Chen, 1999) and then redrew the semi-log plot of K versus a (Figure 8.3). We obtained relationship between K and a from the plot and the relationship was:

$$K = 10^{-5a+0.22} \quad (R^2 = 0.91) \quad (8.1)$$

The relationship between the molecular weight and intrinsic viscosity was frequently described by the MHS equation:

$$[\eta] = K \overline{M}_v^a \quad (8.2)$$

where \overline{M}_v represents the viscosity-average molecular weight. Since \overline{M}_v cannot be accessible experimentally, the weight-average molecular weight \overline{M}_w is frequently used. Thus, equation 8.2 can be rewritten as follows:

$$[\eta] = K \overline{M}_w^a \quad (8.3)$$

By combining equation 8.1 with equation 8.3, we can determine the a value from the molecular weight and intrinsic viscosity data:

$$a = \frac{\log[\eta] - 0.22}{\log \overline{M}_w - 5} \quad (8.4)$$

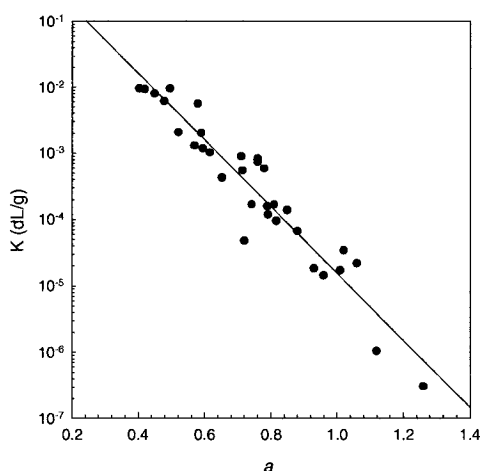


Figure 8.3. The relationship between K and a determined under various temperatures and ionic strengths, pH , DDA and molecular weight ranges (data from Kasaai, 1999; Tsaih and Chen, 1999).

Figure 8.4 shows the calculated K and a values from the measured molecular weight and intrinsic viscosity. The a value increased with increasing cooking time. If the a value is between 0.5 and 0.8, the molecular conformation is random coil, while rod-like conformation occurs for $a > 1$ and sphere for $a \leq 0.5$ (Chen and Tsaih, 2000). Thus, the increase of the a value indicates that the molecular conformation is more extended in terms of the cooking time, resulting in the increase of the viscosity and the chitosan solutions. Increasing temperature decreases hydrogen bonding interactions, resulting in the change of molecular conformation from random coil to unfolded (extend) structures. Thus, this change of the conformation provides the desirable environment to from 3D networks due to exposure of polymer junction zones in the molecules. However, the

extended molecular conformation did not return to original random conformation, shown the increase of a values in terms of cooking time.

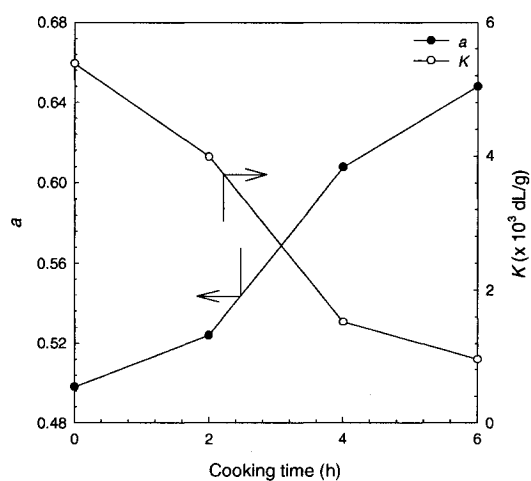


Figure 8.4. Effect of cooking time on MHS constants a and K .

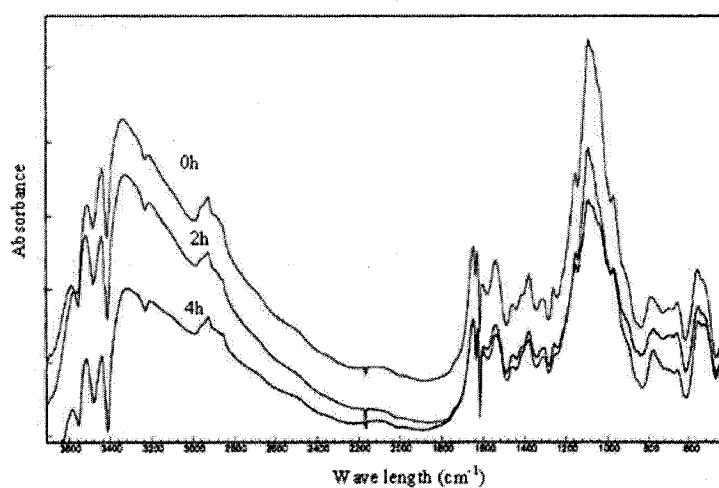


Figure 8.5. Cooking time effect on the FTIR spectra.

8.3.2.3. FTIR measurements

FTIR measurements were used to detect the presence of a chemical reaction between chitosan and β -GP. Figure 8.5 shows the measurement results. We did not find

any distinct difference among the measured spectra. It indicates that the permanent chemical reactions may not exist in the system.

8.4. Effects of storage time and temperature on chitosan solution

8.4.1. Experiments

8.4.1.1. Chitosan solutions preparation

The composition and nomenclature of the chitosan solutions are presented in Table 8.2. A stock solution of chitosan (30 g/L) was prepared by dissolving the biopolymer in 1w/v% acetic acid aqueous solution and mildly stirring with a laboratory magnetic stirrer (PC-420 Corning® Stirrer/Hot Plate, Corning Inc., MA, USA) at room temperature for 6h. During the stirring process, the container of the stock solution was covered with aluminium foil to prevent evaporation. With the stock solution, a series of less concentrated solutions were prepared by adding the acetic acid aqueous solution. Then, glycerophosphate was added very slowly to raise the *pH* of the chitosan solutions above a *pH* of 6.5, the *pK_a* of chitosan at low protonation state (Roberts, 1992). A mixing time of 0.5h was used to homogeneously disperse GP and to avoid the formation of local precipitates. After mixing, the chitosan solutions were left for 3h to degas without stirring at room temperature and stored under various temperatures, *i.e.* at 0°C, 5°C and room temperature. The *pH* (*pH*-meter, Hanna Ltd., Portugal) of each chitosan sample was measured at room temperature in 24 h after the preparation of the solutions.

Table 8.2. Composition, nomenclature and measured *pH* at room temperature of chitosan-GP solutions in 1w/v% AcOH

Sample	C _C (M)*	C _{GP} (M)	<i>pH</i>
5-66	0.05	0.66	6.7
10-33	0.10	0.33	6.5
10-66	0.10	0.66	6.9
10-83	0.10	0.83	7.1
15-66	0.15	0.66	7.0

*Concentration of glucosamine units

8.4.1.2. Visual and rheological investigations

The changes in the chitosan solutions were visually reported in terms of storage temperature and time for various chitosan solutions.

The rheological properties of the chitosan solutions were characterized in terms of storage time at 5°C. The rheometer used was a stress-controlled instrument (AR-2000, TA Instruments, New Castle, DE) with a Couette geometry for the sample 5-66. Low viscosity mineral oil covered the surface of the chitosan solutions in order to hinder evaporation during the measurements. Oscillatory shear measurements were performed in the linear viscoelastic region. The zero-shear viscosity (η_0) was determined from the oscillatory shear data using the three-parameter Carreau model, assuming that the Cox-Merz rule is applicable for the chitosan-GP solution.

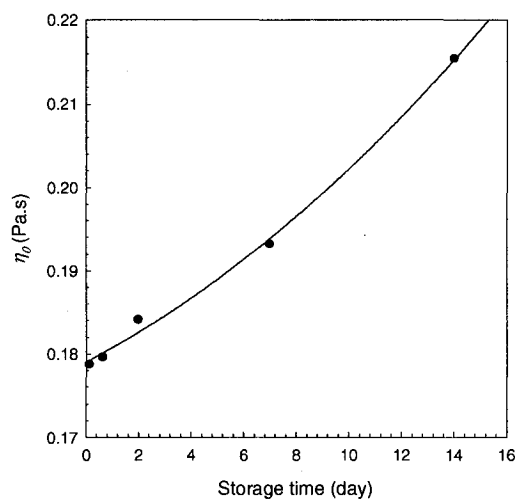


Figure 8.6. Effect of storage time on the zero shear viscosity (η_0) of sample 5-66 at 5°C.

8.4.2. Results and Discussion

8.4.2.1. Rheological measurements

As shown in Figure 8.6 for sample 5-66, η_0 gradually increased when the sample was stored longer. The evolution of the viscosity indicates the formation of physical structures in the system. Chitosan simultaneously has hydrogen bonding and hydrophobic favouring groups in the macromolecule (Roberts, 1992). In general, the hydrogen bonding interactions between polymeric molecules are dominant at low

temperatures. During the storage period at low temperature, the occurrence of hydrogen bonding interactions between chitosan molecules may have caused the increase of the viscosity.

8.4.2.2. Visual investigations

Table 8.3 reports the changes in the chitosan solutions after one month at 0°C. Homogenous gel structures were formed for the most concentrated chitosan solution. The formed gel was opaque. The turbidity of a gel is related to the size of the junction zones. The increase of the turbidity of a system indicates the increase of the size of the junction zones, resulting from the formation of a strong gel system. The chitosan concentration is directly proportional to the number of potential polymer junctions to form a gel. Thus, the gelation occurs more easily at the higher chitosan concentration. At the same chitosan concentration (0.10M), the gelation was more favourable at the higher GP concentration. The addition of GP decreases the protonation of the chitosan molecules as well as increase ionic strength in solution (in Chapter 5), resulting in the association of chitosan molecules. The gelation at 0°C or by freezing is so called “Cryotropic gelation” (Lozinsky *et al.*, 2003). The cryogels can be formed by the forced alignment or association of polymeric molecules by conversion of solvent (mainly water) to ice crystals during freezing (Giannouli and Morris, 2003). The cryogel systems are attractive matrices for chromatography of biological nanoparticles (plasmids, viruses, cell organelles...) and are efficient carriers for the immobilization of biomolecules and cells (Lozinsky *et al.*, 2003).

Table 8.3. Physical state of the chitosan systems after 1 month storage at 0°C.

Sample	State	Color
5-66	Solution	Transparent
10-33	Solution	Transparent
10-66	Solution	Transparent
10-83	Inhomogeneous gel (Cluster)	Light opaque
15-66	Homogenous gel	Opaque

Table 8.4 presents the effect of storage time on the chitosan solutions after a storage of one month in a refrigerator at 5°C. A homogenous opaque gel was formed only for solution 15-66. The other samples remained in solution and transparent, but the solutions were more viscous compared to the original ones, indicating the evolution of physical structures through hydrogen bonding interactions.

Table 8.4. Physical state of the chitosan solutions after 1 month storage at 5°C.

Sample	State	Color
5-66	Solution	Transparent
10-33	Solution	Transparent
10-66	Solution	Transparent
10-83	Solution	Slightly opaque
15-66	Homogenous gel	Opaque

Table 8.5 Physical state of the chitosan solutions after 1 month storage at room temperature.

Sample	State	Color
5-66	Phase separation	Yellow
10-33	Solution	Transparent
10-66	Phase separation	Yellow
10-83	Phase separation	Yellow
15-66	Phase separation	Yellow

Table 8.6. Physical state of the chitosan solutions after 3 months storage at room temperature.

Sample	Gel	Color
5-66	Phase separation	Orange
10-33	Homogenous gel	Slightly opaque
10-66	Phase separation	Orange
10-83	Phase separation	Orange
15-66	Phase separation	Brown

Tables 8.5 and 8.6 show the changes in the chitosan solutions after one month and three months storage at room temperature, respectively. A homogenous light opaque gel system was formed with only the sample 10-33 after 3 months. The remains formed precipitates or phase separation after three months. In general, the driving force to form gel structure is hydrogen bonding interaction at low temperature and hydrophobic interactions at high temperature. With increasing temperature, the hydrogen bonding interactions are getting decreased, but the hydrophobic interactions increase. The hydrophobic interactions are not strong enough to form gel structure at room temperature. The color of the samples was initially transparent; however, it became more opaque when the storage time increased.

8.5. Effect of high temperature on chitosan solution behaviours

8.5.1. Experiments

8.5.1.1. Chitosan solutions preparation

The composition and nomenclature of the chitosan solutions are presented in Table 8.7. A solution of chitosan (30 g/L) was prepared by dissolving the biopolymer in 10g/L acetic acid aqueous solution and mildly stirring with a laboratory magnetic stirrer (PC-420 Corning® Stirrer/Hot Plate, Corning Inc., MA, USA) at room temperature. During the stirring process, the container of the stock solution was covered with aluminium foil to prevent evaporation. Different amounts of AcONa (0 – 0.7M) were incorporated to the chitosan solution to vary ionic strength. All chitosan solutions were left to rest 3h for degassing without stirring at room temperature and then kept in a refrigerator overnight at 5°C. It was found that this overnight storage was essential to the reproducibility of the results, possibly because of the presence of small remaining bubbles. All the samples were used within one week in order to avoid aging effect due to polymer degradation. The pH of the chitosan solutions was measured with a pH meter (Hanna Ltd., Portugal) at room temperature before rheological measurements.

8.5.1.2. Rheological measurements

The rheometer used was a stress-controlled instrument (AR-2000, TA Instruments, New Castle, DE) with a Couette geometry. Mineral oil covered the surface of the chitosan solutions in order to prevent evaporation during the tests. The effect of the mineral oil on the measurements was shown to be negligible. The rheological properties of the chitosan solutions were characterized in terms of time under various ionic strengths at 80°C. A small deformation (γ_0) of 0.01 and a frequency (ω) of 6.28 rad/s were used in order not to disrupt the gel formation during the tests. The gelation time (t_{gel}) was determined as the crossover point of the storage (G') and loss (G'') moduli ($\tan \delta = 1$), despite of the slight dependency on the frequency.

Table 8.7. Composition, nomenclature, ionic strength (I_s) and measured pH at room temperature of each chitosan solution.

Sample	Chitosan (g/L)	AcOH (g/L)	AcONa (M)	I_s^* (M)	pH
30-10-0	30	10	0	4×10^{-5}	4.2
30-10-1	30	10	0.1	0.1	4.2
30-10-3	30	10	0.3	0.3	4.3
30-10-7	30	10	0.7	0.7	4.3

*Ionic strength

8.5.2. Results and Discussion

8.5.2.1. Physicochemical properties of each chitosan solution

The pH of each chitosan solution was measured at room temperature. As shown in Table 8.7, the pH was almost constant regardless of the concentration of sodium acetate (AcONa) in solution. The ionic strength (I_s) was calculated with the following equation (Segel, 1976):

$$I_s = \frac{1}{2} \sum_i \{C_i Z_i^2 + 10^{-pH}\} \quad (8.5)$$

where C_i and Z_i are the concentration and charge number of ion i , respectively. In this expression, the contribution of the protons H^+ is accounted in the separate term on the right-end side. It is important to note that the contribution of the glucosamine units is

also included in equation 8.5. The ionic strength is expressed in a molarity basis. I_S is linearly proportional to the AcONa concentration.

8.5.2.2. Rheological measurements

The complex viscosity at $\omega = 6.28 \text{ rad/s}$ ($\eta^*_{6.28 \text{ rad/s}}$) was reported in terms of ionic strength (I_S). The results are shown in Figure 8.7. The viscosity increased with increasing the magnitude of I_S . On the contrary, the viscosity decreased with increasing I_S at 25°C (Chapter 4). At low temperature, the chitosan is highly protonated (Chapter 5) so that the electrostatic repulsion is of importance for the viscoelastic properties of the solution. The electrostatic repulsion makes the chitosan molecules expand, resulting in the increase of the viscosity. However, the addition of salt neutralizes the electrostatic repulsion (screening effect). It results in the reduction of the molecular volume. Thus, the viscosity is decreased with increasing I_S . However, at high temperature the hydrophobic interactions between the polymeric molecules should be considered as a determinant factor on the rheological properties of the chitosan solutions as well as the screening effect by salt. These hydrophobic interactions are stronger in the condition of high temperature and ionic strength. Thus, the increase of the viscosity can be due to the increase of the number of hydrophobic interactions when I_S increases at 80°C.

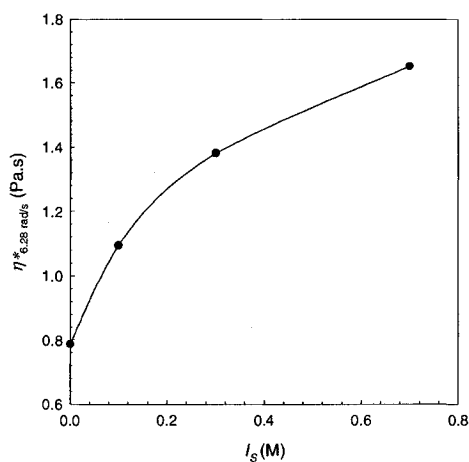


Figure 8.7. Effect of ionic strength (I_S) on the complex viscosity at $\omega = 6.28 \text{ rad/s}$ ($\eta^*_{6.28 \text{ rad/s}}$) at 80°C.

The evolution of the storage G' and loss G'' moduli was monitored during the gelation process at 80°C. Figure 8.8 shows the change in the complex modulus ($G^* = \sqrt{G'^2 + G''^2}$)

during the gelation process. Below $I_S = 0.1\text{M}$, G^* was initially decreased with increasing heating time. It may be due to the degradation of chitosan molecules. G^* was constant following the initial decrease. The constant value of the modulus may result from the balance between the degradation of the polymeric molecules by thermal energy and the association of molecules via hydrophobic interactions. Above an ionic strength (I_S) of 0.3M , the complex modulus G^* gradually increased as a function of heating time due to the formation of a 3D network via hydrophobic interactions. The increasing rate (dG^*/dt) and gel strength were larger when I_S was higher. From the crossover point of G' and G'' , corresponding to $\tan\delta = 1$, the gelation time (t_{gel}) was determined and the results are presented in Table 8.8. t_{gel} decreased with increasing I_S , indicating the acceleration of the gelation process. The acceleration of gelation and the formation of strong gel structure is directly related to the larger number of hydrophobic interactions at higher I_S .

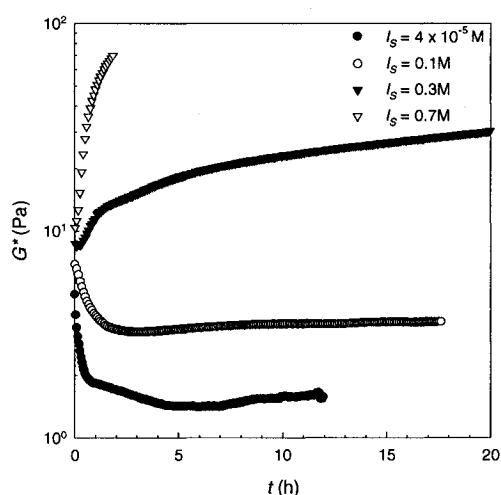


Figure 8.8. The evolution of the complex modulus (G^*) during the gelation process at 80°C ($\gamma_0 = 0.01$ and $\omega = 6.28$ rad/s) under various ionic strength (I_S) ($\text{pH} = 4.2 \sim 4.3$ at room temperature).

8.6. Summary

The formed chitosan- β -GP gels were completely pH -reversible. The viscosity of the recovered chitosan solutions from gel state was proportional to the cooking time, but the flow activation energy was almost constant regardless of the cooking time. The molecular weight decreased with increasing cooking time; however, the higher intrinsic

viscosity presented from the recovered solution increased, explained by a more extended (or higher MHS α constant) molecular conformation. FTIR measurements showed no permanent interactions between chitosan and β -GP.

Table 8.8. Effect of ionic strength (I_S) on gelation time (t_{gel}) at 80°C

Sample	I_S (M)	t_{gel} (h)
30-10-0	4×10^{-5}	×*
30-10-1	0.1	×
30-10-3	0.3	2.67
30-10-7	0.7	0.45

*Gelation time was not observed in the range of experimental time.

The effect of storage time and temperature on chitosan solutions was investigated. At 0°C, cryogels were formed with samples 10-83 (weak) and 15-66 (strong). At 5°C, a homogenous opaque gel system was formed only with the sample 15-66 after one month. Most chitosan samples formed precipitates after one month at room temperature. However, a homogenous light opaque gel system was formed with sample 10-33 after three months at room temperature. A systematic study is required to understand the cryotropic gelation of the chitosan-GP system.

A physical chitosan gel was formed by controlling temperature and ionic strength (I_S) in the absence of β -glycerophosphate. The 3D network was obtained at 80°C when I_S was larger than 0.3M. The driving force of this gelation is considered to be hydrophobic interactions between chitosan molecules. At high I_S , the gelation process was accelerated and stronger gel structures were formed.

Chapter 9

General discussion

In this chapter, five chapters (Chapter 4 – 8) are discussed in a more integral manner. Discussion will be started by the chitosan solution behaviour in dilute regime ($C < C^*$). In the following section, the rheological properties of chitosan solutions in the concentrated regime will be mentioned in terms of various conditions such as salt (or ionic strength), urea, glycerophosphate and polymer concentrations. Then, the evolution of the mechanical properties of the chitosan-glycerophosphate system will be described during the heat-induced gelation. The study of chitosan-based gelation kinetics will be presented in terms of urea, glycerophosphate and polymer concentrations. The thermoreversibility will be mentioned in short. Finally, additional results related to chitosan gels will be presented and discussed.

9.1. Determination of dilute and concentrated regimes

The dilute ($C < C^*$) and concentrated ($C > C_e$) regimes were determined in terms of ionic strength. In this study, the overlap concentration C^* was determined by three different criteria, $1/[\eta]$ (Carreau et al., 1997), the point at which the variation of η_{sp} with $\{C[\eta] + k'(C[\eta])^2\}$ deviates from slope = 1 in a log-log plot (Desbrieres, 2002), and at the concentration where $\eta = 2\eta_s$ (Rubinstein et al., 1994). The entanglement concentration C_e was determined as the concentration at which the final linear domain begins in the log-log plot of η_{sp} and $C[\eta] + k_H(C[\eta])^2$ (Desbrieres, 2002) and as the concentration for which $\eta = 50\eta_s$. (Rubinstein, 1994). The two critical concentrations increased with increasing ionic strength (I). It might be related to the change of the molecular conformation from expanded to collapsed structure due to screening of the electrostatic repulsion between protonated chitosan groups in acidic environment by salt. Both critical concentrations showed a power-law relationship with ionic strength, with $C^* \sim I^{2/9}$ and $C_e \sim I^{1/15}$.

9.2. Solution behaviour in dilute regime

Below the overlap concentration (C^*), the intrinsic viscosity was determined in terms of ionic strength at 25°C. The intrinsic viscosity decreased with increasing ionic strength, resulting from the reduction of the electrostatic repulsion. The molecular radius of gyration calculated from the intrinsic viscosity abruptly decreased from 162 to 113 nm when the ionic strength increased from 8×10^{-4} to 0.1 M. In general, an ionic strength of 0.05 M is sufficient to screen most of the electrostatic repulsion within polyelectrolytes. The persistence length (l_p) was determined to estimate the stiffness of the polymeric molecules from the measured intrinsic viscosity. It decreased from 81 to 32 nm with increasing ionic strength from 8×10^{-4} to 0.40 M and 24 nm at θ condition (or $I = \infty$). Its reduction indicates the increase of the molecular flexibility at high ionic strength. For a polyelectrolyte, the persistence length l_p is a combination of the intrinsic persistence length ($l_{p,0}$) and the electrostatic persistence length ($l_{p,e}$). $l_{p,0}$ is generally used as the persistence length at θ condition. For chitosan solutions, $l_{p,e}$ was linearly proportional to the Debye screening length, $l_{p,e} \sim k^{-1}$, when the ionic strength range was between 0.1 and 0.4M. Dobrynin et al. (Dobrynin et al., 1995) and Ullner et al. (Ullner et al., 1997) also reported that the electrostatic repulsion length of a polyelectrolyte is assumed to be proportional to the Debye screening length.

9.3. Solution behaviour in concentrated regime

In concentrated regime ($C > C_e$), chitosan solutions were characterized using rheological measurements under various ionic strength (or NaCl concentration), urea and glycerophosphate concentrations.

9.3.1 Ionic strength effect

The physical properties of the chitosan solutions (G' , G'' , and η_0) decreased with increasing ionic strength, but were enhanced for highly concentrated chitosan solutions. In addition, the shear power-law index (n) determined from the viscosity curve was gradually getting lower at higher ionic strength and lower chitosan concentration. In

other words, the nonlinear behaviour of the chitosan solutions decreased with increasing ionic strength and decreasing chitosan concentration. At high ionic strength the reduction of the mechanical properties of chitosan solutions results from the reduction of the molecular volume and the increase of the molecular flexibility due to screening of the electrostatic repulsion. In addition, the number of entanglements increases with increasing polymer concentration. Chitosan molecules have simultaneously hydrophobic and hydrogen bonding favouring groups, potential polymer junctions to build-up 3D networks (Roberts, 1992). Amiji (Amiji, 1995) also reported the existence of polymer-polymer associations via hydrophobic interactions for chitosan solutions in semidilute regime with fluorescence measurements. The polymer-polymer association via hydrophobic interactions gradually increase in terms of chitosan concentration (Philippova et al., 2001). Thus, the enhancement of the rheological properties of highly concentrated chitosan solutions is due to larger number of entanglements as well as polymer-polymer interactions.

The zero shear viscosity (η_0) was determined using the three-parameter Carreau model (Carreau et al., 1997). It is exponentially proportional to the chitosan concentration: $\eta_0 \sim C^{4.1}$. The value of 4.1 is similar to 3.94 for chitosan in 0.1M AcOH/0.1M NaCl (Hwang and Shin, 2000), while Desbrières (Desbrières, 2002) determined an exponent of 5.2 in 0.3M AcOH/0.05M AcONa. Muthukumar (Muthukumar, 1997) derived an exponent 4.25 using a theory of dynamics of dilute and semidilute polyelectrolyte in excess salt, similar to our results. On another theoretical view, an exponent of 3.75 was predicted for the reptation of a polyelectrolyte in a semidilute entangled solution in the presence of excess salt (Dobrynin et al., 1995). The higher exponent 4.1 for the chitosan solutions than the reptation-based prediction can be explained in terms of additional physical associates via hydrogen bonding and hydrophobic interactions (Amiji, 1995; Roberts, 1992), which are not considered in the reptation model.

The measured G' and G'' values were used to calculate relaxation spectra. We found that the general shapes of the calculated spectra were similar and showed only one

peak regardless of ionic strength and chitosan concentration, indicating that the main relaxation is unchanged. However, the broadness of the spectra increased with increasing chitosan concentration and decreasing ionic strength due to the enhancement of polymer-polymer interactions as well as entanglements. In the spectra, the mean relaxation time, corresponding to the time at the peak point of the spectra, was exponentially proportional to chitosan concentration: $\tau_H \sim C^{3.1}$. The exponent 3.1 is similar to the power-index 2.6 reported for the longest relaxation time ($\tau = 1/\omega_c$, with ω_c (rad/s) the frequency of G' and G'' cross-over) of a cationic polyacrylamide of 45% charge density (Lauten and Nyström, 1999). When increasing chitosan concentration, the relaxation time increases due to the increase of the number of entanglement and polymer-polymer interactions. The concentration dependence of the mean relaxation time slightly increased with increasing ionic strength, in agreement with other reported experimental findings (Lauten and Nyström, 1999; Yamaguchi et al., 1992). This tendency may be related to the increase of the possibility to build up polymer-polymer associates via mainly hydrophobic interactions at high ionic strength. Using Cole-Cole plots ($G'' \sim G'^P$) (Lauten and Nyström, 1999; Thuresson et al., 1997), we investigated the relaxation behaviour of chitosan solutions. P is equal to 0.5 for one-single Maxwell fluid. All used chitosan solutions presented the P value higher than 0.5, indicating the deviation from single mode Maxwell element behaviour. When chitosan concentration and ionic strength increased, the P value increased. It indicates that the relaxation behaviour becomes more complicated or multimodal at high chitosan concentration and ionic strength.

9.3.2. Urea effect on chitosan-GP solution behaviour

In the presence of glycerophosphate, the chitosan solution behaviour was investigated in terms of urea concentration in order to expand our understanding of the functions of hydrogen bonding and hydrophobic interactions. The rheological physical properties G' at 15°C increased with increasing urea concentration. Higher urea concentration decreased $\tan\delta$, indicating that chitosan solution was less elastic in the

presence of urea. The detrimental effect of urea on polymer-polymer interactions has been abundantly reported (Hammes and Schimmel, 1967; Kim et al., 1996; Kjønsken et al., 2003; Kokufuta et al., 1998; McGrane et al., 20004; Philippova et al., 2001). The relaxation spectra and Cole-Cole plot were determined using both measured G' and G'' moduli. The shape of the relaxation spectra was monomodal and unchanged by the addition of urea. The mean relaxation time decreased with increasing urea concentration. The P value obtained from the Cole-Cole plot gradually decreased with increasing urea concentration, denoting that the stress relaxation becomes more simplified due to the reduction of molecular interactions. Urea hinders polymer-polymer interaction through hydrogen bonding and hydrophobic interactions; thus, it shows much more simplified relaxation process from external forces.

9.3.3. Effects of β -GP and chitosan concentrations on solution behaviour

The effect of glycerophosphate and polymer concentrations on small amplitude oscillatory rheometry data was investigated in the range of temperature 5 to 45°C. The physical properties of chitosan solutions were increased with glycerophosphate content due to the larger number of physical interactions at higher GP concentration (or higher ionic strength). The viscoelastic properties also increased with chitosan concentration due to the entanglements as well as polymer-polymer interactions. The flow activation energies E_{af} was calculated in terms of chitosan and glycerophosphate concentrations. E_{af} was increased in the presence of the low content of glycerophosphate; but it was increased for highly concentrated chitosan solutions. E_{af} represents the sensitivity of physical properties to temperature changes. Therefore, high E_{af} means that the physical properties of polymer solutions show high temperature-dependency. Increasing temperature generally decreases the rheological properties because of the increase of molecular mobility and flexibility of polymer molecules. Chitosan hydrogen bonding and hydrophobic groups are both very sensitive to temperature. Hydrogen bonds are decreased at elevated temperature, but hydrophobic interactions are enhanced at high temperature. In addition, hydrophobic interactions are strengthened at high ionic

strength. The change in ionic strength was calculated in terms of temperature under various glycerophosphate concentrations. The ionic strength was gradually increased at high temperature and the increasing rate was accelerated at the high concentration of glycerophosphate. The enhancement of ionic strength at high glycerophosphate concentration retards the reduction of the physical properties of chitosan solution with temperature due to polymer-polymer associates via hydrophobic interactions. Thus, the rheological properties of chitosan solution showed less sensitivity to temperature at high concentration of glycerophosphate, resulting in lower flow activation energy. The complex viscosity at 0.1rad/s increased with polymer concentration and it presented a power-law relationship with polymer concentrations at three different temperatures, i.e. $\eta_{0.1\text{rad/s}}^* \sim C_C^{5.0}$. This exponent of 5.0 is higher than the one of 4.2 for the chitosan solutions ($\text{pH} = 4.2 (\pm 0.2)$) determined in the absence of glycerophosphate. In the presence of glycerophosphate, the protonation degree in the chitosan chain decreased and the ionic strength was increased. Adding glycerophosphate to the solutions though provides a more favourable environment to form polymer-polymer interactions; thus, the higher power-law index may be the result of more associations.

9.4. Heat-induced gelation

The chitosan-glycerophosphate solutions transformed into gel state when temperature increased (heat-induced gelation). During the gelation process, the evolution of the physical properties of the chitosan-glycerophosphate solutions was characterized using rheological measurements. The gelation of chitosan-glycerophosphate solutions proceeds in three stages. In the first one, chitosan-glycerophosphate solutions showed a viscoelastic fluid-like behavior ($G' < G''$), and both G' and G'' moduli decreased with increasing temperature. Increasing temperature generally decreases the volume of a molecule due to decreasing hydrogen-bonded hydration water (Noguchi, 1981), and results in a decrease of the rheological properties. In the second region, the rheological properties rapidly increased with increasing temperature due to the formation of a three-dimensional network (fast gelation process). In the last zone, the much slower gelation

was caused by the lower diffusivity that resulted from the viscosity increase after gelation (slow gelation process).

9.4.1. Temperature effect on gelation

For chitosan-glycerophosphate systems, the ionization of each species was calculated from the measured *pH* values in terms of temperature. The protonation of chitosan molecules decreased with raising up temperatures, but the ionization of glycerophosphate was enhanced. The ratio of two ions rapidly decreased at elevated temperature, indicating a low possibility of ionic interactions between protonated amine groups and negatively charged phosphoric groups. Hydrogen bonding interactions generally decreases with increasing temperature. This reduction of hydrogen bonds at high temperature might cause a change in the chitosan molecular conformation. At low temperature, chitosan adopts a compact conformation due to intramolecular hydrogen bonds, and the physical junctions that could form a gel are confined inside the coil. It is therefore a poor conformation to build-up a 3D structure due to the difficulty of creating contacts between the junction zones. Increasing temperature reduces the number of intramolecular hydrogen bonds so that the chitosan molecules can unfold freely, thus making gelation more favorable. Finally, water molecules are presumed to form enclosed structures that surround the polymer chains at low temperature (Li et al, 2001). Increasing temperature exceeds the ability of weak hydrogen bonds to orient the dipolar water molecules around the polymer chains (Osada and Kajiwar, 2000). As a consequence, the energized water molecules surrounding the polymer are removed and the dewatered hydrophobic polymer segments begin to associate with each other. The calculated ionic strength (or measured conductivity) of the chitosan-glycerophosphate was increased with temperature. The increased ionic strength in the presence of glycerophosphate involved enhanced screening of electrostatic repulsion and hydrophobic interactions, resulting in favorable conditions to form a gel structure.

9.4.2. Urea effect on gelation

In the presence of urea, the gelation temperature was increased, corresponding to the retardation of the gelation process. In addition, the gel strength was decreased with increasing urea concentration. To explain the effect of urea on gelation, the conductivity of the chitosan-glycerophosphate systems was measured as a function of temperature in the presence of urea. The relative conductivity ratio (i.e. solutions conductivity normalized by that of the solution in the absence of urea) was lower in the presence of urea, and this effect was more pronounced at high temperature. It is known that higher ionic strength increases hydrophobic interactions of chitosan systems (Desbrieres et al., 1996); therefore, the observed decrease of the conductivity was indicative of lower polymer-polymer interactions. Lower ionic strength involves less screening of electrostatic repulsion between protonated chitosan glucosamine groups, and hence fewer possible hydrophobic interactions, resulting in detrimental conditions for gel formation. This study reconfirmed the importance of hydrophobic interactions during the heat-induced gelation process.

9.4.3. 3D sol-gel phase diagram for gelation

The complex G' and G'' moduli measured during the heating process were used to determine gelation point. In this study, the gelation temperature (T_{gel}) was obtained from the crossover point of G' and G'' (or $\tan\delta = 1$), despite of the slight dependency on frequency. T_{gel} was determined under various chitosan and glycerophosphate concentrations and the 3D (T , C_{GP} , C_C) sol-gel phase diagram was plotted for the chitosan-glycerophosphate system. T_{gel} was decreased with increasing chitosan and glycerophosphate concentration. T_{gel} rapidly increased at very low chitosan and glycerophosphate concentrations; however, a synergetic effect at high glycerophosphate and chitosan concentrations resulted in a sudden drop of the gelation temperature. The synergetic effect resulted in a phase transition that is on the edge between concentration-induced and heat-induced gelation.

9.4.4. Gelation kinetics study

Non-isothermal kinetics of the heat-induced gelation was performed in order to quantify the activation energy to form gel structures. The activation energy for gelation (E_{ag}) was determined from the slope of each zone (second and third regimes). First of all, the effect of urea on the activation energy was investigated. The energy increased from 2800 to 5000 kJ/mol in the fast gelation region (Region (2)) with increasing urea concentration, indicating that the development of intermolecular interactions was less favoured energetically in the presence of urea. In the third region, E_{ag} was much lower (about 170 kJ/mol) and was also nearly constant regardless of urea concentration, most probably because gelation was diffusion controlled in this last region. Secondly, the calculated activation energy for gelation (E_{ag}) was determined in terms of glycerophosphate and chitosan concentrations. When chitosan concentration increased from 0.10M to 0.20M, E_{ag} decreased from 3000 to 500kJ/mol in the second regime. It indicated that the development of intermolecular junctions was more favourable energetically for higher polymer content. However, the activation energy was ~ 170kJ/mol and constant regardless of urea concentration in the third regime. The lower gelation activation energy in the last zone suggested that the evolution of the physical networks was also energetically easier, but the gelation was nevertheless strongly slowed down in that region since it was diffusion controlled due to the large viscosity increase. The gelation activation energy was not influenced by glycerophosphate concentration in the second and third zones.

9.4.5. Reversibility of the gel structure formed

The thermoreversibility of the gel structures was investigated by decreasing temperature to 5°C with a constant cooling rate (1°C/min). The physical properties were getting decreased with temperature, but showed a solid-like behaviour ($G' > G''$). It indicates the gel systems showed a partial thermoreversibility due to remaining physical associations. In addition, the gel structures formed were opaque and hard at high temperature; however, the system became transparent, sticky and elastic like rubbers at

5°C. Spontaneous recovery of the gel after high deformation gel break-up at low temperature confirmed this statement and the physical properties were increased with time due to the formation of polymer-networks possibly due to hydrogen bonding interactions.

9.4.6. Gelation below room temperature

Chitosan-GP concentrations was stored at three different temperature (0°C, 5°C, and room temperature) and the change o their physical state was investigated in terms of temperature. At 0 and 5°C, the gel systems were formed at the high contents of chitosan and GP in systems. The gelation at low temperature may mainly be due to the formation of 3D networks via hydrogen bonding interactions. However, phase separation was investigated for all chitosan samples except that the sample 10-33 became a homogenous gel after 3 months. The two important forces, hydrogen bonds and hydrophobicity, are greatly dependent on temperature. Hydrogen bonding interactions are dominant at low temperature, but are reduced at elevated temperature. Hydrophobic interactions enhances at high temperature. Thus, the occurrence of phase separation at room temperature may be due to lack of physical-polymer interactions..

9.4.7. Effects of ionic strength and temperature on gelation

At 80°C, chitosan solutions in the absence of GP (pH ~ 4.2 – 4.3) were characterized in terms of ionic strength using rheological measurements. When ionic strength was lower than 0.1, the viscosity was initially decreased and then was constant. The initial decrease of the viscosity may be due to the mechanical degradation and/or the change of molecular conformation resulting from the loss of hydrogen bonds at high temperature. However, hydrophobic interactions can form 3D networks for chitosan systems at elevated temperature. Thus, the constant viscosity is may be due to balance of the mechanical degradation and/or the loss of hydrogen bonds and hydrophobic interactions. Above an ionic strength 0.3M, the formation of 3D networks via hydrophobic interactions is dominant; thus, the mechanical properties increased. When

ionic strength increased, the gelation process was accelerated and the stronger gel systems were formed. The study also supports that the hydrophobic interactions are the main forces to form 3D networks during the heat-induced gelation.

Chapter 10

Original scientific contributions

- 1) One of the important contributions in this work is the study of the effect of ionic strength at constant pH on the linear and non-linear rheological properties of chitosan solutions in the concentrated regime. The relaxation behaviour of the chitosan solution was extensively characterized with the calculation of continuous relaxation spectra and use of the Cole-Cole plot. It was also compared for the first time with the predictions of the reptation model. This extensive study of the effect of ionic strength provides the fundamental ideas about the chitosan sol behaviour in the concentrated regime (Chapter 4).
- 2) Gelation mechanisms were proposed following the calculation of ionic strength and ionization of each species in the chitosan-glycerophosphate system using the pH values measured in terms of temperature. This approach, coupled to rheometry, was found to be powerful and simple to investigate the gelation process. The calculation permitted to assess the absence of ionic interactions such as ionic bridging and propose the main driving force driving the formation of the gel structure (Chapter 5).
- 3) The 3D sol-gel phase diagram of chitosan and glycerophosphate was generated for the first time. The gelation temperature was used to characterize the structure of the polymer junctions in terms of glycerophosphate concentration. (Chapter 7).
- 4) The feasibility of chitosan heat-induced gelation in the absence of glycerophosphate was shown. The gelation occurred for ionic strengths above 0.3 M. At high ionic strength, the gelation process was accelerated and stronger gel structures were formed. This study informed us of the importance of hydrophobic interactions to form gel structures of chitosan-based systems at high temperature (Chapter 8).

5) We showed the feasibility of cryogelation of the chitosan-glycerophosphate system. The cryogels were formed within one month when the solutions were stored below 0°C. The cryogelation was accelerated at high chitosan and glycerophosphate concentration (Chapter 8).

Chapter 11

Conclusions and perspectives

11.1. Conclusions

In this study, we investigated the sol and gel behavior of chitosan-based systems under various conditions of ionic strength, additives, polymer concentration and temperature. First, we determined the different concentration regimes: dilute, semi-dilute, and concentrated. Then, rheological measurements were performed to characterize chitosan solutions in each regime. In addition, the evolution of rheological and physicochemical properties was thoroughly investigated during the gelation process. The main results are summarized below.

11.1.1. Solution behavior in dilute regime

First of all, the overlapping (C^*) and entanglement (C_e) concentrations were determined as a function of ionic strength and presented power-law relationships with $C^* \sim I^{2/9}$ and $C_e \sim I^{1/15}$. The intrinsic viscosity was shown to decrease with increasing ionic strength as the chain became more flexible and compact with a reduction of the repulsive potential. The persistence length (l_p) decreased with increasing I and the length in a θ solvent ($1/\sqrt{I} = 0$ or $I = \infty$) was 24 nm. White-like precipitates formed above $I = 0.70$ M.

11.1.2. Solution behavior in concentrated regime

The physical properties of chitosan solutions were greatly dependent on ionic strength, urea, glycerophosphate and chitosan concentrations in the concentrated regime. Increasing ionic strength decreased the rheological properties and nonlinear behavior due to the reduction of the electrostatic repulsion force by the salt screening effect. Stress relaxation of the chitosan solutions was more complex and multimodal at high polymer concentration. The relaxation time and the zero-shear viscosity also showed power-law relationships with chitosan concentration (C_C), i.e. $\tau_H \sim C_C^{3.1}$ and $\eta_0 \sim C_C^{4.1}$.

The linear viscoelastic properties were greatly affected by urea, glycerophosphate and chitosan content. The complex viscosity was a power-law function of chitosan concentrations: $\eta_{0.1\text{rad/s}}^* \sim C_C^5$. The flow activation energy was lowered with decreasing glycerophosphate concentration and increased with chitosan concentration. At low temperature, urea lowered viscoelastic properties and shorten relaxation times of chitosan-GP solutions. The relaxation behavior was also more simplified in the presence of urea.

11.1.3. Chitosan gelation

During the heat-induced gelation process, three regions were defined according to rheological properties: 1) a liquid-like behavior at low temperature, 2) a fast gelation process, and 3) a slow gelation process. There are several interactions related to physical gelation – ionic, hydrogen bonding and hydrophobic interactions. These interactions are very sensitive to temperature. We evaluated that the protonation of chitosan molecules ($-\text{NH}_3^+$) was lowered with increasing temperature. However, the ionization of divalent glycerophosphate ($-\text{OP}(\text{O}^-)_2$) was increased, resulting in the increase of the ionic strength. Thus, the ratio of both ions decreased in terms of temperature, indicating a low possibility of ionic interactions such as ionic bridging. The increase of ionic strength promoted polymer-polymer junctions through hydrophobic interactions. In addition, increasing temperature modifies hydrogen bonds distribution and favors polymer-polymer interactions over those of polymer-solvent. Thus, the main driving force of the chitosan-glycerophosphate heat-induced gelation may be hydrophobic interactions. This assumption was supported by the results obtained during gelation tests in the presence of urea.

The gelation temperature (T_{gel}) decreased with increasing chitosan and glycerophosphate concentrations. A synergetic effect was shown by a sudden drop of the gelation temperature at high chitosan and glycerophosphate concentrations. Furthermore,

increasing ionic strength accelerated the gelation process and enhanced gel strength. On the other hand urea retarded gelation.

The gelation activation energy (E_{ag}) calculated from a nonisothermal kinetics model. When chitosan concentration increased from 0.10M to 0.20M, E_{ag} decreased from 3000 to 500 kJ/mol in the fast regime, but it was almost constant (~ 170 kJ/mol) regardless of GP concentration in the slow gelation regime. In both regimes, E_{ag} showed an almost constant value regardless of GP content, indicating that the gelation kinetics is independent on GP concentration. The lower gelation activation energy in the last zone suggested that the evolution of the physical networks was energetically easier, but the gelation was nevertheless strongly slowed down in that region since it was diffusion controlled due to the large viscosity increase.

The gel structure formed at high temperature was only partially thermoreversible upon cooling to 5°C due to the existence of remaining associations. The gel system however showed complete pH-reversibility, and molecular conformation becomes more extended after recovering solution state from gel.

Cryogels were produced with the chitosan-glycerophosphate system below 0°C. The cryogelation process was very slow compared to that of the heated-induced gelation. Additionally, the gelation was more favorable at high chitosan and glycerophosphate concentrations. Precipitation or phase separation occurred after a month for chitosan solutions stored at room temperature due to the absence of a sufficient driving force to form a homogeneous gel.

11.2. Perspectives

In this study, we have thoroughly characterized sol and gel behavior of chitosan solutions under various ionic strength, polymer concentration, additives and temperature. Still we would need to investigate the effect of molecular weight and degree of deacetylation on sol and gelation behavior of chitosan systems. Recently, we found the cryogel formation of chitosan-GP systems at 0°C. However, the investigation was only visually performed. Thus, the physical properties of the system should be measured as a

function of time to characterize the gel strength and gelation time. The gelation rate was very low and it took one month to form gel structure. If possible, we may need to find a way to enhance the gelation process at low temperature.

Many potent and sophisticated drugs have been developed in the pharmaceutical industry; however, many of them cannot be effectively delivered using current drug delivery techniques. The effective drug delivery has been a key issue. Many different strategies have been attempted as a mean to improve drug delivery. In recent studies, microgels have been attracting more attention to develop controlled drug delivery systems with biopolymers. Among various biopolymers, chitosan extracted from crustaceans has been considered because of its non-toxicity, biodegradability, biocompatibility and bioactivities (Kasaai, 1999). For various applications, we may form microgels of chitosan-GP usable for drug release systems. The chitosan-GP system in solution may be mixed with oil and stirred to form emulsions. Some emulsifiers used in the biomedical industry could be employed to stabilize the emulsions, and the emulsified chitosan-GP system could be used to produce microgels by the input of thermal energy.

References

- Alberty, R. A. (1983). Physical chemistry, 6th Ed., John Wiley & Sons Inc.
- Alberty, R. A. and Silbey, R. J. (1996). Physical chemistry, 2nd Ed., John Wiley & Sons, Inc.
- Alonso, D. O. V. and Dill, K. A. (1991). Solvent denaturation and stabilization of globular proteins. Biochemistry, 30, 5974 - 5985.
- Amiji, M. M. (1995). Pyrene fluorescence study of chitosan self-association in aqueous solution. Carbohydrate Polymers, 26, 211 – 213.
- Anthonsen, M. W., Vårum, K. M. and Smidstrød, O. (1993). Solution properties of chitosans: conformation and chain stiffness of chitosans with different degrees of N-acetylation. Carbohydrate Polymers, 22, 193 – 201.
- Argüelles-Mondal, W., Goycoolea, F. M., Peniche, C. and Higuera-Giagara, I. (1998). Rheological study of the chitosan/glutaraldehyde chemical gel system. Polymer Gels and Networks, 6, 429-440.
- Austin, P. R. (1977). German Patent 2,707,164.
- Berger, J., Reist, M., Mayer, J. M., Felt, O., Peppas, N. A. and Gurney, R. (2003). Structure and interactions in covalently and ionically crosslinked chitosan hydrogels for biomedical applications. European Journal of Pharmaceutics and Biopharmaceutics, 57, 19 – 34.

Berry, G. C. and Fox, T. G. (1968). The viscosity of Polymers and their Concentrated Solutions. Advances in Polymer Science, 5, 261 – 357.

Berth, G. and Dauzenberg, H. (2002). The degree of acetylation of chitosans and its effect on the chain conformation in aqueous solution. Carbohydrate Polymers, 47, 39 – 51.

Boris, D. C. and Colby, R. H. (1998). Rheology of Sulfonated Polystyrene Solutions. Macromolecules, 31, 5746 – 5755.

Brugnerotto, J., Desbrières, J., Heux, L., Mazeau, K. and Rinaudo, M. (2001a). Overview on structural characterization of chitosan molecules in relation with their behavior in solution. Macromolecular Symposia, 168, 1-20.

Brugnerotto, J., Desbrieres, J., Roberts, G. and Rinaudo, M. (2001b). Characterization of chitosan by steric exclusion chromatography. Polymer, 42, 9921 – 9927.

Burchard, W. (2001). Structure Formation by Polysaccharides in Concentrated Solution. Biomacromolecules, 2, 342 – 353.

Capitani, D., De Angelis, A. A., Crescenzi, V., Masci, G. and Sergre, A. L. (2001). NMR study of a novel chitosan-based hydrogel. Carbohydrate Polymers, 45, 245 – 252.

Carreau, P. J., De Kee, D. C. R. and Chabra, P. R. (1997). Rheology of Polymeric Systems: Principles and Applications, Hanser Publishers, Munich, Germany.

Chaput, C. and Chenite, A. (2001). Mineral-polymer hybrid composition, WO 01/41822.

Cheetham, N. W. H. and Tao, L. (1997). Amylose conformational transition in binary DMSO/water mixtures. Starch/Stärke, 49, 407 – 415.

Chen, R. H. and Lin, J. H. (1994). Effects of pH, ionic strength, and type of anion on the rheological properties of chitosan solution. Acta Polymerica, 45, 41 – 46.

Chen, R. H. and Tsaih, M. L. (1998). Effect of temperature on the intrinsic viscosity and conformation of chitosans in dilute HCl solution. International Journal of Biological Macromolecules, 23, 135 – 141.

Chen, R. H. and Tsaih, M. L. (2000). Urea-induced conformational changes of chitosan molecules and the shift of break point of Mark-Houwink equation by increasing urea concentration. Journal of Applied Polymer Science, 75, 452 – 457.

Chenite, A., Buschmann, M., Wang, D., Chaput, C. and Kandani, N. (2001). Rheological characterisation of thermogelling chitosan/glycerol-phosphate solutions. Carbohydrate Polymers, 46, 39 – 47.

Christianziana, P., Lelj, F., Amodeo, P., Barone, G. and Barone, V. (1989). Journal of the Chemical Society. Faraday transactions II. Molecular and Chemical Physics, 85, 621.

Cox, W. and Merz, E. (1958). Correlation of dynamic and steady flow viscosities. Journal of Polymer Science, 28, 619 – 622.

Crescenzi, V., Imbriaco, D., Velasquez, C. L., Dentini, M. and Ciferri, A. (1995). Novel types of polysacchride assemblies. Macromolecular Chemistry and Physics, 196, 2873 – 2880.

De Angelis, A. A.; Capitani, D. and Crescenzi, V. (1998). Sythesis and ^{13}C CPMAS NMR charaterisation of a new chitosan-based polymeric network. Macromolecules, 31, 1595 – 1601.

de Gennes, P. G. (1976). Dynamics of Entangled Polymer Solutions. II. Inclusion of Hydrodynamic Interactions. Macromolecules, 9, 594.

Desbrieres, J., Martinez, C. and Rinaudo, M. (1996). Hydrophobic derivatives of chitosan: Characterization and rheological behaviour. International Journal of Biological Macromolecules, 19, 21-28.

Desbrières, J. (2002). Viscosity of semiflexible chitosan solution: influence of concentration, temperature, and role of intermolecular interactions. Biomacromolecules, 3, 342 – 349.

Dobrynin, A.V., Colby, R. H. and Rubinstein, M. (1995). Scaling theory of polyelectrolyte solutions. Macromolecules, 28, 1859 – 1871.

Doczi, J. (1957). US Patent 2,795,579.

Doi, M. and Edward, S. F. (1986). The theory of Polymer Dynamics, Clarendon Press, Oxford.

Domard, A. (1987). pH and c.d. measurements on a fully deacetylated chitosan: application to CuII —polymer interactions. International Journal of Biological Macromolecules, 9, 98 – 104.

Dubin, P. and Stauss, U. P. (1973). Conformational transitions of hydrophobic polyacids in denaturant solutions. Effect of urea. Journal of Physical Chemistry, 77, 1427 - 1431.

Ferry, J.D. (1980). Viscoelastic properties of polymers, J. Willey & Sons, New York.

Finny, J. L. and Soper, A. K. (1994). Solvent structure and perturbations in solutions of chemical and biological importance. Chemical Society Reviews, 23, 1 – 10.

Frenkel. I. (1946). Kinetic Theory of Liquids, Oxford University Press, London, England.

Fuoss, R. M. (1948). Viscosity function for polyelectrolytes. Journal of Polymer Science, 3, 603 – 604.

Fuoss, R. M. (1949). Viscosity function for polyelectrolytes. Journal of Polymer Science, 4, 96.

Goldberg, R. N., Kishore, N. and Lennen, R. M. (2002). Thermodynamic Quantities for the ionization Reaction of Buffers. Journal of Physical and Chemical Reference Data, 31, 231 – 370.

Hamedine, M. (2004). Propriétés viscoélastiques d'hydrogels de chitosane avec acides organiques et inorganiques. Master's Thesis, École Polytechnique de Montréal, Université de Montréal.

Hammes, G. G. and Schimmel, P. R. (1967). An Investigation of Water-Urea and Water-Urea-Polyethylene Glycol Interactions. Journal of the American Chemical Society, 89, 442 – 446.

Hayes, E. R. and Davies, D. H. (1978). Characterization of Chitosan. I. Thermoreversible chitosan gels. Proceedings 1st international conference on

chitin/chitosan, Muzzarelli, R. A. A. and Pariser E. R. (eds), MIT Sear Grant Program Report MITSG 78-7, 193 - 197.

Hirano, S. (1989). Chitin and chitosan, Skjak-Break, G., Anthonsen, T., and Standford, P. (eds). Elsevier Applied Science, 51 – 69.

Hwang, J. K. and Shin, H. H. (2000). Rheological properties of chitosan solutions. Korea-Australia Rheology Journal, 12, 175 – 179.

Imeri, A. G. and Knorr, D. (1998). Journal of Food Science, 53, 1124 - 1128.

Iversen, C., Kjoniksen, A.L., Nystrom, B., Nakken, T., Palmgren, O. and Tande T. (1997). Linear and nonlinear rheological responses in aqueous systems of hydrophobically modified chitosan and its unmodified analogue. Polymer Bulletin, 39, 747 – 754.

Jackson, D. S. (1987) Chitosan-Glycerol-Water Gel, USA Patent 4.659,700.

Jiang, W. H. and Han, S. J. (1999). The interactions of chitosan-poly(ethylene glycerol) in the presence of added salt in water: viscosity effect. European Polymer Journal, 35, 2079 – 2085.

Jones, D. S. (1999). Dynamic mechanical analysis of polymeric systems of pharmaceutical and biomedical significance. International Journal of Pharmaceutics, 179, 167 – 178.

Kasaai, M. R. (1999). Depolymerization of chitosan. Doctoral Thesis, Université Laval, Quebec, Canada.

Kasaai, M.R., Arul, J. and Charlet, G. (2000). Intrinsic viscosity-molecular weight relationship for chitosan. Journal of Polymer Science: B: Polymer Physics, 38, 2591 - 2598.

Kienzle-Sterzer, C.; Rodriguez-Sanchez, D.; and Rha, C. (1982). Dilute Solution Behavior of a Cationic Polyelectrolyte, Journal of Applied Science, 27, 4467 – 4470.

Kim, S. S., Lee, Y. M. and Cho, C. S. (1995). Synthesis and properties of semi-interpenetrating polymer networks composed of β -chitin and poly(ethylene glycerol) macromer, Polymer, 36, 4497 – 4501.

Kim, S., Sarathchandra, D. and Mainwaring, D. E. (1996). Effect of Urea on Molecular and Colloid Aggregation of Proanthocyanidin Polymers from *Pinus radiata*. Journal of Applied Polymer Science, 59, 1979 – 1986.

Kjonisken, A.-L., Hiorth, M., Roots, J., Nystrom, B. (2003). Shear-induced Association and Gelation of Aqueous Solutions of Pectin. Journal of Physical Chemistry B., 107, 6324-6328.

Knaul, J. (1998). Improved mechanical properties of chitosan fibres: applications to degradable radar countermeasure chaff. Ph. D. Thesis, Royal Military College, Kingston, ON, Canada.

Knorr, D. (1985). Proc. Biochem., 6, 90 – 92.

Kokufuta, E., Suzuki, H., Yashida, R., Yamada, K., Hirata, M. and Kaneko, R. (1998). Role of Hydrogen Bonding and Hydrophobic Interactions in the volume Collapse of a Poly(ethylenimine) Gel. Langmuir, 14, 788.

Kopperud, H. M., Hansen, F. K. and Nyström, B. (1998). Effect of surfactant and temperature on the rheological properties of aqueous solutions of unmodified and hydrophobically modified polyacrylamide. Macromolecular Chemistry and Physics, 199, 2385 – 2394.

Krause, W. E., Tan, J. S. and Colby, R. H. (1999). Semidilute solution rheology of polyelectrolytes with no added salt. Journal of Polymer Science Part B: Polymer Physics, 37, 3429 – 3437.

Kulicke, W.-M., Arendt, O. and Berger, M. (1998). Rheological characterization of the dilatant flow behavior of highly substituted hydroxypropylmethylcellulose solutions in the presence of sodium lauryl sulphate. Colloid & Polymer Science, 276, 617 – 626.

Kumar, M. N. V. R. (2000). A review of chitosan and chitosan applications. Reactive & Functional Polymers, 46, 1 – 27 (2000).

Lauten, R. A. and Nystrom, B. (1999). Linear and nonlinear viscoelastic properties of aqueous solutions of cationic polyacrylamides. Macromolecular Chemistry and Physics, 201, 677 – 684.

Li, L., Thangamathesvaran, P. M., Yue, C. Y., Tam, K. C., Hu, X. and Lam, Y. C. Gel Network Structure of Methylcellulose in Water. Langmuir, 17, 8062-8068.

Lide, D. R. (2003/2004). CRC Handbook of Chemistry and Physics: A Ready-Reference Book of Chemical and Physical Data, 83rd Ed., CRC Press.

McGrane, S., Mainwaring, D. E., Cornell, H. J. and Rix, C. J. (2004). The Role of Hydrogen Bonding in Amylose Gelation. Strach/Stärke, 56, 122 – 131.

Mi, F. L., Sung, H. W. and Shyu, S. S. (2000). Synthesis and characterization of a novel chitosan-based network prepared using naturally occurring crosslinker. Journal of Polymer Science. Part. A. Polymer Chemistry, 38, 2804 – 2814.

Mitchell, J.R. and Ledward, D. A. (1996). Functional properties of food macromolecules, Elsevier Applied Science Publishers.

Morel and Hering (1993). Principles and Applications of Aquatic Chemistry, Wiley.

Mucha, M. (1997). Rheological characteristics of semi-dilute chitosan solutions. Macromolecular Chemistry and Physics, 198, 471 – 484.

Mukherjee, D. P. (2001). USA Obvious 6.310,188.

Muzzarelli, R. A. A., Tanfani, F., Emanuelli, M., and Gentile, S. (1980). J. Appl Biochem, 2, 380.

Muzzarelli, R. A. A., Tomasetti, M., and Iiari, P. (1994). Depolymerization of chitosan with the aid of papain. Enzyme Microb. Technol., 16, 110 – 114.

Noda, I. and Takahashi, Y. (1996). Bunsen-Gesellschaft - Physical Chemistry Chemical Physics, 100, 696.

Noguchi, H. (1981) Hydration around hydrophobic groups. Water activity: Influences on food quality, Rocklan, L. B. and Stewart, G. F. Eds., Academic Press.

Noguchi, J., Arato, K., and Komai (1969). Kogyu Kogaku Zasshi, 72, 796.

Nystrom, B., Kjøniksen, A.-L. and Iversen, C. (1999). Characterization of association phenomena in aqueous systems of chitosan of different hydrophobicity. Advances in Colloid and Interface Science, **79**, 81 – 103.

Osada, Y. and Kajiwara, K. (2000). Gels Handbook, Academic Press.

Pa, J.-H. and Yu, T. L. (2001). Light scattering study of chitosan in acetic acid aqueous solutions. Macromolecular Chemistry and Physics, **202**, 985 – 991.

Park, J. W., Choi, K.-H. and Park, K. K. (1983). Acid-base equilibria and related properties of chitosan. Bulletin of Korean Chemistry Society, **4**, 68 – 72.

Pearson, D. S. (1987). Recent advances in the molecular aspects of polymer viscoelasticity. Rubber Chemistry and Technology Journal, **60**, 439 – 498.

Philippova, O. E., Volkov, E. V., Sitnikova, N. L., Khokhlov, A., Desbrieres, J. and Rinaudo, M. (2001). Two Types of Hydrophobic Aggregates in Aqueous Solution of Chitosan and Its Hydrophobic Derivative. Biomacromolecules, **2**, 483 – 490.

Raymond, L., Morin, F. G. and Marchessault, R. H. (1993). Degree of deacetylation of chitosan using conductometric titration and solid-state NMR. Carbohydrate Research, **246**, 331 – 336.

Rinaudo, M., Milas, M. and Le Dung, P. (1993). Characterization of chitosan. Influence of ionic strength and degree of acetylation on chain expansion. International Journal of Biological Macromolecules, **15**, 281 – 285.

Rinaudo, M., Pavlov, G. and Desbrières, J. (1999). Influence of acetic concentration on the solubilization of chitosan. Polymer, **40**, 7029 – 7032.

Rinaudo, M., Pavlov, G. and Desbrières, J. (1999). Solubilization of chitosan in strong acid medium. International Journal of Polymer Analysis and Characterization, 5, 267 – 276.

Roberts, G. A. F. (1992). Chitin Chemistry, The Macmillan Press Ltd.

Roberts, G. A. F. (1995). Structure-property relationships in chitin and chitosan. Chitin and Chitosan, the versatile environmentally friendly modern materials. Mat B. Zakaria et al. (eds), Penerbit Universiti Kebangsaan Malaysia, Bangi, 94 – 108.

Roseman, M. and Jenks, W. P. (1975). Interactions of urea and other polar compounds in water. Journal of the American Chemical Society, 97, 631 - 640.

Rubinstein M., Colby R. H. and Dobrynin, A.V. (1994). Dynamics of Semidilute Polyelectrolyte Solutions. Physical Review Letter, 73, 2776 - 2779.

Rutherford, F. A. and Austin, P. R. (1977). Proceedings 1st international conference on chitin/chitosan, Muzzarelli, R. A. A. and Pariser E. R. (eds), MIT Sear Grant Program Report MITSG 78-7, 182.

Singla, A. K. and Chawla, M. (2001) Chitosan: some pharmaceutical and biological aspects – an update. Journal of Pharmacy and Pharmacology, 53, 1047 – 1067.

Soto-Perlata, N. V., Maller, H. and Knorr, D. (1988). Journal of Food Science, 54, 495 – 496.

Takahashi, Y., Isono, Y., Noda, I. and Nagasawa, M. (1985). Zero-shear viscosity of linear polymer solutions over a wide range of concentration. Macromolecules, **18**, 1002 – 1008.

Tako, M. and Hanashiro, I. (1997). Evidence for a conformational transition in curdlan. Polymer Gels and Networks, **5**, 241 – 250.

Tsaih, M. L. and Chen, R. H. (1997). Effect of molecular weight and urea on the conformation of chitosan molecules in dilute solutions. International Journal of Biological Macromolecules, **20**, 233 – 240.

Tsaih, M. L. and Chen, R. H. (1999). Molecular weight determination of 83% degree of decetylation chitosan with non-Gaussian and wide range distribution by high-performance size exclusion chromatography and capillary viscometry. Journal of Applied Polymer Science, **71**, 1905 – 1913.

Ullner, M., Jönsson, B., Peterson, C., Sommelius, O. and Söderberg, B. (1997). The electrostatic persistence length calculated from Monte Carlo, variation and perturbation methods. Journal of Chemical Physics, **107**, 1279 – 1284.

Wallqvist, A. and Covell, D. G. (1998). Hydrophobic Interactions in Aqueous Urea Solutions with Implications for the Mechanism of Protein Denaturation, Journal of the American Chemical Society, **120**, 427 – 428.

Wang, D. (1999). Characterization of thermoreversible pH-sensitive physical gels of chitosan. Master's Thesis, Ecole Polytechnique de Montreal, Quebec, Canada.

Wang, W. and Xu, D. (1994). Viscosity and flow properties of concentrated solutions of chitosan with different degrees of deacetylation. International Journal of Biological Macromolecules, 16, 149 – 152.

Watchter, R. and Stenberg, E. (1996). Hydagen® CMF in cosmetic applications, Efficacy in different in-vivo and in-vivo measurements, Advances in chitin and chitosan, 1, Domard, A.; Jeuniaux, C.; Muzzarelli, R. A. A.; & Roberts, G. A. F. (eds), Jacques Andre Publisher, Lyon, France, 381 – 388.

Wetton, R. E., Marsh, R. D. L. and Ven-de-Velde, J. G. (1991). Theory and application of dynamic thermal analysis. Thermochimica Acta, 175, 1 – 11.

Yamaguchi, M., Wakutsu, M., Takahashi, Y. and Noda, I. (1992). Viscoelastic properties of polyelectrolyte solutions. 2. Steady-state compliance. Macromolecules, 25, 475 – 478.

Yomota, C., Miyazaki, T. and Okada, S. (1993). Determination of the viscometric constants for chitosan and the application of universal calibration procedure in its gel permeation chromatography. Colloid & Polymer Science, 271, 76 – 82.

Yong, R. J. and Lovell, P. A. (1991). Introduction to polymers, Chapman & Hall.

Appendices

Appendix I. Conference paper 1 – Rheological properties and gelation of chitosan and β -glycerophosphate solutions

: Jaepyoung Cho, Marie-Claude Heuzey, André Begin, and Pierre J. Carreau, *Advances in Chitin Science*, Montreal, QB, CANADA, 7, 191 – 195, 2003 .

Appendix II. Conference paper 2 – Gelation study of chitosan/ β -glycerophosphate solutions by rheological measurements

: Jaepyoung Cho, Marie-Claude Heuzey, André Begin, and Pierre J. Carreau, *Proceedings of the XIVth International Congress on Rheology (ICR2004)*, FB09-1 – 3, 2004.

Appendix III. Conference paper 3 – Concentrations effect on the gelation of chitosan and glycerophosphate

: Jaepyoung Cho, Marie-Claude Heuzey, André Begin, and Pierre J. Carreau, *Proceedings of Polymer Processing Society (PPS) Asia/Australia*, 30-O-S5-07, 2004.

Appendix IV. Conference Paper 4 – Rheology of heat-induced gelation f chitosan solutions

: Jaepyoung Cho, Marie-Claude Heuzey, André Begin, and Pierre J. Carreau, *The Society of Plastics Engineers (SPE) Annual Technical Conference (ANTEC) 2005*.

Appendix I.

Conference paper 1 - Rheological properties and gelation of chitosan / β -glycerophosphate solutions

Jaepyoung Cho^a, Marie-Claude Heuzey^a, André Bégin^b and Pierre J. Carreau^a

^aGénie Chimique, École Polytechnique de Montréal, C.P. 6079, succ. Centre-Ville, Montréal, Québec, H3C 3A7, Canada

^bCentre de recherche et de développement sur les aliments, 3600, boul. Casavant Ouest, Saint-Hyacinthe, Québec, J2S 8E3, Canada

Abstract

In this work, gel formation was investigated for chitosan / β -glycerophosphate (β -GP) solutions by dynamic mechanical measurements to understand the nature of the gelation process. In solution, the zero shear viscosity was linearly proportional to storage time below room temperature. Heating resulted in the gelation between 78 and 79°C. Decreasing temperature from 90°C to 10°C, the gel strength gradually decreased as indicated by the gradual decrease in the measured G' . However, the chitosan/ β -GP system retained a gel-like structure below room temperature. At 5°C, the gel formed had a cohesion energy (E_c) of 20.4 mJ/m³ and showed recovery after break-up. The flow activation energy (E_{af}) was determined with the solutions transformed from gel structures, cured at 80°C for different times (0 – 6 h), into liquid-like state by controlling the pH from 6.6 to 4.5 with the addition of HCl. The calculated activation energy was between 34 – 37 kJ/mol. From the study of the non-isothermal kinetics of the gel formation, we found that the gelation can be described by a three-step process corresponding to three different temperature ranges. The activation energy for gelation (E_{ag}) was 125 kJ/mol between 71 – 77°C, 4090 kJ/mol between 77 – 79°C and 315 kJ/mol between 79 – 90°C for the gel formation of the chitosan/ β -GP system during the heating process.

1. Introduction

Chitosan is a biopolymer obtained by alkaline deacetylation of chitin, extracted from the shells of crustaceans and the exoskeletons of arthropods. This biopolymer is a non-toxic, biocompatible and biodegradable material. It has been used in many areas such as food, medical, cosmetic and pharmaceutical industries [1].

Below a pH of 6.2, chitosan becomes a positively charged polyelectrolyte due to the protonation of free amine groups, causing electrostatic repulsion [2]. The addition of a base to chitosan solutions reduces the

electrostatic repulsion so that it results in the formation of gel-like structure above a pH of 6.2. There are three important forces related to the gelation of chitosan solutions: electrostatic repulsion, hydrogen bonding and hydrophobic interactions. The forces are mainly dependent on the degree of deacetylation (DDA) of chitosan, pH, ionic strength and temperature [3-5]. Recently, a thermoreversible chitosan gel system for biomedical applications was prepared by neutralizing highly deacetylated semidilute chitosan solutions with β -glycerophosphate, β -GP. The system remained in solution at physiological pH of 7.2 and changed into a

hydrogel system upon heating at physiological temperature (37°C) [6,7]. The gel formation of chitosan/ β -GP system was investigated in terms of pH, temperature, DDA and acid [8,9].

In this work, the evolution of a similar gel-like system was investigated using a highly deacetylated and high molecular weight chitosan and β -GP. The aim of this work was to investigate the nature of the gelation process of the chitosan/ β -GP system. First, the effect of the storage time on the physical properties of the chitosan solutions was investigated before gelation tests. Then, the variation in the storage modulus (G') was investigated by heating and cooling at a constant rate. The G' data measured during the structure development was used to analyze the non-isothermal kinetics related to gel formation. The gel system was characterized at low temperature by dynamic mechanical testing. Finally, the gel was transformed to liquid-like state by lowering the pH from 6.6 to 4.5. The viscosity of the resulting solutions was measured at different temperatures in order to investigate the stiffness of the chitosan molecules.

2. Experiments

2.1. Materials and methods

Chitosan from Marinard Biotech (QC, Canada) was used in this study. The weight average molecular weight (\overline{M}_w) and DDA of the chitosan were 2×10^6 g/mol and 93%, respectively. Acetic acid (AcOH) was used to dissolve chitosan. The addition of β -glycerophosphate disodium salt (β -GP) (Sigma-Aldrich, ON, Canada) increased the pH of the chitosan solution without causing immediate precipitation or gel formation below room temperature. The composition of the chitosan solution was 0.87%(w/w) chitosan/ 0.86%(w/w) AcOH/

13.7 %(w/w) β -GP. The chitosan solution was left to rest 3 h for degassing without stirring at room temperature and then kept in a refrigerator ($< 5^\circ\text{C}$). The pH of the solution was 6.6 between 2 - 5°C .

2.2. Rheological measurements

The stability of the chitosan solution was monitored as a function of storage time by measuring the zero shear viscosity (η_0). Gelation was carried out by increasing temperature from 5 to 90°C and decreasing from 90 and 5°C at a constant rate of $1^\circ\text{C}/\text{min}$. Small deformation (γ_0) of 0.01 and low frequency (ω) of 1 Hz were used in order not to disturb the gel formation. The gelation temperature (T_g) was determined as the crossover point of the storage (G') and loss (G'') moduli. The G' modulus data was used to analyze non-isothermal kinetics related to gel formation. The gel system formed was characterized by small amplitude oscillatory shear at 5°C . In a separate test, the chitosan solution was cured at 80°C as a function of time (0 – 6 h) and the resulting gel system formed was cooled down at room temperature for 24 h. It was later transformed into liquid-like state by controlling the pH from 6.6 to 4.5 with 37% HCl. The viscosity of the solutions obtained was measured at different temperatures (5, 25, 45°C) to determine the flow activation energy (E_{af}). The rheometer used was a stress-controlled rheometer AR-2000 (TA Instruments, Del, USA) with a Couette geometry. Mineral oil covered the surface of the chitosan solutions in order to hinder evaporation during the measurements.

3. Results

3.1. Characterization of chitosan solutions

After preparation, chitosan/ β -GP solutions were stored in a refrigerator ($T <$

5°C). The solutions were characterized by frequency sweep test and steady shear test at 5°C. The Cox-Merz rule ($\eta(\dot{\gamma}) = \eta^*(\omega)$) was valid for this system. The zero shear viscosity (η_o) was determined from frequency sweep test data with the three-parameter Carreau model [10]. The Carreau model is given by:

$$\eta = \frac{\eta_o}{\left[1 + (\lambda\dot{\gamma})^2\right]^{\frac{n-1}{2}}} \quad (1).$$

The parameters are η_o , λ and n . The characteristic time λ has units of time and the parameter n is dimensionless. When the steady shear rate ($\dot{\gamma}$) becomes zero, the model predicts the zero shear viscosity η_o and the slope in the power-law region (or the high frequency region in the figure) is given by $1-n$. Figure 1 shows the effect of the storage time on η_o of the chitosan solution. The viscosity increased linearly with storage time. The total increase was 8.1% after one week and 20.5% after two weeks. The increase in the viscosity may be due to the interactions between chitosan-chitosan and chitosan/ β -GP molecules. The solutions used to perform gelation were stored for less than one week in order to keep the viscosity variation below 10%. Figure 2 shows the results of the frequency sweep test performed at 5°C within the linear viscoelastic region, where G' and G'' are independent of the strain amplitude. G'' is larger than G' in the whole range of frequency. G' and G'' have a power-law dependence to frequency in the terminal zone: $G' \sim \omega^2$ and $G'' \sim \omega^1$. This is the typical behaviour of a viscoelastic solution.

3. 2. Thermoreversible gelation

For gelation, the evolution of G' and G'' was investigated as a function of increasing and decreasing temperature to examine thermoreversibility. The gelation

test was repeated five times in the same conditions and the relative standard deviation of G' was within 20%. This deviation value is reasonable for the gelation test. Figure 3 shows the results of the temperature ramp test. At low temperature, the chitosan/ β -GP solutions showed solution behaviour ($G' \ll G''$) unlikely those obtained with the addition of NaOH, which exerts immediate precipitation. In the first part of the whole heating process, G' continuously decreased as a function of temperature before gel formation. This is the common thermal behavior of a liquid system [11]. Between 78 and 79°C, there was a crossover between G' and G'' , which is generally considered as the gelation point. After this point, G' abruptly increased as a function of temperature. When the gel system formed was cooled down from 90 to 5°C, G' decreased up to 10°C and then slightly increased below 10°C. It indicates that the gel formed partially thermoreversed between 90 to 10°C but the gelation continued to be evolved between 10 to 5°C. Figure 4 (a), (b) and (c) show the rheological characterization of the gel system at 5°C. In Figure 4(a), the oscillatory test clearly shows the gel nature of the system with G' larger than G'' . Both moduli show a slight dependence on frequency, which is a typical of a physical gel system. In Figure 4(b), the effect of strain on the gel is shown. Both G' and G'' moduli remained constant for low strains, but decreased at strains larger than 0.05. The strain value of 0.05 is the critical strain (γ_c) at which a polymeric solution begins to show a non-linear viscoelastic behavior. γ_c can be used to calculate the cohesion energy [12]:

$$E_c = \int_0^{\gamma_c} \sigma d\gamma_c = \int_0^{\gamma_c} G'_c \gamma_c d\gamma_c = \frac{1}{2} \gamma_c^2 G'_c \quad (2)$$

where E_c is the cohesion energy and G'_c represents the storage modulus at the critical strain. The cohesion energy E_c is related to the energy involved in the formation of physical crosslinks between the polymer chains. E_c calculated was 20.4 mJ/m³. The gel formed was broken at higher strains. The break-up of the gel formed resulted in the reduction of the G' and G'' moduli. Figure 4 (c) presents the evolution of G' at 5°C. The storage modulus increased continuously due to the formation and rearrangement of junction zones. After all experiments, the gel system was transparent, sticky and elastic-like rubbery materials.

3. 3. Characterization of pH-reversed chitosan solutions

To explore the role of β -GP on gel formation, the zero shear viscosity (η_0) was measured after transforming gel-like structures, cured at 80°C for different times (0 – 6 h), into liquid-like state by controlling the pH from 6.6 to 4.5 with the addition of 37% HCl. The viscosity was measured at three different temperatures (25, 35 and 45°C). It was proportional to the curing time at 80°C as shown in Figure 5 (a). In general, the zero shear viscosity of polymer melts and solutions has a power-law dependence on molecular weight. Thus, an increase in the zero shear viscosity may result from increasing molecular weight due to interactions between chitosan or chitosan/ β -GP molecules. FTIR and intrinsic viscosity measurements will be used to investigate the source of the viscosity increase. In Figure 5(b), the zero shear viscosity is plotted as a function of the inverse of the absolute temperature $1/T$. This temperature dependence is a useful way to characterize the stiffness of the polymer molecule because it relates to the activation energy (E_{af}) for the flow process. Higher flow activation energy represents higher stiffness. The calculated activation

energy was between 34 – 37 kJ/mol. Wang [5] determined for a chitosan concentration of 2g/dL (in 0.2M AcOH/0.1M AcONa) that the activation energy was 25 kJ/mol for a DDA of 91% and 15 kJ/mol for a DDA of 75% [13]. Desbrieres [14] reported that the activation energy of a concentration-induced chitosan gel (5.285g/dL) in 0.3M AcOH/0.05M AcONa was 25.4 kJ/mol in the temperature range from 273 to 323K. The chitosan used had a molecular weight of 1.93×10^3 g/mol and a DDA of 88%. In this work, the activation energy is very high compared to other results due to the use of a high molecular weight (2×10^6 g/mol) and high DDA (93%) chitosan. The effect of curing time on the activation energy is small (Figure 5(b)). This may be because the high molecular weight and high DDA chitosan macromolecules used in this work had already a very high stiffness.

4. Discussion

4. 1. Gelation of chitosan/ β -GP solutions

When a strong base such as NaOH is added to a chitosan solution, it precipitates instantly. However, the addition of β -GP to a chitosan solution leaves it in a solution-state ($G' \ll G''$) even for pH above 6.2 at room temperature, as shown in Figure 3. It may be due to the mild alkalinity of β -GP (pKa = 6.34) [9] and the interactions of O⁻ ionized in β -GP molecules and protonated amine groups (NH₃⁺) in chitosan molecules, decreasing electrostatic intra and intermolecular repulsions and inhibiting chitosan chain-chain aggregation. In addition, it is in solution-state at low temperature because the water structure prevents the contacts between chitosan-chitosan molecules. However, chitosan/ β -GP solutions were transformed into gel-like structures when heated. As shown in Figure 3, G' rapidly increased above 79°C. Upon heating, the water structure formed at low

temperature is broken so that it is possible to form chitosan-chitosan chain aggregation. Furthermore, the induction of thermal energy increases the hydrophobic interactions between biopolymeric molecules [9,11]. Thus, the increase in hydrophobic interactions accelerates the gel formation of chitosan solutions.

After heating up to 90°C, the cooling process was done at a cooling rate of 1°C/min. G' increased in the beginning of the cooling process and then gradually decreased up to 10°C. When temperature was decreased below 10°C, G' was slightly increased again due to the continuing gel formation. At 5°C, the system showed a typical gel behavior ($G'' < G'$). The evolution of the physical structure at low temperature may be related to the aggregation of chitosan molecules by hydrogen bonding and/or chemical reaction between chitosan molecules and β -GP molecules. FTIR and intrinsic viscosity measurements will be carried out to explain the build up of the physical structure at low temperature [15,16].

4. 2. Non-isothermal gelation kinetics

To use non-isothermal kinetics models, gelation tests should be carried out at a constant heating rate. The kinetic model used in this work is a combination of the Arrhenius equation and the time-temperature relationship, yielding:

$$\ln\left(\frac{1}{G'^n} \frac{dG'}{dt}\right) = \ln k_o - \left(\frac{E_{ag}}{RT}\right) \quad (3)$$

where G' is the storage modulus, n the reaction rate, t the time, k_o the Arrhenius frequency factor, E_{ag} the activation energy for gelation, R the ideal gas constant and T the absolute temperature [17]. This equation, however, does not always cover the whole range of experimental temperatures.

To determine E_{ag} from this equation, the first step is the determination of the parameter n , a complex and difficult process because of the dependency of temperature on n . Thus, in this work we assumed that the reaction rate n was equal to 2. This value represents the collision of two macromolecules as the most probable first stage in intermolecular aggregation, giving rise to second-order kinetics. Figure 6(a) shows the determination of the gelation rate (dG'/dt) data at each temperature. The gelation rate was determined from the slope of the three G' data points. We observed that dG'/dt increases as a function of time (or temperature). Assuming the reaction rate $n = 2$, E_{ag} was determined from the plot of $\ln(1/G'^2 * dG'/dt)$ and $1/T$ as shown in Figure 6(b). The gelation can be described by a three-step process corresponding to three different temperature ranges. E_{ag} was 125 kJ/mol between 71 – 77°C, 4090 kJ/mol between 77 – 79°C and 315 kJ/mol between 79 – 90°C for the gel formation of the chitosan solution during the whole heating process. In Figure 3, the gelation temperature was shown to be between 78–79°C. The higher activation energy between 77 – 79°C indicates that gel formation is very difficult; moreover, the development of intra and intermolecular interactions is only possible when enough thermal energy is provided. Over 79°C, the evolution of the physical three-dimensional network is energetically easier and the activation energy is lower. However, the viscosity increase should eventually hinder the diffusion of the molecules and slow down the gelation process.

5. Conclusions

In this work, the evolution of a gel-like structure was investigated for chitosan/ β -GP solutions to understand the nature of the gelation process. The zero shear viscosity of

the chitosan/ β -GP solutions increased linearly as a function of storage time below room temperature. The chitosan solutions showed typical solution behavior below room temperature. When curing was induced, gelation started between 78 – 79°C and continuously progressed up to 90°C. Decreasing the temperature from 90 to 10°C, the gel strength gradually decreased as indicated by the gradual decrease of the measured G' . However, between 10 and 5°C, G' increased slightly and the chitosan/ β -GP system kept a gel-like structure. The cohesion energy of the gel formed was 20.4 mJ/m³ at 5°C. After break-up, the gel showed recovery as demonstrated by the elastic modulus (G') increase as a function of time measured at small strain and low frequency. The increase in G' at low temperature may result from increased hydrogen bonding interactions or the chemical interactions between chitosan and β -GP. The flow activation energy (E_{af}) was determined with the solutions transformed from gel structures, cured at 80°C for different times (0 – 6 h), into liquid-like state by controlling the pH from 6.6 to 4.5 with the addition of HCl. The calculated activation energy was between 34 – 37 kJ/mol. From the study of the non-isothermal kinetics related to gel formation, we found that gelation can be described by a three-step process corresponding to three different temperature ranges. The higher activation energy, occurring between 77 – 79°C, indicates that the gel formation is difficult. However, above 79°C, the evolution of the physical three-dimensional network is energetically easier and the activation energy for gelation is lower.

Acknowledgements

The authors gratefully acknowledges the financial support of Conseil De Recherches en Pêche et en Agroalimentaire du Québec (CORPAQ).

References

1. Kassai, M. R., Depolymerization of Chitosan, Doctoral Thesis, Université Laval (1999).
2. Park, J. W., Choi, K.-H., and Park, K. K., *Bul Korean Chem Soc*, Vol. 41, No. 2, 68 – 72 (1983).
3. Vachoud, L., Zydowicz, N. and Domard, A., *Carbohydr Res*, 302, 169 – 177 (1997).
4. Vachoud, L., Zydowicz, N. and Domard, A., *Carbohydr Res*, 326, 295 – 304 (2000).
5. Wang, D., Characterization of thermoreversible pH-sensitive physical gels of chitosan, Master's Thesis, École Polytechnique de Montréal in Quebec, Canada (1999).
6. Chaput, C. and Chenite, A., WO 01/41822 A1 (2001).
7. Chenite, A., and Chaput, C., Wang, D., and Selmani, A., WO 01/3600 A1 (2001).
8. Chenite, A., Chaput, C., Wang, D., Combes, C., Bushmann, M., Hoemann, C., Leroux, J., Atkinson, B., Binette, F., and Selmani, A., *Biomaterials*, 21, 2155 – 2161 (2000).
9. Chenite, A., Bushmann, M., Wang, D., Chaput, C., and Kandani, N., *Carbohydr Polym*, 46, 39 – 47 (2001).
10. Carreau, P. J., Chhabra, R. P., and De Kee, D. C. R., *Rheology of Polymeric Systems: Principles and Applications*, Hanser Publishers, Munich (England) (1997).
11. Li, L., Thangamathesvaran, P. M., Yue, C. Y., Tam, K. C., Hu, X. and Lam, Y. C., *Langmuir*, 17, 8062 – 8068 (2001).
12. Lessard, D. G., Ousalem, M., Zhu, X. X., Einsenberg, A., and Carreau, P. J., *J Polym Sci Phys Polym*, 41, 1627 – 1637 (2003).
13. Wang, W. and Xu, D., *Int J Biol Macromol*, 19, 149-152 (1994).

14. Desbrieres, J., *Biomacromolecules*, 3, 342-349 (2002).
15. Matsumoto, T., Kawai M. and Masuda, T., *Biorheology*, 30, 435 – 441 (1993).
16. Ramos, V. M., Rodriguez, N. M., Diaz, M. F., Heras, A. and Augllo, E., *Carbohydr Polym*, 52, 39 – 46 (2003).
17. Lopes de Silva, J. A., Gonçalves, M. P. and Rao, M. A., *Int J Biol Macromol*, 17(1), 25 - 32 (1995).

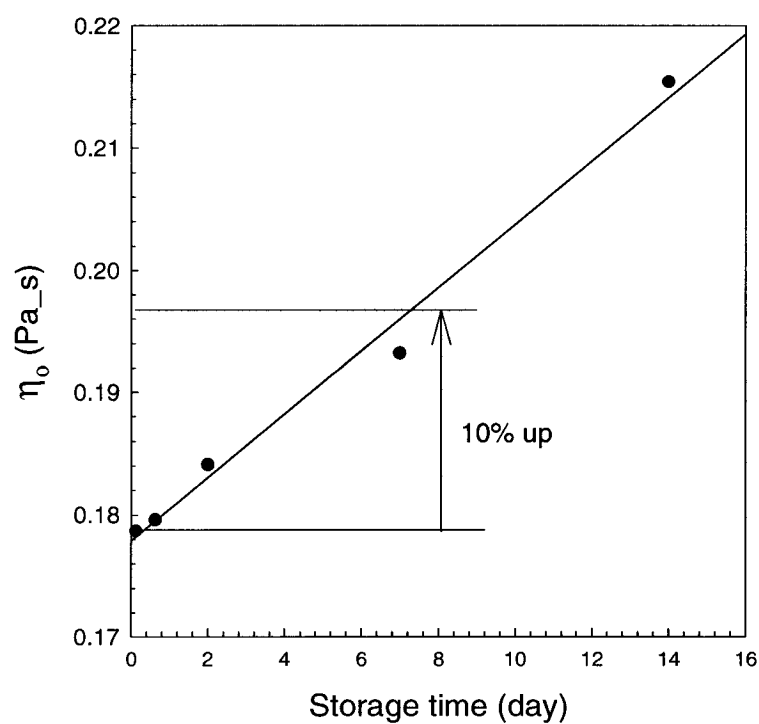


Figure 1. Zero shear viscosity (η_0) as a function of storage time ($T < 5^\circ\text{C}$). The composition of the chitosan solutions was 0.87%(w/w) chitosan/ 0.86%(w/w) AcOH/ 13.7 %(w/w) β -GP (pH = 6.6).

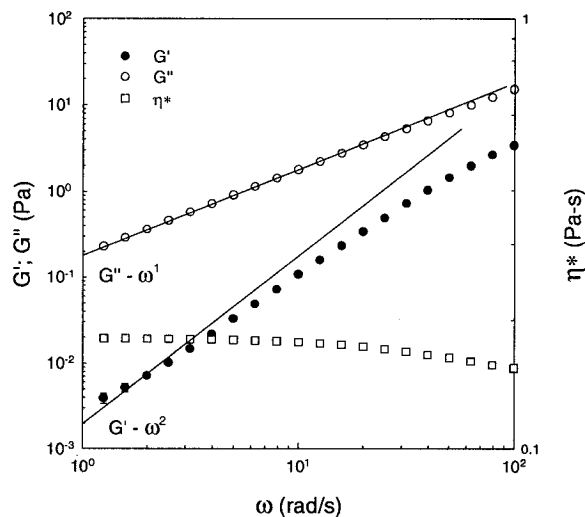


Figure 2. Storage (G') and loss (G'') moduli as functions of frequency for the chitosan solution (0.87%(w/w) chitosan/ 0.86%(w/w) AcOH/ 13.7%(w/w) β -GP (pH = 6.6)) before gelation at 5°C. The test was performed in the linear viscosity regime.

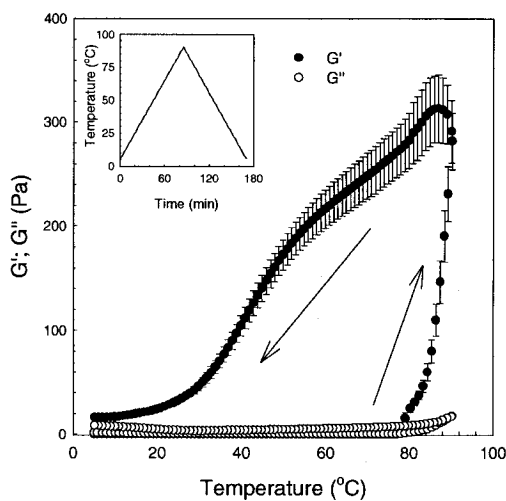


Figure 3. Storage modulus (G') and loss modulus (G'') as a function of temperature during heating and cooling processes with 0.87%(w/w) chitosan/ 0.86%(w/w) AcOH/ 13.7%(w/w) β -GP solution. The heating and cooling rates were 1°C/min. The strain and frequency used were 0.01 and 1Hz, respectively.

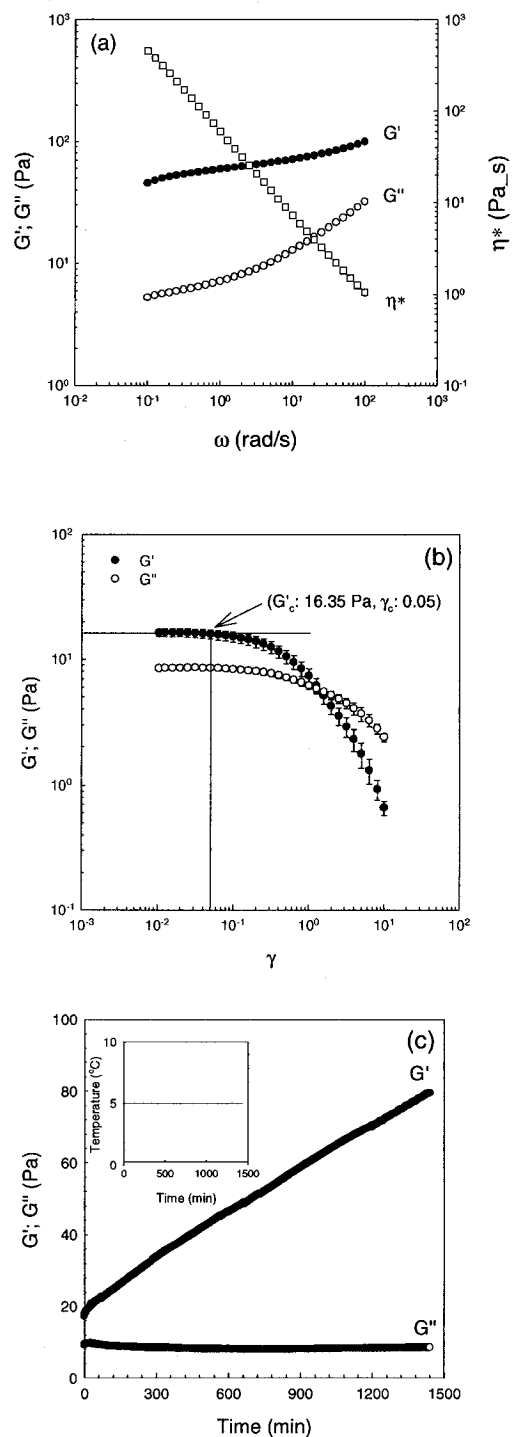


Figure 4. Gel systems characterized by (a) frequency sweep ($\gamma_0 = 0.01$); (b) strain sweep ($\omega = 1$ Hz) and (c) time sweep ($\gamma_0 = 0.01$ and $\omega = 1$ Hz) tests at 5°C. Results (a), (b) and (c) were done in sequence.

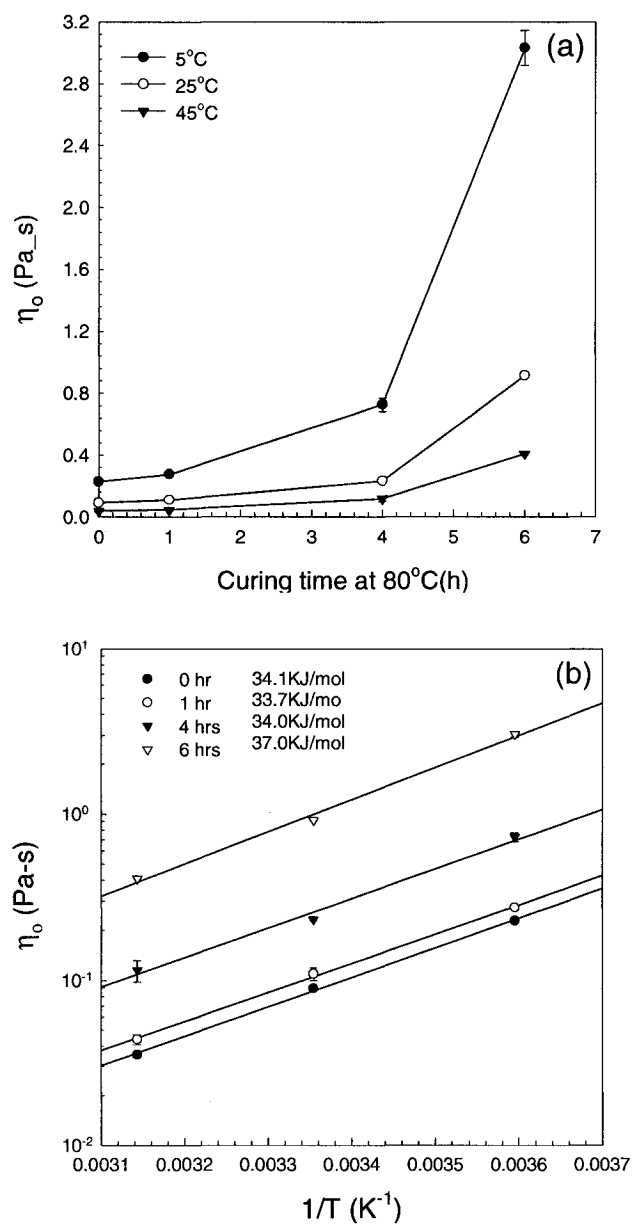


Figure 5. (a) Zero-shear viscosity of the solutions obtained from gels formed at 80°C as a function of curing time. (b) Zero shear viscosity as a function of $1/T$.

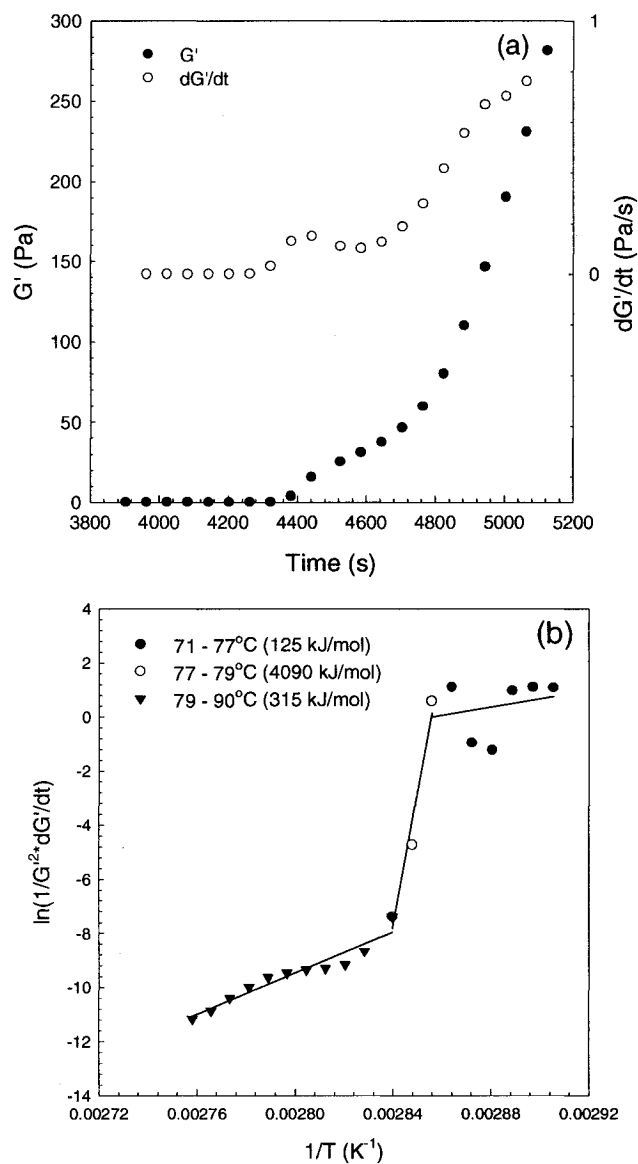


Figure 6. Non-isothermal kinetic analysis of G' data obtained from temperature ramp test. (a) Gelation rate (dG'/dt) was determined from the slope of three G' data points and (b) activation energy (E_{ag}) was calculated from the slope of the plot of $\ln(1/G'^2 \cdot dG'/dt)$ versus $1/T$ (K^{-1}).

Appendix II

Conference paper 2 – Gelation study of chitosan/ β -glycerophosphate solutions by rheological measurements

Jaepyoung Cho^a, Marie-Claude Heuzey^a, André Bégin^b and Pierre J. Carreau^a

^aCenter for Applied Research on Polymers (CRASP), Chemical Engineering, Ecole Polytechnique, PO Box 6079, Stn Centre-Ville, Montreal, Quebec, H3C 3A7, Canada

^bFood Research and Development Center, 3600 Casavant Blvd West, Saint-Hyacinthe, Quebec, J2S 8E3, Canada

ABSTRACT

To understand the nature of gelation of chitosan/ β -glycerophosphate solutions, the physical properties of the sol-gel transition were characterized by dynamic mechanical testing under different polymer and urea concentrations. In these gelation tests, the evolution of the storage (G') and loss (G'') moduli was monitored as a function of temperature. Heating resulted in sol-gel transition at a critical temperature, called gelation temperature (T_{gel}). To determine T_{gel} , we used two criteria: 1) $\tan\delta = 1$ and 2) $\tan\delta \sim \omega^0$ or $G' \sim G'' \sim \omega^n$, with $n = 0.65 \pm 0.01$. The two methods showed slightly different T_{gel} , as discussed by Chambon and Winter [1]. At low temperatures, chitosan-*GP* mixtures remained in solution and the complex viscosity (η^*) showed a power-law relationship with chitosan concentration, i.e. $\eta^* \sim C^{4.5}$ (at 45°C). For sol-gel transition, increasing chitosan concentration resulted in a lower T_{gel} , corresponding to an earlier onset of the gelation process. However, it also slowed down the gelation rate due to the reduction of diffusivity by the increase of viscosity. The addition of urea increased T_{gel} , indicating that hydrogen bonding is an important interaction of the gel formed.

INTRODUCTION

Chitosan is a biopolymer obtained by alkaline deacetylation of chitin, extracted from the shells of crustaceans and the exoskeletons of arthropods. It is chemically composed of 2-amino-2-deoxy-D-glucopyranose (*NGlc*) and 2-acetamido-2-deoxy-D-glucopyranose (*AcNGlc*) units. An important characteristic of the molecular structure is the degree of deacetylation (*DDA*), or the number percentage of *NGlc* in the chitosan molecule. The copolymer is generally accepted as "chitosan" when the *DDA* is larger than 50% [2]. It has been used in many areas such as food, medical, cosmetic and pharmaceutical industries due to its non-toxic, biocompatible and biodegradable character [3].

Chitosan becomes a positively charged polyelectrolyte below a *pH* of 6.2 due to the

protonation of the free amine groups ($pK_a = 6.2$), causing electrostatic repulsion [4,5]. Screening electrostatic repulsion by excessive salt leads to the formation of white-like precipitates [6]. Similarly, gels can be obtained by controlling the *pH*. The addition of a base to a chitosan solution reduces electrostatic repulsion so that it eventually results in the formation of a gel-like structure above a *pH* of 6.2. Using a strong base such as NaOH causes phase separation or precipitation. However, homogenous thermoreversible gels can be prepared by neutralizing highly deacetylated semi-dilute chitosan solution with a weak base such as β -glycerophosphate (*GP*) ($pK_{a,2} = 6.34$) [7]. The system remains in solution at physiological *pH* of 7.2 and room temperature and changes into a gel upon heating at physiological temperature [7,8]. There are four important interactions related to chitosan physical gelation: screening of electrostatic repulsions, hydrogen bonding,

hydrophobic interactions and entanglements. The interactions are dependent on ionic strength, DDA, chitosan concentration, pH, temperature and molecular weight. However, there is sparse information about the gelation nature of the chitosan/GP system. In this work, the gelation process of the chitosan/GP system is investigated by rheological measurements for various chitosan and urea concentrations. The aim of this work is to understand the nature of the chitosan/GP system gelation process.

EXPERIMENTAL

The chitosan studied (Marinard Biotech, Rivière-au-Renard, QC, Canada) has a high DDA (93.5%) and molecular weight ($\bar{M}_w = 2.0 \times 10^6$ g/mol). Aqueous solutions containing acetic acid (1 wt%) were used to dissolve the chitosan. The addition of GP (Sigma-Aldrich, Oakville, ON, Canada) (13.8 wt%) increased the pH of the chitosan solution without the immediate formation of precipitation or gel below room temperature. Urea (1M-5M) was added to control hydrogen bonding interactions. The range of chitosan concentration was 0.86-4.3 wt%. The chitosan solutions were left to rest 3h for degassing without stirring at room temperature and then kept in a refrigerator ($T \sim 5^\circ\text{C}$). The pH of chitosan solutions was measured at 5°C .

Gelation tests under oscillatory shear were carried out by increasing temperature at a constant heating rate ($1^\circ\text{C}/\text{min}$). A small deformation of 0.01 was applied not to disturb the gel formation. The critical temperature T_{gel} was determined by two criteria: 1) the crossover point of G' and G'' ($\tan\delta = 1$), 2) $\tan\delta$ independent of frequency ($\tan\delta \sim \omega^0$ or $G' \sim G'' \sim \omega^n$) [1]. For $\tan\delta = 1$, temperature ramp tests were performed at a single frequency (1Hz). To determine the point of $\tan\delta \sim \omega^0$, several frequencies (1-10Hz) were simultaneously used when the temperature ramp test was performed. The slope of the log-log plot of $\tan\delta$ and ω was determined at each temperature. The rheometer used was a stress-controlled rheometer (AR-2000, TA Instruments, Del, USA) with a Couette geometry. Mineral oil covered the surface of the

chitosan solutions to prevent evaporation during the tests. The effect of the mineral oil on the measurements was shown to be negligible.

Table 1. pH of chitosan-GP solutions

Urea concentration	0M	1M	3M	5M
Chitosan 1.72 wt%	6.7	6.8	7.0	7.1
Chitosan 3.44 wt%	7.1	×	×	×

RESULTS AND DISCUSSION

The pH of the chitosan solutions was slightly increased by increasing chitosan and urea concentrations (Table 1). This may be due to the consumption of H^+ ions by the protonation of the free amine groups in chitosan molecules and urea.

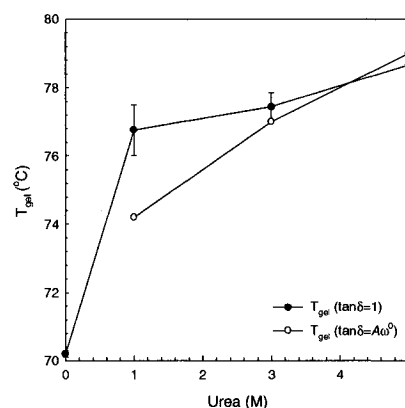


Figure 1. The effect of urea concentration on gelation temperature. The lines are drawn to guide the eye.

Figure 1 shows the comparison of T_{gel} obtained by both methods in the presence of urea for a chitosan concentration of 1.72 wt%. They result in slightly different values, as predicted for $n \neq$

0.5 [1]. In our case, n was found to be 0.65 ± 0.01 . However, both criteria indicate the same tendency in terms of urea effect, i.e. increasing urea concentration increases T_{gel} , thus making gelation more difficult. Since adding urea destroys hydrogen bonding interactions [9], it indicates that these interactions are important in the heat-induced chitosan-GP sol-gel transition.

During the gelation process, the evolution of G' and G'' was investigated as a function of temperature. As shown in Figure 2, three regions clearly appear. In Region (1), all chitosan solution samples (0.86-3.4 wt%) show liquid-like behavior ($G' < G''$, G'' not shown), and G' slightly decreases with increasing temperature.

This is the common thermal behavior of a polymer solution [10]. In this region, the complex viscosity (η^*) shows a power-law relationship with chitosan concentration, i.e. $\eta^* \sim C^{4.5}$, at 45°C. This exponent (4.5) is slightly higher than the value of 4.1-4.2 found for the same material in increasing ionic strength solutions ($I = 0.1$ - 0.4 M) [6]. Chitosan can remain in solution at these low temperatures even above a pH of 6.2 due to the mild alkalinity of GP [7]. However, the chitosan concentration of 4.3 wt% makes a spontaneous homogenous gel without any thermal treatment, even below room temperature.

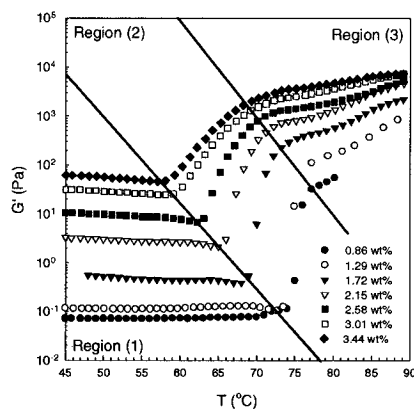


Figure 2. The effect of chitosan concentration on sol-gel transition (no urea).

In Region (2), G' abruptly increases upon heating, indicating a fast gelation process. Increasing temperature modifies hydrogen bonds distribution, favoring polymer-polymer interactions over those of polymer-solvent. Furthermore, $(\text{PO}_4)^{2-}$ ionic groups in GP can make ionic interactions with NH_3^+ positive chitosan amine groups, since their ionization intensifies with temperature. Finally, the induction of thermal energy increases

hydrophobic interactions [7,10], resulting in an acceleration of the gelation process of chitosan/GP solutions.

We also observe in Region (2) that the slope of G' as a function of temperature, related to gelation rate, decreases as chitosan concentration increases. This is due to the reduction of diffusivity, as expected, from the increase of viscosity with chitosan concentration. However, the onset of gelation is earlier, and the final modulus G' is also larger. This is explained by the fact that larger chitosan concentration increases the number of entanglements as well as the number of junctions, e.g. hydrogen bonds and hydrophobic sites. Overall, it makes more favorable gelation conditions.

Finally, the slower gelation observed in Region (3) is caused by the lower diffusivity that results from the viscosity increase during network formation.

SUMMARY

Gelation tests were performed for various chitosan and urea concentrations. The gelation temperature was determined by two criteria: $\tan\delta = 1$ and $\tan\delta \sim \omega^0$ or $G' \sim G'' \sim \omega^n$, with $n=0.65 \pm 0.01$. T_{gel} obtained by the two methods showed slightly different values, but presented the same tendency, i.e. urea retards the sol/gel transition. This indicates that hydrogen bonding interactions should be considered as an important factor of the chitosan-GP system gelation. At low temperatures, chitosan remains in solution due to the use of a weak base (GP) and favorable polymer-solvent hydrogen bonding interactions. The complex viscosity shows a power-law relationship with chitosan concentration, i.e. $\eta^* \sim C^{4.5}$, at 45°C. Increasing temperature results in enhanced polymer-polymer hydrogen bonding over polymer-solvent, the build-up of ionic attractions and the increase of hydrophobic interactions. Thus, increasing temperature accelerates sol/gel transition. Increasing chitosan concentration decreases T_{gel} and increases the storage moduli; however, it decreases the gelation rate due to the

reduction of diffusivity caused by the increase of viscosity. The chitosan concentration of 4.3 wt% makes a spontaneous homogenous gel in the presence of *GP* without any thermal treatment, even below room temperature.

REFERENCES

1. F. Chambon and H.H. Winter, *J Rheol*, 31, 683 (1987).
2. J. Brungenerotto, J. Desbrières, L. Heux, K. Mazeau, and M. Rinaudo, *Macromol Symp*, 168, 1 (2001).
3. M. R. Kassai, *Depolymerization of chitosan*, Doctoral thesis, Université Laval (1999).
4. J.-W. Park, K.-H. Choi and K.-K. Park, *Bul Korean Chem Soc*, 4, 68 (1983).
5. L. Vachoud, N. Zydowicz, A. Domard, *Carbohydr Res*, 302, 169 (1997).
6. J. Cho, M.-C. Heuzey, A. Bégin, and P. J. Carreau, *J Food Eng*, submitted.
7. A. Chenite, M. Bushmann, D. Wang, C. Chaput, and N. Kandani, *Carbohydr Polym*, 46, 39 (2001).
8. A. Chenite, C. Chaput, D. Wang, C. Combes, M. Bushmann, C. Hoemann, J. Leroux, B. Atkinson, F. Binette, and A. Selmani, *Biomaterials*, 21, 2155 (2000).
9. M. L. Tsaih, R. H. Chen, *Int J Bio Macromol*, 20, 233 (1997).
10. L. Li., P. M. Thangamathesvaran, C. Y. Yue, K. C. Tam, X. Hu and Y. C. Lam, *Langmuir*, 17, 8062 (2001).

Appendix III

Conference paper 3 – Concentrations effect on the gelation of chitosan and glycerophosphate

Jaepyoung Cho⁽¹⁾, Marie-Claude Heuzey⁽¹⁾, André Bégin⁽²⁾, Pierre J. Carreau⁽¹⁾,

(1) Center for Applied Research on Polymers (CRASP), Chemical Engineering, Ecole Polytechnique, PO Box 6079, Stn Centre-Ville, Montreal, Quebec, H3C 3A7, Canada

(2) Food Research and Development Center, 3600 Casavant Blvd West, Saint-Hyacinthe, Quebec, J2S 8E3, Canada

Abstract

The gelation of the chitosan solutions was studied by dynamic mechanical testing for various chitosan and urea concentrations. During the gelation tests, the evolution of the storage (G') and loss (G'') moduli was monitored as a function temperature. Heating resulted in sol-gel transition at a critical temperature, called gelation temperature (T_{gel}). It was found that increasing chitosan decreases T_{gel} ; however, it decreases the gelation rate due to the reduction of diffusivity resulting from the increase of the viscosity. A chitosan concentration of 4.3 wt% spontaneously forms a homogenous gel without the addition of thermal energy. The addition of urea increases T_{gel} , corresponding to the retardation of the gelation process. It indicates that hydrogen bonding is an important interaction of the gel formed.

Introduction

Chitosan is a biopolymer obtained by alkaline deacetylation of chitin, extracted from the shells of crustaceans and the exoskeletons of arthropods. This chitosan has been attracting much attention because of its various bioactivities such as antifungal, antitumor, antiallergic and immune activating characters. In addition, the chitosan is a non-toxic, biocompatible and biodegradable material. Therefore, it has been extensively used in food, medical, cosmetic and pharmaceutical industries.

Chitosan is positively charged below a pH of 6.2 due to the protonation of the free amine groups ($pK_a = 6.2$), causing electrostatic repulsion. Screening electrostatic repulsion by excessive salt leads to the formation of white-like precipitates [1].

Gel structure can be formed by controlling the pH. The addition of a base to a chitosan solution reduces electrostatic repulsion so that it eventually results in the formation of a gel-like structure above a pH of 6.2. Homogenous thermoreversible gels can be prepared by neutralizing semi-dilute chitosan solution with a weak base such as β -glycerophosphate (GP) [2]. The system remains in solution at physiological pH of 7.2 and room temperature and changes into a gel upon heating at physiological temperature 37°C. There are four important interactions related to chitosan physical gelation: screening of electrostatic repulsion, hydrogen bonding, hydrophobic interactions and entanglements. The interactions are dependent on ionic strength, the degree of deacetylation (DDA), chitosan concentration, pH, temperature and molecular weight. However, there is sparse information about the gelation nature of the chitosan/GP system. In this work, gelation tests were performed by dynamic mechanical testing for various chitosan solutions to understand the nature of the gelation process.

Experimental

The chitosan studied (Marinard Biotech, QC, Canada) has a high DDA (93.5%) and molecular weight ($\bar{M}_w = 2.0 \times 10^6$ g/mol). 1 wt% aqueous acetic solution was used to dissolve the chitosan. GP of 13.8 wt% (Sigma-Aldrich, ON, Canada) was added to increase the pH of the chitosan solutions without the immediate formation of precipitation or gel below room temperature. Urea (1M-5M) was added to control hydrogen bonding interactions. The range of chitosan concentration used was 0.86 - 4.3 wt%. The chitosan solutions were left to rest 3h for degassing without stirring at room

temperature and then kept in a refrigerator ($T \sim 5^{\circ}\text{C}$). The pH of chitosan solutions was measured at 5°C .

Gelation tests under oscillatory shear were carried out by increasing temperature at a constant heating rate ($1^{\circ}\text{C}/\text{min}$). A small deformation of 0.01 was applied not to disturb the gel formation. The gelation temperature (T_{gel}) was determined by two methods 1) the crossover point of G' and G'' ($\tan\delta = 1$) and 2) $\tan\delta$ independent of frequency ($\tan\delta \sim \omega^0$ or $G' \sim G'' \sim \omega^n$) [3]. For $\tan\delta = 1$, temperature ramp tests were performed at a single frequency (1Hz). To determine the point of $\tan\delta \sim \omega^0$, several frequencies (1-10Hz) were simultaneously used when the temperature ramp test was performed. The slope of the log-log plot of $\tan\delta$ and ω was determined at each temperature. The rheometer used was a stress-controlled rheometer (AR-2000, TA Instruments, Del, USA) with a Couette geometry. Mineral oil covered the surface of the chitosan solutions to prevent evaporation during the tests. The effect of the mineral oil on the measurements was shown to be negligible.

Results

To follow gelation, the evolution of G' and G'' was investigated as a function of temperature. Three regions are clearly shown during the gelation process. Initially all chitosan solutions in the range of 0.86 and 3.4 wt% present liquid-like behavior ($G' < G''$) and both moduli G' and G'' slightly decrease with increasing temperature. This is common behavior of a polymer solution. Increasing temperature generally decreases the volume of a molecule due to decreasing hydrogen-bonded hydration water. Thus, the reduction of the molecular size results in the reduction of the rheological properties of the chitosan solutions with increasing solution temperature. However, the chitosan concentration of 4.3 wt% makes a spontaneous homogenous gel without any thermal treatment, even below room temperature.

Above the temperature at the point presenting the minimum G' , both G' and G'' moduli show different behaviors. G' abruptly increases upon heating, indicating a fast gelation process. However, the loss modulus G'' still gradually decreases with increasing temperature. This difference between G' and G'' in this region

suggests that the evolution of the gel structure mainly contributes to the increases in the elasticity of the system. In addition, the gelation rate decreases with increasing chitosan concentration. This is due to the reduction of diffusivity, as expected, from the increase of viscosity with chitosan concentration. However, the onset of gelation is earlier, and the final modulus G' is also larger. This is explained by the fact that larger chitosan concentration increases the number of entanglements as well as the number of junction zones, e.g. hydrogen bonds and hydrophobic sites. Overall, it makes more favorable gelation conditions.

The induction of thermal energy and the change in ionic strength increase hydrophobic interactions [4]. Thus, increasing temperature results in an acceleration of the gelation process of chitosan/GP solutions. In addition, increasing temperature furthermore modifies hydrogen bonds distribution, favoring polymer-polymer interactions over those of polymer-solvent.

Finally, the slower gelation observed at high temperature region is caused by the lower diffusivity that results from the viscosity increase during network formation.

T_{gel} determined by the two methods shows slightly different values, but presents the same tendency; i. e. urea retards the sol-gel transition, thus making gelation more difficult since adding urea destroys hydrogen bonding interactions [5]. It indicates that hydrogen bonding interactions is important in the heat-induced chitosan/GP sol-gel transition.

Conclusions

Gelation tests were performed for various chitosan and urea concentrations by rheological measurements. During gelation process, three regions are clearly observed depending on temperature range: solution behavior, fast gelation and slow gelation. When increasing the chitosan concentration, the gelation process is accelerated due to the increase of the number of entanglements and junctions such as hydrogen bonds and hydrophobic parts. A very highly concentrated chitosan solution spontaneously forms a homogenous gel without inputting any thermal energy, even below room temperature. Adding urea to chitosan solution increases T_{gel} , corresponding to the retardation of the gelation process. It indicates that hydrogen bonding is

important in the chitosan-GP gelation process, even at high temperature

References

1. J. Cho, M.-C. Heuzey, A. Bégin and P. J. Carreau, *J. Food Eng.*, submitted.
2. A. Chenite, C. Chaput, D. Wnag, C. Combes, M. Bushmann, C. Hoemann, J. Leroux, B., Atkinson, F. Binette and A. Selmani, *Biomaterials*, 21, 2155 (2000).
3. F. Chambon and H.H. Winter, *J. Rheol.*, 31, 683 (1987).
4. J. Desbrieres, C. Martinez and M. Rinaudo, *Int. J. Bio. Macromol.*, 19, 21 (1996).
5. M. L. Tsaih, R. H. Chen, *Int. J. Bio. Macromol.*, 20, 233 (1997).

Appendix IV

Conference Paper 4 – Rheology of heat-induced gelation of chitosan solutions

Jaemyoung Cho¹, Marie-Claude Heuzey¹, André Bégin² and Pierre J. Carreau¹

¹CRASP, École Polytechnique de Montréal, Québec, Canada

²Food Research and Development Center, Québec, Canada

Abstract

The physiochemical and rheological properties of the chitosan system in liquid and gel state were measured in terms of temperature under various urea concentrations. Increasing temperature decreases the degree of the protonation of the chitosan and increases the total ionic strength of the system used. In solution state, adding urea decreases the rheological properties. Heating resulted in sol-gel transition at a critical temperature, called gelation temperature (T_{gel}). It was found adding urea decreased the gel strength and increased T_{gel} , corresponding to the retardation of the gelation process.

Background

Chitosan is a biopolymer, prepared from crustaceans with a series of chemical treatments. It is non-toxic, biocompatible and biodegradable. It has been used in many industries such as food, medical, cosmetic and pharmaceutical, and numerous international patents have claimed the

applications of chitosan in these areas. The advantage of this biopolymer is the ability to form three-dimensional networks or gel structure by controlling pH, ionic strength, and temperature. The physiochemical and rheological properties of the polymeric system during gelation is very useful tools to understand the mechanism of the gel formation and gelation process. The aim of this paper is to present the physiochemical and rheological properties of the chitosan-based system during gelation process under the various concentration of urea, a well-known hydrogen breaking agent [1]. The pH and conductivity measured are used to calculate the degree of the protonation of the chitosan and assume the ionic strength of the chitosan system in terms of temperature. The rheological measurement results are used to characterize the whole gelation process and determine the gel strength and gelation temperature.

Experimental

Materials and solution preparation

A high DDA (93%) and high molecular weight

(M_w : 8.5×10^5 g/mol) chitosan (Marinard Biotech, QC, Canada) was used to gel structure. Acetic solution was used to dissolve the chitosan. *GP* (Sigma-Aldrich, Canada) was added to increase the *pH* of the chitosan solution without the immediate formation of precipitation below room temperature. 0 – 5 M urea (Sigam[®], USA) was added to control hydrogen-bonding interactions. The final chemical composition for the chitosan solution prepared was 1.72 wt% chitosan/ 13.8 wt% *GP*/ 0.86 wt% *GP*/ 0 – 5 M urea.

***pH* and conductivity measurements**

Each chitosan solution was characterized in terms of *pH* (*pH*-meter, Hanna Ltd., Portugal) and conductivity (conductance meter, YSI model 35, YSI Inc., USA) under various temperatures. Water bath (Model BT-15, Cole-Parmer, USA) was used to increase temperature increased with a constant rate (0.8°C/min). Since *pH* and conductivity are temperature-dependent, we compensated temperature effect on the two-physiochemical values measured. The results of the *pH* measurements were used to estimate the degree of the protonation (α) of the chitosan applying the method of Rinaudo et al. [2]. The conductivity results indicate the ionic strength (*I*) of the sample used.

Rheological measurements

In solution state, the dynamic mechanical properties of the chitosan solution were

characterized at 5°C by frequency sweep test, performed in the linear viscoelastic regime. The zero shear viscosity (η_0) was determined from the shear data with the Carreau-Yasuda model [3]. The evolution of the rheological properties of the chitosan was investigated as a function of temperature by oscillatory shear measurements. Temperature increased from 5 to 90°C with a constant heating rate (+1°C/min) during the gelation test. Small deformation (γ_0) of 0.01 and low frequency (ω) of 1 Hz were used in order not to disturb the gel formation. The gelation temperature (T_{gel}) was determined as the crossover point of the storage (G') and loss (G'') moduli ($\tan \delta = 1$). The rheometer used was a stress-controlled rheometer (AR-2000, TA Instruments, DE, USA) with a Couette geometry. Mineral oil covered the surface of the chitosan solutions to prevent evaporation during the tests. The effect of the mineral oil on the measurements was shown to be negligible.

Results and Discussion

Effect of temperature on *pH* and conductivity

The *pH* and conductivity of the chitosan solutions were measured as a function of temperature. Figure 1 shows the effect of temperature on *pH* and conductivity. Increasing temperature decreases the *pH* values regardless of the chemical composition of each sample; however, increases the conductivity values, indicating that the ionic strength increases with

increasing temperature. Adding GP increased up to a pH of 6.9 at 25°C without instant precipitation or gel formation due to the neutralizing effect of the phosphate groups (base) [4]. However, adding urea did not affect the pH value of the chitosan solution.

The determination of the degree of the protonation (α)

In the absence of GP, the α value of the chitosan can be estimated with the method of Rinaudo et al. [2]. To calculate, the α value of the chitosan, the pK_a value of the acetic acid at each temperature should be recalculated by using the following equation [5]:

$$pK_{a,T} = -(R \ln 10)^{-1} \left[-\left\{ \ln(10) \frac{RT pK_{a,\theta}}{\theta} \right\} + \Delta_r H_\theta^\circ \left\{ \left(\frac{1}{\theta} \right) - \left(\frac{1}{T} \right) \right\} \right] + \Delta_r C_{p,\theta}^\circ \left\{ \left(\frac{\theta}{T} \right) - 1 + \ln \left(\frac{T}{\theta} \right) \right\} \quad \text{Eq (1).}$$

where R is the ideal gas constant; the subscripts T and θ denote the temperature to which a quantity pertains; the subscript P a constant pressure; and the subscript r the quantity to refer to a reaction. $pK_{a,\theta}$ is the pK_a value at the standard temperature θ (298.15 K), $\Delta_r H_\theta^\circ$ the enthalpy and $\Delta_r C_{p,\theta}^\circ$ the heat-capacity change at 298.15 K, $I = 0$ and $P = 0.1$ M Pa. The $pK_{a,\theta}$, $\Delta_r H_\theta^\circ$ and $\Delta_r C_{p,\theta}^\circ$ can be found in elsewhere [5]. The equation (1) can be used only between 274 and 350K and $I = 0$. Even though the ionic strength of the solution used was not zero in this study, the α values were determined with Rinaudo et al. putting pK_a at each temperature value determined from Eq (1).

Figure 2 clearly shows that α decreases with increasing temperature. The decrease in the α value at high temperatures results in decreasing the electrostatic repulsion so that the chitosan molecules can more easily contact with other chitosan molecules. At high temperatures, increasing the ionic strength more effectively screens the electrostatic repulsion caused by protonated amine groups and enhances the polymer-polymer interactions via hydrophobic interactions instead of polymer-solution interactions. Thus, increasing temperature provides a favourable environment to form gel structure.

Effect of urea on chitosan solution behaviors

The dynamic mechanical properties of the chitosan solutions were investigated by oscillatory shear tests in the linear viscoelastic zone under various urea concentrations at 5°C. Figure 3 shows the effect of the urea concentration on the G' and G'' moduli. Both moduli decrease with increasing the urea concentration. In the absence of urea, the plateau modulus in G' shows at the low frequency regime, indicating the formation of the structure due to hydrogen bonding interactions. However, the addition of urea makes the plateau modulus disappeared. The zero shear viscosity (η_0) decreases with increasing urea concentration. Urea mainly hinders the formation of the intermolecular hydrogen bonds leading to macromolecular or colloidal structuring in more

concentrated solutions [1,6]. Thus, the reduction of the number of the hydrogen bonding interactions results in the decrease of the rheological properties of the chitosan solution in the presence of urea.

Effect of urea on gelation behaviors

During the gelation process, the evolution of G' and G'' was investigated as a function of temperature. As shown in Figure 4, three regions clearly appear: Region (1) liquid-like behavior ($G' < G''$, G'' not shown); Region (2) a fast gelation process; and Region (3) a slow gelation process. Increasing urea concentration increases T_{gel} and gel strength, corresponding to the retardation of gelation. Since adding urea destroys hydrogen-bonding interactions [1,6], it indicates that these interactions are important in the heat-induced chitosan-*GP* sol-gel transition.

The addition of *GP* to the chitosan solution increases the *pH* and ionic strength and screens the electrostatic repulsions caused by the protonated amine groups in the chitosan molecules as well as it controls the hydrophobic and hydrogen bonding interactions [4]. Amiji [7] reported that chitosan could be associated by intermolecular hydrophobic interactions between *N*-acetyl-D-glucosamine groups. Philippova et al. [8] showed the existence of intermolecular hydrophobic aggregates both in chitosan and in hydrophobically modified chitosan from pyrene fluorescence study. The

induction of thermal energy and the increase in the ionic strength enhances hydrophobic interactions [9]. Thus, increasing temperature results in an acceleration of the gelation process of chitosan/*GP* solutions. From the *pH* and conductivity results, we confirmed that the degree of the protonation of the chitosan decreases and the ionic strength increases when increasing temperature. Thus, increasing temperature provides the favourable environment to form gel structure. Finally, increasing temperature may cause the change of the chitosan molecular conformation due to the reduction of hydrogen bonding interactions. At a low temperature, chitosan molecule has a randomly coil conformation or compacted structure due to hydrogen bonding interactions. If the molecular conformation is random coil, the physical junction zones to form gel may in the coil. Thus, it is a poor conformation to build-up gel structure due to the difficulty of contacts between the junction zones. On the other hand, increasing temperature reduces the number of hydrogen bonding interactions so that the chitosan molecules can be freely unfolded. This unfolded structure is favourable to form gel due to exposure of the physical junction zones. Thus, gelation will be easier at high temperature.

Conclusions

The physiochemical properties and Gelation tests were performed for various urea concentrations in terms of temperature.

Increasing temperature decreases the pH values regardless of the chemical composition of each sample; however, increases the conductivity values, indicating that the ionic strength increases with increasing temperature. The degree of the protonation of the chitosan calculated decreases with increasing temperature. The higher ionic strength and less electrostatic repulsion enhance the polymer-polymer interactions via hydrophobic interactions at higher temperatures.

In solution state, adding urea decreases the rheological properties (G' , G'' , and η_0). It is caused by the reduction of the number of hydrogen bonding interaction due to urea. During the gelation tests, heating resulted in sol-gel transition at a critical temperature, called gelation temperature (T_{gel}). It was found that adding urea decreased the gel strength and increased T_{gel} , corresponding to the retardation of the gelation process. It indicates that hydrogen bonding is an important interaction of the gel formed even at high temperature.

Acknowledgement

The authors gratefully acknowledge the financial support of Conseil de Recherches en Pêche et en Agroalimentaire du Québec (CORPAQ).

References

1. McGrane, S. J., Mainwaring, D. E., Cornell, H. J., and Rix, C. J., The role of hydrogen bonding in amylose gelation, *Starch/Stärke*, 56, 122 – 131 (2004).
2. Rinaudo, M., Pavlov, G., and Desbrières, J., Influence of acetic acid concentration on the solubilization of chitosan, *Polymer*, 40, 7092 – 7032 (1999).
3. Carreau, P. J., De Kee, D. C. R. and Chhabra, R. P., Rheology of Polymeric Systems: Principles and Applications, Munich (England): Hanser Publishers (1997).
4. Wang, D., Characterization of thermoreversible pH-sensitive physical gels of chitosan, Master's thesis, École Polytechnique de Montréal, QC, Canada (1999).
5. Lide, D. R., CRC Handbook of Chemistry and Physics: A Ready-Reference Book of Chemical and Physics Data, 84th Ed., CRC press, 7-9 – 7-13 (2003/2004).
6. Kokufuta, E., Suzuki, H., Yoshida, R., Yamada, K., Hirata, M., and Kaneko, F., Role of hydrogen bonding and hydrophobic interactions in the volume collapse of a poly(ethylenimine) gel, *Langmuir*, 14, 788 – 795 (1998).
7. Amiji, M. M., Pyrene fluorescence study of chitosan self-association in aqueous solution, *Carbohydrate Polymers*, 26, 211-213 (1995).

8. Philippova, O. E., Volkov, E. V., Sitnikova, N. L., and Khokhlov, A. R., Two types of hydrophobic aggregates in aqueous solutions of chitosan and its hydrophobic derivative, *Biomacromolecules*, 2, 483-490 (2001).
9. Desbrieres, J., Martinez, C., and Rinaudo, M., Hydrophobic derivatives of chitosan: Characterization and rheological behaviour, *International Journal of Biological Macromolecules*, 19(1), 21-28 (1996).

Key words

Chitosan, Urea, Gelation, rheology, pH, ionic strength, temperature, hydrogen bonding, hydrophobic interactions

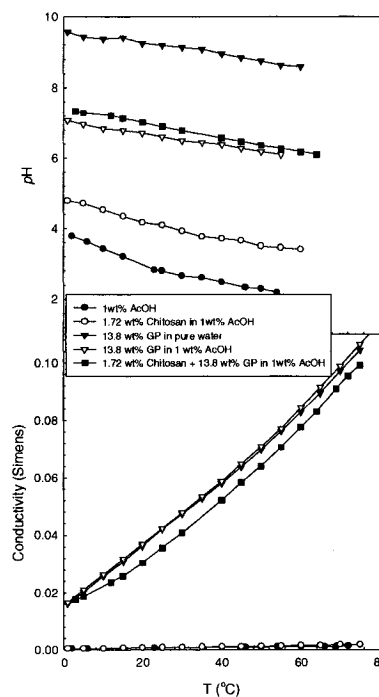


Figure 1. The pH and conductivity measurements as a function of temperature for each solution.

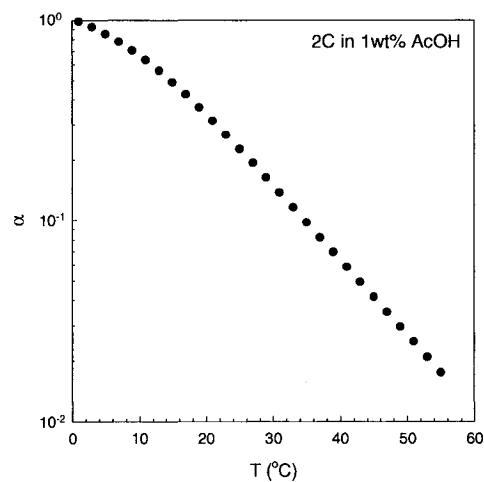


Figure 2. The degree of the protonation (α) calculated of the chitosan at each temperature.

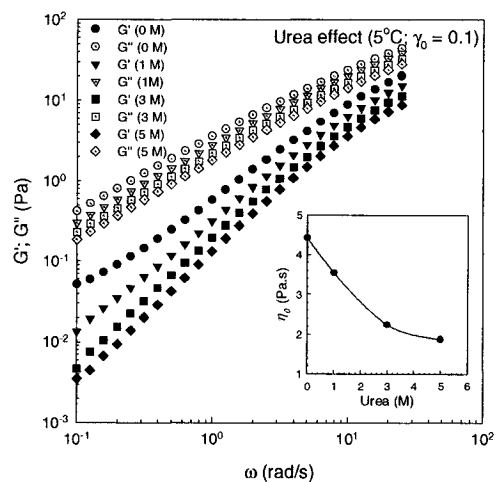


Figure 3. The effect of urea on the physical properties of the chitosan solutions.

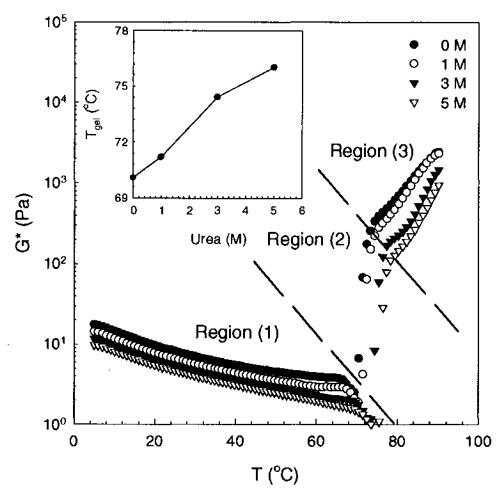


Figure 4. The effect of urea concentration on the gelation process.